NEI-NO--915

WILLIAM BAILEY

N09805305

AN EVALUATION OF CALCULATION PROCEDURES AFFECTING THE CONSTITUENT FACTORS OF EQUIVALENT CIRCULATING DENSITY FOR DRILLING HYDRAULICS

MASTER

DISTRIBUTION OF THIS DOCUMENT IS UNLIMITED
FOREIGN SALES PROHIBITED

NTNU
Norges teknisk-naturvitenskapelige universitet
Trondheim

DOKTOR INGENIØRAVHANDLING 1996:96
INSTITUTT FOR PETROLEUMSTEKNOLOGI
OG ANVENDT GEOFYSIKK
TRONDHEIM

IPT-rapport 1996:5

Erratum

Errata found in "An Evaluation of Calculation Procedures Affecting the Constituent Factors of Equivalent Circulating Density for Drilling Hydraulics."

Page 44, section 3.1.6, unnumbered equation in item 3 should read:

$$D_{\mathrm{L}} = \sqrt{D_o^2 + D_i^2 - \frac{D_o^2 - D_i^2}{\ln\left(D_o / D_i\right)}}$$

Page 45, section 3.1.6, Eq.(3.10) should read:

$$D_{\mathrm{hy}} = \frac{1}{2}\sqrt[4]{D_o^4 - D_i^4 - \frac{\left(D_o^2 - D_i^2\right)^2}{\ln\left(D_o / D_i\right)}} + \frac{\sqrt{D_o^2 - D_i^2}}{2}$$

Page 79, section 4.2.2, Eq.(4.2) should read:

$$f\left(v_p\right) = \frac{1}{\sqrt{2\pi m p(1-p)}} \exp\left[-\frac{1}{2mp(1-p)}\left(\frac{v_p - v_{p,\min}}{v_{p,\max} - v_{p,\min}} - p\right)^2\right]$$

Page 80, section 4.2.3, second unnumbered display equation in item 2 should read:

$$y = S_z^{\mathrm{M}} U_2$$

An Evaluation of Calculation Procedures Affecting the Constituent Factors of Equivalent Circulating Density for Drilling Hydraulics

by

William J. Bailey

December 1996

A dissertation in partial fulfillment
of the requirement for the degree of
Doktor Ingeniør
(Doctor of Philosophy)

Division of Petroleum Engineering
and Applied Geophysics
The Norwegian Institute of Technology
Norges Teknisk-Naturvitenskapelige Universitet (NTNU)
The University of Trondheim, Norway

This work was typeset by the author in $\LaTeX\ 2\varepsilon$ using Scientific Word.
The author welcomes any communication and may be contacted
via e-mail at `w.bailey@ic.ac.uk`

DISCLAIMER

Portions of this document may be illegible electronic image products. Images are produced from the best available original document.

Summary

The purpose of drilling hydraulics is to provide information about downhole pressure, suitable surface pump rates, the quality of hole cleaning and optimum tripping speeds during drilling operations. Of the different calculations performed, a good estimate of equivalent circulating density (ECD) is possibly the most significant. This is because it indicates potential violation of formation integrity: a failure of which can result in either loss of valuable circulating fluids to the formation or in an uncontrolled influx of reservoir fluids to the well. The objective of this thesis is to investigate the procedures affecting this calculation in order to provide more reliable ECD estimates. To achieve these objectives the following main issues were addressed:

1. *Selection of the Rheological model.* The RMS measures of goodness-of-fit, calculated from a large data set, show that alternatives to commonly employed rheological models provide significantly improved drilling fluid characterisation over a wide range shear rates. The study encompasses both direct and nonlinear least squares parameter solution procedures. It is shown through various statistical treatments that for the latter parameter solution methodology, a reparameterised form of the Sisko model provides the most consistently reliable and accurate fluid characterisation possible - and could be considered as a suitable default.
2. *System pressure losses due to friction.* Inconsistencies existing in the contemporary treatment of flow functions are addressed by the introduction of a generalised flow behaviour index, N. This parameter can be defined for *any* rheological model, is flowrate dependent and does not rely on any simplifying assumptions concerning conduit geometry. This parameter also provides a mechanism by which some consistency and generality may be applied to the pressure loss calculation for laminar, turbulent and transitional flow as well as in flow regime transition criteria. The performance of an implicit, generalised, laminar flow function (making no assumptions about conduit geometry, the presence of plug flow nor the form of the rheological model), along with a hybrid turbulent flow friction factor correlation, is compared against measured data with reasonable agreement. The generalised laminar flow function is further treated in order to provide confidence intervals of its result. This procedure is considered significant in that it can furnish confidence intervals for the pressure loss component of ECD (which may prove beneficial when drilling within a tight tolerance) and for *any* fitted nonlinear function. Utilitarian functions for approximating pressure losses over downhole tools are also presented.
3. *Density of mud with cuttings.* Simple functions for use within a material balance to determine composite fluid density as a function of salinity, temperature and downhole pressure are proposed. Slip velocity calculation procedures within a multivariate environment are presented. This method provides a means to accommodate actual distributions of cuttings size, cuttings shape and velocity profiles in the calculation of cuttings concentration.

The thesis concludes with simulations conducted on four different sections of an actual North Sea well with reasonable agreement to measured SPP's when rotational and annulus eccentricity effects are considered.

Acknowledgements

In a work of this kind there are many to thank. Firstly I must express my sincere gratitude to my supervisor Professor Michael Golan of the Institute for Petroleum Technology and Applied Geophysics, Norges Teknisk-Naturvitenskapelige Universitet (NTNU). I am also deeply indebted to Dr. T. Sezgin Daltaban, Elf senior lecturer at the department of Earth Resources Engineering, Imperial College of Science, Technology and Medicine, University of London and Professor at the Ecole Nationale Supérieure du Pétrole et des Moteurs, Paris, for his support and encouragement.

It would not be an overstatement to say that this thesis would not have been completed if it was not for the help, advice and, above all, friendship of Dr. Iain S. Weir, Department of Mathematics, University of Bristol. Your contribution was invaluable.

I must also express my sincere gratitude to Dr. Erik Skjetne for his contributions, Richard Carrington for navigating me through some grammatical minefields and Dr. G. Stephenson of Imperial College for valuable mathematical guidance. I am also grateful to the various service companies who allowed me access to their hydraulics simulation packages and/or relevant documentation.

I would like to thank Dr. John Daniel Friedmann, Saga Petroleum A/S, Professor Dr.-Ing. Volker Köckritz, Freiberg University of Mining and Technology, Germany, Professor Bernt Aadnøy, Høgskolesenteret i Rogaland, Stavanger, Norway and Professor dr.ing. Knut L. Sandvik, Institutt for geologi og bergteknikk, NTNU for serving in my Graduate Committee.

I am fortunate to have had the support of my friends: Dave Ashley and Lou, Séan Bartindale, Chris Bray, Matthew Carrington, Mark 'Snowboy' Cotgrove (always steps ahead of the rest), Branimir Cvetković, André DiBiaggio, Darryl (Chye) Goon and family, Dag Edvardson and the TBF (Svein Omdal, Tom Erik Holte *et al.*), Rolf Helland, David Jackman, Ole Lie, Frederic Meyer, Shane Ó'Ríórdain, Donald 'Jock' Paterson, Dag Pedersen, Southend United F.C., Svein Tollefsen, Philip Wiltshire, Dr. Su Ze. I also owe thanks to my colleagues at Imperial College and NTNU.

This study was made possible with financial support of European Community COMETT and ERASMUS scholarships and the understanding of my bank manager. Finally I wish to express my deepest gratitude to my parents for their unwavering support.

This work is dedicated *To Them.*

Preface

Sections 2.5 and 3.4 are taken directly from the following SPE paper, with only minor revisions:

Weir, I.S., and Bailey, W.J.: "A Statistical Study of Rheological Models for Drilling Fluids," paper SPE 36359, accepted for publication in *Soc. Pet. Eng. J.* on 8th July 1996, scheduled for publication in the December 1996 issue.

Consequently the author wishes to acknowledge the significant contribution to these particular sections made by Dr. Iain S. Weir.

Table of Contents

List of Tables

List of Figures

Chapter 1

Drilling Hydraulics

Drilling hydraulics calculations form an integral part of the planning and operational decision making processes involved in the drilling of oil- and gas-wells. With a greater number of deviated, deeper (long reach) and slimhole wells being drilled, an ability to establish accurate system hydraulics is becoming increasingly important. A good understanding of drilling hydraulics in the well can result in both monetary savings and enhanced safety. Such benefits emerge if the calculation is properly applied in order to determine pump rates required to:

- provide the necessary amount of hole cleaning (cuttings transport, carrying capacity) and prevent re-grinding of drill-cuttings due to particle re-sedimentation;
- provide the necessary degree of pressure maintenance so as to prevent loss-of-circulation and the uncontrolled influx of reservoir fluids, without damaging the formation;
- provide optimum drill bit performance in terms of penetration rate, bit wear, operational costs and the prevention of bit-clogging;
- provide sufficient energy for efficient/effective performance of any downhole tools such as positive displacement motors (PDM's), turbines and so on;
- allow for safe operating margins for the surface pumps (as determined either by pump capacity or pop-off valve [POV] setting);
- provide sufficient lubrication to all drillstring components;
- allow sufficient filter-cake formation (when desired);
- provide conditions conducive for rapid tripping without exposing the system to adverse swab or surge pressures.

In essence, drilling hydraulics calculations attempt to establish surface pump rates that minimise parasitic losses without compromising hole cleaning and downhole tool requirements, but providing sufficient energy for optimum bit performance: all without jeopardising the safety imperative. For well-planning applications, drilling hydraulics calculations help to establish reasonable operating margins while the equivalent real-time (rig-site) calculation is conducted to provide the information necessary for decision making and to ensure acceptable equivalent circulating densities when considered alongside utilitarian standpipe pressures (Parigot, 1985).

1.1 Components of the Circulating System

Ordinarily, drilling hydraulics calculations act over the whole circulating system encompassing the path followed by the drilling fluid (or cement) in the well being drilled plus certain top-side installations. Various authors (e.g., Pigott, 1941; Moore, 1974; Randall & Anderson, 1982) have described the mud circulation system and its component parts in detail. For the purposes of this work, the circulation system is considered to comprise the following main elements (in sequence and in the direction of fluid flow):

1. Surface connection lines incorporating all tubing from the mud pump manifold up to, and including, the standpipe, rotary hose, kelly and/or top drive. Lengths and geometries of these tubings (often referred to as 'surface equipment') may vary considerably between each installation[1].
2. Drillpipe.
3. Bottom hole assembly (BHA) incorporating some, or all, of the following:
   - Heavy weight drill pipe (HWDP) or nonmagnetic drillpipe (NMDP),
   - Drill collars (DC),
   - Measurement while drilling (MWD) tools,
   - The PDM or turbine,
   - Jar(s),
   - Cross-over sub(s) (XO sub),
   - Additional specialised tubing/equipment.

   The drillpipe and BHA assembly together is referred to as the 'drillstring'.
4. Drill bit (roller cone, diamond, PDC) or core barrel.
5. Annulus around the BHA.
6. Annulus around the drill pipe.
7. Annulus in the riser system (with or without riser-boosters) for offshore operations only.
8. System outlet, often taken to be at the shale shaker (assumed at atmospheric conditions).

Figure 1.1 presents a schematic (not to scale) of a typical drilling circulating system and indicates its complexity with annular and circular flow paths, tortuous routings through downhole tools and sudden throttling at the bit). Compressibility and thermal expansion of the circulating fluid provides further complications, especially in extended reach wells where fluid residence times are longer. In addition there exist the effects of drill cuttings, hole-inclination, drillstring rotation, annular eccentricity, changes in fluid rheology and mud-cake formation. All of the aforementioned contribute to the critical decision of establishing appropriate pump rates.

[1] Calculation of surface equipment losses (between 1% and 5% of total system loss) is facilitated by classifying surface equipment as belonging to one of four classes – Types I to IV (Comité des Techniciens, 1982). North Sea installations are typically represented as Type IV which is defined as – Standpipe: 45ft, 4″ ID; Rotary Hose: 55ft, 3″ ID; Swivel: 6ft, 3″ ID and Kelly: 40ft, 4″ ID. Although these tubings do not fully represent modern top drive installations used in many North Sea operations, use of this definition has gained some consensus in the field.

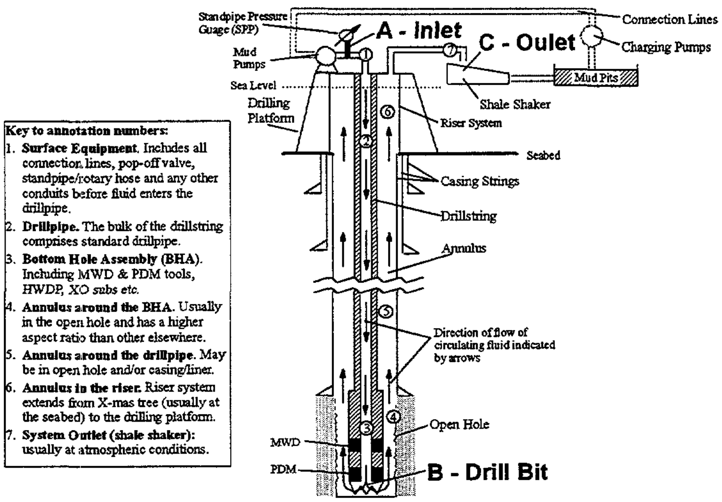

Figure 1.1: Schematic of a typical drilling hydraulics system (not to scale). Dashed lines represent connection lines not directly considered in the analysis. Point '**A**' represents the inlet of the circulating system. Point '**B**' is the drill bit (or core barrel) where the fluid exits the drillstring arrangement (essentially a circular profile) and enters the system annulus. Point '**C**' represents the outlet of the circulating system (usually at the shale shaker and at atmospheric conditions).

1.2 Contemporary Drilling Hydraulics Solutions

To enable the solution of the drilling hydraulics calculation, most operating companies, service companies and some research institutions have access to, or have developed their own, proprietary drilling hydraulics software. These tools, however, vary widely in sophistication. At one extreme are simple printed calculation forms, tables and charts that often rely on *rules of thumb* or extreme simplifications of the system under investigation (for example Paul, 1978). While these methods are suitable for hand computations they are strictly limited in the scope and accuracy of the information they are able to convey. Although their utility cannot be casually dismissed due to their historical significance, modern drilling operations now require more immediate, detailed and accurate information than could otherwise be provided. At the other extreme are large and intricate, mainframe-based, dynamic computer simulation packages for non-Newtonian multiphase fluids; e.g., GasKick (Rommetveit, 1988; Bjørge, Kvalvaag & Vefring, 1990) and SideKick (White & Walton, 1969). Designed specifically for kick simulation, such programs provide a vital tool for the control and simulation of gas kicks during drilling operations. GasKick employs Bingham Plastic and Power Law models while SideKick utilises the Casson model. Such packages are, however, impractical for practical day-to-day operational needs since they are not designed for the specific requirements of drilling hydraulics calculations. Consequently, practical drilling hydraulics is conducted using specialised, often PC-based, computer programs capable of generating rapid output in a format suitable for quick interpretation by interested personnel. Service companies are the principle suppliers of such programs, often as part of their contractual obligations. Whilst the author had access to a number of proprietary hydraulics programs for evaluation and study, as well as for use under actual operational scenarios (for both well planning and rig-site analysis), it is not the intention of this work to critique these products. Consequently this work will refrain from making any direct reference to specific products, vendors or program-components unless generally available in the public domain. Occasional reference will be made, however, to the HYCAT simulation package (NOS, 1993) which the author was involved in developing.

Although such software packages can sometimes provide reasonable predictions of standpipe pressures (SPP's), calibration of the simulation pivots upon a single surface-read value - the measured SPP, (a calibration often conducted through manipulation of certain, essentially unknown, variables in the system - such as the bit discharge coefficient). This practice casts some doubt on the validity of inferring simulation accuracy to critical parts of the system (e.g., at the casing shoe and open hole) by assuming that the magnitude of the error between measured and observed SPP applies to all parts of the system uniformly. Excessive over-estimation of drillstring friction losses, coupled with severe under-estimation of annulus friction losses, cuttings concentration and fluid compressibility may indeed precisely match SPP at the surface but provide poor modelling accuracy at critical points elsewhere in the system.

The primary area of interest of this study is, therefore, to help establish methods and procedures to determine more accurate, system-wide, drilling hydraulics calculations that permit greater confidence to be placed on simulated downhole values; in particular ECD.

1.2.1 The Importance of Equivalent Circulating Density

Accurate evaluation of downhole ECD (sometimes referred to as 'annular specific weight' or 'effective circulating density') is crucial in preventing both loss of circulation of the drilling fluid and the influx of any formation fluids (kicks). The prevention of the latter is an absolute priority during any drilling operation. The gravity of such an occurrence requires little elaboration as its consequences are all too well documented.

Conditions conducive to a kick will occur if the pressure acting on the open hole by the drilling fluid is below the formation's pore pressure. Conversely, conditions conducive to loss of circulation (loss of valuable circulating fluid to the formation) will occur if the pressure acting on the open hole by the fluid is above that required to fracture the rock formation. Both occurrences are undesirable and translate into additional expenses and operating hazards. Equivalent circulating density provides the information necessary to determine how close the operation is within given safety margins, provided by geological and actual drilling data. A generalised fracture- and pore-pressure diagram is shown in Fig. 1.2. Such a plot provides the driller with a clear indication of appropriate operating ECD values.

1.2.2 Calculation of Equivalent Circulating Density

Equivalent circulating density represents the total actual bottom-hole pressure exerted on the open-hole/casing and is usually presented in terms of an equivalent specific gravity that, whilst retaining the acronym 'ECD', implies (incorrectly) the dimensions of density. ECD, at the point in question, is the sum of the static specific weight of the fluid, the additional pressure drop due to the weight of drilled cuttings suspended in the fluid in the annulus and the friction and acceleration pressure losses over the measured length of the annulus. The additional 'weight'

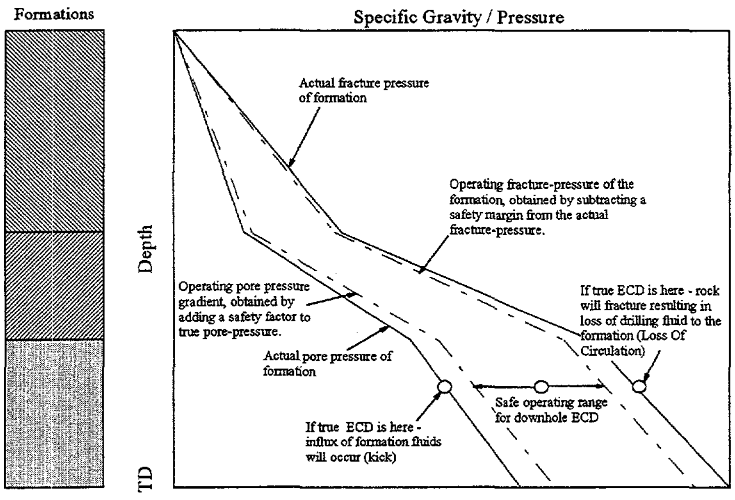

Figure 1.2: A pore- and fracture-pressures versus depth diagram. Prevention of kicks and loss of circulation requires that downhole ECD remains within the given boundaries.

resulting from the annular pressure losses may be of considerable importance when drilling through fragile and/or soft formations. This is especially important in slimhole activities due to the frequency of (soft) sedimentary formations drilled using this technique (Delwiche, Lejeune, Mawet & Vighetto, 1992) and the high associated annular friction losses. In equation form ECD can be expressed in a number of ways: as a specific gravity,

$$\mathrm{ECD} = (\gamma)_{\mathrm{ecd}} = (\gamma)_{\mathrm{mwc}} + \frac{(\Delta p)_{\mathrm{ann}}}{10\,000L}, \tag{1.1}$$

or in terms of a quantity with dimensions of density (kg/m^3):

$$\mathrm{ECD} = (\rho)_{\mathrm{ecd}} = (\rho)_{\mathrm{mwc}} + \frac{(\Delta p)_{\mathrm{ann}}}{10L},$$

or in terms of a quantity with the units of pressure (Pa):

$$\mathrm{ECD} = (\Delta p)_{\mathrm{ecd}} = 10L\,(\rho)_{\mathrm{mwc}} + (\Delta p)_{\mathrm{ann}}.$$

Eq.(1.1) is presented in Table 1.1, for two different sets of commonly employed units.

1.3 Calculation Procedure Overview

In general, drilling hydraulics calculations consist of several distinct elements and disciplines rolled into a single activity, namely:

S.I. units	$(\gamma)_{\text{ecd}} = 0.001\,(\rho)_{\text{mwc}} + \dfrac{(\Delta p)_{\text{ann}}}{10\,000\,L}$
Imperial units	$(\gamma)_{\text{ecd}} = 0.11983\,(\rho)_{\text{mwc}} + \dfrac{2.26\,(\Delta p)_{\text{ann}}}{L}$

Table 1.1: ECD, expressed in terms of specific gravity (SG), for two common sets of units, for S.I.: L = m; Δp = Pa and $(\rho)_{\text{mwc}} = \text{kg/m}^3$. For Imperial units: L = ft; $\Delta p = \text{lb}_\text{f}/\text{in}^2$ and $(\rho)_{\text{mwc}} = \text{lbs}_\text{m}/\text{gal}$.

1. Rheological description of the drilling fluid/cement slurry.
2. Laminar, transitional and turbulent friction losses in annular and circular conduits.
3. Pressure losses through downhole tools (e.g., MWD's, PDM's and turbines).
4. Fluid compressibility and expansion.
5. Cuttings transportation.
6. Drillstring rotation.
7. Pressure losses through the drill bit/core barrel.
8. Incidental calculations: i.e., swab-surge, bit optimisation.

Whilst this list presents the basic activities associated with conventional drilling hydraulics calculations, the different software packages available vary widely in the nature and treatment of the procedures employed in the solution. The calculation process first requires the identification of system geometry to the program: drillstring/BHA (described by the 'tally-book'); casing and open-hole geometry (provided by the 'welly-book'); hole inclination and azimuth (from deviation surveys). Once rheological data (usually taken from Fann viscometer readings at four, six or eight rotation speeds) and other input requirements have been fulfilled, program-flow switches are then selected (e.g., rheological model, cuttings transport model, bit discharge coefficient, calculation step length etc.). The steady state integration scheme progresses step-wise through the system (either upstream from the fluid outlet at atmospheric conditions to the mud pumps, or downstream in the direction of flow from the mud pumps to the fluid outlet at the shale shaker). Depending on what is required (standard SPP calculation, bit optimisation, swab-surge calculations etc.) the results are then formatted and outputted for interpretation, analysis and decision making.

While a detailed analysis of the so-called 'conventional' solution procedures is presented in the relevant chapters, the formulations utilised by most of the proprietary software considered are founded and/or constructed on some, or all, of the following generalisations and assumptions:

1. Restricted selection of rheological models available to describe the non-Newtonian behaviour of the fluid.
2. An apparent desire to have analytical tractability for all flow equations.

3. Reliance on the unrepresentative slot-flow assumption to describe annular geometry: an assumption applied to make flow equations more manageable.
4. Concentric annulus geometry throughout.
5. Inconsistent application of calculated parameters between flow regimes.
6. Inconsistent application of conventional models in pressure loss functions, critical Reynolds numbers and other dimensionless quantities.
7. Possible discrete/separate application of different rheological models over certain parts of the continuous circulating system.
8. Rheological model parameters calculated using over-simplistic procedures.
9. Generalisations concerning drill-cuttings size and shape with transportation occurring in a uniform annular velocity field.
10. Incompressible circulating fluids.
11. Empirical, or best-guess, approaches to pressure loss estimation over downhole tools.
12. Similarly empirically-based approaches to drill bit/core barrel pressure loss estimation.
13. No compensation for pipe rotation effects (helical flow and Taylor vortices).
14. Often unreasonably large step-lengths in the integration process.
15. Certain integration schemes that treat the node in each calculation 'cell' as a separate, independent, body detached from other calculation cells except for pressures at cell boundaries.
16. Steady state solutions only.

While the effect and implications of some of these assumptions are discussed in more detail later, it is clear that such generalisations are likely to have an effect on the accuracy and validity of the calculation. It is apparent that these 'limitations' are a legacy of a time where rig-site computation facilities were not readily available and conventions and simplifications necessary for expedient calculation were subsequently incorporated into the design of drilling hydraulics programs.

1.4 Study Objectives and Document Outline

Drilling hydraulics calculations are served by three main references (Comité des Techniciens, 1982; Exlog, 1985; Bourgoyne, Chenevert, Millheim & Young, 1986) which approach the subject from an essentially operational standpoint. While presenting conventional formulations and procedures, they are quite assumption-loaded and restricted in their scope of applicability, especially in the light of the increasing number of slim-hole operations. Consequently, this work examines contemporary procedures associated with fluid characterisation, unobstructed conduit pressure losses, downhole tool losses, compressibility and thermal expansion of the drilling fluid and the treatment of cuttings concentration. In précis, the general objective of this study is to investigate the calculation procedures involved in quantifying downhole ECD. The basic components of ECD are, however, required in incidental drilling hydraulics calculations encompassing nozzle-sizing (bit optimisation), swab-surge, SPP matching, and setting surface pump rates etc.

The document itself comprises five chapters (including this one) that consider the following:

- Chapter 1: a general introduction of the application of hydraulics calculations in drilling operations and the importance of downhole ECD.
- Chapter 2: an analysis of contemporary fluid characterisation procedures and proposes alternative rheological models and model selection criteria (with a suggested 'best' rheological model being recommended for default application).
- Chapter 3: contemporary pressure loss estimation procedures and proposes a generalised and consistent model for laminar, transitional and turbulent flow in unobstructed pipes and annular conduits that is independent of the form of the rheological model. The model is compared against measured data for actual drilling fluids in pipes and annuli with good agreement. Empirical downhole tool pressure loss expressions are presented to furnish approximate tool pressure losses. Finally procedures for establishing confidence bounds for laminar pressure losses are dicsussed, thereby providing a mechanism whereby some degree of confidence can be attributed to ECD estimates. It should be noted that bit losses are not explicitly considered in this work as this involved topic is beyond the scope of this study.
- Chapter 4: fluid compressibility and thermal expansion with published data being translated into useable expressions in terms of downhole pressure and temperature. Cuttings transport calculations are considered within a procedure enabling conventional, single-value, expressions for particle slip to be applied within a multivariate framework. Simulations on an actual well in the North Sea are outlined and compared against measured SPP values, with reasonable agreement.
- Chapter 5: general conclusions and recommendations for further work. The chapter is followed by nomenclature, references and nine appendices.

Chapter 2

Fluid Characterisation

The pseudoplastic behaviour of time-independent non-Newtonian drilling fluids and cement slurries is characterised by rheological models that provide relationships between the rate of shear and the instantaneous shear stress of the fluid. A number of such models exist in the literature with formulations based on empirical observations of the flow of specific fluids, purely theoretical formulations or a combination of both. This chapter examines the limitations of contemporary industry conventions in determining the flow properties of drilling fluids and cement slurries from given rotational viscometer readings and presents more rigorous procedures for the selection of suitable rheological model(s) and the calculation of their parameters.

2.1 Conventional Calculation Procedures

The contemporary engineering approach to rig-site fluid characterisation of drilling fluids and cement slurries is through viscometer readings (most commonly the Fann rotational viscometer[1]). These readings are taken at regular intervals during the day at predetermined, or contracted, rotation speeds at a constant fluid temperature. A number of operating companies in the North Sea require readings to be taken at 600/300, 200/100, 60/30 and 6/3 rpm, while others may specify readings at six, or less, rotation speeds, although readings at 600/300 and 6/3 rpm are almost universally measured: this specific data provides nearly all rig-site fluid characterisation.

While there are a large number of rheological models present in the public domain, only two have gained any widespread acceptance within the petroleum industry: Bingham Plastic[2] (Bingham, 1916) and Ostwald–de Waele (de Waele, 1923; Ostwald, 1925) models - the latter often being referred to as the 'Power Law'. Their popularity can be explained by the tractable form of their related laminar flow friction pressure loss equations (Melrose, Savins, Foster & Parish, 1957; Savins, 1958) and the ease by which model parameters may be estimated - ordinarily they are calculated directly from Fann viscometer readings at 600/300 rpm.

[1]While it is accepted that alternatives to rotational viscometer data may be more suitable for characterising certain pipe-flow phenomenon, this work concentrates on examining only conventional rig-site procedures; hence the need to focus on results provided by the Fann rotational viscometer (Fann International Corporation, Houston, Texas). It is almost universal for mud logging companies to record such data using these, or similar, devices. For completeness, however, well documented procedures for correcting rotational viscometer readings for improved pipe-flow characterisation are presented in section 2.4.3 on page 21.

[2]Eugene Bingham, a physicist at the US Bureau of Standards, postulated the notion of the 'ideal plastic' after noticing anomalous viscosities during investigations of the flow properties of paints which were found to act like a solid until a certain stress was applied.

2.1.1 Limitations of Conventional Procedures

The main limitations, or concerns, identified with conventional rig-site fluid characterisation procedures relate to the following:

- the failure of popular rheological models to characterise the non-Newtonian flow behaviour of the drilling fluid or cement slurry on a rheogram for all shear rates encountered in the circulating system, which may result in
- *ad hoc* and discrete application of different rheological models over distinct sections of the circulating system, and
- over-simplistic procedures for evaluating rheological model parameters from the available measured data.

No single rheological model is able to accurately represent the flow behaviour of most pseudoplastic and yield-pseudoplastic fluids over the full spectrum of shear rates (Chilingarian & Vorabutr, 1983; Okafor & Evers, 1992). Nevertheless, the historical need for analytically useable flow equations has resulted in the persistent dominance of Bingham Plastic and Power Law models in practical drilling hydraulics calculations[3]. Furthermore, these models have been used extensively, either directly or indirectly, in the interpretation and analysis of research and experimental investigations in the following areas:

- solids transportation (examples include: Valentik & Whitmore, 1965; Ansley & Smith, 1967; Okrajni & Azar, 1986; Peden & Luo, 1987; Martin, Georges, Bisson & Konirsch, 1987; Bizanti & Robinson, 1988; Franco & Verduzco, 1988; Becker, Azar & Okrajni, 1991),
- temperature effects on rheology (examples include: McMordie, Bennet & Bland, 1975; Politte, 1985; Houwen & Geehan, 1986; Alderman, Gavignet, Guillot & Maitland, 1988),
- rheometer evaluation (examples include: Bannister, 1980; Clark, 1995),
- laminar flow models in concentric and eccentric annuli (examples include: Wallick & Savins, 1969; Guckes, 1975; Iyoho & Azar, 1981; Langlinais, Bourgoyne & Holden, 1985; Üner, Özgen & Tosun, 1988 & 1989; Haciislamoglu, 1989; Yuejin Luo & Peden, 1990).

The continued reliance upon Bingham Plastic or Power Law models has resulted in a meretricious convention which often assumes that the Power Law provides better characterisation at lower shear rates (where the model better represents the rheogram), while Bingham Plastic provides greater precision at higher shear rates (where the flow curve is often near-linear). This belief sometimes results in the separate application of the Power Law in the annulus and Bingham Plastic in the drillpipe and BHA (NOS, 1993; Strømnes & Lydvo, 1993). A consequence of this is the discontinuous application of dissimilar characterisation models over a single and continuous hydraulic system. The somewhat impetuous application of the Power Law in the annulus is likely to fail to deliver reasonable fluid characterisation when the *in situ* aspect ratio is high (such as around the BHA and in slim-hole drilling) due to high localised shear rates or at very low

[3]Standard drilling hydraulics packages supplied by several major service companies essentially offer a choice of only Bingham Plastic or Power Law models (or those derived directly from them, i.e., 'ARTEP' models, the Hughes Tool Co. Inc. model, and those presented in the book by Preston Moore).

shear rates (such as in the riser system) when the fluid exhibits a discernible yield stress. Other conventions consider the use of the Power Law for all hydraulics calculations up to the 12 1/4″ section to be appropriate and then Bingham Plastic thereafter. This crude simplification reflects the existence of a greater cross-sectional annular flow area for the upper sections, acknowledging the lower shear rates inherent under such conditions; but fails to account for the extensive region of higher shearing in the drillstring.

The third main concern is directed at the common practice of employing viscometer readings at only 600 and 300 rpm in order to determine rheological model parameters. Calculating constant parameters, determined at specific shear rates (which will correctly describe the fluid in only certain portions of the circulating system), cannot be expected to furnish accurate shear stresses over the whole circulating system where shear rates will vary considerably.

The consequence of these limitations to rig-site fluid characterisation procedures is likely to be a failure in accurately modelling non-Newtonian flow behaviour over the whole range of shear rates encountered in the circulating system. This inaccuracy inevitably introduces an added element of uncertainty in both calculated parasitic pressure losses and ECD estimates.

2.1.2 Alternative Models Proposed to Industry

To compensate for the limitations outlined in the previous section, a number of alternative rheological models have been proposed to the petroleum industry, namely: Robertson & Stiff (1976; with subsequent revisions to the flow equations presented by Beirute & Flumerfelt, 1977); Graves & Collins (1978), usually referred to as the 'Collins-Graves' model, appearing first, as a proper publication, in the paper by Haut, Collins & Graves (1978); Casson (1959; first proposed to the industry by Lauzon & Reid, 1979); Herschel-Bulkley (1926; comprehensively documented in the book edited by Whittaker, (Exlog, 1985)); the linear annular shear model (essentially a modified Bingham Plastic model based on limited empirical observations) proposed by Taylor & Smalling (1973) and the polynomial model proposed by Gavignet & Wick (1986). All these models claim to provide more accurate fluid characterisation over a wider range of shear rates than possible using Bingham Plastic and Power Law models. Of these alternatives only the Robertson-Stiff and Casson models can be manipulated into analytically tractable, but implicit, velocity profile and laminar pressure loss functions for both drillpipes and annuli. The implicit annular flow expressions derived from the aforementioned models are themselves merely approximations due to the need to apply the slot-flow assumption in order to yield tractability.

The cumbersome nature of the flow functions for the aforementioned alternatives possibly accounts for their lack of widespread acceptance in the field, even though studies have shown that they indeed yield greater precision in fluid characterisation over a wide range of shear rates. Hemphill, Campos & Pilehvari (1993) demonstrated how the Herschel-Bulkley model better described the behaviour (for two oil-based muds and one water-based drilling fluid) than Bingham Plastic and Power Law models. Beirute & Flumerfelt (1977) found the Robertson-Stiff model to be an improved fitting equation over the Herschel-Bulkley model in describing the rheological behaviour of cement slurries. Okafor (1982) demonstrated how Robertson-Stiff yielded improved fluid characterisation over Bingham Plastic, Power Law and linearised Power Law models in a study involving two different water-based drilling fluids. This finding was supported by Lenchow (1993) in a study involving two further drilling fluids. Cloud & Clark (1980) predicted that the Herschel-Bulkley model would provide better modelling to yield-pseudoplastic cross-linked fracturing fluids at low rates of shear while Robertson-Stiff would provide more satisfactory results at higher shear rates; with both models demonstrating greater accuracy than Bingham Plastic, Power Law or Newtonian models. Khataniar, Chukwu & Hua Xu (1994) demonstrated the improved fluid characterisation provided by both Robertson-Stiff and Herschel-Bulkley models over Bingham Plastic and Power Law models in an exercise comparing four water-based fluids. Wang Zhongying & Tang Songren (1982) found that the Casson model provided better fluid characterisation than Bingham Plastic or Power Law models in a study of 14 different pseudoplastic fluids. Houwen & Geehan (1986) showed how the Herschel-Bulkley and Casson models yielded improved fluid characterisation over the Bingham Plastic model for oil based muds at different temperatures, with Casson being found to be more reliable than Herschel-Bulkley for the purpose of extrapolating the function beyond the data region. Finally, Aadnøy & Ravnøy (1994) demonstrated that the Collins-Graves model was preferred over Bingham Plastic and Power Law models for a limited number of drilling fluids.

It should be noted that other rheological formulations exist in the wider literature (refer to Reiner, 1960; Skelland, 1967; Govier & Aziz, 1972), however, the aforementioned alternatives were explicitly presented to, and evaluated for, application within the petroleum industry.

2.2 Parameter Estimation

Detailed procedures for the solution of Bingham Plastic and Power Law model parameters, principally using Fann viscometer dial readings at 600/300 rpm ($\theta_{600}/\theta_{300}$) are well documented (e.g. Bourgoyne *et al.*, 1986). It has already been recognised that defining a global parameter at a specific, and localised, shear rate for general application is likely to result in poor fluid characterisation when *in situ* shear rates are decades away (on a semi-log scale) from the shear rate at which the parameters themselves were evaluated. Two approaches to parameter estimation are presented; the 'direct' approach and nonlinear least squares with contrasting performances being judged against a large data set of Fann viscometer readings taken from fluids used in actual drilling operations in the North Sea.

2.2.1 Data

General conclusions as to whether one rheological model is preferable over another, made from a comparison using only a few fluid samples (as outlined in section 2.1.2 on the page before), must be considered flimsy at best - or even inconclusive. A larger sample of fluids exhibiting greater variety in pseudoplastic and yield-pseudoplastic behaviour is required before any reliable conclusions can be drawn. To achieve this, a large sample of 414 different Fann viscometer reading sets was employed in the analysis, taken from a variety of different drilling fluids used in a number of North Sea drilling operations. The data comprises four principle drilling fluids: bentonite/polymer, sea water/pac, KCl/polymer and oil based muds (OBM's). The range of values of some essential properties, and the number of data sets for each of the four fluids, are presented in Table A.1 (page 110) with the full data set presented in Tables A.2 to A.5 inclusive while Table A.6 (page 120) presents more complete fluid details for four representative samples, one from each major fluid type. Readings were taken using a Fann rotational viscometer at 600/300, 200/100, 60/30 and 6/3 rpm at a constant test temperature of 50°C.

2.2.2 Statistical Measures

The R^2-test has been cited as a goodness-of-fit measure for model fitting (e.g., Comité des Techniciens, 1982; Jensen & Sharma, 1987). However, its interpretation as being "the proportion of explained variation" is not true for nonlinear models and since (apart from Bingham Plastic) the rheological models considered are nonlinear, its use is not relevant. Ratkowsky (1990), with regard to use in nonlinear model fitting, states "R^2 has no rôle to play in such evaluation and need never be calculated." Other objections to R^2 have been raised in some definitive statistical literature (Draper, 1984; Healy, 1984; Helland, 1987) which highlighted how it can be a misleading measure. It is standard practice to analyse residuals in order to detect inadequacies of a model, however, with a small number of data observations this too may be misleading; for example Daniel & Wood (1971) demonstrated obvious patterns in cumulative distribution plots of 16 generated random standard normal deviates. Instead, the performance measure used in subsequent analysis, as recommended by Healy, is the magnitude of the residual mean square (RMS) given by

$$\mathrm{RMS} = \frac{\mathrm{RSS}(\phi)}{n-p}$$

where

$$\mathrm{RSS}\,(\phi) = \sum_{i=1}^{n} \left[\tau_i - f\left(\dot{\gamma}_i, \phi\right)\right]^2,$$

with n being the number of data points (eight for all entries in this analysis) and p being the number of parameters in the rheological model. Unlike R^2, this simple measure takes into account the varying number of parameters between the models and gives an estimate of the error variance. Each model is compared by examining their RMS performance over the 414 Fann viscometer data sets. It is interesting, therefore, to compare for each model the empirical distribution of RMS values, with box-and-whisker plots providing the most suitable vehicle for such representation (Tukey, 1977).

2.3 Direct Parameter Estimation

Direct rheological model parameter solution refers to the procedure using viscometer readings in expressions constructed from successive substitution of the rheological model itself. With a conventional set of eight Fann viscometer readings a 2-parameter model will have 28 (${}_8C_2$) possible combinations of readings that will provide legitimate solutions for that model. For a 3-parameter model this figure rises to 56 (${}_8C_3$) legitimate solution combinations and 70 (${}_8C_4$) for a 4-parameter model.

2.3.1 Non-Conventional Direct Solutions

There is little documented evidence to confirm (or disprove) convincingly the general suitability of certain Fann viscometer readings over others. Widespread use of a procedure based on industry practice is no guarantee of accuracy or aptness of that procedure. The convention suggesting $\theta_{600}/\theta_{300}$ be preferred to those recorded at lower rotation speeds may be mistaken. The non-Newtonian fluid being characterised at these typically high rotations will, more often than not, be in the region of nonlaminar flow due to the high local shearing of the fluid. Consequently, laminar flow (which exists at lower shear rates) is often poorly served by concentrating rheological parameter solution on higher rotation readings. It is therefore appropriate to consider parameters calculated from non-conventional rotation speeds as being legitimate.

2.3.2 Models Considered

Twelve different models are considered in this part of the study including Bingham Plastic, Casson, Collins-Graves, Herschel-Bulkley, Power Law and Robertson-Stiff. Less familiar models selected for analysis include: Cross (1965); Ellis, Lanham, & Pankhurst (1955, with subsequent modifications by Reiner, 1960); Prandtl-Eyring (Prandtl, 1928; Eyring, 1936); Reiner-Philippoff (Reiner, 1930; Philippoff, 1935) and Sisko (1958). The final model considered (the Hyperbolic model, see section 2.3.3) has four parameters and employs a novel approach to rig-site parameter solution. All of the models considered, along with their simultaneous direct parameter solution equations (if applicable), are presented in Appendix B.

The criteria upon which model selection was conducted was whether the model could be reduced to a set of generalised simultaneous implicit and/or explicit expressions. Other models not considered were those proposed by Symonds, Rosenthal & Shaw (1955); Spencer & Dillon (1948); Spencer (1950); Williamson (1929) and Reiner & Rivlin (1928), as these relate only to pseudo-shear curves ($8\bar{v}/D$ versus τ_w, as discussed by Mooney, 1931). While pseudo-shear diagrams provide a useful method for establishing shear stress/shear rate relationships at conduit walls (through average velocities), such models have limited usefulness in drilling hydraulics calculations as they do not provide *in situ* values of τ and $\dot{\gamma}$.

2.3.3 The Hyperbolic Rheological Model

Observation of yield-pseudoplastic data profiles from standard sets of Fann viscometer readings can be considered to follow the path described by that portion of a hyperbola occupying the positive quadrant of a $\dot{\gamma} - \tau$ plane (Skjetne, 1996). Consequently a form of the expression for a hyperbola with a horizontal transverse axis can be used to describe the fluid profiles, namely:

$$\tau = \tau_{cp} + b\sqrt{\left(\frac{\dot{\gamma} - \dot{\gamma}_{cp}}{a}\right)^2 - 1}. \tag{2.1}$$

This expression is illustrated in Fig. 2.1 which also defines the four principal expression parameters; $a, b, \dot{\gamma}_{cp}$ and τ_{cp}. Dilatant fluids can also be characterised by modifying the model as follows:

$$\tau = \tau_{cp} + b\sqrt{\left(\frac{\dot{\gamma} - \dot{\gamma}_{cp}}{a}\right)^2 + 1}.$$

Conventional direct parameter solution procedures would necessitate the reduction of Eq.(2.1) into four simultaneous equations. The implicit solutions to the cumbersome expressions generated for this approach were found to be highly unstable and unsuitable for general application. However, explicit parameter solutions are possible through reparameterisation that involves components with more practical meaning to drilling engineers. The relationships defining the reparameterisation are as follows:

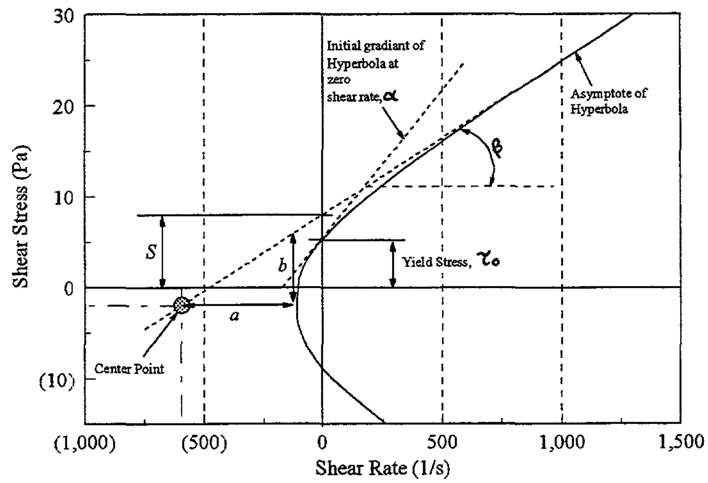

Figure 2.1: Definition of parameters employed in the Hyperbolic rheological model.

a (the shear rate defining the distance from the centre-point to the point of inflection of the hyperbola) is given by

$$a = \frac{S - \tau_\circ}{\beta}\sqrt{\frac{1+(\beta/\alpha)}{1-(\beta/\alpha)}};$$

b (the shear stress defining the distance between the point of inflection and the asymptotic gradient of the positive branch of the hyperbola) is calculating using

$$b = (S - \tau_\circ)\sqrt{\frac{1+(\beta/\alpha)}{1-(\beta/\alpha)}};$$

$\dot{\gamma}_{cp}$ (the shear rate at the centre-point of the hyperbola) is expressed as

$$\dot{\gamma}_{cp} = -\frac{S - \tau_\circ}{\beta\left[1-(\beta/\alpha)\right]};$$

and τ_{cp} (the shear stress at the centre-point of the hyperbola) being given by

$$\tau_{cp} = S - \frac{S - \tau_\circ}{1-(\beta/\alpha)}.$$

Intermediate model parameters, $\alpha, \beta, \tau_\circ$ and S, are illustrated in Fig. 2.1 and are defined as:

- α is the gradient of the hyperbola at $\dot{\gamma} = 0$, and may be approximated for rig-site application by taking the gradient between viscometer reading pairs at 6 and 3 rpm.

- β represents the gradient of the positive branch of the hyperbola at infinite shear rate. Similar to the approach used to determine plastic viscosity for the Bingham Plastic model, β is estimated as the gradient of the flow curve at the highest recorded rotation speeds. For rig-site application this will be the gradient between readings taken at 600 and 300 rpm.

- τ_o is the fluid's yield stress, and is approximated by the intercept of the line through the data points at 6 and 3 rpm with the ordinate.

- S is the plastic yield stress and represents the intercept of the hyperbola asymptote with the ordinate, namely the intercept of the line with gradient β passing through the data points at θ_{300} and θ_{600}.

The above represents a field-orientated approach to intermediate model parameter value estimation. For the purposes of the following analysis these expedient intermediate parameter definitions are not rigidly adhered to so that non-conventional measurement selection may be applied to the model.

2.3.4 Test Procedure and Results

Employing an ANSI C program written for the task, parameters for each of the models were calculated using the 414 data sets at one unique combination of readings. The associated RMS value was then calculated for this particular Fann viscometer reading combination data set, with a running tally providing a cumulative RMS figure. This procedure was repeated until all valid combinations of readings and data sets were exhausted. Detailed results for each rheological model are presented in Appendix C, Tables C.1 to C.11, which presents results for each possible combination of Fann viscometer readings for one rheological model and in addition: the number of solutions (maximum 414); lower and upper RMS extremes; lower- and upper-quartile RMS's; the median RMS with 95% confidence limits; the cumulative (maximum) RMS and the number of outliers (as defined by the box-and-whisker plot construction procedure, Appendix D).

Table C.1 (page 136) shows how the conventional Fann viscometer combination at $\theta_{600}/\theta_{300}$ furnishes poor fluid characterisation compared to those obtained using other legitimate reading combinations. The maximum RMS for this combination (159.4 Pa^2 under column labelled 'Max. RMS') was substantially higher than that found for other combinations with implications for pressure loss predictions and other related quantities. The θ_{600}/θ_{30} reading combination row has the lowest RMS value (31.97 Pa^2) of all possible combinations tested, with potentially beneficial implications for hydraulic calculation accuracy. Further examination of the results presented in Table C.1 shows that a high proportion of non-conventional Fann viscometer reading combinations yielded smaller RMS values and spreads than a conventional $\theta_{600}/\theta_{300}$ combination.

A box-and-whisker plot constructed for all models represented by parameters calculated using the highest viscometer rotation speed readings ($\theta_{600}/\theta_{300}$ for 2-parameter models, $\theta_{600}/\theta_{300}/\theta_{200}$ for 3-parameter models and $\theta_{600}/\theta_{300}/\theta_{200}/\theta_{100}$ for the Hyperbolic model) is presented in Fig. 2.2 on page 28. This provides a clear visual representation of the degree of RMS density and spread obtained from selections of 'conventional' Fann readings[4]. Both Casson and Hyperbolic models appear to out-perform others when basing predictive quality upon median RMS's with each

[4]It is assumed that 'conventional' in this case (namely θ_{600} and θ_{300}) also applies to lesser-employed rheological models where no such standard convention can be said to exist. Convention is also assumed to include θ_{200} for 3-parameter models and θ_{100} for the Hyperbolic model.

Model	Fann Speeds	Lower ext.	Lower q'tile	Med.	Upper q'tile	Upper ext.	Median 95% Conf. Limits	Max. RMS	No. Outs
Bi-Pl	600/30	0.3402	1.6710	2.3470	5.1300	9.400	(2.080 , 2.615)	31.97	76
Cass	600/60	0.0149	0.4305	0.7458	2.0570	4.417	(0.620 , 0.872)	10.03	59
Co-Gr	600/100/6	0.3198	0.8812	1.1820	2.0880	3.810	(1.088 , 1.275)	9.689	57
Ellis	600/100/6	0.0118	0.1048	0.1605	0.2885	0.548	(0.146 , 0.175)	4.555	23
He-Bu	600/100/6	0.0114	0.1085	0.1817	0.3028	0.584	(0.167 , 0.197)	4.442	23
Hyper	600/300/6/3	0.0877	0.6849	1.1450	5.9450	12.71	(0.738 , 1.550)	44.88	77
P-Law	600/100	0.0155	1.4790	6.1070	7.6390	15.98	(5.631 , 6.584)	27.04	3
Pr-Ey	600/100	0.4603	11.230	17.310	20.770	34.44	(16.57 , 18.05)	63.90	4
Re-Ph	600/200/6	0.0731	0.4951	0.6959	0.9973	1.655	(0.632 , 0.760)	4.360	6
Ro-St	600/100/6	0.0109	0.1463	0.2941	0.4379	0.871	(0.272 , 0.317)	4.324	17
Sisko	600/200/6	0.0139	0.0630	0.1082	0.1986	0.401	(0.098 , 0.119)	2.287	32

Table 2.1: RMS values for the 11 rheological models considered using 'best' Fann speed combinations. All models achieved 414 out of a possible 414 solutions except Reiner-Philippoff (Re-Ph) which managed only 154 solutions.

model demonstrating very narrow inter-quartile spreads, which implies an increased certainty that these models will provide reasonable fluid characterisation. Bingham Plastic and Power Law models, on the other hand, exhibit higher median RMS values than for all but the Collins-Graves, Prandtl-Eyring and Reiner-Philippoff models. Bingham Plastic exhibits the greatest spread of inter-quartile RMS's of any model and also exhibits a preponderance of outliers whose density and depth of spread is indicative of an increased likelihood of poor fluid characterisation. This introduces further incertitude into an already uncertain system of full-scale hydraulic calculations. It should be noted that for this combination only of Fann readings, results for the modified Power Law[5] are also presented and indicate no clear advantage in using this alternative model. Both modified and standard Power Law models exhibit greater lower-quartile spreads than any other model thereby demonstrating that the Power Law cannot be relied upon to furnish consistently reasonable fluid characterisations. All other models examined appear to yield only moderate fluid characterisation gauged from RMS performance. Of most concern, however, is the magnitude and spread of RMS's produced by all of the models. Even Casson and Hyperbolic fail to provide RMS spreads that could indicate reasonable fluid characterisation. An empirically determined gauge as to what constitutes 'reasonable' fluid characterisation was considered to be any model exhibiting a low RMS spread (say, no higher than 10 Pa^2), with narrow inter-quartile ranges, a median RMS as near to zero as possible and with few outliers. None of the aforementioned models utilising 'conventional' Fann readings satisfy this general requirement and, therefore, it can be concluded that the conventional selection of Fann viscometer readings is unlikely to furnish reasonable fluid characterisation. Furthermore, use of this data in Bingham Plastic and Power Law models provided significantly poorer modelling capabilities than most of the other models considered. The conventional procedure to fluid characterisation is, therefore, suspect.

Due to the large number of input data combination considered in the analysis, it was deemed impractical to present box-and-whisker plots for all possible combinations along with accompanying remarks. To facilitate concise presentation, the 'best' input data combinations (those having the smallest median RMS) for each model are presented in a single table (Table 2.1) with an accompanying box-and-whisker plot (Fig. 2.3 on page 28). Of significance is the omission of

[5]The modified Power Law (Appendix B, section B.12) acts on the consistency factor and applies only when this parameter is solved using the viscometer reading at 300 rpm. This is because the modification acts to compensate for the fact that the conventional solution to the Power Law consistency factor neglects the dial factor of 1.0678 and assumes a Newtonian shear rate of 511 s^{-1}, see Exlog (1984).

any $\theta_{600}/\theta_{300}$ Fann viscometer selections for any model in this list of superior performing combinations. The left-hand box-and-whisker sub-plot of Fig. 2.3 presents the density and spread of RMS's of the poorest performing rheological models with the vertical scale extending over 60 Pa^2 (namely, Bingham Plastic, Power Law, Prandtl-Eyring and Hyperbolic models). Dividing the plot was necessary to exhibit fairly the better performing models which are shown in the right-hand box-and-whisker sub-plot of Fig. 2.3 with the vertical scale reduced to an RMS of 10 Pa^2. Even at this higher resolution, marked differences in the comparative performance of the models are manifest. It is clear from this figure that the 3-parameter model proposed by Sisko out-performs all others, not just by having the smallest maximum RMS, but also by demonstrating the smallest median RMS value and lower- and inter-quartile spreads. Ellis *et al.* and Herschel-Bulkley models also perform well while Reiner-Philippoff and Robertson-Stiff models, although having smaller maximum RMS values, display greater lower- and inter-quartile RMS spreads. Although Casson and Collins-Graves exhibit the poorest performance of those presented in the right-hand box-and-whisker sub-plot, they substantially out-perform the four models presented on the left-hand sub-plot of this figure.

These findings indicate that not only are Bingham Plastic and Power Law models significantly out-performed by alternative rheological models, but non-conventional input data combinations provide marked improvements in fluid characterisation over standard Fann viscometer input combination conventions.

2.3.5 Solution Robustness

The selection of different viscometer readings was found to result in non-convergence during solution of some of the models evaluated indicating a limited robustness in the direct solution approach. Table 2.2 presents the average number (and percentage) of data sets successfully solved for all reading combinations considered. Also shown is the percentage of tested combinations achieving a solution to all 414 Fann viscometer data sets. Both entries provide indicators to possible model sensitivity to the choice of viscometer reading combinations employed.

While all 2-parameter models achieved 100% solution success, higher-order models showed less consistent stability. Only Herschel-Bulkley demonstrated 100% solution success for all 414 data sets. All other 3-parameter models exhibited some degree of numerical divergence during the solution of their implicit functions[6], although with varying degrees of severity. The Collins-Graves model showed limited robustness with an average of 372 solutions for all input combinations with only 10.7% of the combinations tested yielding solutions to all 414 data sets. The Ellis *et al.* model is seen to be almost insensitive to the combination of Fann viscometer readings used to determine model parameters. This is indicated by this model having an average number of 413 solutions with 75% of all possible combinations yielding solutions to all 414 data sets. Convergence failure was most acute for the Cross model which failed to converge on at least 96% of the data sets for any combination of input data. The severity of these divergencies disqualifies this model for presentation alongside the others and from future analysis. The next-least robust model (Reiner-Philippoff) managed a minimum convergence success of 16.7% and an average convergence success of 41.8%, substantially higher than for Cross. The reasons for Cross's lack of robustness can only be attributed to the characteristics of the cumbersome direct parameter solution expressions [see Appendix B, section B.5 on page 124, Eqs.(B.2 to B.4)].

[6]The van Wijngaarden-Dekker-Brent bisection algorithm '`zbrent()`' was used throughout the analysis (available in *Numerical Recipes* by Press, Flannery, Teukolsky & Vetterling, 1988,).

Model	Number of Parameters	Sol'n Convergence Number	[%]	Sol'n [%]
Bingham Plastic	2	414	100	100
Casson	2	414	100	100
Collins-Graves	3	372	89.8	10.7
Ellis *et al.*	3	413	99.8	75.0
Herschel-Bulkley	3	414	100	100
Hyperbolic	4	405	97.9	25.7
Power Law	2	414	100	100
Prandtl-Eyring	2	386	93.2	39.3
Reiner-Philippoff	3	173	41.8	0
Robertson-Stiff	3	410	99.0	57.1
Sisko	3	412	99.4	69.6

Table 2.2: Direct parameter solution analysis solution robustness: The average number of convergences of each model for all reading combinations tested over the full 414 readings data set. The far right-hand column presents the percentage of combinations achieving solution to all 414 data sets.

2.4 Nonlinear Parameter Estimation

The method of nonlinear least squares was applied to parameter solution of the aforementioned rheological models and to a further eight revised and/or novel models constructed for this analysis.

2.4.1 Models Evaluated

The rheological model assumes that the expected shear stress, τ, for a given shear rate, $\dot{\gamma}$, is determined by a function of the shear rate and p parameters $\phi = (\phi_1, \phi_2, \ldots, \phi_p)$. An observed reading is subject to an additive random error term, ϵ, which accounts for measurement precision and instrument error; the relationship can be written as:

$$\tau = f(\dot{\gamma}, \phi) + \epsilon.$$

The errors between observations are assumed to be independent and identically normally distributed with zero mean and constant variance, σ^2.

The identification of a suitable choice for the deterministic function, $f(\dot{\gamma}, \phi)$, should be the principle aim of the fluid characterisation stage in the drilling hydraulic calculation procedure. Tables 2.7 & 2.8 (presented at the end of this chapter) summarise the 20 candidate functions considered in this comparison. Twelve of these models have already been introduced in section 2.3.2. In the spirit of the inclusion of a yield stress term that distinguishes the Power Law and Herschel-Bulkley models, five models are proposed that are simple adaptations of those published involving either the inclusion, or removal, of an additive parameter representing a yield stress component: namely, Collins-Graves*, Hyperbolic*, Prandtl-Eyring*, Robertson-Stiff* and Sisko*. Two hybrid models are proposed that reflect the commonly held belief that the Power Law and Bingham Plastic models are suitable for conditions of lower and higher shear rates respectively. The first hybrid, Power Law/linear, correspondingly joins the two models together at a shear rate that is itself a parameter to be determined and is restricted to characterising fluids within the range of the equivalent shear rate settings used in the viscometer measurements.

The two segments of the model are designed to form a continuous smooth function; these two constraints lead to a 3-parameter model (refer to Appendix B, section B.13 on page 129). The second hybrid, Herschel-Bulkley/linear, is similar to Power Law/linear in that it too comprises of two expressions whose use is conditioned about a shear rate that is itself a parameter requiring evaluation. This model differs from Power Law/linear in that the yield-Power Law relationship (Herschel-Bulkley) replaces the purely Power Law component thereby resulting in a 4-parameter model (refer to Appendix B, section B.8 on page 126). Finally, a new single function, 3-parameter model is proposed, Inverse ln-cosh, which was formulated from observations of flow curve profiles of the data set, (see in Appendix B, section B.11 on page 128).

2.4.2 Parameter Estimation Procedure

The generalised method of model parameter estimation using as many data points as parameters has been shown (1) to provide fluid characterisations of widely differing quality, (2) questionable solution robustness and (3) rarely being capable of providing consistently satisfactory estimates with non-negligible RMS spreads and magnitudes. The reason for this is that the direct approach does not take into account the random error in an observation and the fit is strongly influenced by the choice (often arbitrary) of data points selected for parameter estimation. Far more satisfactory estimates can be obtained by employing more data points than parameters and estimating them through least squares. Consider n observations $(\tau_i, \dot{\gamma}_i), i = 1, 2, \ldots, n$, then the least squares estimator is the value of ϕ which minimises the residual sum of squares,

$$\mathrm{RSS}(\phi) = \sum_{i=1}^{n} \left[\tau_i - f(\dot{\gamma}_i; \phi)\right]^2 .$$

For nonlinear models this will require iterative numerical methods such as Gauss-Newton, steepest descent, Marquardt's compromise or various derivative-free methods (Seber & Wild, 1989). The choice of methodology is dependent on the form of the model, taking into account the ease of partial derivative calculation and any parameter constraints. Regardless of the method employed, convergence to least squares estimation is aided by providing good initial parameter values.

Tables 2.7 & 2.8 presents the parameter constraints for the various models; these are derived from the requirement that shear stresses are positive and increase with shear rate. The majority of the models have just simple bounds, the exceptions being Hyperbolic and its adaptation, Hyperbolic*, that have linear constraints between two of their parameters. For the models with just simple bounds the NAG library (1988) routine `E04LAF` was employed using first partial derivative information (provided for all applicable models in Appendix B) and the respective initial parameter values given in Tables 2.7 & 2.8. This routine is a proprietary algorithm for finding the minimum of a function subject to fixed upper and lower bounds. Note that the constraints on Bingham Plastic necessitate the use of such an algorithm as opposed to the explicit least squares solution that is otherwise available for a simple linear model. The algorithm was found to be generally insensitive to initial values, the exceptions being the models of Ellis *et al.* and Reiner-Philippoff which required a grid of initial values in order to find the global least squares minimum. For Hyperbolic and Hyperbolic* the NAG library routine `E04UCF` was employed as it was necessary to utilise an algorithm designed to solve the minimisation of a smooth nonlinear function subject to a set of constraints on the variable (Gill, Hammarling, Murray, Saunders & Wright, 1986). The routine was executed using first partial derivative information and the given initial values, and was not found to be sensitive to initial values. Obviously the precision of the estimates will improve with a corresponding increase in the number of data points used, thereby supporting the desirability of, and preference for, more rig-site readings than are currently recorded.[7]

2.4.3 Results

Tables 2.9 & 2.10 (pages 36 & 37) present the parameter estimates and RMS values obtained for the various models applied to the four specific data sets presented in Table A.6 on page 120. It can be seen that several models perform well on all four data sets: in particular Herschel-Bulkley/linear, Hyperbolic, Power Law/linear and Sisko whose fitted models are presented in Figs. 2.4 to 2.7 respectively (from page 29 onwards). The fits demonstrate that these models are flexible enough to accommodate the variety of profile shapes exhibited by these specific drilling fluids. The effect of the adaptations to the published models can be considered by examining the corresponding RMS values. For Collins-Graves* and Prandtl-Eyring* the adaptations result in lower RMS values for all four data sets, however Robertson-Stiff* only had lower values for two data sets, Hyperbolic* only one and Sisko* did not signify any improvement.

In Fig. 2.8 (page 31) a visual representation of the relative RMS rankings of the models using the four data sets is presented; it can be seen that there is no clear choice for an overall 'best' model. In order to aid selection of an appropriate preferred rheological model, the empirical distribution of RMS results for the full 414 data sets are examined; in Table 2.3 the resulting RMS summary statistics for the various models are presented. The corresponding RMS box-and-whisker plots for poor- and good-fitting models are presented in Figs. 2.9 & 2.10 respectively (pages 31 & 32); note that in order to facilitate comparisons the models are grouped according to spread and that not all outliers are displayed. It can be seen that the two industry preferences, together with Prandtl-Eyring, perform poorly. Five models are considered to be superior and have similar location and spread: Herschel-Bulkley/linear, Hyperbolic, Hyperbolic*, Sisko and Sisko*. Table 2.3 reveals that the maximum RMS values for these models are of the same order as the lower-quartile of the two industry-favoured models. It is, therefore, clear that the aforementioned models are considerably more appropriate for the characterisation of the pseudoplastic behaviour of the large data set than the conventional choice of rheological models.

[7] It should be noted that when a non-Newtonian fluid is sheared in any coaxial cylindrical rotational viscometer, the prevailing shear rate can not generally be calculated exactly (Yang & Krieger, 1978). Various solutions to the integral equation of the concentric cylinder, put forth independently by Krieger & Elrod (1953) and Pawlowski (1953), have been presented (such as the series solutions presented by Krieger, 1969 and Code & Raal, 1973). While it is acknowledged that the shear rate correction provided by the integral equation, namely:

$$\Omega = \frac{1}{2}\int_{c\tau_b}^{\tau_b} \tau^{-1} f^{-1}(\tau;\phi)\mathrm{d}\tau,$$

is likely to provide more representative non-Newtonian shear rates, the ensuing analysis remains valid as all data is treated in a consistent manner for all models. Future nonlinear least squares may benefit from proper application of this correction factor expression so long as all necessary viscometer data is known. The exact diameter ratios for all the devices used in the recording of the rheological data were not available thereby preventing any confident application of this correction factor in this study.

Model	Lower extreme	Lower quartile	Median	Upper quartile	Upper extreme	Max. RMS	No. outs.
Bingham Plastic	0.2029	1.4263	2.0042	4.1329	7.8531	26.939	76
Casson	0.0063	0.3067	0.5351	1.5185	3.2397	7.5357	59
Collins-Graves	0.0327	0.5474	0.7463	1.2464	2.2879	4.2944	51
Collins-Graves*	0.0186	0.2902	0.5128	0.7545	1.4423	3.0800	10
Cross	0.0073	0.3561	1.1358	1.6629	3.5957	12.094	16
Ellis *et al.*	0.0207	0.7905	1.3773	1.9648	3.6337	5.5704	18
Herschel-Bulkley	0.0061	0.0699	0.1284	0.2277	0.4642	1.6344	16
Herschel-Bulkley/linear	0.0019	0.0440	0.0805	0.1455	0.2966	1.4100	24
Hyperbolic	0.0018	0.0312	0.0579	0.1115	0.2272	1.3833	27
Hyperbolic*	0.0072	0.0494	0.0917	0.1513	0.2932	1.5225	41
Inverse ln-cosh	0.0080	0.0698	0.1329	0.2145	0.4215	1.4240	24
Power Law	0.0115	1.1470	5.2797	6.6760	14.030	20.448	3
Power Law/linear	0.0026	0.1879	0.3721	0.5169	0.9958	2.0321	16
Prandtl-Eyring	0.3904	9.2380	15.228	18.477	30.924	57.444	3
Prandtl-Eyring*	0.0135	0.5171	0.7277	1.1711	2.1010	4.3876	57
Reiner-Philippoff	0.0118	0.4541	0.6381	0.8944	1.5320	12.708	37
Robertson-Stiff	0.0046	0.1037	0.2156	0.3417	0.6904	1.9646	11
Robertson-Stiff*	0.0050	0.0805	0.1588	0.2756	0.5612	2.0430	18
Sisko	0.0077	0.0384	0.0693	0.1178	0.2287	1.1938	35
Sisko*	0.0047	0.0263	0.0487	0.0988	0.2074	1.2691	26

Table 2.3: RMS summary statistics for all rheological models considered.

2.5 Estimation Behaviour Comparison

While it is possible to recommend confidently the five short-listed models (section 2.4.3 on the page before) as being capable of providing a reasonably high degree of accuracy for pseudoplastic fluid characterisation purposes, it would be preferable for time-constrained rig-site applications, to establish a single 'default' model that will furnish consistently accurate pseudoplastic fluid characterisations over all shear rates. Further treatment and analysis is therefore required before a single preference from the short-listed models can be confidently recommended.

2.5.1 Statistical Measures Employed

As indicated by Seber & Wild (1989) the least squares estimates of a linear model with independent and identically distributed normal errors have the desirable properties of being unbiased, normally distributed and have minimum variance among linear unbiased estimates. However, least squares estimates of nonlinear models achieve these properties asymptotically. The extent to which the behaviour of the estimates approximates the asymptotic properties is model dependent; those models that display the properties even when the sample sizes are relatively small are termed 'close-to-linear' models (Ratkowsky, 1983; Ratkowsky, 1990). Since only eight data observations are used in model fitting, it is important that a close-to-linear model is chosen. It is this criterion which is used to judge the appropriateness of the five 'best' models identified in section 2.4, page 19. Here, the extent of the nonlinear behaviour of the estimates is examined using the Bates & Watts (1980) curvature measures and the Hougaard (1985) γ_1 statistic of skewness behaviour.

	Bentonite/ polymer	Sea water/ pac	KCl/pac	Oil Based Mud
Herschel-Bulkley/linear				
IN	1.6033	0.0209	0.0130	0.4632
PE	476.93	10.287	2.3186	5.4230
$\gamma_1(a)$	0.5239	3.7510	0.8998	0.4106
$\gamma_1(b)$	9.0209	0.2995	0.1949	0.5175
$\gamma_1(c)$	-1.5870	0.0324	0.0185	-0.2330
$\gamma_1(d)$	1.2221	3.7691	0.9418	0.5650
Hyperbolic				
IN	2.7064	0.1575	0.1422	0.1826
PE	15.868	17.740	15.133	2.0960
$\gamma_1(a)$	5.2721	1.9572	1.5148	0.5932
$\gamma_1(b)$	4.6653	1.4007	1.0921	0.5447
$\gamma_1(\dot{\gamma}_{cp})$	-5.5199	-1.9534	-1.5138	-0.6351
$\gamma_1(\tau_{cp})$	-5.3900	-0.4376	-0.2864	-0.6115
Hyperbolic*				
IN	0.0275	0.0275	0.0241	0.0102
PE	65.334	2.8819	3.2599	0.2642
$\gamma_1(a)$	7.3959	1.0198	0.7211	0.0402
$\gamma_1(b)$	4.7890	0.6641	0.5090	0.0056
$\gamma_1(\dot{\gamma}_{cp})$	-7.5323	-1.0240	-0.7215	-0.0659
Sisko				
IN	0.0242	0.0392	0.0237	0.0213
PE	0.3137	1.3409	0.8311	0.4170
$\gamma_1(a)$	-0.0783	-0.3183	-0.1673	-0.0897
$\gamma_1(b)$	0.0941	0.1830	0.0997	0.0791
$\gamma_1(c)$	0.0255	0.0812	0.0503	0.0412
Sisko*				
IN	0.7965	0.0631	0.0445	0.1012
PE	7899.7	31.815	25.465	72.003
$\gamma_1(\tau_o)$	-58.551	-0.4946	-0.4107	-1.3192
$\gamma_1(a)$	-3.4080	-0.8588	-0.5109	-0.8394
$\gamma_1(b)$	59.342	0.9981	0.7176	1.8307
$\gamma_1(c)$	-0.2993	0.0672	0.0383	0.0439
Sisko^R				
IN	0.0242	0.0392	0.0237	0.0213
PE	0.0252	0.0098	0.0067	0.0056
$\gamma_1(\tau_1)$	-0.0055	-0.0000	-0.0002	0.0011
$\gamma_1(\tau_2)$	0.0001	-0.0000	-0.0005	-0.0008
$\gamma_1(c)$	0.0255	0.0812	0.0503	0.0412

Table 2.4: Bates & Watts maximum curvature measures and Hougaard γ_1 statistics using the four specific drilling fluids data presented in Table A.6. Critical values at the 5% level for Bates & Watts measures are 0.2150 and 0.1978 for 3- and 4-parameter models respectively.

2.5.2 Bates & Watts Curvature Measures

The solution locus of a linear model is a plane that can be traversed at uniform 'speed' as the parameter set varies. However, neither of these phenomenon are true for nonlinear models. Bates & Watts propose two corresponding measures to examine the degree of their departures from linear behaviour: *intrinsic nonlinearity* (IN) and *parameter effects* (PE) respectively. Both measures are zero for a linear model and increase with departure away from their respective linear characteristic. The consequence of a significantly large intrinsic nonlinearity is that the fitted values and the error estimate are biased. It is, therefore, important that the IN value is below an acceptable limit. A large parameter effects nonlinearity invalidates the confidence interval and t-test formula given later in Chapter 3, section 3.4.1 (page 69) and could result in difficulty in obtaining the least squares solution. As a guide, Ratkowsky recommends that the

	Lower extreme	Lower quartile	Median	Upper quartile	Upper extreme	No. outs.	No. n.s.
Herschel-Bulkley/linear							
IN	0.0000	0.0346	0.4851	0.9313	2.1176	63	151
PE	1.0653	7.0488	12.372	40.376	87.227	88	0
Hyperbolic							
IN	0.0336	0.1957	0.3328	0.5226	0.9734	23	106
PE	0.9729	3.2319	5.2982	14.039	29.865	58	0
Hyperbolic*							
IN	0.0068	0.0156	0.0214	0.0305	0.0526	44	412
PE	0.2013	0.5668	0.8208	2.0000	4.1236	43	2
Sisko							
IN	0.0093	0.0232	0.0302	0.0396	0.0640	28	414
PE	0.1361	0.4295	0.6007	0.8599	1.4936	34	5
Sisko*							
IN	0.0171	0.0812	0.1592	0.2384	0.4741	22	265
PE	8.7238	48.766	131.14	331.61	728.61	59	0
Sisko^R							
IN	0.0093	0.0232	0.0302	0.0396	0.0640	28	414
PE	0.0000	0.0042	0.0066	0.0102	0.0193	42	414

Table 2.5: Summary Bates & Watts maximum curvature measures. Critical values at the 5% level are 0.2150 and 0.1978 for 3- and 4-parameter models respectively. (n.s.: non-significant values).

statistical significance of the IN and PE values be assessed by comparison with $1/\left(2\sqrt{F}\right)$, where $F = F_{[p,(n-p);\alpha]}$ is the F-distribution value corresponding to the significance level α, available in standard tables. The value of IN is fixed given a model and data set combination, whereas the value of PE can be altered via reparameterisation.

2.5.3 Hougaard γ_1 Statistic of Skewness

One way of measuring deviations from normality of a sample is through the coefficient of skewness (Wetherill, 1972). This measure is zero for normal distributions, positive for distributions with long tails to the right and negative for distributions with long tails to the left. The magnitude of the statistic increases with the degree of skewness. Hougaard presented a direct measure of skewness for nonlinear least squares estimates that can be used to assess nonlinearity. It can be interpreted in a similar manner to the coefficient of skewness. As a consequence Ratkowsky suggests the following *rule-of-thumb*: if $|\gamma_1| \leq 0.1$, the estimator is very close-to-linear; if $0.1 < |\gamma_1| < 0.25$, it is reasonably close-to-linear; for $|\gamma_1| \geq 0.25$, skewness is very apparent and $|\gamma_1| \geq 1$ indicates considerable nonlinear behaviour. If there is a high PE value, then the various γ_1 values can assist a modeller with reparameterisation; consequently only those parameters whose estimators demonstrate skewness need consideration. Both Bates & Watts maximum curvature measures and Hougaard γ_1 statistics were evaluated from FORTRAN algorithms presented by Ratkowsky (1990).

	Lower extreme	Lower quartile	Median	Upper quartile	Upper extreme	No. outs.	Freq. in category			
							VL	RL	SA	CN
Hyperbolic*										
$\gamma_1(a)$	-0.3388	0.0723	0.1212	0.5493	1.2634	37	159	118	137	54
$\gamma_1(b)$	-0.4749	0.0018	0.0316	0.3680	0.8857	34	265	21	128	31
$\gamma_1(\dot{\gamma}_{cp})$	-1.2012	-0.5716	-0.1968	-0.1344	-0.0456	41	37	224	153	54
Sisko										
$\gamma_1(a)$	*-0.3098*	*-0.1831*	*-0.1348*	*-0.0979*	*-0.0338*	*42*	*110*	*240*	*64*	*8*
$\gamma_1(b)$	0.0348	0.0879	0.1160	0.1519	0.2476	36	147	231	36	3
$\gamma_1(c)$	0.0114	0.0420	0.0547	0.0719	0.1158	35	373	34	7	0
Sisko^{R}										
$\gamma_1(\tau_1)$	-0.0041	-0.0003	0.0001	0.0022	0.0060	78	414	0	0	0
$\gamma_1(\tau_2)$	-0.0005	-0.0002	0.0000	0.0001	0.0002	54	414	0	0	0
$\gamma_1(c)$	0.0114	0.0420	0.0547	0.0719	0.1158	35	373	34	7	0

Table 2.6: Summary Hougaard γ_1 statistics for the three selected rheological models. Abbreviations for the four Ratkowsky *rule-of-thumb* categories are: VL: very close-to-linear; RL: reasonably close-to-linear; SA: skewness apparent; CN: considerable nonlinear behaviour.

2.5.4 Results

The Bates & Watts maximum curvature and Hougaard γ_1 statistics for the short-listed five 'best' models using the data of the four specific drilling fluids is given in Table 2.4. The critical values associated with the curvature measures for assessing whether the nonlinearity is significant at the 5% level are 0.2150 and 0.1978 for the 3- and 4-parameter models respectively. Only the Hyperbolic* and Sisko models have IN values below their respective critical values for all four data sets, however, neither model has any non-significant PE values. For the OBM data set the Hougaard γ_1 statistics for the Hyperbolic* model are satisfactory. For the other data sets they indicate nonlinear behaviour for all three parameters and thus suggests a total reparameterisation in order to obtain non-significant PE values. Despite having significant PE values for all four data sets, the Sisko model has satisfactory Hougaard γ_1 statistics for all but parameter a on the sea water/pac data set; thus there is no clear suggestion of which parameters require reparameterisation. The Hyperbolic and Sisko* models have non-significant IN values on three data sets while Herschel-Bulkley/linear has only two. All of the PE values for these models are significant.

Table 2.5 summarises the Bates & Watts maximum curvature measures for the full data set with the corresponding box-and-whisker plots displayed in Fig. 2.11. It can be seen that only the Hyperbolic* and Sisko models consistently have low IN values; the Sisko model has no significant values on all 414 data sets while Hyperbolic* only has two. Since the other models did not perform so reliably they shall not be considered further. The PE values for the Hyperbolic* and Sisko models are disappointing with only two and five non-significant values respectively; both, models could, therefore, benefit from a reparameterisation. The summary Hougaard γ_1 statistics and corresponding box-and-whisker plots for the two models are displayed in Table 2.6 and Fig. 2.12 (page 33) respectively. The Hyperbolic* values do not reveal a pattern that would indicate a general reparameterisation. The Sisko values, however, reveal that parameter c is generally well behaved and thus only the other two parameters need further consideration. For this reason, and because the RMS empirical distribution is slightly better than Hyperbolic*, only Sisko shall be considered for further treatment.

2.5.5 Reparameterisation

Reparameterisation in this case involves expressing the new parameter as a function only of the old parameters without reference to $\tau, \dot{\gamma}$ or the error term. The least squares estimators of the new parameters can be obtained from the functional relationship and the least squares estimators of the old parameters. The fitted values of the two parameterisations will be identical as will the IN value, however the PE value alters. It is desirable to find a suitable reparameterisation of a good-fitting model that has a non-significant IN value but a significant PE value. The Hougaard γ_1 statistics are useful for indicating which parameters may benefit from a reparameterisation. Ross (1975) proposed *expected value* parameters which correspond to the fitted values of the response variable. This class of parameter exhibits close-to-linear behaviour.

The Hougaard γ_1 statistic for the Sisko model suggests that the two parameters a and b could benefit from a reparameterisation. In order to replace them with expected value parameters we need to choose two values of the explanatory variable $\dot{\gamma}$ that fall within the observed data range, say $\dot{\gamma}_1$ and $\dot{\gamma}_2$. The expected values for these two constants are given by

$$\tau_1 = a\dot{\gamma}_1 + b\dot{\gamma}_1^c$$

and

$$\tau_2 = a\dot{\gamma}_2 + b\dot{\gamma}_2^c$$

respectively. Solving these two equations for a and b, one obtains

$$a = \frac{\tau_2\dot{\gamma}_1^c - \tau_1\dot{\gamma}_2^c}{\dot{\gamma}_1^c\dot{\gamma}_2 - \dot{\gamma}_2^c\dot{\gamma}_1} \tag{2.2}$$

and

$$b = \frac{\tau_1\dot{\gamma}_2 - \tau_2\dot{\gamma}_1}{\dot{\gamma}_1^c\dot{\gamma}_2 - \dot{\gamma}_2^c\dot{\gamma}_1}. \tag{2.3}$$

Substituting Eqs.(2.2 & 2.3) into the Sisko equation one constructs the required reparameterisation (Sisko^{R}):

$$\tau = \frac{(\tau_2\dot{\gamma}_1^c - \tau_1\dot{\gamma}_2^c)\,\dot{\gamma} + (\tau_1\dot{\gamma}_2 - \tau_2\dot{\gamma}_1)\,\dot{\gamma}^c}{\dot{\gamma}_1^c\dot{\gamma}_2 - \dot{\gamma}_2^c\dot{\gamma}_1}$$

which has eliminated the original parameters a and b in favour of the two new parameters τ_1 and τ_2. The choice of the two constants $\dot{\gamma}_1$ and $\dot{\gamma}_2$ will affect the resulting PE value, it is desirable to choose them so that its value is as low as possible with criteria for finding an optimal set of values presented by Clarke (1987). In this analysis a grid of values with regular spacing of 12.5 s^{-1} such that $12.5 \le \dot{\gamma}_1 < \dot{\gamma}_2 \le 1012.5$ s^{-1} is taken with the combination that provides the minimum PE value being chosen.

The new Bates & Watts curvature measures and Hougaard γ_1 statistics for Sisko^{R} for the four specific fluids are presented in Table 2.4, page 23. It can be seen that the reparameterisation has led to non-significant PE values for all four drilling fluid types. The chosen reparameterisation constants are $(\dot{\gamma}_1, \dot{\gamma}_2) = (112.5, 812.5)$, $(162.5, 962.5)$, $(162.5, 1012.5)$ and $(212.5, 1012.5)$ for the bentonite/polymer, sea water/pac, KCl/pac and oil-based muds respectively. The summary Bates & Watts curvature measures and Hougaard γ_1 statistics for the complete 414 data sets for Sisko^R are given in Tables 2.5 and 2.6 respectively, and the corresponding box-and-whisker plots are presented in Figs. 2.11 & 2.12 (pages 32 & 33). It can be seen that the PE values are now non-significant in all of the data sets and that the Hougaard γ_1 statistics verify that all three parameters have very close-to-linear behaviour. Figure 2.13, page 33, presents a grey-scale 2-dimensional histogram of the chosen reparameterisation constants; combinations chosen have values that are towards the two extreme shear rate settings of the Fann viscometer. The most frequently chosen combination was (212.5, 887.5) which could be used in future as an initial value for a more sophisticated search in order to find a combination with a lower PE value.

2.6 Chapter Summary

The examination of conventional oilfield procedures for non-Newtonian fluid characterisation has been found wanting. The continued application of Bingham Plastic and Power Law models to expedite analytic solutions cannot be justified due to the availability of suitable rig-site computation tools. Most of the different rheological models considered in this analysis, along with alternative parameter solution procedures, consistently outperformed the accuracy of conventional calculation methods and models. The comparison of different models against a large data set exhibiting diverse pseudoplastic profiles showed that substantial gains in modelling accuracy are possible. Nonlinear least squares analysis provided a short-list of five alternative rheological models that yielded consistently high degrees of modelling accuracy. Further treatments based on Bates & Watts and Hougaard γ_1 statistics established that the reparameterised Sisko model may be considered as the most reliable and accurate of all the 20 rheological models considered.

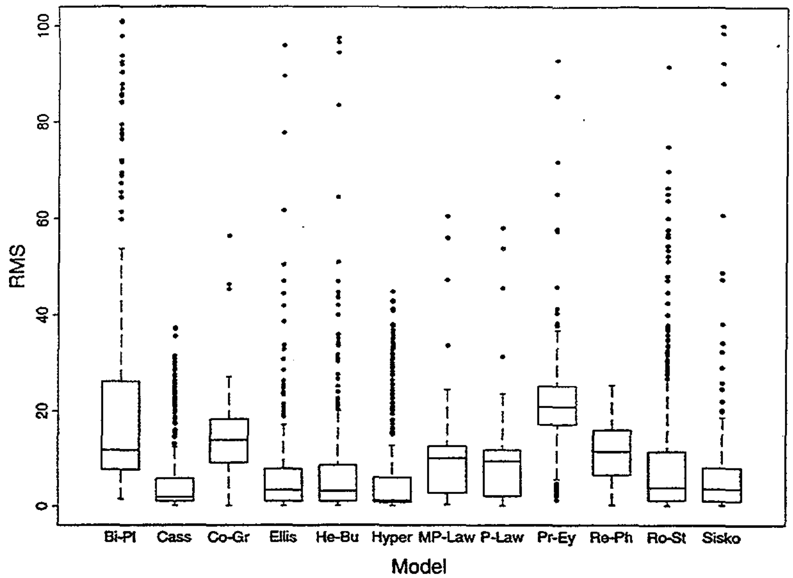

Figure 2.2: RMS box-and-whisker plots for 12 rheological models with parameters calculated using the direct parameter solution approach employing $\theta_{600}/\theta_{300}$ (for 2-parameter models) plus θ_{200} for 3-parameter models and θ_{100} for the Hyperbolic model.

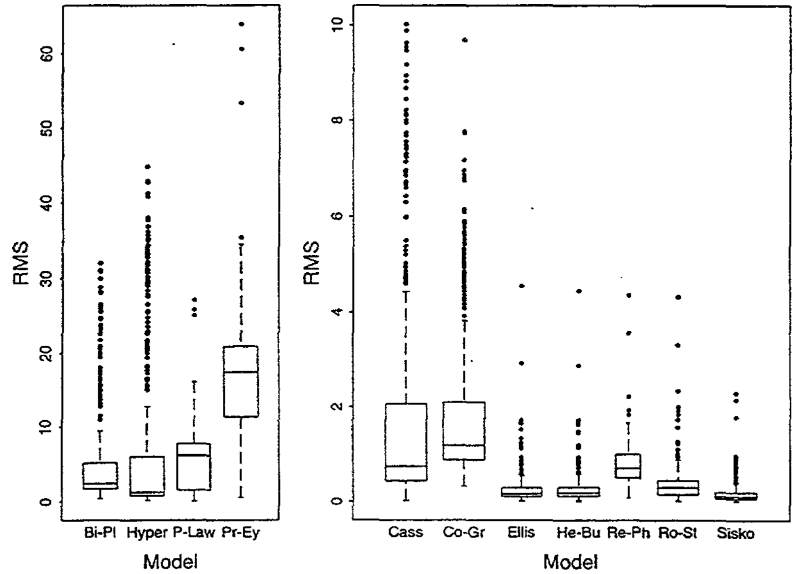

Figure 2.3: Best RMS values for 11 rheological models with parameters calculated from different non-conventional combinations of Fann viscometer readings (Table 2.1) using the direct parameter solution approach.

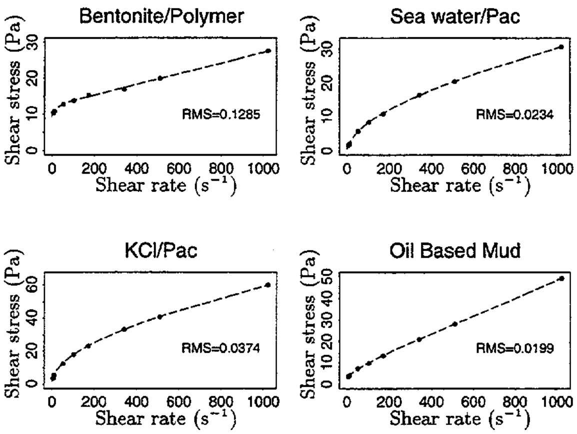

Figure 2.4: Herschel-Bulkley/linear: Fitted models for the four specific drilling fluids data.

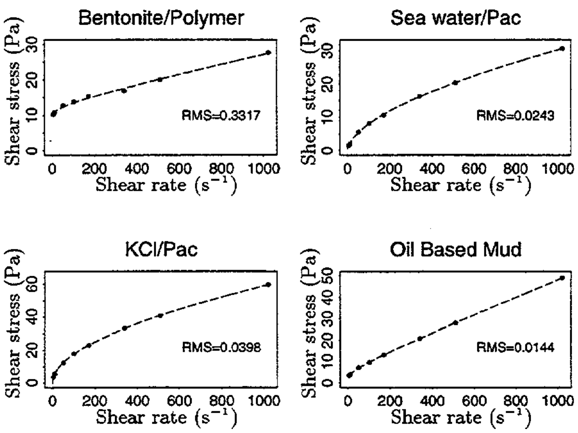

Figure 2.5: Hyperbolic: Fitted models for the four specific drilling fluids data.

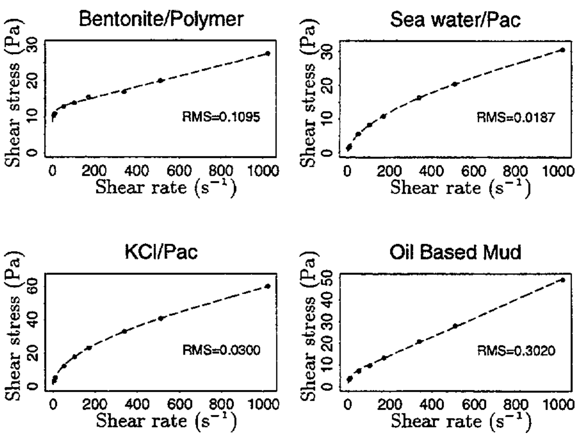

Figure 2.6: Power Law/linear: Fitted models for the four specific drilling fluids data.

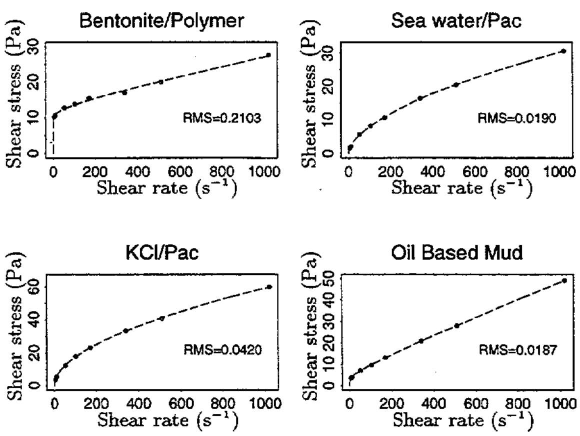

Figure 2.7: Sisko: Fitted models for the four specific drilling fluids data.

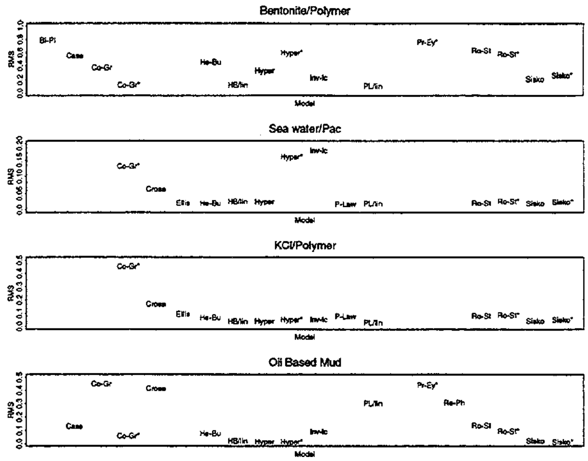

Figure 2.8: Relative RMS rankings of models using the four specific drilling fluids data.

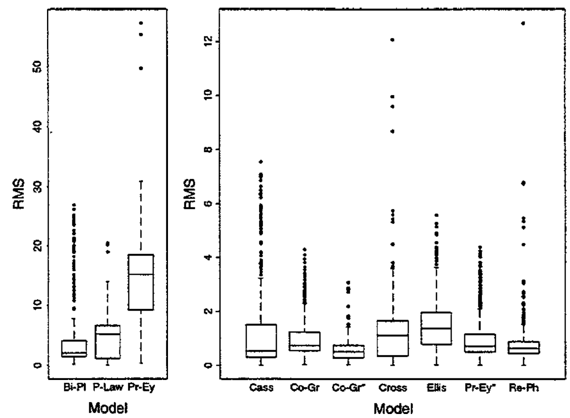

Figure 2.9: RMS box-and-whisker plots of poor-fitting models.

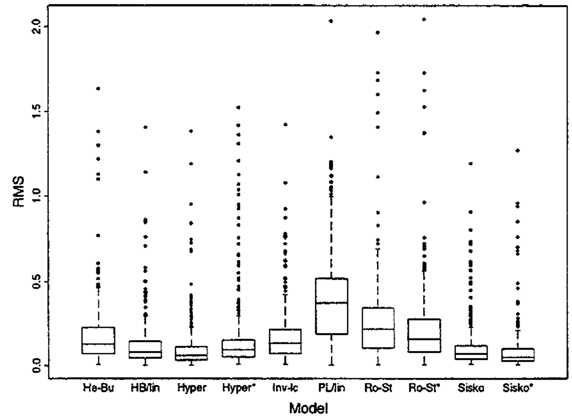

Figure 2.10: RMS box-and -whisker plots of good-fitting models.

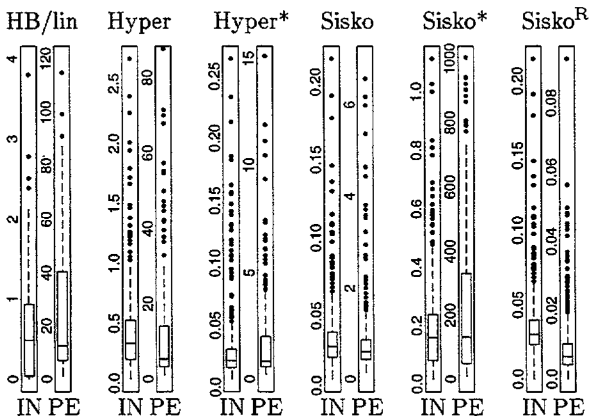

Figure 2.11: Bates and Watts curvature measures. Critical values at the 5% level are 0.2150 and 0.1978 for 3- and 4-parameter models respectively.

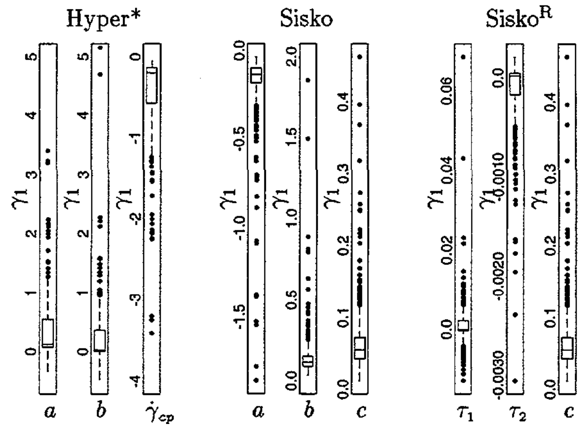

Figure 2.12: Hougaard γ_1 statistics for Hyperbolic*, Sisko and Sisko^R models.

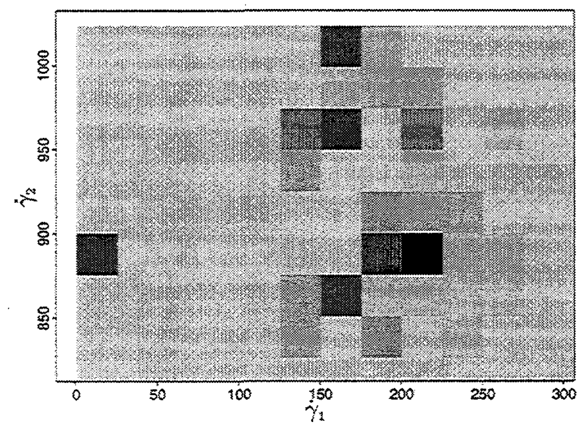

Figure 2.13: Grey-scale 2-dimensional histogram of the chosen values of the Sisko^R model's constants $\dot\gamma_1$ and $\dot\gamma_2$ taken from all 414 data sets; the number of counts increases with darkness.

Model	Equation	Constraints/initial values
Bingham Plastic (Bi-Pl)	$\tau = \tau_\circ + \mu_\infty \dot{\gamma}$	$\tau_\circ \geq 0$, $\mu_\infty > 0$ $\tau_\circ = 0$, $\mu_\infty = 0.05$
Casson (Cass)	$\tau = \left(\sqrt{\tau_\circ} + \sqrt{\mu_\infty \dot{\gamma}}\right)^2$	$\tau_\circ \geq 0$, $\mu_\infty > 0$ $\tau_\circ = 0$, $\mu_\infty = 0.05$
Collins-Graves (Co-Gr)	$\tau = (\tau_\circ + k\dot{\gamma})\left(1 - e^{-\beta\dot{\gamma}}\right)$	$\beta > 0$, $k > 0$, $\tau_\circ \geq 0$ $\beta = 1$, $k = 0.05$, $\tau_\circ = 0$
Collins-Graves* (Co-Gr*)	$\tau = \alpha + (\tau_\circ + k\dot{\gamma})\left(1 - e^{-\beta\dot{\gamma}}\right)$	$\alpha \geq 0$, $\beta > 0$, $k > 0$, $\tau_\circ \geq 0$ $\alpha = 0$, $\beta = 1$, $k = 0.05$, $\tau_\circ = 0$
Cross	$\tau = \dot{\gamma}\left(\mu_\infty + \frac{\mu_0 - \mu_\infty}{1 + \alpha\dot{\gamma}^{2/3}}\right)$	$\alpha \geq 0$, $\mu_\circ \geq 0$, $\mu_\infty \geq 0$ $\alpha = 1$, $\mu_\circ = 0.1$, $\mu_\infty = 0.05$
Ellis *et al.* (Ellis)	$\dot{\gamma} = (\phi_0 + \phi_1 \tau^{\alpha - 1})\tau$	$\alpha \geq 0$, $\phi_0 \geq 0$, $\phi_1 \geq 0$ Grid
Herschel-Bulkley (He-Bu)	$\tau = \tau_\circ + k\dot{\gamma}^m$	$\tau_\circ \geq 0$, $k > 0$, $0 < m < 1$ $k = 1$, $m = 0.5$, $\tau_\circ = 0$
Herschel-Bulkley/ linear (HB/lin)	$\tau = a + bd^c(c-1) + b\dot{\gamma}^c \quad \dot{\gamma} \leq d$ $a + bcd^{c-1}\dot{\gamma} \quad \dot{\gamma} > d$	$a \geq 0$, $b \geq 0$, $0 < c < 1$, $\dot{\gamma}_{\min} \leq d \leq \dot{\gamma}_{\max}$ $a = 0$, $b = 1$, $c = 0.5$, $d = 10$
Hyperbolic (Hyper)	$\tau = \tau_{cp} + b\sqrt{\left(\frac{\dot{\gamma} - \dot{\gamma}_{cp}}{a}\right)^2 - 1}$	$0 < a \leq -\dot{\gamma}_{cp}$, $b > 0$, $\dot{\gamma}_{cp} < 0$ $a = 500$, $b = 10$, $\dot{\gamma}_{cp} = -500$, $\tau_{cp} = 0$
Hyperbolic* (Hyper*)	$\tau = b\sqrt{\left(\frac{\dot{\gamma} - \dot{\gamma}_{cp}}{a}\right)^2 - 1}$	$0 < a \leq -\dot{\gamma}_{cp}$, $b > 0$, $\dot{\gamma}_{cp} < 0$ $a = 500$, $b = 10$, $\dot{\gamma}_{cp} = -500$

Table 2.7: Rheological models summary: abbreviations, equations, parameter constraints and initial values employed in least squares fitting. Models marked with an asterisk are adaptations of existing models. 'Grid' indicates that the model required a grid of initial values in order to find the global least squares minimum. $\dot{\gamma}_{\min}$ and $\dot{\gamma}_{\max}$ respectively denote the minimum and maximum shear rates of the observed data.

Model	**Equation**	**Constraints/initial values**
Inverse ln-cosh (Inv-lc)	$\tau = \tau_\circ + A\cosh^{-1}\left[\exp(\dot\gamma/B)\right]$	$\tau_\circ \geq 0,\ A > 0,\ B > 0$ $\tau_\circ = 0,\ A = 10,\ B = 200$
Power Law (P-Law)	$\tau = k\dot\gamma^n$	$k > 0,\ 0 < n < 1$ $k = 1,\ n = 0.5$
Power Law/ linear (PL/lin)	$\tau = k\dot\gamma^n \quad \dot\gamma \leq c$ $kc^n(1-n) + knc^{n-1}\dot\gamma \quad \dot\gamma > c$	$k > 0,\ 0 < n < 1,\ \dot\gamma_{\min} \leq c \leq \dot\gamma_{\max}$ $k = 1,\ n = 0.5,\ c = 10$
Prandtl-Eyring (Pr-Ey)	$\tau = A\sinh^{-1}(\dot\gamma/B)$	$A > 0,\ B > 0$ $A = 10,\ B = 100$
Prandtl-Eyring* (Pr-Ey*)	$\tau = \tau_\circ + A\sinh^{-1}(\dot\gamma/B)$	$\tau_\circ \geq 0,\ A > 0,\ B > 0$ $\tau_\circ = 0,\ A = 10,\ B = 100$
Reiner-Philippoff (Re-Ph)	$\dot\gamma = \tau\left(\mu_\infty + \frac{\mu_\circ - \mu_\infty}{1+(\tau/\tau_s)^2}\right)^{-1}$	$\mu_\circ \geq 0,\ \mu_\infty \geq 0,\ \tau_s > 0$ Grid
Robertson-Stiff (Ro-St)	$\tau = A(\dot\gamma_\circ + \dot\gamma)^B$	$0 < B < 1,\ A > 0,\ \dot\gamma_\circ \geq 0$ $B = 0.5,\ A = 1,\ \dot\gamma_\circ = 0$
Robertson-Stiff* (Ro-St*)	$\tau = \tau_\circ + A(\dot\gamma_\circ + \dot\gamma)^B$	$0 < B < 1,\ A > 0,\ \dot\gamma_\circ \geq 0,\ \tau_\circ \geq 0$ $B = 0.5,\ A = 1,\ \dot\gamma_\circ = 0,\ \tau_\circ = 0$
Sisko	$\tau = a\dot\gamma + b\dot\gamma^c$	$a \geq 0,\ b \geq 0,\ 0 < c < 1$ $a = 0,\ b = 1,\ c = 0.5$
Sisko*	$\tau = \tau_\circ + a\dot\gamma + b\dot\gamma^c$	$a \geq 0,\ b \geq 0,\ 0 < c < 1,\ \tau_\circ \geq 0$ $a = 0,\ b = 1,\ c = 0.5,\ \tau_\circ = 0$

Table 2.8: Rheological models summary: abbreviations, equations, parameter constraints and initial values employed in least squares fitting. Models marked with an asterisk are adaptations of existing models. 'Grid' indicates that the model required a grid of initial values in order to find the global least squares minimum. $\dot\gamma_{\min}$ and $\dot\gamma_{\max}$ respectively denote the minimum and maximum shear rates of the observed data.

	Bentonite/ polymer	Sea water/ pac	KCl/pac	Oil Based Mud
Bingham Plastic				
$\tau_\circ$	1.1434×10	4.1855	9.7624	4.7446
μ_∞	1.6170×10^{-2}	2.8059×10^{-2}	5.3396×10^{-2}	4.4284×10^{-2}
RMS	0.7839	5.5702	25.1719	1.1786
Casson				
$\tau_\circ$	9.1227	2.1539	5.3916	1.8849
μ_∞	4.5203×10^{-3}	1.7040×10^{-2}	3.0313×10^{-2}	3.0765×10^{-2}
RMS	0.5489	1.5541	7.0495	0.1317
Collins-Graves				
$\tau_\circ$	1.1985×10	9.0171	1.8894×10	5.6163
k	1.5349×10^{-2}	2.1376×10^{-2}	4.0572×10^{-2}	4.2986×10^{-2}
β	3.3200×10^{-1}	1.3930×10^{-2}	1.6689×10^{-2}	1.4211×10^{-1}
RMS	0.3747	0.5452	3.1566	0.4505
Collins-Graves*				
α	9.6378	1.2756	3.3194	3.3786
$\tau_\circ$	2.7114	8.7520	1.7942×10	3.4636
k	1.4821×10^{-2}	2.0242×10^{-2}	3.7821×10^{-2}	4.1359×10^{-2}
β	4.6565×10^{-2}	9.7831×10^{-3}	1.0618×10^{-2}	1.8673×10^{-2}
RMS	0.1268	0.1305	0.4523	0.0593
Cross				
α	4.9435×10^{4}	1.8079×10^{-1}	3.1059×10^{-1}	2.2276×10^{4}
$\mu_\circ$	1.3601×10^{5}	3.5507×10^{-1}	1.2312	3.0954×10^{4}
μ_∞	0.0000	1.2387×10^{-2}	2.1479×10^{-2}	3.3988×10^{-2}
RMS	13.9996	0.0627	0.1663	0.4157
Ellis, Lanham & Pankhurst				
α	4.7837	1.7359	1.8933	1.4190
ϕ_0	1.4904×10^{-7}	0.0000	0.0000	0.0000
ϕ_1	2.4207×10^{-4}	2.6903	4.4600×10^{-1}	4.2073
RMS	5.6800	0.0205	0.0932	3.4172
Herschel-Bulkley				
$\tau_\circ$	1.0467×10	6.1634×10^{-2}	4.3414×10^{-1}	3.3481
k	8.2674×10^{-2}	5.5350×10^{-1}	1.4271	1.1656×10^{-1}
m	7.6695×10^{-1}	5.7893×10^{-1}	5.3759×10^{-1}	8.6135×10^{-1}
RMS	0.4568	0.0199	0.0689	0.0766
Herschel-Bulkley/linear				
a	1.2362×10	1.1338×10	2.2872×10	7.0135
b	1.9305	5.7710×10^{-1}	1.6106	1.6392×10^{-1}
c	2.6713×10^{-1}	5.7231×10^{-1}	5.1867×10^{-1}	8.0546×10^{-1}
d	1.2709×10^{2}	8.0250×10^{2}	6.8226×10^{2}	4.0040×10^{2}
RMS	0.1285	0.0234	0.0374	0.0199
Hyperbolic				
a	3.1920×10^{2}	3.0341×10^{3}	4.0865×10^{3}	2.1543×10^{2}
b	4.3122	3.6230×10	8.0045×10	8.6107
$\dot\gamma_{cp}$	-3.1920×10^{2}	-3.0398×10^{3}	-4.0865×10^{3}	-2.3117×10^{2}
τ_{cp}	9.7947	-1.5739	-2.6898×10^{-1}	-2.7416×10^{-1}
RMS	0.3317	0.0243	0.0398	0.0144
Hyperbolic*				
a	2.9015×10^{3}	1.2221×10^{3}	3.4301×10^{3}	2.0622×10^{2}
b	2.6739×10	2.0024×10	7.2297×10	8.2651
$\dot\gamma_{cp}$	-3.1325×10^{3}	-1.2221×10^{3}	-3.4301×10^{3}	-2.1973×10^{2}
RMS	0.5965	0.1601	0.0533	0.0118

Table 2.9: Least squares parameter estimates and RMS values for various models using the four specific drilling fluids data.

	Bentonite/ Polymer	Sea water/ Pac	KCl/Pac	Oil Based Mud
Inverse ln-cosh				
$\tau_\circ$	9.7486	0.0000	0.0000	1.6099
A	4.4114	1.7926×10	6.1120×10	6.9424
B	3.0808×10^2	9.6563×10^2	2.4465×10^3	1.6572×10^2
RMS	0.2322	0.1782	0.0549	0.0929
Power Law				
k	5.7002	5.6547×10^{-1}	1.5319	3.6329×10^{-1}
n	2.0905×10^{-1}	5.7606×10^{-1}	5.2817×10^{-1}	7.0471×10^{-1}
RMS	4.7333	0.0171	0.0777	2.8477
Power Law/linear				
k	8.5121	5.7638×10^{-1}	1.6101	1.7187
n	1.0471×10^{-1}	5.7249×10^{-1}	5.1872×10^{-1}	3.8340×10^{-1}
c	9.6609×10	8.0400×10^2	6.8245×10^2	8.4594×10
RMS	0.1095	0.0187	0.0300	0.3020
Prandtl-Eyring				
A	2.6899	1.1236×10	1.9165×10	2.9003×10
B	5.2842×10^{-1}	1.4992×10^2	1.0643×10^2	4.0535×10^2
RMS	8.6440	2.0437	10.1337	8.4530
Prandtl-Eyring*				
$\tau_\circ$	1.1130×10	2.0491	4.9301	4.0711
A	1.5986×10	1.3435×10	2.3337×10	4.8858×10
B	8.4381×10^2	2.5666×10^2	2.0870×10^2	9.7041×10^2
RMS	0.7629	0.8034	3.7120	0.4416
Reiner-Philippoff				
τ_s	1.0361×10^{-1}	6.8453	1.0423×10	3.8488×10^{-2}
$\mu_\circ$	1.9400×10^3	1.7940×10^{-1}	6.1751×10^{-1}	4.0162×10^3
μ_∞	0.0000	2.2823×10^{-2}	4.2098×10^{-2}	4.5890×10^{-2}
RMS	14.0025	0.2376	0.6845	0.3050
Robertson-Stiff				
$\dot{\gamma}_\circ$	2.6207×10^2	2.5411×10^{-1}	6.9519×10^{-1}	4.5735×10
A	4.3109×10^{-1}	5.6173×10^{-1}	1.5028	1.5185×10^{-1}
B	5.7975×10^{-1}	5.7704×10^{-1}	5.3103×10^{-1}	8.2810×10^{-1}
RMS	0.6277	0.0201	0.0808	0.1349
Robertson-Stiff*				
$\tau_\circ$	1.0467×10	6.1634×10^{-2}	4.3414×10^{-1}	3.3481
$\dot{\gamma}_\circ$	0.0000	0.0000	0.0000	0.0000
A	8.2674×10^{-2}	5.5350×10^{-1}	1.4271	1.1656×10^{-1}
B	7.6695×10^{-1}	5.7893×10^{-1}	5.3759×10^{-1}	8.6136×10^{-1}
RMS	0.5710	0.0248	0.0861	0.0957
Sisko				
a	1.3052×10^{-2}	1.2551×10^{-3}	5.3848×10^{-3}	3.8687×10^{-2}
b	9.3789	5.8818×10^{-1}	1.6876	2.3290
c	5.8032×10^{-2}	5.6437×10^{-1}	5.0076×10^{-1}	2.0391×10^{-1}
RMS	0.2103	0.0190	0.0420	0.0187
Sisko*				
$\tau_\circ$	0.0000	0.0000	0.0000	1.9950
a	1.3052×10^{-2}	1.2551×10^{-3}	5.3848×10^{-3}	3.6619×10^{-2}
b	9.3789	5.8818×10^{-1}	1.6876	7.5074×10^{-1}
c	5.8032×10^{-2}	5.6437×10^{-1}	5.0076×10^{-1}	3.6824×10^{-1}
RMS	0.2628	0.0237	0.0525	0.0191

Table 2.10: Least squares parameter estimates and RMS values for various models using the four specific drilling fluids data.

Chapter 3

Pressure Losses

This chapter presents a generalised approach to flow regime identification and friction losses in pipes and annuli that is not constrained by system geometry and the form of the rheological model. Procedures for establishing realistic confidence intervals for calculated laminar pressure losses are also presented, providing a mechanism by which a greater degree of certainty in subsequent ECD estimates may be engineered. A brief examination of conventional pressure loss estimation procedures is also provided to support the proposition that an alternative estimation approach is justified. An empirical and generalised approach for estimating losses over specific PDM's, turbines and MWD tools is also proposed.

3.1 Conventional Calculation Procedures

Most contemporary drilling hydraulics software rely upon laminar pressure loss functions derived from Bingham Plastic or Power Law models, or variants thereof. Even the complement of alternative models available in some 'state-of-the-art' programs, (e.g., the HYCAT package and the models outlined by De Sá, Martins & Amaral (1994), Silva & Martins (1989) and others), remain founded on tractable flow functions. This section briefly examines the treatment of models currently used in conventional drilling hydraulics applications and also reviews the approaches adopted in the calculation of hydraulic diameters.

3.1.1 Treatment of Bingham Plastics

Almost all drilling hydraulics programs have Bingham Plastic capabilities. There are, however, apparent differences in the treatment of plug flow, associated dimensionless quantities and the form of the annular flow equations employed. References also vary in the thoroughness of their treatment of Bingham Plastics: Bourgoyne *et al.* (1986), Moore (1974) and the Comité des Techniciens (1982) all present simplified models that exclude the presence of plug flow; meanwhile Skelland (1967), Govier & Aziz (1972) and Exlog (1985) present more rigorous treatments by incorporating plug flow.

Laminar pressure loss relationships for Bingham Plastics in circular pipes are as follows: excluding plug flow,

$$\Delta p \simeq \frac{8L\bar{v}\mu_\infty}{R^2} + \frac{8L\tau_\circ}{3R}, \tag{3.1}$$

and including plug flow,

$$0 = \left(\frac{2L\tau_\circ}{\Delta pR}\right)^4 - 4\left(\frac{2L\tau_\circ}{\Delta pR}\right)\left(1 + \frac{3\mu_\infty\bar{v}}{\tau_\circ R}\right) + 3. \tag{3.2}$$

Eq.(3.2) is a special case of the Buckingham equation (Buckingham, 1921), and while this would ordinarily require a numerical treatment, an explicit field-orientated solution procedure is available (Exlog, pp. 66). Variations of Eq.(3.1) also exist, distinguished by different constants in an attempt to approximate the effect of plug flow. Expressions for laminar flow in concentric annuli are (with the hydraulic diameter being approximated by a circular diameter): excluding plug flow,

$$\Delta p \simeq \frac{12L\bar{v}\mu_\infty}{R^2(1-\psi)^2} + \frac{3L\tau_\circ}{R(1-\psi)},$$

and including plug flow,

$$\frac{12L\mu_\infty\bar{v}}{\Delta pR^2\,(1-\psi)^2} = 1 - \frac{3L\tau_\circ}{\Delta pR(1-\psi)} + 0.5\left[\frac{2L\tau_\circ}{\Delta pR(1-\psi)}\right]^3. \tag{3.3}$$

Eq.(3.3) is based on the somewhat extreme assumption of representing the annulus as two parallel plates (the 'parallel plate' or 'slot-flow' assumption). Exlog provide the full implicit analytic expression for annular flow without applying the parallel plate simplification, but maintaining the equivalent circular diameter concept:

$$\begin{aligned} \frac{8L\bar{v}\mu_\infty}{\Delta pR^2} &= 1 + \psi^2 - 2\lambda_{[+]}\left(\lambda_{[+]} - \frac{2L\tau_\circ}{\Delta pR}\right) - \frac{8}{3}\frac{L\tau_\circ\,(1+\psi^3)}{\Delta pR\,(1-\psi^2)} \\ &\quad + \frac{2}{3}\frac{L\tau_\circ}{\Delta pR\,(1-\psi)^2}\left(2\lambda_{[+]} - \frac{2L\tau_\circ}{\Delta pR}\right)^3, \end{aligned} \tag{3.4}$$

which first requires solution to $\lambda_{[+]}$ from the expression:

$$\begin{aligned} 0 &= 2\lambda_{[+]}\left(\lambda_{[+]} - \frac{2L\tau_\circ}{\Delta pR}\right)\ln\left[\frac{\lambda_{[+]} - \left(\frac{2L\tau_\circ}{\Delta pR}\right)}{\psi\lambda_{[+]}}\right] \\ &\quad + \frac{4L\tau_\circ}{\Delta pR}\,(1-\lambda_{[+]}) + \left(\frac{2L\tau_\circ}{\Delta pR} + \psi\right)^2 - 1, \end{aligned}$$

which contains the pressure drop sought thereby necessitating a trial-and-error solution involving successive substitution of $\lambda_{[+]}$, calculated for each Δp. To facilitate stability and convergence a reasonable initial guess of Δp can be obtained from Eq.(3.3).

While the thoroughness of the integration is distinguished by the form of the flow relationship, related regime identification procedures, based on dimensionless quantities, are generally treated with less consistency. The Bingham Plastic modified Reynolds number ($N_{Re,Bi} = D\bar{v}\rho/\mu_\infty$) and yield number ($N_Y = 2R\tau_\circ/\bar{v}\mu_\infty$) are two such associated dimensionless quantities (as proposed by Govier, 1959). These and their product, the Hedström (1952) number $[N_{He} = D^2\tau_\circ\rho/(\mu_\infty)^2]$, have been used by investigators to establish procedures for identifying the onset of nonlaminar-fully turbulent flow. Hanks (1963) presented a correlation between N_{He} and $N_{Re,cr}$ (the critical Reynolds number) which was later solved by Hanks & Pratt (1967) with predictions confirmed using data from a number of earlier research studies (Wilhelm, Wroughton & Loeffel, 1939; Caldwell & Babbitt, 1941; Alves, Boucher & Pigford, 1952). This approach differs from the primarily graphical procedure presented by Bourgoyne *et al.* in the correlation between N_{He} and $N_{Re,cr}$. The HYCAT simulation package employs the latter approach as an optional validation procedure for regime identification while other packages may employ different approaches, such as that presented by Hedström which correlates $N_{Re,Bi}$ and N_{He} against friction factors with the onset of regime transition occurring approximately between $N_{Re,Bi} = 2000$ and 3000. Ordinarily the onset of nonlaminar flow is accepted as occurring at a Reynolds number (Reynolds, 1884) $N_{Re} \simeq 2100$.

Different formulations of flow relationships, the application of a number of generalising assumptions, various criteria for the cessation of laminar flow along with differing treatments of Bingham Plastics in the literature has resulted in inconsistent application of this fluid model in the field: a state of affairs compounded through the use of different definitions of hydraulic diameters (section 3.1.6, page 44).

3.1.2 Treatment of Power Law Fluids

A Power Law fluid capability is present in almost all mainstream hydraulics applications. As fluids described by the Power Law possess no yield stress, flow relationships are simpler in form resulting in more consistent application. The expression for flow in a circular conduit is given by,

$$\Delta p = \frac{2Lk}{R}\left[\frac{\bar{v}\,(3n+1)}{Rn}\right]^n ,$$

and for flow in concentric annuli (employing the slot-flow assumption and equivalent circular diameters),

$$\Delta p \simeq \frac{2Lk}{R(1-\psi)}\left[\frac{6\bar{v}}{R(1-\psi)}\frac{2n+1}{3n}\right]^n . \quad (3.5)$$

Transition criteria using this model, however, vary between applications. The most familiar criteria for the onset of turbulence is considered to occur at about

$$N_{\mathrm{Re,cr}} \approx 3470 - 1370n, \tag{3.6}$$

which reduces to the accepted Newtonian transition at $N_{\mathrm{Re,cr}} \simeq 2100$ when $n = 1.0$. Schuh (1964) considered this criteria to represent the point of laminar flow cessation only while the onset of fully turbulent flow occurred at a somewhat higher critical Reynolds number;

$$(N_{\mathrm{Re,cr}})_{\mathrm{turb}} \approx 4270 - 1370n, \tag{3.7}$$

with the intermediate region representing transitional flow. Eq.(3.6) represents the criteria most widely employed in the drilling hydraulics packages considered. Ryan & Johnson (1959) defined the locus of the onset of turbulence from a correlation of the Power Law flow behaviour index, the Power Law Reynolds number ($N_{\mathrm{Re,PL}} = D^n \bar{v}^{(2-n)}\rho/k$) and friction factor, f; however this has yet to gain any widespread application, even though the procedure was substantiated by Hanks & Christiansen (1962).

3.1.3 Treatment of Cassonian Fluids

The implicit pipe flow relationship for this model, incorporating plug flow is:

$$0 = \left(\frac{2L\tau_\circ}{\Delta pR}\right)^4 - 28\left(\frac{2L\tau_\circ}{\Delta pR}\right)\left(1 - \frac{3\bar{v}\mu_\infty}{\tau_\circ R}\right) + 48\left(\frac{2L\tau_\circ}{\Delta pR}\right)^{0.5} - 21,$$

and for a concentric annulus, using the parallel plate approximation and equivalent circular diameter concept:

$$\begin{aligned}\frac{12\mu_\infty \bar{v} L}{\Delta p R^2 (1-\psi)^2} &= 1 - \frac{12}{5}\left[\frac{2L\tau_\circ}{\Delta pR(1-\psi)}\right]^{0.5} \\ &\quad + \frac{3L\tau_\circ}{\Delta pR(1-\psi)} - \frac{1}{10}\left[\frac{2L\tau_\circ}{\Delta pR(1-\psi)}\right]^3.\end{aligned} \tag{3.8}$$

It appears that no detailed investigation into the onset of flow regime transitions for purely Cassonian fluids have been presented in the literature.

3.1.4 Treatment of Robertson-Stiff Fluids

While the physical significance of this model's parameters are not fully understood in the field (De Sá *et al.*, 1994), the form of the function permits relatively straightforward mathematical construction of flow relations (Robertson & Stiff, 1976; with revisions by Beirute & Flumerfelt, 1977, to account for plug flow): namely for pipe flow,

$$0 = \left(\frac{2LA\dot{\gamma}_\circ^B}{\Delta pR}\right)^{[3+\frac{1}{B}]} - (3B+1)\left(\frac{2LA\dot{\gamma}_\circ^B}{\Delta pR}\right)^{\frac{1}{B}} \times \left(1 + \frac{3\bar{v}}{R\dot{\gamma}_\circ}\right) + 3B,$$

and for flow in the annulus, (using the parallel plate approximation and equivalent circular diameter concept):

$$\begin{aligned}\frac{12LA\bar{v}\dot{\gamma}_\circ^B}{\Delta pR^2\dot{\gamma}_\circ(1-\psi)^2} &\simeq \frac{3B}{(2B+1)}\left[\frac{\Delta pR(1-\psi)}{2LA\dot{\gamma}_\circ^B}\right]^{\left(\frac{1}{B}-1\right)} \\ &\quad - \frac{3LA\dot{\gamma}_\circ^B}{\Delta pR(1-\psi)} + \frac{3}{2\,(2B+1)}\left[\frac{2LA\dot{\gamma}_\circ^B}{\Delta pR(1-\psi)}\right]^3 . \end{aligned} \tag{3.9}$$

As for Cassonian fluids, no detailed investigation into regime transitions have been performed explicitly for this fluid. Khataniar *et al.* (1994), however, suggest a modified version of the Power Law transition criteria, namely $N_{\mathrm{Re,cr}} \approx 3470 - 1270B$; a substitution partially verified against just one set of measured transition data.

3.1.5 Treatment of Herschel-Bulkley Fluids

Unlike the manageable flow relationships derived for the previous models, the form of the yield-pseudoplastic model does not submit to easy manipulation. While Herschel-Bulkley flow relations for full-form annular flow remain intractable, implicit expressions for Δp in pipes, allowing for a central unsheared plug, are possible:

$$\begin{aligned}\frac{\bar{v}}{R} &= \frac{k^{(-1/m)}}{\frac{\Delta pR}{2L}^3}\left(\frac{\Delta pR}{2L}-\tau_\circ\right)^{\left[\frac{1+m}{m}\right]} \\ &\quad\times\left[\frac{\left(\frac{\Delta pR}{2L}-\tau_\circ\right)^2}{(1+3m)/m}+\frac{2\tau_\circ\left(\frac{\Delta pR}{2L}-\tau_\circ\right)}{(1+2m)/m}+\frac{{\tau_\circ}^2}{(1+m)/m}\right],\end{aligned}$$

although Khataniar *et al.* propose an alternative annular flow model to the above. These authors also suggest substitution of the Herschel-Bulkley flow behaviour index in Eq.(3.6), namely $N_{\mathrm{Re,cr}} \approx 3470 - 1370m$; a proposal partially supported against limited measured data.

Annular flow relations for yield-pseudoplastic fluids based on flow through parallel plates have been proposed (Skelland, 1967):

$$\frac{Q}{wH^2} = \frac{\left(\frac{\Delta pR}{2L}-\tau_\circ\right)^{\left[\frac{1}{m}+1\right]}}{2\left(1+\frac{1}{m}\right)k\frac{\Delta pR}{2L}}\left[1-\frac{\frac{\Delta pR}{2L}-\tau_\circ}{\left(2+\frac{1}{m}\right)\frac{\Delta pR}{2L}}\right].$$

Due to the inaccuracies inherent in applying expressions formulated using the slot-flow assumption to slimhole, and other high aspect-ratio operations, Silva & Martins (1989) employed empirically-calibrated Herschel-Bulkley correlations using experimental data in a large scale simulator.

These five models represent the sum of rheological models presently considered in mainstream, and other published (research-orientated), drilling hydraulics programs. In addition, novel dimensionless characterisation of the Collins-Graves model and associated laminar pipe-flow pressure loss expressions (Aadnøy & Ravnøy, 1994) was also essentially driven by a desire to construct manageable and tractable flow functions from the chosen rheological model.

3.1.6 Treatment of Hydraulic Diameters

It has long been realised that the hydraulic diameter is insufficient for correlating friction pressure losses for Newtonian fluids in concentric annuli (*cf*: Davies & White, 1929; Lamb, 1932; Knudsen & Katz, 1958 among others). While debate continues about the validity of the two principle theoretical approaches to formulation of representative hydraulic diameters[1], the extension of the characteristic length dimension in generalising the Reynolds number for flow in concentric annular conduits for non-Newtonian fluids has yet to receive any general consensus. The lack of consistency in the treatment of this parameter is essentially due to the relative scarcity of published investigations for annular flows of pseudoplastic drilling fluids compared to that available for Newtonian fluids[2]. The few relevant studies available are essentially represented by Hanks (1963), Hanks & Peterson (1982), Okafor (1982) and Langlinais, Bourgoyne & Holden (1985). The length dimension parameter most used in drilling hydraulics computations are based on Newtonian fluid 'hydraulic diameters' (sometimes referred to as 'equivalent diameters') and provides the simplest representation of the annulus. Four principle hydraulic diameter functions exist in conventional hydraulics calculation applications:

1. Equivalent circular diameter: $D_{\mathrm{hy}} = D_{\mathrm{o}} - D_{\mathrm{i}}$.
2. Slot representation: $D_{\mathrm{hy}} = 0.816\,(D_{\mathrm{o}} - D_{\mathrm{i}})$. (It should be noted that Rothfus (1948) states that "while the flat plate criterion is easily visualised, its mathematical justification is obscure," thereby supporting the notion made earlier that the parallel plate assumption is suspect and unsuitable for realistic representation of annular geometry.)
3. The Lamb (1932) criteria (based on an extension of the Hagen-Poiseuille equation for laminar flow through circular pipes):

$$D_{\mathrm{L}} = \sqrt{{D_{\mathrm{o}}}^2 + {D_{\mathrm{i}}}^2 - \frac{D_{\mathrm{o}2} - D_{\mathrm{i}2}}{\ln\left(D_{\mathrm{o}}/D_{\mathrm{i}}\right)}},$$

which is used in the definition of the equivalent diameter, $D_{\mathrm{equiv}} = D_{\mathrm{L}}^2/\left(D_{\mathrm{o}} - D_{\mathrm{i}}\right)$.

[1] One school, principally represented by Prof. Rothfus and co-workers (e.g., Rothfus, Monrad & Senecal, 1955), suggests the need for the aspect ratio to be used as a correlating parameter and the division of the annular flow field into two separate regions with possibly distinct flow regimes bounded about the point of maximum fluid velocity: thereby requiring the separate application of flow regime transition criteria to each radially distinguished annular region. The other main school of thought (typified by Fredrickson & Bird, 1961) suggests that a single flow regime exists radially throughout the annular flow path, with the transition criteria based on laminar flow determined length dimensions using geometrical parameters to maintain dimensional integrity. Sufficient documentary evidence exists to conclude that "neither school adequately predicts magnitudes or trends of objectively confirmed existing data," (Jones & Leung, 1981).

[2] Lohrenz & Kurata (1960) present a detailed review of available studies up to 1960 while Jones & Leung provide references to most post-1960 studies up to 1981.

4. The semi-empirical expression of Crittendon (1959), from investigations of hydraulic fracture treatments:

$$D_{\mathrm{hy}} = \frac{1}{2}\sqrt[4]{{D_{\mathrm{o}}}^4 - {D_{\mathrm{i}}}^4 - \frac{\left(D_{\mathrm{o}2} - D_{\mathrm{i}2}\right)^2}{\ln\left(D_{\mathrm{o}}/D_{\mathrm{i}}\right)}} + \frac{\sqrt{D_{\mathrm{o}2} - D_{\mathrm{i}2}}}{2}. \tag{3.10}$$

In addition to these models, an empirically determined slot-type representation has been suggested (Jensen & Sharma, 1987) whereby coefficients are adjusted to match available data (based on a study on the effect of hydraulic diameters of nine published, and six derived, explicit solutions to the Colebrook friction factor) using $D_{\mathrm{hy}} = \text{Constant} \times (D_{\mathrm{o}} - D_{\mathrm{i}})$.

While Eq.(3.10) has been recommended as a suitable hydraulic diameter (from the simulation of two slimhole operations, Thonhauser, Millheim & Spörker, 1995), once again there exists inconsistent application of hydraulic diameters. HYCAT, for example, provides access to all of the above D_{hy} options, although justification for selection is determined only by the quality of computed versus measured SPP's; Comité des Techniciens present expressions employing equivalent circular diameters only; Moore (1974), the slot approximation; while programs HYDRAULIC (Geoservices drilling hydraulics program manual, 1995) and EAP (Exlog) employ equivalent circular diameters.

3.2 Generalised Flow Regime Transition Criteria

The criteria delimiting flow regime transition are based primarily on empirical observations, with interpretation procedures dependent on the rheological model employed. The proposal herein provides a generalised and consistent procedure for the determination of parameters necessary for estimating flow regime transitions.

3.2.1 Flow Regime Transition in the Drillstring

It has been shown that all fluids which are not time-dependent must obey the conventional Newtonian $f - \mathrm{N_{Re}}$ relationships when in steady state laminar flow - so long as $\mathrm{N_{Re}}$ adequately accommodates the fluid's non-Newtonian characteristics (Skelland, 1967). Metzner & Reed (1955) established that a high degree of correlation existed between data for time-independent non-Newtonian fluids on an f versus $\mathrm{N_{Re}}$ plot when utilising the concept of a dimensionless generalised Reynolds number (GRN). Such representation has the advantage of allowing conventional and tested procedures for calculating Newtonian friction factors to be applied to non-Newtonian fluids. The GRN, and the manner of its definition, provides the necessary mechanism for establishing a consistent and generalised methodology for the determination of parameters necessary to specify flow regime transition criteria.

Assuming that, (1) the fluid is in steady state laminar flow, (2) the fluid is time-independent under the prevailing conditions, and (3) there is no slippage between the fluid and the conduit wall, it is possible to apply the Rabinowitsch-Mooney relationship (Rabinowitsch, 1929; Mooney,

Models	Changes in N (%)					
	$\epsilon_{[0.1\%]}\%$	$\epsilon_{[1.0\%]}\%$	$\epsilon_{[2.0\%]}\%$	$\epsilon_{[3.0\%]}\%$	$\epsilon_{[4.0\%]}\%$	$\epsilon_{[5.0\%]}\%$
Bingham Plastic	0.00755	0.08356	0.16909	0.25577	0.34364	0.43646
Casson	0.00571	0.06311	0.12757	0.19275	0.25868	0.32537
Collins-Graves	0.01171	0.12931	0.26141	0.39500	0.53009	0.66678
Herschel-Bulkley	0.00174	0.01922	0.03893	0.05892	0.07922	0.09982
Hyperbolic	-0.00064	-0.00705	-0.01426	-0.02155	-0.02891	-0.03636
Power Law	nil	nil	nil	nil	nil	nil
Reiner-Philippoff	0.00655	0.07257	0.14712	0.22294	0.30007	0.37853
Robertson-Stiff	0.00111	0.01232	0.02497	0.03784	0.05091	0.06421
Sisko	0.00437	0.04831	0.09756	0.14722	0.19744	0.24815

Table 3.1: Percentage change in generalised flow behaviour index N due to perturbation of volumetric flowrate from 0.1% to 5.0%. $\epsilon_{[x\%]}\%$ represents the percentage change in N from a base established at a perturbation of 0.003%.

1931)[3] to determine wall shear stress, namely:

$$Q = \frac{\pi R^3}{{\tau_w}^3} \int_0^{\tau_w} {\tau_r}^2 \dot{\gamma}_r \, \mathrm{d}\tau_r. \tag{3.11}$$

Khataniar *et al.* (1994) solved this integral for Herschel-Bulkley and Robertson-Stiff fluids by writing $\dot{\gamma}_r$ in terms of these models and formulating implicit functions about τ_w. Eq.(3.11) can, however, be written in a more general form:

$$Q = \frac{\pi R^3}{{\tau_w}^3} \int_0^{\tau_w} {\tau_r}^2 f^{-1}(\tau_r; \phi) \, \mathrm{d}\tau_r, \tag{3.12}$$

which can be solved numerically to furnish τ_w. Using the relationship $\dot{\gamma}_w = f^{-1}(\tau_w; \phi)$, the 'apparent' Newtonian viscosity at the pipe wall is obtained from $\mu_{w,\mathrm{app}} = \tau_w / \dot{\gamma}_w$. The generalised flow behaviour index, N, is then calculated from

$$N = \frac{\mathrm{d}(\ln \tau_w)}{\mathrm{d}(\ln \dot{\gamma}_w)}. \tag{3.13}$$

Eq.(3.13) is somewhat different from the definition of n' defined by Metzner & Reed who relate $\dot{\gamma}_w$ to the Newtonian shear rate $(8\bar{v}/D)$ thereby defining the flow behaviour of a pseudo-shear rheogram and not the instantaneous relationships required for drilling hydraulics computations. If it is accepted that N remains constant over at least a differential range of shear rates then solution to Eq.(3.13) may be obtained by perturbation of the volumetric flow rate by a small amount: a 0.1% perturbation proved satisfactory for all the cases studied. As expected N is unaffected by perturbation for the Power Law as this models' form remains linear due to the logarithm. However, the quality of N calculated from other rheological models does vary upon the magnitude of perturbation. Table 3.1 presents the percentage variation in N observed

[3] According to Savins, Wallick & Foster (1962*a* & *b*) the expression was first developed by Herzog & Weissenberg in 1928.

through different magnitudes of volumetric flow rate perturbations from 0.1% to the maximum value studied, 5%. The perturbation analysis considered eight other rheological models. The percentage error uses

$$\epsilon_{[x\%]}(\%) = \left[\frac{N_{[x\%]} - N_{[@\,0.003\%]}}{N_{[@\,0.003\%]}}\right] \times 100$$

to define $\epsilon_{[x\%]}$ where $N_{[@\,0.003\%]}$ is the value of N obtained from a perturbation of 0.003% and $N_{[x\%]}$ is the generalised flow behaviour index obtained from perturbing the volumetric flow rate by x%.

Table 3.1 shows that, apart from the Power Law, the Hyperbolic model is least sensitive to perturbation, exhibiting a modest −0.036% error at a 5% perturbation. Collins-Graves, however, is the most sensitive to the magnitude of perturbation with a possibly significant 0.666% error at maximum test perturbation. Figure 3.1 is more informative as it presents $\epsilon_{[x\%]}\%$ against flow rate perturbations between 0.003% to 5% (points generated in 0.001% increments). This figure indicates that all significant divergencies in N occurs, for all rheological models (except the Power Law), at perturbations greater than 0.1%. No significant accuracy gains are obtained from smaller perturbations, hence 0.1% is deemed satisfactory for the purposes of future calculation when employing `double` precision in the ANSI C program written for this study.

Metzner (1956) ascertained that n' remained relatively unaffected by sustained fluctuations in temperature. On the other hand other investigators have shown that flow behaviour indices for both water- and oil-based muds may be affected by changes in downhole conditions (Annis, 1967; Bartlett, 1967; de Wolf, Coffin & Byrd, 1983; McMordie, Bennett & Bland, 1975; Politte, 1985; Houwen & Geehan, 1986; Fisk & Jamison, 1989). Although there is relatively little systematic understanding of the processes involved, Alderman, Gavignet, Guillot & Maitland (1988) present findings to show that n increases slightly with rising temperatures while also exhibiting a modest decrease with increasing pressures. If one assumes increasing temperatures are coincident with increasing pressures then it is reasonable to assume that any net variations in n will be approximately nullified at downhole conditions. These observations could be assumed to also apply to N. For systems possessing long fluid residence times (as found in extended reach/horizontal wells) high temperatures may not always correspond to high pressures and a net variation in N may well result. In such circumstances rheology measurements should be taken at different temperatures to determine the severity of any rheological changes and should be considered during hydraulics calculations (necessitating dynamic temperature profiling, for example Beirute, 1991). Rheograms recorded at multiple temperatures will also benefit simulations involving cement slurries (particularly for expansive, freeze-protected, salt and latex-modified cement systems) where the heat released during setting may affect thixotropy substantially.

Reed & Pilehvari (1993), following from investigations led by Professor Metzner and co-workers, presented the following 'effective' diameter for non-Newtonian fluids based on the Metzner generalised pipe shear rate relationship:

$$D_{\text{eff,MR}} = \frac{4n'D}{3n'+1}, \tag{3.14}$$

which represents the imaginary (effective) diameter of a circular pipe which would experience the

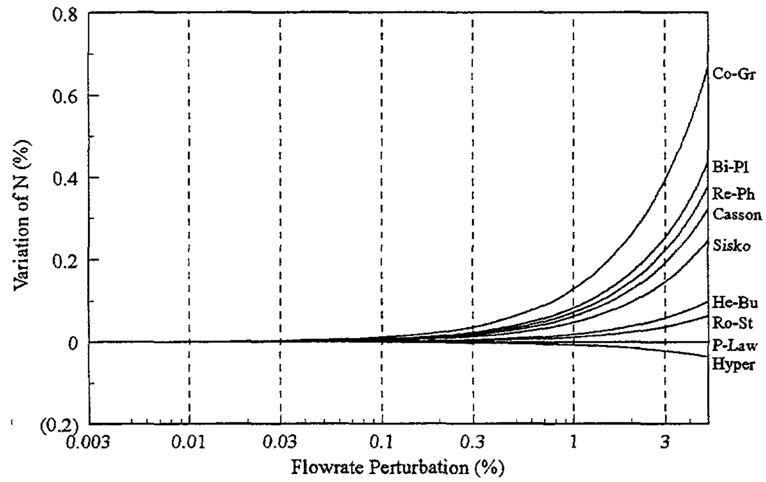

Figure 3.1: Variation of N against perturbation in volumetric flow rates.

same pressure drop for a Newtonian fluid with a viscosity identical to the 'apparent' viscosity of the non-Newtonian fluid, flowing at the same average velocity. For pseudoplastic fluids ($n' < 1$) the effective diameter will be less than the physical diameter while it will be greater for dilatant fluids ($n' > 1$). It can be shown that Eq.(3.14) is proportional to the equivalent wall shear rate $[(\dot{\gamma}_w)_{MR}]$ calculated at the average fluid velocity in the conduit. Consequently, the generalised effective diameter for *in situ* fluid velocity is redefined as follows:

$$D_{\text{eff,G}} = \kappa \frac{4ND}{3N+1},$$

where $\kappa = (\dot{\gamma}_w)_{MR}/\dot{\gamma}_w$ and represents a correction factor to compensate for the average velocity in Metzner & Reed parameters. This expression is independent of the form of the rheological model and represents the diameter of a pipe with an effective fluid-contact circumference equating to that over which the wall shear stress acts. With $\mu_{w,\text{app}}$ and $D_{\text{eff,G}}$ defined, the generalised Reynolds number can be calculated from:

$$\mathrm{N}_{\text{Re,G}} = \frac{\rho \bar{v} D_{\text{eff,G}}}{\mu_{w,\text{app}}}. \tag{3.15}$$

3.2.2 Critical Reynolds Numbers

Both Khataniar *et al.* and Reed & Pilehvari suggest substitution of Robertson-Stiff and Herschel-Bulkley flow behaviour exponents into Eqs.(3.6 & 3.7) to define a more flexible critical transition criteria. Subsequently, substitution of the generalised flow behaviour index, N, into similar expressions using the GRE extends the generality of the critical transition criteria to all rheological models: delimiting steady state laminar to nonlaminar flow,

$$(\mathrm{N_{Re,G,cr}})_L \approx 3470 - 1370N, \tag{3.16}$$

and the criteria defining transitional to fully turbulent flow,

$$(\mathrm{N_{Re,G,cr}})_U \approx 4270 - 1370N. \tag{3.17}$$

Eq.(3.16) reduces to the accepted Newtonian laminar/turbulent transition ($\mathrm{N_{Re,G,cr}} \simeq 2100$) when $N = 1.0$, while Eq.(3.17) reduces to the empirically determined upper critical value for fully turbulent flow, $\mathrm{N_{Re,G,cr}} \approx 2900$ (Schuh, 1964). While the former fixed-transition criteria represents an accepted truth concerning Newtonian flow, observations of non-Newtonian fluids in pipes fail to confirm the wholesale validity of these criteria (for example, Khataniar *et al.* validated their proposals against just one data set).

Tables E.2 to E.7 (inclusive) present critical volumetric flow rates (in lpm) calculated from data observed for two drilling fluids flowing in three sizes of pipe (Table E.1). Alongside these calculated values are visually-determined critical flow rates as determined from inspection of measured pressure data. Figures E.1, E.3, E.5, E.7, E.9 & E.11 present measured data (pressure drops and volumetric flow rates) with calculated lower- and upper-'fixed' transition zones superimposed for each rheological model (note: vertical positioning of tie-lines is arbitrary). The left-hand open-circle represents $(Q_{cr})_L$ while the right-hand open-circle marks $(Q_{cr})_U$ with tie-lines indicating the region of transitional flow.

1″ pipe transitions for mud 'A' provides consistent over-prediction in critical values. All models, except Reiner-Philippoff, over-predict $(Q_{cr})_L$ by a minimum of 23% (Bingham Plastic) to a maximum of 52% (Ellis *et al.*). For $(Q_{cr})_U$, the smallest over-prediction was 10% (Bingham Plastic) with the largest again being provided by Ellis *et al.* (37%) - refer to Table E.2 on page 151. Inspection of the superimposed tie-lines against the measured data reveals a strong orientation of the fixed-transition model to predict transitional flow over what is essentially turbulent flow. Such a propensity will result in pressure loss under-prediction. Predicted transitions for mud 'B' flowing in the same conduit appear more reasonable, except for Reiner-Philippoff which demonstrates substantial over-predictions (66% and 115% for $(Q_{cr})_L$ and $(Q_{cr})_U$ respectively). Calculated transitions provide modest under-predictions of the observed laminar-transitional flow transition (maximum under-estimation being -21% by the Power Law) and provides modest over-prediction of transitional to fully-turbulent flow transitions (maximum over-prediction being 17% by Collins-Graves). Good straddle positioning of the transitional flow region by model tie-lines is, of course, desirable. It is questionable whether the straddling exhibited by the fixed-transition criteria approach for mud 'B' could be considered reasonable as the observed region of transitional flow (delimited by lower and upper critical flow rates of 92 and 98 lpm respectively) is extremely narrow. Fixed-value transition delineation is insensitive to variations in the magnitude of the transitional flow region. Although the transitional flow region described by mud 'A' [$(Q_{cr})_L$ = 52 lpm and $(Q_{cr})_U$ = 80 lpm] is more reasonably represented by the fixed-transition model, the relative positioning of calculated tie-lines was poor (situated to the right of the transitional flow region). While Reiner-Philippoff provided the most appropriate tie-line positioning for mud 'A', this was not repeated for mud 'B' where it provided the worst transition marking of any model. Consequently, this model is considered to be highly sensitive to N and for this reason is considered unreliable: verification of which is provided by similarly poor behaviour in both the 2″ and 3″ pipes.

Calculated transitions for 2″ pipe, mud 'A' data (Table E.4, page 155, and depicted in Fig. E.5, page 156), indicates good tie-line straddling over the transition region with only modest over- and under-predictions. On the other hand, transitions calculated for mud 'B' in the same pipe provided somewhat poorer quality transition marking. While an element of doubt exists concerning the quality of the measured data for this system (uncharacteristic laminar flow pressure drop profiles and a [too] extensive transitional flow region, estimated to exist from 140 to 232 lpm), superpositioning of transition tie-lines reveals consistent and substantial over-prediction of transitions. Excluding Reiner-Philippoff (which lies off the scale in Fig. E.7), the minimum over-prediction of $(Q_{cr})_L$ is 47%, and for $(Q_{cr})_U$ is 23% (both for Bingham Plastic). Subsequent pressure drop over-estimation will ensue.

Transitions for both muds in the 3″ pipe demonstrated poor quality flow regime transition predictions (Tables E.6 & E.7, illustrated in Figs. E.9 & E.11). All models over-estimated transitions. While calculations applicable for mud 'A' may be considered adequate for some purposes, those provided for mud 'B' cannot be accepted due to the significant over-estimation of transitions with tie-lines for all models being situated well to the right of the data.

Although the fixed-transition criteria generally over-predicted transitions, it does provide acceptable values for both mud types examined in 1″ and 2″ pipes. Acceptability of prediction is stretched somewhat for mud 'A' in the 3″ pipe and is unacceptable for mud 'B'. As the fluids examined are pseudoplastic ($N < 1$), the N-criteria in Eqs.(3.16 & 3.17) will provide even greater over-estimation of critical values. As mud 'B' is characterised by a lower value of N than for mud 'A' the form of the N-criteria transition expressions will result in substantially greater over-estimation of transitions and longer tie-lines. This is demonstrated in Tables E.2 to E.7 (from page 151, inclusive) where critical flow rates (and associated errors against observed critical values) for the N-criteria are presented alongside critical values for the fixed-transition method. While it is accepted that just six samples is insufficient to draw any substantive conclusions, it is clear that any over-estimations in transitions determined from the fixed-transition approach will be exaggerated if Eqs.(3.16 & 3.17) are employed for pseudoplastic fluids. It is also clear that while critical values are more or less insensitive to N, certain models are over-sensitive to this parameter, namely Reiner-Philippoff and, to a lesser extent, Ellis *et al.* As such, these models are deemed unsuitable for the robust requirements of drilling hydraulics calculations. For these reasons the fixed-transition criteria is preferred over the N-criteria approach for pseudoplastics with characteristically low numerical values of flow behaviour indices. Finally, it is apparent that the degree of disagreement between observed and calculated critical values is not just related to the rheological properties of the fluid, but is also reflected in the diameter of the conduit: the 3″ pipe exhibiting substantially poorer predictions for the same fluid type than for smaller diameter pipes.

Exploratory data analysis (EDA) established that the rheological-dependent term in Eqs.(3.16

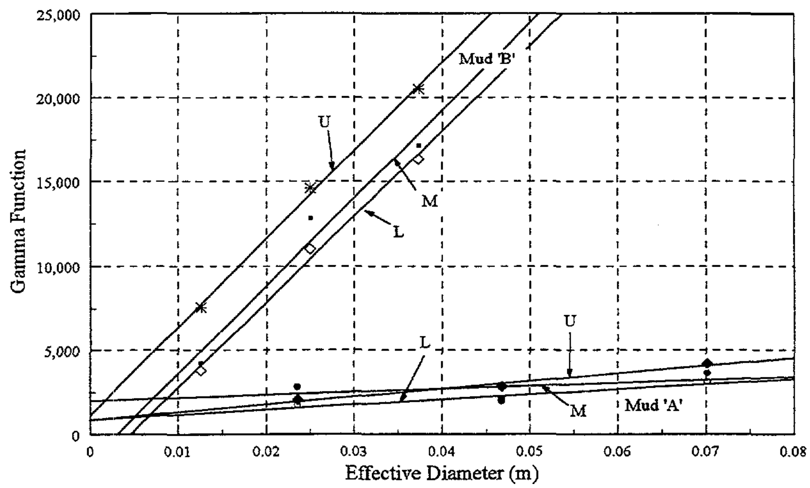

Figure 3.2: Γ-function versus $D_{\mathrm{eff,G}}$ for muds 'A' & 'B'. Laminar to nonlaminar (transitional), laminar to fully turbulent and nonlaminar (transitional) to fully turbulent flow regime transitions are indicated by annotations 'L', 'M' and 'U' respectively.

& 3.17), currently fixed at 1370, forms an approximately linear relationship when modified to equate to observed critical values. Figure 3.2 presents the equivalent rheological-dependent term (referred to as the Γ-coefficient) corresponding to the observed regime transitions. Consequently one may write the transition criteria, thus: for laminar to nonlaminar flow,

$$(\mathrm{N_{Re,G,cr}})_{L\,(\&\,M)} \approx 3470 - \Gamma N, \tag{3.18}$$

and for nonlaminar (transitional) to fully turbulent flow,

$$(\mathrm{N_{Re,G,cr}})_{U} \approx 4270 - \Gamma N. \tag{3.19}$$

Further basic analysis provided the following function for Γ:

$$\Gamma = (a + bN)\, D_{\mathrm{eff,G}} + (c + dN)\,,$$

with model constants provided in Table 3.2, which provides a third set of constants intended for application to a single transition zone (namely no transitional flow) - designated the 'middle' value.

The lower halves of Tables E.2 to E.7 (inclusive) present calculated critical flow rates corresponding to lower, middle and upper flow regime transitions determined from Eqs.(3.18 & 3.19).

Application	Constants			
	a	b	c	d
Laminar to transitional: Eq.(3.18)	706978.4	-973725.3	-2946.3	6991.2
Transitional to turbulent: Eq.(3.19)	699247.7	-922677.1	1262.8	-562.3
Laminar to turbulent: Eq.(3.18)	684822.9	-924976.2	-3502.4	6168.0

Table 3.2: Correlation flow regime transition approximation constants for function $\Gamma = (a + bN)\, D_{\text{eff,G}} + (c + dN)$.

Results are also illustrated in Figs. E.2, E.4, E.6, E.8, E.10 & E.12 for the three pipe diameters and the two fluid types.

Comparison between the fixed- and correlation-transition criteria for the 1″ pipe shows marked differences in predicted critical values. For mud 'A' the spread of tie-lines for the correlated-transition approach are larger than for the fixed method. For mud 'B' the opposite is true. The correlation-transition approach can, therefore, reflect the extent of the transition region. This approach, however, exhibits greater errors and inconsistent transition locations for the 1″ pipe. Tie-lines for mud 'B' are unevenly located over Fig. E.2, while Fig. E.1 (also on page 152) shows an evenness in tie-line distribution and spread. For this pipe size, the fixed-transition approach is preferred over the correlation-transition method. Similarly for mud 'A' in the 2″ pipe, the correlation method provides less consistent and accurate critical values than provided by the fixed-transition criteria approach. For mud 'B', only the Power Law and Ellis *et al.* models benefit from the correlation approach. As the correlation may yield negative values, computation 'checks' were necessary and any negative values were replaced by fixed-transition criteria to maintain solution integrity. Application of the correlation approach to the 3″ pipe data also yielded poor results and demonstrated a lack of solution robustness (Figs. E.10 & E.12). Consequently the correlation approach, as currently defined, cannot be recommended for robust calculation requirements and the fixed transition criteria approach is preferred. The poor performance of the correlation approach is not unexpected due to the paucity of data on which the EDA was conducted and with only two data sets, linearity was imposed onto a nonlinear system.

3.2.3 Flow Regime Transition in the Annulus

Skelland (1967) extended the Rabinowitsch-Mooney relationship for flow between flat parallel plates under the same assumptions presented in section 3.2.1, page 45, thus:

$$Q = \frac{wH^2}{2{\tau_w}^2} \int_0^{\tau_w} {\tau_r}^2 f^{-1} (\tau_r; \phi)\, \mathrm{d}\tau_r. \tag{3.20}$$

While providing reasonable solutions for τ_w in circulating systems with low to medium aspect ratio values, errors resulting from the use of the parallel plate assumption are expected in systems where the aspect ratio is higher.

A general expression relating Q and τ_w for laminar flow of time-independent fluids in a concentric annulus without employing any geometrical simplifications (accepting the assumptions given in section 3.2.1) is proposed as follows:

$$Q = \pi \int_{R\psi}^{R} r^2 f^{-1}(\tau_r;\phi)\,\mathrm{d}r. \tag{3.21}$$

This relationship (refer to Appendix F for derivation) integrates over the (more logical) annulus radius, and not over a constant [namely τ_w as used in Eq.(3.12) and Eq.(3.20)]. $f^{-1}(.)$ above represents $\dot{\gamma}_r$ which may be written in terms of wall shear stress and radial position using the relationship:

$$\tau_r = \tau_w \left| \frac{\lambda^2 - z^2}{z(\lambda^2 - 1)} \right|.$$

Eq.(3.21) also assumes that a single flow regime is prevalent throughout the annulus. The generalised effective diameter incorporating both rheological and geometric effects is given by,

$$D_{\mathrm{eff,G}} = \frac{D_{\mathrm{hy}}}{G}. \tag{3.22}$$

The hydraulic diameter correlation factor $G = f(N)$ (originally defined by Fredrickson & Bird (1958) using the Power Law flow behaviour index) is obtained from the following set of expressions (developed by Exlog), but making use of the generalised flow behaviour index:

$$G = \frac{[1 + (Z/2)]\,[(3 - Z)N + 1]}{(4 - Z)N},$$

where $Z = 1 - \left[1 - (\psi)^Y\right]^{1/Y}$ and $Y = 0.37N^{-0.34}$.

While the Fredrickson-Bird formulation strictly relates to laminar flow of a Power Law fluid, usage of N generalises the function to any rheological model, a proposal validated somewhat by Reed & Pilehvari who successfully utilised the Herschel-Bulkley flow behaviour index, m, in the determination of G. Finally, the GRN for flow in concentric annuli is calculated from Eq.(3.15) which may be used in Eqs.(3.18 & 3.19) to delimit flow regime transitions. The Exlog book generalises the transition from laminar to fully turbulent flow as occurring at critical Reynolds numbers some 50% higher than those proposed for pipe flow while the Comité des Techniciens make no such claim and employ unadjusted pipe flow critical Reynolds number criteria to the annulus. Although it is admitted that annulus-specific critical Reynolds numbers are subject to some uncertainty and debate, the GRN provides an element of consistency in application, although further investigation is necessary to determine more precise rheological- and geometrical-dependent $\mathrm{N_{Re,G,cr}}$ flow regime punctuators (annulus pressure loss data provided by Okafor did not extend into transitional and turbulent flow).

Hanks's (1963) critical Reynolds number defining the transition from laminar to nonlaminar flow provides an alternative criteria to Eqs.(3.16 and 3.17) for inner- and outer-annular sections, and is given by:

$$\left(\mathrm{N_{Re,cr}}\right)_{i,o} = \frac{808\phi^{1.5}}{\left(1 - \bar{\xi}^2 + 2\lambda^2 \ln \bar{\xi}\right)\left|\bar{\xi} - \frac{\lambda^2}{\bar{\xi}}\right|}, \tag{3.23}$$

where $\phi = 1 + \psi^2 - 2\lambda^2$, and $\xi = r/R$. $\bar{\xi}$ represents the radial fraction at which Hanks' K-factor is a maximum (definition and values of which are presented by Hanks, 1980). This critical Reynolds number considers the division of the annular flow field as comprising two separate regions (per Rothfus, 1948), with geometrical similarity allowing Eq.(3.23) to apply to both inner- and outer-regions. The limiting value at $\psi = 1$ provides $(\mathrm{N_{Re,cr}})_i = (\mathrm{N_{Re,cr}})_o = 2285$.

3.3 Pressure Loss Estimation

While selection of alternative, possibly more esoteric, rheological models may provide eminently suitable fluid characterisations, their practical usefulness is usually restricted by the lack of a suitable application vehicle. The proposed model, originally based on the work of Herzog & Weissenberg (1928), attempts to provide such a mechanism.

3.3.1 Drillstring Friction Losses - Laminar Flow

A general method for assaying the characteristics of laminar pressure losses in pipes, without any initial assumptions regarding the nature of the rheological function to pressure drop and volumetric flowrate (kinematical) quantities, provides the basis of the following 'differential method' (Hersey, 1932) expression:

$$\bar{v} = 2R \int_0^1 y \int_0^1 f^{-1}\left(\frac{\Delta p R z}{2L}; \phi\right) \mathrm{d}z \, \mathrm{d}y, \tag{3.24}$$

which represents the general form of the flow relation for any fluid without a yield stress. Savins, Wallick & Foster (1962*a*) provide a review to the development of a different form of Eq.(3.24) and cite Alves *et al.* (1952) as being the first to presented the classical 'differential method' expressions[4] in terms of volumetric flowrate through the introduction of the second integral.

The radial fraction term, z, takes values $0 \leq z \leq 1$ such that at the centre of the pipe $(Rz = 0)_{z=0}$, and at the inner pipe wall $(Rz = R)_{z=1}$. Inspection of Eq.(3.24) shows that if $f^{-1}(.)$ is replaced by a simple and explicit function for $\dot{\gamma}$, an analytic solution is possible: Newtonian and Power Law fluid flow functions can be easily constructed from such treatment. The inner integral represents the velocity profile for the specified Δp such that:

$$v(z) = R \int_0^1 f^{-1}\left(\frac{\Delta p R z}{2L}; \phi\right) \mathrm{d}z = \int_0^1 \dot{\gamma} \, \mathrm{d}r, \tag{3.25}$$

while the outer integral solves $\mathrm{d}Q = 2\pi R^2 y \, v(z) \, \mathrm{d}y$ (the differential expression for volumetric flowrate) thus:

[4] Herzog & Weissenberg (1928) and Eisenschitz, Rabinowitsch & Weissenberg (1929) are considered to be the pioneers of the differential method, although others attribute the basic concept to Rabinowitsch (1929) and Mooney (1931).

$$f(Q) = 2\pi R^3 \int_0^1 yv(z)\,\mathrm{d}y,$$

and in terms of velocity,

$$f(v) = 2R \int_0^1 yv(z)\,\mathrm{d}y.$$

As seen from Eq.(3.25), the value of $f^{-1}(\tau_r;\phi)$ is dependant upon the unknown laminar pressure drop, Δp. The desired value of Δp is, therefore, the root of:

$$f\left(\Delta p\right) = f\left(v\right) - \bar{v} = 0.$$

Accepting the Rothfus conjecture that the two distinct annular regions about the radial point of maximum velocity are geometrically similar (Hanks, 1980) one can then extend the Herzog & Weissenberg approach to velocity distributions discretely over distinct portions of the conduit, and by integrating a second time, pressure loss may then be written in terms of the known (measured) quantity, Q. Consequently the general expression for fluids possessing a yield stress is:

$$\bar{v} = 2R\left[\int_0^\lambda y \int_0^\lambda f^{-1}\left(\frac{\Delta pRz}{2L};\phi\right)\mathrm{d}z\,\mathrm{d}y + \int_\lambda^1 y \int_\lambda^1 f^{-1}\left(\frac{\Delta pRz}{2L};\phi\right)\mathrm{d}z\,\mathrm{d}y\right],$$

or

$$\bar{v} = 2R\left[\int_0^\lambda y\,v(z)\,\mathrm{d}y + \int_\lambda^1 y\,v(z)\,\mathrm{d}y\right].$$

λ is the dimensionless radial fraction delimiting the boundary between the plug and laminar flow regions where $0 \leq \lambda \leq 1$, and is obtained from:

$$\lambda = \tau_y \frac{2L}{\Delta pR}.$$

The required pressure drop is then the root of:

$$f\left(\Delta p\right) = \left(f(v)_{\mathbf{plug}} + f(v)_{\mathbf{lam}}\right) - \bar{v} = 0.$$

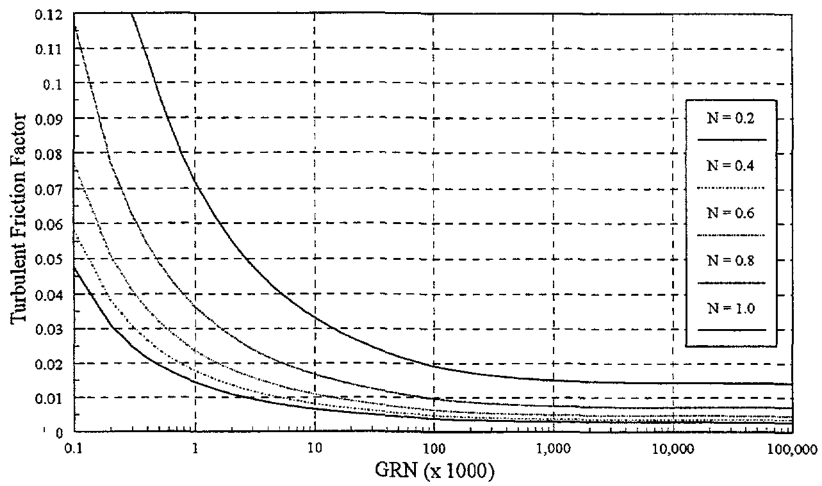

Figure 3.3: Turbulent friction factor for different N values.

3.3.2 Drillstring Friction Losses - Turbulent and Transitional Flow

To maintain consistency in application of concepts it is desirable to apply generalised parameters to turbulent flow formulations. The generalised turbulent flow pressure loss expression is given by

$$\Delta p = f_{\text{turb}} \frac{2\rho\bar{v}L}{D_{\text{eff,G}}}.$$

Table 3.3 on the next page presents RMS values for four published friction factor expressions developed specifically for non-Newtonian fluids and one Newtonian-based friction factor correlation. It should be noted that the expression of Clapp (1961) utilises Deissler's (1951) values of constants required in the original expression, while the Dodge & Metzner (1959) expression, based on dimensional analysis procedures proposed by Millikan (1939), utilises constants determined from a study of time-independent viscous aqueous Carbopol. The near-precise explicit approximation of the Colebrook (1938/39) implicit friction factor expression of Zigrang & Sylvester (1982) was selected as the Newtonian fluid friction factor model[5]. It is clear that the four empirical non-Newtonian friction factor expressions failed to provide consistently reasonable predictions while the Zigrang & Sylvester Newtonian expression provided somewhat better modelling (as indicated by having the smallest average RMS).

As the generalised flow behaviour index essentially superimposes a yield-Power Law-type parameter to any fluid model over the elemental region of shear rates for the section of the system

[5]While Jensen & Sharma (1987) considered nine published explicit approximations to the Colebrook equation and their ability to model non-Newtonian fluids, their reliance on the R^2-test goodness-of-fit measure on these nonlinear models limits the confidence one may have on their conclusions.

Model	Mud 'A' RMS values			Mud 'B' RMS values			Avg.
	1″	2″	3″	1″	2″	3″	RMS
Clapp (1961)	3423.33	57.37	5.53	3498.85	359.56	128.84	1245.58
Dodge & Metzner (1959)	2289.54	94.79	1.65	2448.49	214.77	76.31	854.26
Tomita (1959)	1879.66	12.46	0.96	1186.44	79.60	42.15	533.35
Torrance (1963)	3848.25	86.61	11.15	3385.20	365.51	139.62	1306.06
Zigrang & Sylvester (1982)	2218.73	20.76	1.77	204.98	1.34	9.97	409.56
Eq.(3.26)	282.41	38.64	10.39	104.03	4.89	0.48	73.47

Table 3.3: RMS values for different turbulent flow friction factor correlations and measured turbulent flow pressure losses for three different pipe diameters. PVC pipe roughness was assumed to be 0.002 mm.

under investigation, it is reasonable to assume that friction factor models employing Power Law-type flow behaviour indices be deemed suitable for further analysis. However, the varying quality of RMS's for the four non-Newtonian friction factor correlations, and the improved accuracy provided by the Colebrook Newtonian model, suggests an alternative model may be appropriate. A hybrid model, receptive to the unifying generalised flow behaviour index (and related quantities), but of a Colebrook-form, would appear to provide the necessary improvement in turbulent flow modelling for the two fluids considered. Reed & Pilehvari (1993), in their melding together of the Dodge & Metzner and Colebrook functions (retaining all Dodge & Metzner constants), provided one hybrid that could accommodate pipe roughness, n' and GRN's. This hybrid provided poorer predictions (as determined by RMS) than the conventional Dodge & Metzner expression. The explicit hybrid model proposed here is based on the first iteration of the numerical solution to the standard Colebrook function but with constants modified to account for non-Newtonian fluid characteristics, namely:

$$\frac{1}{\sqrt{f_{\mathrm{turb}}}} = -\left(A_1 + A_2 e^N\right)\log_{10}\left[\frac{\epsilon}{A_3 D_{\mathrm{eff,G}}} - \frac{A_4}{\mathrm{N_{Re,G}}}\log\left(\frac{\epsilon}{A_3 D_{\mathrm{eff,G}}} + \frac{(A_5)^N}{\mathrm{N_{Re,G}}}\right)\right], \tag{3.26}$$

where constants $A_1 = 6.66410$, $A_2 = -1.70664$, $A_3 = 2.9$, $A_4 = 5.02$ and $A_5 = 1.26$. EDA revealed that RMS's were most sensitive to the pseudo-gradient term in the conventional Colebrook function, originally at a value of -2.0, and could be best described by a function of N, namely $\left(A_1 + A_2 e^N\right)$. While the constants suggested for this function yield the smallest error for both fluid types examined, the somewhat extreme values of flow behaviour indices (from about 0.17 to 0.71) means that some degree of compromise in their determination was necessary, namely they yield the smallest RMS values for both fluids. It is apparent that for systems operating with fluids possessing less variable values of N, different values for A_1 and A_2 may provide improved solution accuracy. And as the pseudo-gradient has a significant effect on the solution, application of this model to other fluids may benefit from a nonlinear least squares analysis (as long as suitable data is available). The remaining constants have a limited effect on solution accuracy. Table 3.3 presents the RMS values obtained from Eq.(3.26) and shows substantial improvements in modelling accuracy: the average RMS is just 18% of the next-best average RMS value obtained from the full two iteration Zigrang & Sylvester approximation to the Colebrook expression and just 14% of the best non-Newtonian model (Tomita, 1959). While these results clearly demonstrate significant improvements upon existing data, more tests are required to verify conclusively the model.

Procedures for extending friction factors over all flow regimes (e.g., Wilson & Azad, 1975; Churchill, 1977) require empirical constants, with published values determined from investigations of Newtonian fluids. Reed & Pilehvari present a modification to the Churchill model involving n', Dodge & Metzner turbulent friction factor constants and the accepted criterion of $N_{Re,G,cr} \simeq 2100$; namely $f_{trans} = C(N) \times (N_{Re,G})^2$, with $C(N) = x/(y - zN)^2$, where $x = 9.4 \times 10^{-9}$, $y = 4.767$ and $z = 2.167$ respectively. These expressions failed to provide reasonable correlations against measured data and as such linear interpolation between laminar and turbulent friction losses (calculated at their respective critical GRN's) proved more satisfactory (refer to Appendix G for results).

3.3.3 Drillstring Equipment Losses - MWD's

MWD tool losses cannot be described by simple geometrical representations based on the assumption of a continuous unobstructed flow path due to the tortuous, throttling and often divisive flow aspect of such devices. While constituting a very small fraction of the total length of the drillstring, their contribution to system losses may be substantial (system losses of over 15% are not uncommon). Integration of vendor-supplied tool-loss data and drilling hydraulics applications is patchy at best with such devices often being ignored, given fixed losses regardless of operating conditions or through manual insertion of 'best guess' tool losses. Loss estimation is further complicated by the paucity and non-uniformity of vendors' data. Some provide reasonably detailed product performance data[6] while others fail to provide any such data.

Entirely empirical in form, the proposed method utilises vendor-supplied pressure loss data represented as a fourth-order polynomial, thus:

$$(\Delta p)_{MWD} \simeq \gamma \sum_{j=1}^{5} a_j Q^{(j-1)},$$

where a_j are tool-specific polynomial coefficients. Table 3.4 provides these coefficients for a selected number of tools from two major vendors along with the fluid SG's at which data was obtained (Anadrill MWD Tool Catalogue, 1993): interpolation between operating SG's will be necessary. While it is acknowledged that this approach is somewhat crude, it does provide a flexible method of including MWD tools in the drilling hydraulics calculation through appropriate tool database management.

[6]Sperry Sun Drilling Services (SSDS) conducted extensive laboratory tests for nine MWD toolstring configurations and provided equivalent tool internal diameters for use within a Darcy-Weisbach-type model for a range of fluid types with the friction factor being given by $f = 10^a$ where $a = -\left[\log_{10}(25.05Q\rho/\mu) + 8.3688\right]/5.86$. SSDS MWD tool losses are given by (Sperry-Sun, 1989):

$$(\Delta p)_{MWD} \simeq f \frac{T\rho L Q^2}{2129.48\,(D_{eff})^5},$$

all units are in SI. Effective diameters for SSDS tools (in inches) are: RLL with DGR & EWR sensors: 1.92 (with RTDT: 1.81; with CNØ sensors: 1.92 and with CNØ & RTDT: 1.84). MPT with DGR & EWR sensors: 1.78 (*std.*), 1.84 (*hf*); [with directional sensors; 1.74 (*std.*), 1.81 (*hf*); with CNØ sensors: 1.80 (*std.*), 1.85 (*hf*), or with both: 1.76 (*std.*), 1.84 (*hf*)] or with just the directional sensor: 1.68 (*std.*), 1.77 (*hf*). CNØ: compensated neutron porosity; DGR: dual gamma ray; EWR: electromagnetic wave resistivity; RLL: recorded lithology logging; RTDT: retrieving tool for data transmission; *hf*: high flow tool; *std*: standard tool.

Mud SG	Polynomial Coefficients					Valid for
	$a_1 \times 10^3$	$a_2 \times 10^5$	$a_3 \times 10^8$	$a_4 \times 10^8$	$a_5 \times 10^9$	Tool
Anadrill Drilling Services MWD Tools						
1.0000	-6.827358	8.346245	7.009699	5.056968	-2.519700	7″ & 8″ *std.*
1.0000	-6.682658	2.415737	4.577591	-1.272003	1.053814	9″ *std.*
1.0000	-1.215963	1.897576	4.122917	1.640302	-1.061027	6 1/2″ CDR
1.0000	-3.316288	4.493185	5.145181	4.180898	-3.024768	6 1/2″ CDN
1.0000	-1.248292	1.889564	0.915146	3.103912	-2.847095	8″ CDR
1.0000	-3.386808	5.790541	1.117237	7.674651	-6.349326	8″ CDN
1.0000	32.79840	-27.88220	1.113733	-10.7361	4.925302	9 1/2″ CDR
Halliburton Energy Services MWD Tools						
1.0784	2.298250	-0.932412	3.928430	-4.766620	0.0	All
1.1983	1.969929	2.645364	4.567608	-7.626575	0.0	All
1.4379	1.805771	12.46793	5.196566	-10.48645	0.0	All
1.6776	4.268186	13.53041	5.856356	-11.43971	0.0	All
1.9172	5.088986	7.263919	7.279349	-21.92643	0.0	All

Table 3.4: Polynomial coefficients for a small selection of MWD tools from two major vendors. Coefficients valid for the expression: $(\Delta p)_{\text{MWD}} \simeq \gamma \sum_{j=1}^{5} a_j Q^{(j-1)}$. CDR: compensated dual resistivity; CDN: compensated density neutron.

3.3.4 Drillstring Equipment Losses - PDM's and Turbines

Disruption of flow is more acute for PDM's (also known as Moineau motors) and turbines than for MWD tools. While tool losses contribute significantly to parasitic pressure losses (up to 25%, or more for tools fitted with nozzles), no published investigation has been found that considers such tool losses in any real detail. Most contemporary hydraulics calculation procedures for PDM/turbine pressure loss estimation involve: (1) manual input of tool loss (often relying on *rule-of-thumb* estimates) or, (2) fixed pressure loss values (regardless of operating conditions) or, (3) are omitted from the calculation completely. It is accepted in the field that tool losses are essentially a function of downhole torque and, to a lesser extent, WOB. The type of formation drilled, volumetric flow rate, internal tool configuration (lubrication requirements, by-pass settings, rotor-nozzle size, rotor-stator ratio etc.), mud weight and rheology also affect losses, but to a lesser extent[7]. The proposed empirical tool pressure loss function has the form:

$$(\Delta p)_{\text{PDM}} \approx (\Delta p)_{\text{nl}} + \Omega \left[\left(\frac{(\Delta p)_{\text{max}} - (\Delta p)_{\text{nl}}}{\text{WOB}_{\text{max}}} \right) \times \text{WOB} \right], \tag{3.27}$$

and is illustrated in Fig. 3.4. Ω is a dimensionless 'reactive torque factor' which adjusts the sensitivity of WOB to differential pressure (default = 1.0). This expression assumes: (1) mud weight, volumetric flow rate and rheology have a negligible effect on tool loss, (2) WOB emulates downhole torque linearly with zero torque corresponding to zero WOB, (3) differential pressure losses are linear between no-load to stall-out pressures, (4) stall-out pressure corresponds to the point just above the maximum allowable WOB, and (5) WOB can be accurately measured (or calculated) at the surface. Tool loss approximations are further complicated by the paucity and non-uniformity of vendors' data. While acknowledging the relative crudity of this method, the lack of any suitable alternative and the prevalence of these tools justifies its implementation until better alternatives are found.

[7]These observations are based on the authors' operational experience and numerous discussions with service personnel and directional drillers.

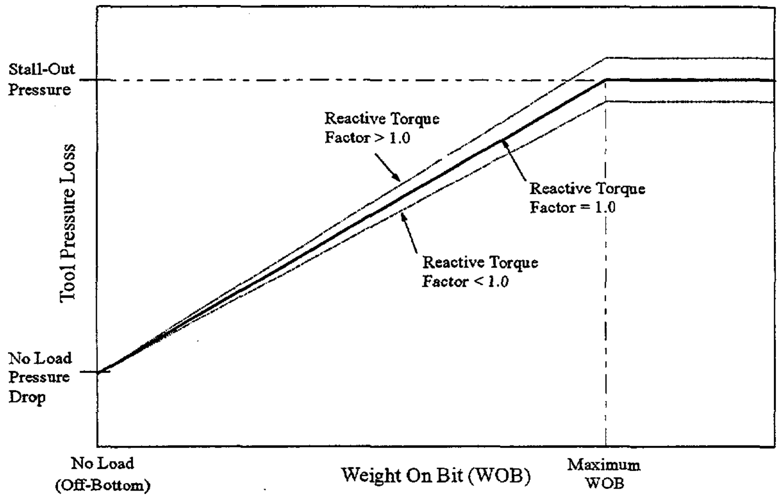

Figure 3.4: Schematic of PDM/turbine pressure loss function.

Flowrate	Polynomial Coefficients					
[lpm]	$a_1 \times 10^{-1}$	$a_2 \times 10^{-4}$	$a_3 \times 10^{-7}$	$a_4 \times 10^{-11}$	$a_5 \times 10^{-15}$	$a_6 \times 10^{-19}$
757	9.857	1.587	-2.716	8.842	-10.47	3.333
1514	9.930	-3.141	0.580	-0.247	-0.258	0.0
2272	9.903	-4.825	1.594	-2.583	1.603	0.0
3028	9.881	-6.338	2.674	-5.339	3.954	0.0
3785	9.887	-7.374	3.445	-7.404	5.792	0.0
4542	9.880	-7.963	3.834	-8.381	6.641	0.0

Table 3.5: Polynomial coefficients for 'Toms phenomenon' (for six different volumetric flowrates) for the expression: $\mathrm{T} = \sum_{j=1}^{6} a_j x^{(j-1)}$ where x is the concentration of drag-reducing polymer (in ppm).

3.3.5 Friction-Reducing Polymers

Experimental data descibing the effect of drag-reducing polymers (polymethyl methacrylate in monochlorbenzene) through straight tubes at large Reynolds numbers (Toms, 1948; Hoyt, 1972) has been translated into 6th-order polynomial coefficients to fit the expression: $\mathrm{T} = \sum_{j=1}^{6} a_j x^{(j-1)}$. T ('Toms phenomenon' factor) is a dimensionless multiplier used to adjust normalised calculated pressure losses (for all regimes and system components), x is polymer concentration (in ppm) with coefficients presented in Table 3.5. Coefficients are valid for concentrations: $0 \leq x \leq 5000$, and flow rates: $757 \leq Q \leq 4542$ lpm.

Model	Mud 'A' RMS's			Mud 'B' RMS's			Avg. RMS
	1″	2″	3″	1″	2″	3″	
Bingham Plastic (*npf*)	12.91	0.19	1.48	10.49	5.05	4.10	5.70
Bingham Plastic (*pf*)	8.44	0.44	1.28	6.86	1.43	4.30	3.79
Casson (*npf*)	5.32	0.10	1.17	2.35	2.03	3.19	2.36
Casson (*pf*)	5.05	0.17	1.12	4.79	1.24	3.56	2.65
Collins-Graves	15.55	1.82	0.98	7.82	2.15	5.76	5.68
Ellis *et al.*	4.42	0.04	1.69	21.93	3.04	2.13	5.54
Herschel-Bulkley (*npf*)	5.03	0.01	1.44	2.29	1.98	3.36	2.35
Herschel-Bulkley (*pf*)	4.91	0.03	1.37	6.52	1.41	3.81	3.01
Hyperbolic (*npf*)	7.22	0.05	1.85	-	-	-	3.04
Hyperbolic (*pf*)	6.75	0.02	1.66	-	-	-	2.81
Power Law	3.32	0.04	1.51	6.94	1.49	2.48	2.63
Reiner-Philippoff	46.03	2.69	1.59	906.2	53.35	50.62	176.7
Robertson-Stiff (*npf*)	4.65	0.01	1.50	2.00	1.89	4.18	2.38
Robertson-Stiff (*pf*)	4.75	0.04	1.38	15.42	4.50	9.39	5.91
Sisko	5.42	0.10	1.26	2.48	2.00	3.04	2.37

Table 3.6: RMS values for ten different rheological models considered in the laminar pipe flow analysis. *npf*: plug flow was not considered in the calculation; *pf*: plug flow was considered in the calculation.

3.3.6 Drillstring Friction Losses - Model Comparison

Predictions provided by the proposed model were compared against data obtained from three pipe diameters and two drilling fluids for laminar, transitional and turbulent flow (Okafor, 1982). Appendix G presents detailed tabular and graphical results for the ten rheological models considered in this part of the analysis. These ten models included all those previously presented to the industry as well as Ellis *et al.*, Hyperbolic, Reiner-Philippoff and Sisko. Restricting the number of models considered was deemed necessary in order to reduce the weightiness of result tables/figures, to facilitate visibility and ease interpretation of results without compromising analytical substantiality.

Table 3.6 summarises laminar flow pressure loss RMS's (with and without plug flow). While it is clear that Reiner-Philippoff provided the poorest quality predictions for all six cases (with an average RMS of 176.7), it is apparent that no single model has an outright advantage for both fluid types and all conduit sizes examined. While one model may perform better than another for one mud type, it may perform significantly worse for another (e.g., Ellis *et al.* and Robertson-Stiff). The results support the conclusions of the detailed rheological model comparison (section 2.5 on page 22) where it was established that Sisko furnished the most consistent and accurate fluid characterisation. The small RMS of 2.37 for the Sisko model (compared to RMS's of 2.35 for Herschel-Bulkley, without plug flow, and 2.36 for the Casson model, without plug flow) supports the suposition that this model indeed provides reliable results for fluids not represented in the large data set upon which the model's recommendation was drawn.

Figures G.1 to G.12 (from page 192 onwards) present measured and calculated pressure losses for laminar, transitional and turbulent flow versus average fluid velocity. Examination of only the laminar flow portions of Figs. G.1 & G.2 for the 1″ pipe, mud 'A' clearly indicates excellent agreement between calculated and measured pressure losses for all except Collins-Graves, Bingham Plastic and Reiner-Philippoff models. The former model deviates beyond the ±5% data measurement accuracy markers[8] at lower velocities. Bingham Plastic consistently under-predicted pressures (below the acceptable ±5% error bound) while the latter provided somewhat extreme under-predictions. For mud 'B' (Figs. G.3 & G.4) one sees less consistency in predictive quality with Ellis *et al.* over-predicting pressures and Bingham Plastic under-predicting over all laminar shear rates (velocity equivalent). Reiner-Philippoff yielded very poor modelling quality due to near-unity values of N (emulating a Newtonian fluid) while the Power Law provided moderate over-predictions at average velocities less than 1.0 m/s. The remaining models predict laminar pressure losses within acceptable error bounds. Figures G.5 & G.6 (mud 'A', 2″ pipe) reveal similar patterns of over- and under-prediction, although the over-prediction provided by Collins-Graves is more pronounced than observed for the 1″ pipe. Figures G.7 & G.8 demonstrate similarly less consistent modelling quality to that observed in the 1″ pipe, however deviations are more extreme. Some doubt exists as to the quality of the measured data at velocities below 0.6 m/s where observed pressure loss profiles deviate from expected trends. Nevertheless, most of the models considered provide predictions within acceptable margins, although the pseudo-Newtonian performance of Reiner-Philippoff was clearly unacceptable. Figures G.9 & G.10 present results for mud 'A' in the 3″ pipe and shows poor modelling by Bingham-Plastic Casson, Collins-Graves and Reiner-Philippoff. Surprisingly Sisko slightly over-predicted pressures between 0.30 to 0.55 m/s while Herschel-Bulkley, Hyperbolic and Robertson-Stiff provided reasonable modelling over most of the laminar flow region. Finally, Figs. G.11 & G.12 (3″ pipe, mud 'B') reveals consistently poor laminar flow modelling by most models with only Sisko providing more acceptable predictions. These findings imply that most of the models considered will furnish reasonable laminar flow friction pressure losses for commonly employed drill pipes so long as the drilling fluid is characterised by generalised flow behaviour indices closer to unity than zero. Where the fluid is characterised by small values of N, laminar flow losses in nominal 3″ drill pipes will experience poorer modelling quality. In this case the Sisko model is expected to furnish more reasonable results (again supporting the notion that this model is suitable as a default).

Tables G.1 to G.24 (from page 168 onwards) provide detailed results (for laminar, transitional and turbulent flow) for the ten rheological models and the three pipe sizes considered. Near-linear $N_{\mathrm{Re,G}}$, τ_w and $\dot{\gamma}_w$ profiles were obtained when plotted against velocity while nonlinear profiles for N and $D_{\mathrm{eff,G}}$ for most rheological models, typified by Fig. G.13, page 198, were obtained. Such nonlinearity is expected due to the pseudoplastic profiles having a steeper gradient at lower shear rates than at higher shear rates. As N represents the instantaneous rate of change of the rheogram, any quantity derived from the gradient of the rheogram will inevitably be reflected in the profiles of derived quantities, as observed in the figure.

The effect of considering plug flow in the calculation does not demonstrate any regularity in improved solution. Modest improvements in average RMS's are apparent in two models: Bingham Plastic (from 5.70 to 3.79) and Hyperbolic (from 3.04 to 2.81) while a small deterioration is present for Herschel-Bulkley (from 2.35 to 3.01), Casson (from 2.36 to 2.65) and Robertson-Stiff (from 2.37 to 5.91). Figure G.14 on page 198 presents calculated values of λ (labelled 'radial fraction') against velocity for the 1″ pipe. These results confirm the expected behaviour of λ with velocity trends. As velocity increases, the unsheared plug begins to shed finite concentric layers to the laminar flow region, thereby decreasing the radius of the plug flow region. The rate of layer-shedding is initially more rapid and reduces as velocity increases. The usual

[8] The Sensotec pressure transducers used to record the data have a stated accuracy of ±5%.

over-estimate of the Bingham Plastic yield-stress, τ_o, results in more pronounced plug flow layer shedding than for other models who more accurately predict τ_y. Furthermore, Bingham Plastic λ-values do not correspond to other λ-values, indicating constant over-estimation in the size of the plug flow region. What remains uncertain is the apparent instantaneous break-down of the plug flow region at the cessation of laminar flow. Maintenance of a plug flow region in transitional flow is possible if one accepts the Rothfus conjecture of discrete flow regimes co-existing in the same conduit element. It may be possible for plug flow to survive in the centre while turbulence exists in the outer regions of the conduit, only to be eroded away, and then cease, as fluid velocity increases. On the other hand, if one accepts the Fredrickson-Bird argument that only one regime may exist in a conduit element at any one time then at termination of laminar flow the plug flow region will experience an instantaneous break-down as transitional or turbulent effects renders any remaining unsheared region apart. Neither of these postulations can be confirmed or disproved from this analysis alone, hence extension of calculated λ's beyond purely laminar flow is represented as dashed lines. Figures G.15 & G.16 presents λ (labelled radial fraction) versus average velocity plots for 2″ and 3″ pipes and shows very similar behaviour to that discussed for the 1″ pipe. While these results are insufficient to conclude whether plug flow should be considered or not in the calculation, in operational environments one may need to evaluate the benefits of including plug flow against the added computation time required to perform the additional iterations.

3.3.7 Annular Friction Losses - Laminar Flow

It has already been stated that the annular flow field may be described in terms of two separate regions (Rothfus, 1948): (1) the inner, or core, region describing the fluid from the central pipe to the point in the annular flow field of maximum *in situ* fluid velocity (marked by the dimensionless radial fraction parameter λ), and (2) an outer, or wall, region describing the fluid from λ to the outer conduit inner wall. If one accepts the assumptions stated previously in section 3.2.1, page 45, one can extend both the concentric annular flow-field segregation concept to an expanded Herzog—Weissenberg-type formulation to provide a generalised laminar pressure loss expression that can include plug flow and any rheological model.

For a fluid possessing no yield stress the generalised implicit flow function is given by:

$$\begin{aligned}\bar{v} \;=\; & 2R\int_{\psi}^{\lambda} y \int_{\psi}^{\lambda} f^{-1}\left(\frac{\Delta pR}{2L}\left|\frac{\lambda^2}{z}-z\right|;\phi\right)\mathrm{d}z\,\mathrm{d}y \\ & +2R\int_{\lambda}^{1} y \int_{\lambda}^{1} f^{-1}\left(\frac{\Delta pR}{2L}\left|\frac{\lambda^2}{z}-z\right|;\phi\right)\mathrm{d}z\,\mathrm{d}y,\end{aligned} \tag{3.28}$$

where the shear stress at any radial position is given by:

$$\tau = \frac{\Delta pR}{2L}\left|\frac{\lambda^2}{z}-z\right|. \tag{3.29}$$

Geometrical parameters used in Eq.(3.28) are illustrated in Fig. 3.5. Initial guesses of λ can be

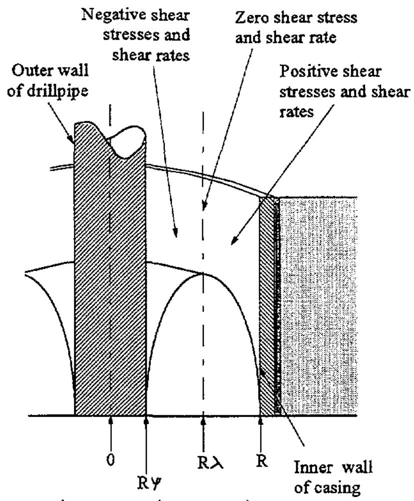

Figure 3.5: Geometries in a concentric annulus without plug flow.

obtained from either setting it to be half-way in the annular flow field using $\lambda = (1+\psi)/2$, or from the expression derived from purely Newtonian fluids $\lambda^2 = \left(\psi^2 - 1\right) / (2\ln(\psi))$.

The rigorous solution for λ is provided by satisfying the following implicit function obtained from the fact that fluid velocity at conduit walls is zero (the no-slip assumption):

$$0 = \int_{\psi}^{\lambda} f^{-1}\left(\frac{\Delta pR}{2L}\left|\frac{\lambda^2}{z} - z\right|;\phi\right)\,\mathrm{d}z + \int_{\lambda}^{1} f^{-1}\left(\frac{\Delta pR}{2L}\left|\frac{\lambda^2}{z} - z\right|;\phi\right)\,\mathrm{d}z. \tag{3.30}$$

Numerical root-finding for the value of λ that satisfies Eq.(3.30), where $\psi \leq \lambda \leq 1$, is necessary. For fluids possessing a yield stress the generalised implicit flow function is as follows:

$$\begin{aligned}
\bar{v} \;=\; & 2R\int_{\psi}^{\lambda_{[-]}} y \int_{\psi}^{\lambda_{[-]}} f^{-1}\left(\frac{\Delta pR}{2L}\left|\frac{{\lambda_{[-]}}^2}{z} - z\right|;\phi\right)\,\mathrm{d}z\,\mathrm{d}y \\
& +2R\int_{\lambda_{[-]}}^{\lambda_{[+]}} y \int_{\lambda_{[-]}}^{\lambda_{[+]}} f^{-1}\left(\frac{\Delta pR}{2L}\left|\frac{\lambda^2}{z} - z\right|;\phi\right)\,\mathrm{d}z\,\mathrm{d}y \\
& +2R\int_{\lambda_{[+]}}^{1} y \int_{\lambda_{[+]}}^{1} f^{-1}\left(\frac{\Delta pR}{2L}\left|\frac{{\lambda_{[+]}}^2}{z} - z\right|;\phi\right)\,\mathrm{d}z\,\mathrm{d}y.
\end{aligned} \tag{3.31}$$

The geometrical quantities involved are presented in Fig. 3.6. Further manipulations of Eq.(3.29)

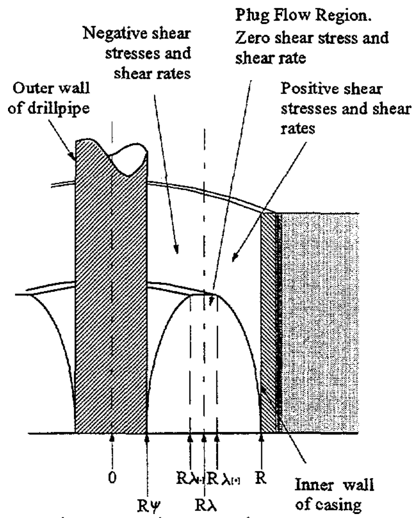

Figure 3.6: Geometries in a concentric annulus with plug flow.

allows construction of the following relationship: $\lambda = \sqrt{\lambda_{[+]} \cdot \lambda_{[-]}}$, which is partially derived from:

$$R \left| \frac{\lambda^2}{\lambda_{[+]}} - \lambda_{[+]} \right| = \tau_y \frac{2L}{\Delta p}.$$

Consequently the three annular flow fields represented in Eq.(3.31) can be solved through a combination of these equations.

3.3.8 Annular Friction Losses - Turbulent and Transitional Flow

Eq.(3.26) is also valid for turbulent flow in a concentric annulus as N, $D_{\text{eff},\text{G}}$ and $\text{N}_{\text{Re},\text{G}}$ can be defined for annular geometry. Similarly, treatment of transitional flow is also valid so long as consistency in parameter usage is maintained. As stated in section 3.2.3, page 52, uncertainty remains in establishing proper/reasonable critical Reynolds numbers for the demarcation of flow regimes. Consequently $\text{N}_{\text{Re},\text{G},\text{cr}} \simeq 2100$ and $\text{N}_{\text{Re},\text{G},\text{cr}} \approx 2900$ are used (in the absence of more precise alternatives) in subsequent analysis to define lower- and upper-transitional flow regime delimiters.

3.3.9 Drillstring Rotation

Drillstring rotation effects on annular pressure loss is governed by two principle phenomena: helical flow and Taylor vortices. The latter phenomenon (Drazin & Reid, 1981; Barnes, Hutton & Walters, 1989) is associated with increased pressure losses, with a succinct summary provided by Marken, Xiaojun He & Saasen (1992). Helical laminar flow may be visualised as concentric fluid 'shells' sliding over one another in a regular screw-like motion with no fluid transfer radially between 'shells' (unlike Taylor vortices). Walker & Al-Rawi (1970) verified experimentally the theoretical expectation that helical flow will result in reduced pressure losses as inner-pipe rotation increases (Bird, Armstrong & Hassager, 1977). Confirmation of expected pressure variations due to both helical and Taylor vortices effects in slimhole operations, have been presented by various investigators (Delwiche *et al.*, 1992; Cartalos & Dupuis, 1993; McCann, Quigley, Zamora & Slater, 1993; Ribeiro, Podio & Sepehrnoori, 1993) who also considered drillstring vibration and eccentricity effects.

Eqs.(3.28 & 3.31) can accommodate *in situ* tangential shear rates at any radial point by substituting the *in situ* axial shear rate term (denoted previously as $\dot{\gamma}_r$ or simply $\dot{\gamma}$) for:

$$\dot{\gamma}_{z,\mathrm{hel}} = \sqrt{\dot{\gamma}^2_{z,\mathrm{x}} + \left(\frac{1-z}{1-\psi}\right)^m \times \dot{\gamma}^2_{w,\mathrm{tan}}}, \tag{3.32}$$

where $\dot{\gamma}_{z,\mathrm{x}}$ represents the *in situ* axial shear rate and $\dot{\gamma}_{w,\mathrm{tan}}$ is the tangential shear rate acting on the rotating pipe wall, given by Guillot (1990) as

$$\dot{\gamma}_{w,\mathrm{tan}} = \frac{\omega D_\mathrm{i}}{D_\mathrm{o} - D_\mathrm{i}}.$$

Eq.(3.32) differs from that presented by Marken *et al.* (1992) in that it does not require an average axial wall shear rate and the inclusion of a $\dot{\gamma}_{w,\mathrm{tan}}$ decay term, the rate of which is determined by the exponent m.

3.3.10 Annular Eccentricity

While a number of investigations have proposed several different corrections for eccentric annular flow (Vaughn, 1965; Wallick & Savins, 1969; Mitsuishi & Aoyagi, 1973; Iyoho & Azar, 1980; Yuejin Luo & Peden, 1990), all such proposals were constructed on equations valid for concentric annular flows only, thereby failing to obtain satisfactory results. The model (Haciislamoglu, 1989; Haciislamoglu & Langlinais, 1990) was not formulated upon concentric flow models and is, by far, the simplest, most accurate and versatile of any in the available literature. Based on dimensional analysis of a bi-polar co-ordinate translation of annular geometry for Herschel-Bulkley fluids (grounded on the approach proposed by Guckes, 1975), and fitted to a simple equation using nonlinear least squares, Haciislamoglu developed an expression valid for eccentricities from 0.0 to 0.95 with aspect ratios of 0.3 to 0.9 and yield-Power Law flow behaviour indices of 0.4 to 1.0. If one accepts the proposition that the generalised flow behaviour index suitably mimics yield-Power Law-type indices for all fluid models then it is reasonable to extend Haciislamoglu's correlation to incorporate generalised parameters thus:

Model	Mud 'A' RMS's		Mud 'B' RMS's		Avg.
	1″× 3″	1.5″× 3″	1″× 3″	1.5″× 3″	RMS
Bingham Plastic	0.750	5.167	7.380	57.70	17.75
Bingham Plastic, Eq.(3.4)	0.750	5.167	7.380	57.70	17.75
Bingham Plastic, Eq.(3.3)	0.690	555.8	2.186	159.5	179.5
Casson	0.365	4.524	6.675	46.86	14.61
Casson, Eq.(3.8)	0.106	5.929	8.546	395.5	102.5
Collins-Graves	1.174	14.87	2.928	23.98	10.74
Ellis *et al.*	1.974	1.381	6.731	36.97	11.76
Herschel-Bulkley	0.396	4.466	8.008	54.63	16.87
Hyperbolic	0.426	6.277	-	-	(3.35)
Power Law	1.739	1.183	1.281	11.69	3.97
Power Law, Eq.(3.5)	0.036	2.178	2.106	14.10	4.60
Reiner-Philippoff	10.01	14.98	187.8	241.9	113.7
Robertson-Stiff	0.331	5.245	9.224	59.86	18.66
Robertson-Stiff, Eq.(3.9)	0.398	7.102	10.75	96.34	28.64
Sisko	0.766	2.263	0.870	3.934	1.96

Table 3.7: RMS values for ten different rheological models considered in the laminar concentric annular flow analysis. Aspect ratios: $\psi = 0.43077$ for 1″× 3″ and $\psi = 0.62306$ for 1.5″ × 3″. Unless specified otherwise, all entries are calculated from either Eq.(3.31) for models possessing a yield stress, or Eq.(3.28) for models not possessing a yield stress.

$$\mathrm{R} = 1 - 0.072\frac{\epsilon}{N}(\psi)^{0.8454} - 1.5\epsilon^2\sqrt{N}(\psi)^{0.1852} + 0.96\epsilon^3\sqrt{N}(\psi)^{0.2527}, \tag{3.33}$$

where ϵ is a dimensionless representation for annular eccentricity. For concentric annuli, $\epsilon = 0$, and for fully eccentric conditions, $\epsilon = 1$. Eccentricity for strings with no centralisers is given by $\epsilon = 2\delta/(D_o - D_i)$, and when the string possesses a centraliser or other stabilising components (assumed to contact the outer conduit wall), eccentricity is given by $\epsilon = (D_o - D_c)/(D_o - D_i)$. The stated accuracy of Eq.(3.33) against the full-form model is ±5%, and is used in Eq.(3.34) to predict pressure loss gradients in eccentric annular geometry from

$$\left(\frac{\Delta p}{\Delta L}\right)_{\mathrm{ecc}} = \mathrm{R} \times \left(\frac{\Delta p}{\Delta L}\right)_{\mathrm{conc}}. \tag{3.34}$$

3.3.11 Annular Friction Losses - Model Comparison

Laminar flow losses provided by Eq.(3.28), page 63, or Eq.(3.31), page 64, were compared against published laminar flow pressure loss data obtained for two drilling fluids in two concentric annular geometries (Okafor, 1982). Appendix H presents detailed tabular and graphical results for the same ten rheological models considered in the pipe flow comparison (section 3.3.6).

Table 3.7 summarises model RMS's (in kPa^2) calculated for conduits: 1″× 3″ ($\psi = 0.43077$) and 1.5″× 3″ ($\psi = 0.62306$). This table shows that the Sisko model provided the lowest average RMS (at 1.96), less than 50% of the next-best performing model (Power Law). Reiner-Philippoff proved unreliable with a significantly greater RMS (113.7) than any other model and can, therefore, be dismissed from further consideration. There were little real differences in the performance of the remaining models with RMS's residing in a narrow spread between

10.74 (Collins-Graves) and 18.66 (Robertson-Stiff). As for the pipe flow analysis, numerical divergencies developed in the solution to the Hyperbolic model for mud 'B' only and casts some doubt on the Hyperbolic model solution robustness, while also prohibiting a like-with-like performance comparison with other models.

Unlike the predictions provided for pipe flow, those for annular flow show more deviation about expected values - Figs. H.1 to H.8 inclusive (page 212 onwards), with detailed results presented in Tables H.1 to H.10 respectively (pages 202 to 211 inclusive). For mud 'A' in the $\psi = 0.431$ conduit, Bingham Plastic in Fig. H.1 (page 212) shows clear over-prediction of laminar pressure losses at average fluid velocities less than 0.6 m/s whilst tending to under-predict values at velocities greater than 1.1 m/s. Nevertheless, the low associated RMS value of 0.750 indicates good agreement with expected values. Behaviour of Collins-Graves at lower average velocities was markedly poor, however at velocities higher than 1.0 m/s it became the only model to furnish predictions within the $\pm 5\%$ tolerances. Sisko provided almost exact matching for the first four data points in Fig H.2 while slightly under-estimating losses at higher velocities. Herschel-Bulkley provided good estimates at lower flow rates, but then under-predicted pressure losses at higher velocities. Although not explicitly stated by Okafor, it is believed that cessation of laminar flow occurs close to the upper data points thereby indicating that the consistent under-predictions at higher velocities supplied by all models will have only a limited impact on final annular system laminar pressure loss estimates.

Figures H.3 & H.4 (page 213) illustrate predictions for mud 'A' in the $\psi = 0.62306$ conduit and shows very modest over-predictions of pressures for all but Collins-Graves and Reiner-Philippoff models. This is reflected in characteristically low RMS's (Table 3.7) with all but the aforementioned models producing RMS's being below 7 kPa^2, indicating good modelling. Greater inconsistency and deviation was, however, observed for mud 'B' in the 1″× 3″ conduit. The over-predictions exhibited by Collins-Graves in Figs. H.1 & H.3 are no-longer apparent in Fig. H.5 (page 214) where the model under-predicts all those presented on the figure over most of the velocity range plotted. Figure H.6 (page 214) shows that the Power Law and, in particular, Sisko furnished very good agreement with expected values. This is demonstrated by Sisko having the smallest RMS of all models (0.870) with the Power Law having an RMS of 1.281. The remaining models (excluding Reiner-Philippoff which performed consistently poorly) also displayed acceptable RMS's (ranging from 2.928 for Collins-Graves to 9.224 for Robertson-Stiff). Figures H.7 & H.8 (page 215) present the results for the mud 'B', $\psi = 0.62306$ aspect ratio system where, again, more deviation from expected is observed. For this case, Sisko yields a significantly lower RMS than any of the other models (3.934, compared to the next best RMS of 11.69 for the Power Law).

As expected, the implicit-exact flow expression for Bingham Plastics, Eq.(3.4), furnished identical pressure loss predictions to those provided by Eq.(3.31). The slot-flow derived equivalent expression, Eq.(3.3), yielded higher RMS values than those obtained from the rigorous method. The modest RMS differences between the two approaches for the low aspect ratio system is not unexpected (see Exlog, pp. 99). Differences in RMS's between the rigorous and slot-flow derived flow models were also obtained for Power Law, Casson and Robertson-Stiff: Eqs.(3.5, 3.8 & 3.9) respectively (Table 3.7). The marked differences resulting from applying the slot-flow assumption for the higher aspect ratio system are substantial enough to warrant application of the rigorous approach. For slimhole and/or high aspect ratio systems therefore, the rigorous approach is likely to be the most appropriate solution.

A minor reservation is levelled at the measured data used in this comparison. It is not certain whether the 10.9728 m long inner pipe in the measurement apparatus employed was kept completely central through the deployment of centralizers. Consequently it is likely that measured data have values slightly under what would have been recorded if centralizers were used. This may account for (in part) the modest over-predictions provided in the higher aspect-ratio system. In short, one is unable to draw fully convincing conclusions from this data alone. More rigorous and substantial data (covering a range of aspect ratios, flow rates and fluid types) is required to provide the confirmation needed.

The pressure loss reducing effects of helical flow due to concentric drillpipe rotation are illustrated in Figs. H.9 & H.10 (page 216). These figures present the ratio of pressure with rotation to the loss with a static drillpipe versus rotation speed for six different annular aspect ratios. Both figures represent results for a single average fluid velocity of 0.636 m/s with the shear rate decay exponent set at $m = 3$. Increasing the decay exponent in Eq.(3.32) has the effect of reducing the pressure ratio and *vice versa.* Of interest is the observation that pressure reduction is more pronounced for fluids with smaller values of N. For example, at a rotation of 150 s^{-1} (88 rpm) mud 'A' flowing in a concentric annulus with a low aspect ratio ($\psi = 0.4$) experiences a pressure of about 0.84 of that of the equivalent static system, while for mud 'B' this proportion increases to about 0.95. It is also observed that helical flow effects are less marked on high aspect ratio annuli. This may be of significance for slimhole operations where pipe rotation and annular aspect ratios are characteristically high and where annular pressure losses are also high.

3.4 Determining Confidence Intervals

The nonlinear fits of the rheological model detailed in section 2.4, page 19, are of restricted utility. One of their primary purposes is to determine laminar friction losses in the circulating system. If one lets all other variables in the system be fixed, then *cetarus paribus* the various calculated quantities that use the fitted model are simply nonlinear functions of the fitted model parameters. This section presents formulae that allow calculation of approximate confidence intervals and tests of significance of the function to be performed.

3.4.1 Statistical Formulae

Let $h(\hat{\phi})$ be the nonlinear function of interest that is obtained using the estimated rheological model parameters, $\hat{\phi}$. Then, using the results of Gallant (1987), an approximate $100(1-\alpha)\%$ confidence interval estimate of the true value of the nonlinear function is given by

$$h(\hat{\phi}) \pm t_{[(n-p);\alpha]}\sqrt{\hat{H}\left(\hat{F}^T\hat{F}\right)^{-1}\hat{H}^T s^2} \tag{3.35}$$

where

$$\hat{H} = \begin{pmatrix} \frac{\partial[h(\hat{\phi})]}{\partial\phi_1} & \frac{\partial[h(\hat{\phi})]}{\partial\phi_2} & \cdots & \frac{\partial[h(\hat{\phi})]}{\partial\phi_p} \end{pmatrix} \tag{3.36}$$

is the row vector of partial derivatives of $h(\hat{\phi})$ with respect to the rheological model parameters,

Shear Rate [s^{-1}]	Observed Shear Stress [Pa]	Expected Shear Stress [Pa]	95% Confidence Interval [Pa]
5.11	9.8188	9.9966	(9.2970 , 10.6961)
10.22	11.0162	10.7365	(10.1365 , 11.3365)
170.33	15.3269	15.5803	(14.9904 , 16.1702)
340.67	17.9612	18.1536	(17.5959 , 18.7114)
511.00	20.8349	20.3545	(19.8492 , 20.8598)
1022.00	26.1035	26.2393	(25.3527 , 27.1258)

Table 3.8: Observed rheological data, reparameterised Sisko expected values and confidence limits.

$$\hat{F} = \begin{bmatrix} \frac{\partial[f(\dot{\gamma}_1;\hat{\phi})]}{\partial\phi_1} & \frac{\partial[f(\dot{\gamma}_1;\hat{\phi})]}{\partial\phi_2} & \cdots & \frac{\partial[f(\dot{\gamma}_1;\hat{\phi})]}{\partial\phi_p} \\ \frac{\partial[f(\dot{\gamma}_2;\hat{\phi})]}{\partial\phi_1} & \frac{\partial[f(\dot{\gamma}_2;\hat{\phi})]}{\partial\phi_2} & \cdots & \frac{\partial[f(\dot{\gamma}_2;\hat{\phi})]}{\partial\phi_p} \\ \vdots & \vdots & & \vdots \\ \frac{\partial[f(\dot{\gamma}_n;\hat{\phi})]}{\partial\phi_1} & \frac{\partial[f(\dot{\gamma}_n;\hat{\phi})]}{\partial\phi_2} & \cdots & \frac{\partial[f(\dot{\gamma}_n;\hat{\phi})]}{\partial\phi_p} \end{bmatrix} \tag{3.37}$$

is the $n \times p$ matrix of partial derivatives of the rheological model evaluated at $\hat{\phi}$ and the n data points $\dot{\gamma}_i$, s^2 is the estimated error variance given by the RMS value, and $t_{[(n-p);\alpha]}$ is the t-distribution value corresponding to the significance level α. The approximate t-test of the null hypothesis that h_0 is the true value of the nonlinear function is

$$t = \frac{h(\hat{\phi}) - h_0}{\sqrt{\hat{H}\left(\hat{F}^T\hat{F}\right)^{-1}\hat{H}^T s^2}}$$

and has $(n-p)$ degrees of freedom. The accuracy of the above approximations will increase with sample size; for small data sets, a close-to-linear model is necessary to ensue that the above formulae are valid.

3.4.2 Example

An application of the methodology presented previously is applied to the calculation of laminar pressure losses due to friction in a circular pipe using Eq.(3.24). Since the inverse rheological relationship cannot be expressed explicitly, the value of $f^{-1}(\tau;\phi)$ needs to be found numerically from the root of

$$0 = f^{-1}\left(\frac{\Delta p R z}{2L};\phi\right) - \dot{\gamma},$$

for which NAG routine `C05ADF` was used (a routine that locates a zero of a continuous function in a given interval). The double integral is numerically approximated using routines `D01AJF` and `D01AHF` for the inner- and outer-integral respectively. Both of these routines are general purpose integrators that calculate an approximation to the integral of a function over a finite

Average Velocity [m/s]	Observed Pressure Drop [kPa]	Expected Pressure Drop [kPa]	95% Confidence Interval [kPa]
0.5617	31.0057	30.7040	(29.6503 , 31.7576)
0.5995	31.1712	31.1161	(30.0623 , 32.1705)
0.6931	32.3502	32.0907	(31.0390 , 33.1423)
0.7324	32.7983	32.4829	(31.4336 , 33.5322)
0.8431	34.0256	33.5422	(32.5025 , 34.5819)
1.0104	35.6045	35.0454	(34.0258 , 36.0651)
1.1506	36.2181	36.2341	(35.2332 , 37.2350)
1.2802	37.4178	37.2875	(36.3034 , 38.2716)

Table 3.9: Observed laminar pressure drops for mud 'B' flowing in a 10.9728 m long, 1″ [nominal] (2.59944×10^{-2}) i.d. horizontal pipe. Also presented are expected values and 95% confidence intervals calculated using the fitted reparameterised Sisko model.

range. Finally, C05AJF is used to locate the zero of Eq.(3.24). The vector of partial derivatives $\hat{H}$ is estimated using the routine D04AAF. This routine uses an extension of the Neville algorithm (Lyness & Moler, 1967) and bases the results on 21 function values at points determined by a user supplied step length. The accuracy of the results is critically dependent on the choice of step length; examination of the routine's estimate of the absolute error can be used to provide a suitable value.

Data presented by Okafor was used to investigate laminar pressure loss predictions. The rheological data from the six Fann viscometer settings for mud 'B', a 1,036.3 kg/m^3 clay-water drilling fluid, is given in Table 3.8. The resulting Sisko nonlinear least squares parameter estimates are $a = 9.39968 \times 10^{-3}$, $b = 8.49260$ and $c = 9.70027 \times 10^{-2}$, and give a RMS value of 0.15346. The IN and PE values are 0.01386 and 0.26630 respectively and are compared to the critical value of $1/\left(2\sqrt{F_{[3,3;0.05]}}\right) = 0.16413$. The IN value is non-significant but the PE value is significant, thus a reparameterisation is required. Using the same grid employed in section 2.5.5, page 26, the chosen Sisko$^{\mathrm{R}}$ constants are $(\dot{\gamma}_1, \dot{\gamma}_2) = (87.5, 812.5)$ giving a non-significant PE value of 0.03015. The corresponding parameters are $\tau_1 = 13.9270$, $\tau_2 = 23.9040$ and $c = 9.70027 \times 10^{-2}$. The expected shear stresses and 95% confidence intervals for the data are given in Table 3.8. The latter are calculated using Eqs.(3.35 to 3.37) where the nonlinear function of interest, $h(\hat{\phi})$, is the expected shear stress and $\hat{H}$ is the fitted model's vector of partial derivatives evaluated at the required shear rate. For example, consider the slowest conventional shear rate at which data is recorded (5.11 s^{-1}), the corresponding values are:

$$\hat{H} = (0.86730, -0.08711, -25.1004)\,,$$

$$\hat{F} = \begin{bmatrix} -0.33721 & 1.29416 & -6.03211 \\ 0.46867 & 0.57845 & 6.47482 \\ 0.71623 & 0.34215 & 7.92002 \\ 0.93097 & 0.10938 & 5.34668 \\ 0.91924 & -0.08642 & -19.7156 \\ 0.86730 & -0.08711 & -25.1004 \end{bmatrix},$$

with $t_{[3;0.05]} = 2.35338$, and $s^2 = 0.15346$.

Inserting the above values into Eq.(3.35), the interval $(9.2970, 10.6961)$ is obtained. Note, for all interval calculations $\hat{F}$, s^2 and the t-distribution values remain constant. In Fig. 3.7 the observed rheological data, expected values and 95% confidence limits are presented; it can be seen that all observed data points fall within the limits.

Table 3.9 presents the observed pressure losses together with their respective average fluid velocities are given. For each average fluid velocity, the expected pressure drop and 95% confidence interval were calculated using Eqs.(3.35 and 3.37) and Eq.(3.24), and given in Table 3.9. In Fig. 3.8 the observed laminar pressure losses are displayed together with the expected values and confidence limits over a suitable range of average fluid velocities. Whilst Okafor's observed values are not exact (the pressure transducers used in the recording of the data have a stated error of ± 0.1723 kPa), it is reassuring to see that Sisko^{R} provides reasonable modelling of the data and that all of the observed values fall within the confidence limits.

3.5 Chapter Summary

Contemporary treatment of Bingham Plastic, Power Law, Casson, Herschel-Bulkley and Robertson-Stiff rheological models within drilling hydraulics calculations was examined with a number of concerns raised relating to the consistency of their treatment and the assumptions inherent in the formulation of their respective flow functions. Proposals for the generalised and consistent treatment of flow regimes and laminar flow functions (without imposing any assumptions concerning annular geometry nor the presence of an unsheared plug flow region) were made based on perturbation of the *in situ* portion of the rheogram. A related fully turbulent flow friction factor correlation was presented that utilises parameters common to the laminar flow relationships which are themselves independent of the form of the rheological model. Novel application of statistical procedures were applied to the generalised flow function to provide realistic confidence intervals for laminar pipe flow pressure loss predictions provided by the reparameterised Sisko model. This procedure could be extended to full-scale simulations so as to provide more representative confidence bounds on the laminar annular pressure loss component of the ECD and *any* other fitted nonlinear function. Such information could furnish the driller with a means to better determine surface pump rate, mud weight, ROP and related activities subject to ECD requirements.

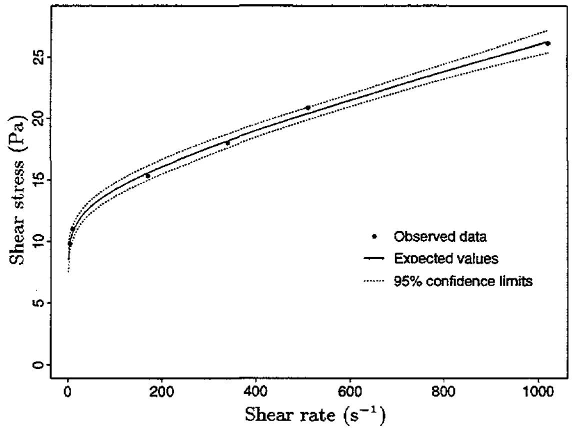

Figure 3.7: Observed rheological data, Sisko^R expected values and confidence limits.

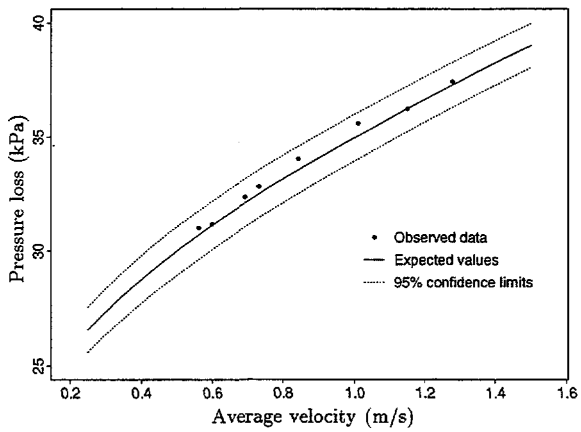

Figure 3.8: Observed laminar pressure loss data, expected values and confidence limits calculated using the fitted Sisko^R model.

Chapter 4

Equivalent Circulating Density

This chapter considers the remaining factors affecting ECD. The discussion includes a brief review of compressibility and thermal expansion of make-up fluids found in the literature with data translated into simple expressions for implementation into the hydraulics calculation. An alternative procedure for estimating cuttings transportation that compensates for the multivariate nature of the associated independent variables is also discussed. Simulations, incorporating the procedures presented in this and previous chapters, are compared against surface SPP measurements with reasonable agreement.

4.1 Fluid Compressibility and Thermal Expansion

A number of investigations have furnished data for the compressibility and thermal expansion of drilling fluids (McMordie *et al.*, 1975; McMordie, Bland & Hauser, 1982; Politte, 1985; Kutasov, 1988), however, their utility is restricted due to the specific nature of the fluids considered. A more general material balance for determining fluid density (or SG), as a function of temperature and pressure, was developed by Hoberock, Thomas & Nickens (1982), and requires a knowledge of the response of individual fluid constituents to downhole conditions:

$$\gamma(p,T) = \frac{(\gamma_{\mathrm{o}} f_{v,\mathrm{o}}) + (\gamma_{\mathrm{w}} f_{v,\mathrm{w}}) + (\gamma_{\mathrm{s}} f_{v,\mathrm{s}}) + (\gamma_{\mathrm{c}} f_{v,\mathrm{c}})}{1 + f_{v,\mathrm{o}}\left(\frac{\gamma_{\mathrm{o}}}{\gamma_{\mathrm{o},[p,T]}} - 1\right) + f_{v,\mathrm{w}}\left(\frac{\gamma_{\mathrm{w}}}{\gamma_{\mathrm{w},[p,T]}} - 1\right) + f_{v,\mathrm{s}}\left(\frac{\gamma_{\mathrm{s}}}{\gamma_{\mathrm{s},[p,T]}} - 1\right) + f_{v,\mathrm{c}}\left(\frac{\gamma_{\mathrm{c}}}{\gamma_{\mathrm{c},[p,T]}} - 1\right)}.$$

Peters, Chenevert & Chunhai Zhang (1990) state that the compressibility and thermal expansion of solid weighting agents (denoted by subscript 's') and chemical additives (denoted by subscript 'c') are essentially negligible, permitting the compositional model above to be simplified, thus:

$$\gamma(p,T) = \frac{(\gamma_{\mathrm{o}} f_{v,\mathrm{o}}) + (\gamma_{\mathrm{w}} f_{v,\mathrm{w}}) + (\gamma_{\mathrm{s}} f_{v,\mathrm{s}}) + (\gamma_{\mathrm{c}} f_{v,\mathrm{c}})}{1 + f_{v,\mathrm{o}}\left(\frac{\gamma_{\mathrm{o}}}{\gamma_{\mathrm{o},[p,T]}} - 1\right) + f_{v,\mathrm{w}}\left(\frac{\gamma_{\mathrm{w}}}{\gamma_{\mathrm{w},[p,T]}} - 1\right)}. \tag{4.1}$$

Eq.(4.1) requires knowledge of constituent-fluid SG's at initial and elevated pressures and temperatures (denoted by the subscript '$[p,T]$').

Property	Base Oil				
	Oil 'A'	Oil 'B'	Oil 'C'	Oil 'D'	Diesel
$a_1 \times 10^{-9}$	1.8693	2.0954	2.0764	2.0050	2.0304
$a_2 \times 10^{-7}$	4.6156	4.8691	4.6238	4.3174	4.1016
a_3	-0.6522	-0.6738	-0.6392	-0.6225	-0.6586
a_4	852.503	832.588	802.044	811.870	853.465
γ_{std}	0.84	0.84	0.82	0.79	0.80
Aromatics [wt.%]	30-50	16	10-13	0.9	<0.1
Viscosity [@ 38°C]	2.7	2.7	1.8	1.6	1.7

Table 4.1: Thermal expansion and compressibility correlation coefficients for five base-oils with some basic fluid properties. Coefficients to fit expression: $\rho_{[p,T]} = (a_1T + a_2)p + (a_3T + a_4)$, and are valid between $20 \leq T \leq 280$°C and $0.1 \times 10^6 \leq p \leq 138.0 \times 10^6$ Pa.

A correlation for NaCl brine densities with molal concentrations from 0 to 25, temperatures between 20 and 250°C and pressures between 0 and 29,000 psig has been developed[1] (Kutasov, 1989 & 1991) based on analysis of available thermodynamic data. Melbouci (1991) provided regression coefficients for a 400 g/l (mass salt/mass pure water) CaCl brine used specifically in the make-up of certain proprietary oil-based muds[2].

Whilst pure water and NaCl brine behaviour is adequately served by the Kutasov correlation (Babu, 1996), no equivalent generalised expression exists for base oils. Furthermore, there is a paucity of published data relevant to oil-phase behaviour. Nonlinear regression on the available data for diesel oil and four base oils yielded the coefficients presented in Table 4.1, along with known fluid properties, to fit the expression:

$$\rho_{[p,T]} = (a_1T + a_2)\,p + (a_3T + a_4)\,,$$

where ρ is in kg/m^3, T is in °C and p is in Pa. This linear function provides good characterisation demonstrated by having a minimum R^2 value of 0.998. Melbouci provides regression coefficients for one specific base-oil (see footnote 2) with the following properties: γ_{std}: 0.814; aromatics: 6 (vol.%); parafinicity: 59 (vol.%); naphthenes: 35 (vol.%); viscosity at 20°C: 5.0 mm^2/s and at 100°C: 1.3 mm^2/s.

Figure 4.1 illustrates the compressibility and thermal expansion for two base-oils which are visibly quite significant. The effect of this fluid behaviour on calculated ECD at the bit in

[1]The correlation proposed by Kutasov is:

$$\rho = \rho_{std} \exp\left[\alpha p + \beta\,(T - T_{std}) + \gamma\,(T - T_{std})^2\right],$$

where α, β and γ are constants (Table 1, pp. 48, Kutasov, 1991), p is in psig, T is in °F, ρ is in ppg. T_{std} is taken to be 59°F and ρ_{std} is brine density at 0 psig and T_{std}.

[2]Melbouci's regression analysis provided coefficients to fit the expression:

$$\gamma_{[p,T]} = (a_1T + b_1)\,p^2 + (a_2T + b_2)\,p + a_3T + b_3,$$

where pressure, p, is in bars and temperature, T, is in °C. Expression coefficients for the two fluid types considered are given in the table below (valid for $30 \leq T \leq 150$°C and $70 \leq p \leq 910$ bars):

Fluid Type	Regression Coefficients					
	$a_1 \times 10^{-10}$	$a_2 \times 10^{-7}$	$a_3 \times 10^{-4}$	$b_1 \times 10^{-8}$	$b_2 \times 10^{-5}$	b_3
400 g/l CaCl Brine	-1.26	2.52	-6.74	-0.137	3.86	1.2461
SN91/HDF200 Base Oil	-1.66	4.01	-7.36	-1.750	6.65	0.8241

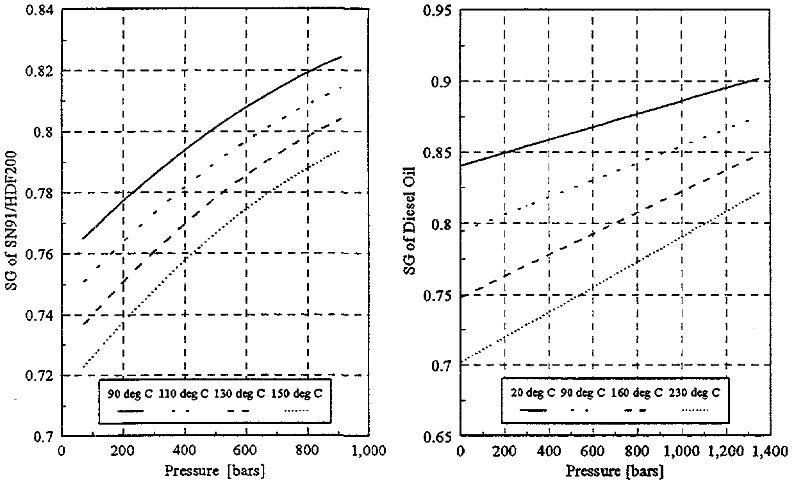

Figure 4.1: Compressibility and thermal expansion of Diesel Oil and SN91/HDF200 base-oil.

an actual drilling operation was found to be severe enough to warrant continual monitoring of the expansion/compressibility of oil-based muds during drilling hydraulics calculations (Bailey, 1992). With a statutory operating safety margin of 0.04 off pore- and fracture-pressure equivalent ECD's, an operational simulation on a North Sea well[3] using an 1.72 SG oil-based mud, predicted an ECD at the bit of 1.813 without considering compressibility and thermal expansion effects, and 1.845 with. *Cetarus paribus*, this difference represents a possible 80% encroachment on operating safety margins and does not consider the added, quantifiable, uncertainties attributed to the annular pressure loss calculations (refer to section 3.4, page 69) and estimable uncertainties concerning cuttings concentration (see next section). Calculated SPP's from this simulation do not, however, provide any tangible indication of possible downhole safety margin violation: without thermal expansion and compressibility; 297.4 bars and 298.62 bars with (compared to a measured value of 306 bars). Additional uncertainties concerning annular eccentricity, drillstring rotation and bit losses are likely to contribute to further ECD inaccuracies which may be sufficient to exceed the operating safety margins.

4.2 Cuttings Transportation

The technology to model particle slip velocity has not kept pace with the rapid developments in inclined, horizontal and/or extended reach wells. The problem of assuring adequate cuttings transportation is hindered by the lack of any universally applicable model by which transport data may be correlated (Becker, 1987). This deficiency is compounded by an inability

[3]Simulation conducted on an 8.5″ hole section; flowrate: 1870 lpm; bit depth: 4864 [m MD], 2002 [m TVD]; Power Law flow equations; volume fractions: oil: 54.9% (SN91), brine: 18.3%, solids: 26.8%; bottom-hole temperature: 70°C; flow-line temperature: 50°C; ROP: 25 m/h; WOB: 10 tons; bit TFA: 0.5177 in^2.

to measure/quantify dependent variables (slip velocity, cuttings bed size, volumetric cuttings concentration) from independent variables (cuttings size distribution, density, geometry and influx rate; fluid density, rheology and velocity; annular eccentricity, inclination, aspect ratio and drillstring rotation) in operational environments. Bin-Haddah (1988) studied the parameters governing hole cleaning and concluded that a complete solution is likely to be uneconomical, possibly unattainable and that approximate solutions must suffice. Whilst it is acknowledged that a precise solution is unlikely to be forthcoming, it is possible, at least, to reduce the severity of uncertainty through a procedure for treating single-value slip velocity correlations within a multivariate environment.

4.2.1 Contemporary Calculation Procedures

Faced with the uncertainties alluded to above, it is little wonder that contemporary treatment of slip velocity within drilling hydraulics programs is so diverse in both the thoroughness of the expressions coded and the extent to which the independent variables are considered. These programs may also be inconsistent in their application of rheological model-specific particle slip velocity formulations within an environment defined by another rheological model.

Since Pigott (1941) first addressed the issue, cuttings transportation has been the subject of many publications. While most transportation models are empirical or semi-empirical in form, it was not until the 1960's (i.e., Saffman, 1965) that purely theoretical formulations for the lateral lift force on spherical particles exposed to shear flow were developed. Such mechanistic models, however, required precise knowledge of *in situ* velocities and shear rate profiles plus the exact radial location of the suspended particle. Consequently, hydraulics calculations have reverted to simpler, semi-mechanistic, solutions. Of recent importance are the widely used particle slip models of Sze-Foo Chien (1972), Moore (1974; later employed in the finite difference algorithm of Iyoho, Horeth & Veenkant, 1988) and Walker & Mayes (1975) - all of which are reproduced in standard texts. Of additional interest are the models of Zeidler (1974, with confirmation of model suitability for field-application by Hussaini, 1977), Thomas (1978), Iyoho & Azar (1980), Bin-Haddah (1988), Gavignet & Sobey (1989), Peden, Ford & Oyeneyin (1990) and, in particular, the model proposed by Becker (1987, see section 4.2.2).

Nevertheless, no matter how detailed the formulations applied, or rigorous the treatment of the independent variables, all the hydraulics packages considered (and accompanying citations) have a common denominator: the insistence of the formulations employed to utilise a single size of cuttings, a single cuttings-density, a single generalised cuttings shape, a uniform/average fluid velocity field, and a single apparent viscosity. Despite the attempts of each hydraulics package to provide realistic average/representative values to their respective slip velocity expression parameters, the fact remains that contemporary procedures relent to the dictats of the expression, thereby imposing homogeneity (deemed necessary for expediency by Sifferman, Myers, Haden & Wahl, 1973) into an essentially heterogeneous system (Zandi & Govatos, 1967).

4.2.2 The Multivariate Nature of Cuttings Transportation

It has been long recognised that cuttings transport involves complex processes that are poorly served by abstract generalisations: Hall, Thompson & Nuss (1950) and Williams & Bruce (1951) first recognised the axial velocity and annular profile effects on transportation efficiency as

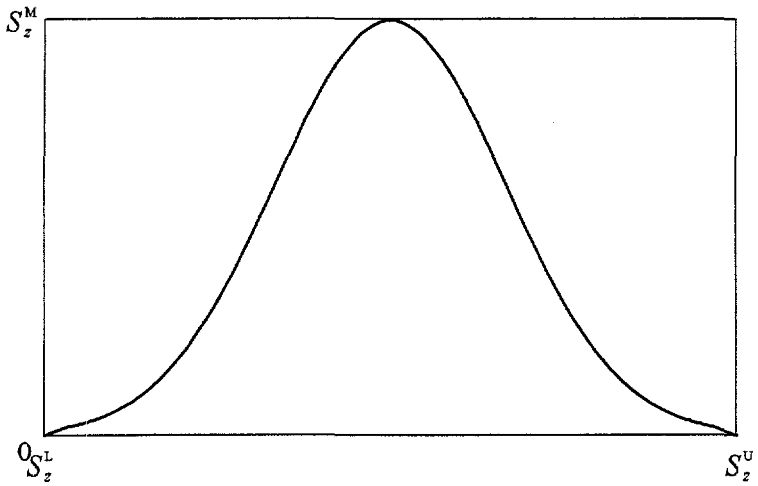

Figure 4.2: 'Boxing-in' of marginal S_z for governing parameter z. S_z^{L} and S_z^{U}: lower- and upper-distribution bounds; S_z^{M}: median value of the S_z marginal.

well as particle shape. Zeidler (1974) confirmed the influence of annular velocity profiles and presented semi-empirical expressions for settling velocities based on the Power Law, employing simple characterisation of irregular drilled particles. Wani, Sarkar & Mani (1982) developed a correlation using a single 'representative' particle size determined from particle size distributions of observed data. Becker (1987) was the first, however, to mathematically approximate particle velocity distributions within a useable transport model. This significant work utilises a binomial distribution function to account for the relative frequency of particle slip within an approximated velocity field:

$$f\left(v_p\right) = \frac{1}{\sqrt{2\pi mp(1-p)}}\,\mathrm{e}^{\mathrm{xp}}\left[-\frac{\left(\frac{v_p - v_{p,\min}}{v_{p,\max} - v_{p,\min}} - p\right)^2}{2mp(1-p)}\right], \tag{4.2}$$

where parameter m is proportional to the variance of the distribution and p describes the degree of symmetry in the bell-curve. In essence, this expression accounts for the frequency of particle slip velocity, v_p, within an assumed laminar annular velocity profile. Eq.(4.2) provides a univariate technique to handle slip velocity expressions requiring single equivalent particle diameters, fluid viscosities and so on. In the spirit of Becker, the logical progression would be to enable treatment of actual concentric annular velocity profiles, variations in particle sphericity Ψ (refer to Bourgoyne *et al.*, 1986, pp. 172; with a simple correlation estimating the effects of Ψ on slip velocity presented by Gavignet & Wick, 1987) and variations in particle diameters within the calculation procedure. The methodology proposed is termed the 'Rejection Method of Simulation for Particle Transport' (RMSPT).

4.2.3 The Rejection Method of Simulation for Particle Transport

The proposal presented here is speculative. At the time of writing, the conjecture could not be substantiated due to the lack of suitable data. The supposition relates only to the treatment, and not the form, of the cuttings transport model and is founded on proven statistical methodologies for establishing confidence bounds for multivariate systems.

It is assumed that (1) cuttings size, sphericity and annulus axial laminar velocity profiles are independent, (2) distributions are known and bounded (i.e., no long tails), (3) the geometric annular profile is concentric, (4) axial particle slip velocity may be calculated from any suitable particle slip function requiring single-valued parameters, and (5) relevant cuttings size and sphericity distributions (marginals) are available.

Consider the simple case of a bivariate distribution (say, axial laminar annular velocity and cuttings size). Any sample drawn from the size marginal and the velocity marginal will have then been sampled from a bivariate distribution. For example: if the free-fall particle slip velocity is computed using the Moore correlation, the sample from the bivariate distribution will be drawn with a unique pairing of particle size and *in situ* velocity specific apparant viscosities. The sampling procedure is repeated n times to obtain a distribution of n valid parameter pairs from which particle transport velocities are calculated: $v_t = (v_{t,1}, v_{t,2}, \ldots, v_{t,n})$.

It is necessary to 'box-in' the distributions which are obtained from known lower- and upper-bounds (assumption 2) and the maximum value of the application function. Figure 4.2 illustrates the 'boxing-in' of a uni-modal governing parameter marginal S_z (where subscript z represents, say, cuttings size). Distribution density variations, such as that illustrated in Fig. 4.2 with multi-modal profiles are also permitted. Sampling from the governing parameter marginal involves the following steps:

1. Generate two random numbers between 0 and 1, say $U_1, U_2 \sim U(0,1)$ where U represents a uniform $(0,1)$ distribution.

2. Let
$$x = S_z^{\mathrm{L}} + \left(S_z^{\mathrm{U}} - S_z^{\mathrm{L}}\right) U_1,$$
and
$$y = S_z^{\mathrm{M}},$$
where superscripts 'L' and 'U' represent lower- and upper-bounds respectively, while 'M' represents the median value of governing parameter z.

3. If $y > f(x)$, i.e., $S_z^{\mathrm{M}} U_2 > f\left[S_z^{\mathrm{L}} + \left(S_z^{\mathrm{U}} - S_z^{\mathrm{L}}\right) U_1\right]$, then reject (U_1, U_2), otherwise permit the calculated value of x. The value of x then comes from the z marginal. If rejection occurs, generate new values for U_1, U_2 and repeat until success.

4. Once a point from the z marginal has been accepted, the above process is repeated for the y marginal S_y (where subscript y represents, say, fluid velocity). The resulting combination of particle size and fluid velocity represents the desired sample from a bivariate distribution, from which $v_{t,1}$ is subsequently calculated.

The procedure itemised above is depicted in Fig. 4.3 which illustrates rejection and acceptance of two samples taken from each of the marginals. One can extend this approach to trivariate

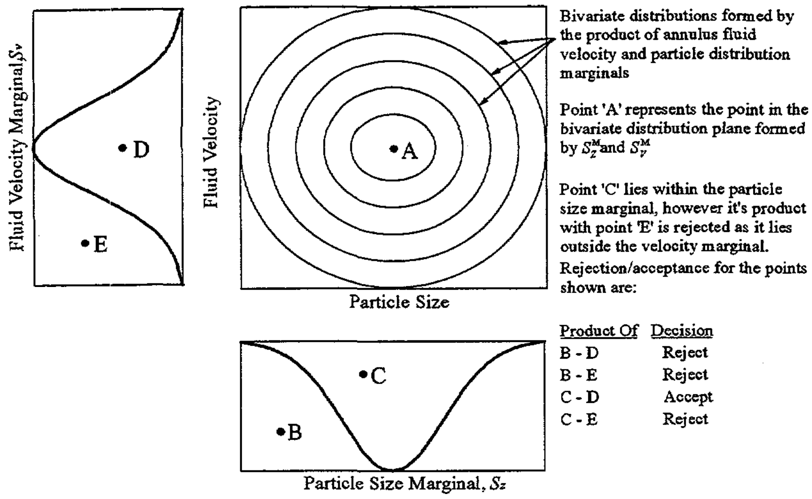

Figure 4.3: Illustration of the RMSPT procedure for a bivariate distribution with examples of rejection and acceptance of bivariate products.

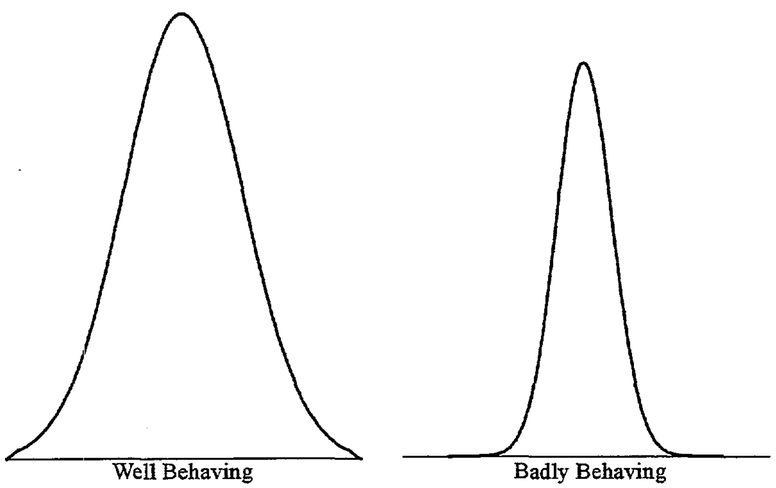

Figure 4.4: Illustration of well- and badly-behaving marginal profiles. 'Badly behaving' can be construed as having a narrow, strongly leptokurtic, parameter distributions.

(or higher) distributions, however all marginals must still be defined over a finite range and, in addition, should possess reasonably flat (mesokurtic or platykurtic) profiles. Figure 4.4 presents cartoons of 'well' and 'badly' behaved profiles. Velocity profiles are likely to be well-behaved while size, and possibly shape, profiles may possess leptokurtic (spiked) profiles. In these instances, the long tails should be terminated near the spike thereby flattening out the profile over the given boundary. RMSPT still operates in the presence of distributions with highly leptokurtic profiles but the acceptance rate will be poor (unduly lengthening run-time thereby hindering real-time monitoring capabilities).

Having obtained a sample of n points, $v_{t,[1...n]}$ is computed which provides $f(v_t)$, the multivariate frequency distribution of transport velocities, and represents a reasonably rigorous distribution which can be presented in a suitable fashion (e.g., histograms, ogives). Reasonable non-parametric confidence intervals can then be readily calculated to provide time-averaged particle transport velocities.

Becker (1987) details treatment of such time averaged values for a number of operational scenarios. Time-average transport velocities can now be accompanied by confidence bounds which then impact on cuttings concentration (hence density of mud with cuttings, ρ_{mwc}) which may be added to the confidence bounds already attributed to annular laminar flow losses (section 3.4, page 69). In this way ECD gains a confidence interval which, if displayed during real-time monitoring of drilling operations, could furnish the drilling engineer with an additional safeguard against unwelcome formation pore- or fracture-pressure violations: enhancing operational efficiency and, above all, safety.

4.3 Simulations

An ANSI C program was written to enable drilling hydraulics calculations to be performed on an actual North Sea well utilising the various procedures presented herein. The volume of data available for comparison purposes was not substantial enough to allow firm conclusions to be drawn concerning the expected benefits of the alternative procedures discussed. As such, this analysis serves only to demonstrate a practical application, not to provide confirmation of its suitability. The program is triggered by command-line arguments and a keyword-driven ASCII input file (an example of which is presented in Appendix I, Table I.1, pages 218 to 220 inclusive) with keywords being accompanied by some '$'-bounded text, indicating required units and basic explanations. The input file comprises six main parts, namely:

Part 1 Contains general administrative information such as the bit run number, bit name, BHA number, well name and simulation date.

Part 2 Contains general hydraulic input data: bit depth, bit discharge coefficient, bit nozzles, bottom depth, circulating fluid make-up and SG, Fann viscometer readings, measured SPP, ROP, temperature (bottom hole), volumetric flowrate and WOB.

Part 3 Contains program control switches and selects bit type and the rheological model while toggling on and off fluid compressibility model and annular eccentricity.

Part 4 Describes the drillstring (the 'tally-book'). Downhole tools are described by an identifying flag after the relevant keyword, along with its length (as these usually vary between

	BHA #2		BHA #6		BHA #9		BHA #20	
Measured SPP [bars]	145.0		275.0		253.0		260.0	
Pore Pressure (meas)	0.93		1.19		1.59		1.60	
LOT/FIT (meas)	1.57		1.63		1.83		1.90	
Results for Sisko								
SPP (1) [bars]	157.1	+ 8.3%	297.0	+8.0%	266.7	+5.4%	273.2	+5.1%
SPP (2) [bars]	149.6	+ 3.2%	291.3	+5.9%	260.2	+2.8%	265.8	+2.2%
SPP (3) [bars]	149.6	+ 3.2%	288.6	+4.9%	257.5	+1.8%	262.1	+0.8%
ECD (bit)	1.41		1.54		1.75		1.82	
Results for Conventional Bingham Plastic								
SPP [bars]	163.8	+13.0%	298.3	+8.5%	271.5	+7.3%	292.7	+12.5%
ECD (bit)	1.43		1.56		1.78		1.88	
Results for Conventional Power Law								
SPP [bars]	157.3	+ 8.5%	294.7	+7.2%	267.6	+5.8%	281.2	+8.1%
ECD (bit)	1.42		1.55		1.76		1.87	

Key:

SPP (1): calculated SPP without rotation or annular eccentricity.

SPP (2): calculated SPP with rotation but no annular eccentricity.

SPP (3): calculated SPP with both rotation and annular eccentricity.

Table 4.2: Full-scale simulation results conducted on the four well sections.

jobs). Drill pipe specifications are also recognised by a similar flag.

Part 5 Describes the casing and open hole configuration (the 'welly-book').

Part 6 Contains deviation survey information (measured depth, total vertical depth and inclination).

The bit discharge coefficients employed are as recommended by Warren (1989) while the approaches for fluid compressibility and thermal expansion effects given earlier in section 4.1 are employed throughout (with an assumed linear temperature profile). The simulations themselves were performed on four hole sections of a single deviated North Sea well where measured SPP's and LOT/FIT data were available. Data relevant for each of these sections (from daily drilling reports) are presented in Table I.2, page 221. Detailed bottom hole assemblages (BHA's) for each simulated section are presented in Tables I.3 & I.4 on page 222, describing each component, their diameters (given in inches) and their individual lengths (refer to document nomenclature for definitions of acronyms used). Component depths (both measured and vertical) for each element of the BHA are presented in Tables I.5 to I.8, inclusive.

Table 4.2 presents concise results of simulations conducted on the four systems defined. SPP's were calculated for the Sisko model under three different conditions: (1) without any rotational and annulus eccentricity effects, (2) with rotational effects considered but excluding eccentricity effects, and (3) with both rotational and eccentricity effects considered in the calculation process. Calculated SPP's using conventional Bingham Plastic and Power Law models (namely those employing the slot flow assumption) are also presented. Fluid compressibility and thermal expansion effects are applied throughout. All simulations over-predict measured SPP's, although the degree of such is more severe for the conventional, slot-flow assumption Bingham Plastic (13% for BHA #2 and 12.5% for BHA #20). Over-predictions for the conventional Power Law are less severe with maximum and minimum values of 8.5% and 5.8% respectively. These

SPP's compare less favourably with those calculated using the Sisko model and the generalised-consistent procedure. Although Sisko consistently over-predicts SPP's for all simulations, the severity of the largest difference is only 8.3% (BHA #2) and reduces when rotation and eccentricity effects are considered. There is a general trend of reducing calculated SPP's when rotation and eccentricity effects are considered. These effects are most beneficial for BHA #20 where the residual reduces to only 0.8%. It is uncertain whether such exactitude will persist for other simulations of similar systems. Of note are the calculated values of ECD at the drill bit. While all simulations predict ECD's within known bounds, all values are closer to measured FIT/LOT values than measured pore pressure SG equivalents. Both Bingham Plastic and Power Laws err towards higher ECD's than those provided from the procedures outlined herein, thereby indicating an area of possible improvement in drilling performance by increasing surface pump rates without violating formation integrity.

All simulations are tinged with an element of doubt due to a number of uncertainties in the system: (1) losses over the drill bit are based on 'best-guess' estimates of discharge coefficients and bit status, (2) down hole tool losses are also uncertain, especially in the presence of PDM's where it is assumed that the reactive torque factor is unity and that the WOB recorded is correct at the instant when SPP was recorded, (3) assumptions inherent in the drill cuttings concentration calculation were necessary, (4) a linear fluid flowing temperatures estimate only, and (5) annular eccentricity is assumed to be a function of inclination only. All the above instils an element of caution in the interpretation of any results concerning surface-only matched values and any inferences to downhole conditions and values. Despite the reluctance to draw any firm conclusions from such a small, assumption loaded example, it is clear that rotational effects and annular eccentricity can play a rôle in matching surface SPP's.

4.4 Chapter Summary

Nonlinear least squares performed on fluid compressibility and thermal expansion data for a number of make-up fluids (brines, diesel oil and five specific base oils) from various sources were translated into simple expressions for use within a generalised material balance expression. Cuttings transport was also briefly examined and a novel procedure for utilising single-value particle transport expressions within a multivariate environment was presented using the approach of the rejection method of simulation. Simulations performed on four sections of a North Sea well furnished reasonable agreement against measured SPP's and also indicate that rotational and eccentricity effects are likely to improve SPP matching. The reduced calculated ECD at the drill bit using the procedures discussed herein, as compared to those furnished by conventional procedures, implies that some room for improved drilling efficiency through increasing pump rates exists, although such conclusions are tentative due to the nature of the assumpions required to perform the simulations themselves.

Chapter 5

Conclusions & Recommendations

This chapter presents conclusions derived from this study. Suggestions for future work are also outlined - with the goal of reducing to acceptable levels (in a real-time, operational, environment) the degree of uncertainty attributed to ECD and other calculated downhole quantities.

5.1 Conclusions

A number of conclusions have been drawn from this study, namely:

1. The recommended measure of goodness-of-fit of any nonlinear rheological model capable of characterising the pseudoplastic profiles exhibited by most drilling fluids (and cement slurries) is RMS. Examination of the statistical literature reveals that reliance on the commonly employed R^2 measure provides an unreliable indication of the degree of explained variation for fitted nonlinear models.

2. It has been established from RMS results drawn from a large data set that contemporary procedures for direct evaluation of Bingham Plastic and Power Law model parameters from a restricted and essentially *ad hoc* selection of Fann viscometer readings will yield poor fluid characterisations. Direct rheological model parameter solution utilising non-standard viscometer reading combinations furnished demonstrably better fluid characterisation than those provided by conventional use of θ_{600} and θ_{300} readings. The median RMS for Bingham Plastic using these Fann readings was 11.71 as compared to only 2.347 when using θ_{600} and θ_{30}. For the Power Law conventional solution yields a median RMS of 9.380 as compared to only 6.107 when using θ_{600} and θ_{100}.

3. It is shown that improved fluid characterisation may be gained when alternative rheological models are used to describe the rheogram, particularly when non-conventional Fann readings are employed in the direct solution of their parameters. The 3-parameter Sisko rheological model, for example, yielded a median RMS of 0.108 when parameters were calculated using θ_{600}, θ_{200} and θ_{6}. This median RMS is just 1.772% and 4.610% of the 'best' median RMS's provided by the Power Law and Bingham Plastic models respectively. All but one of the alternative rheological models considered yielded considerably better median RMS's than the aforementioned models.

4. The differences between the best RMS's obtained for each model using the direct (contemporary) approach were generally 25% to 65% worse than those calculated using nonlinear least squares. The smallest median RMS of all the candidate functions considered using nonlinear least squares was provided by Sisko (at 0.069), about two-thirds of that obtained from the 'best' direct approach Fann reading input combination. Consequently the selection of a representative function of the pseudoplastic profile of the drilling fluid (or cement slurry) could be enhanced if: (*i*) rheological model parameters were determined from nonlinear least squares, and (*ii*) the model selected would possess the smallest median RMS values. Such treatment should ensure that the most representative function is employed in subsequent calculations.

5. Bates & Watts curvature measures and the Hougaard γ_1 statistic are suitable for determining estimation behaviour of nonlinear rheological models and were instrumental in the recommendation of the reparameterised Sisko model as a suitable default (due to it possessing very close-to-linear behaviour).

6. Laminar flow pressure loss functions generated from the Bingham Plastic model have been shown to suffer from some inconsistencies in the literature, namely by the inclusion or exclusion of a plug flow region and different numerical values of certain flow function parameters.

7. The generalised flow behaviour index, N, can provide a means by which to link turbulent, laminar and transitional pressure loss functions as well as providing a consistent flow regime delineation parameter. The parameter is also unrestricted to the choice of rheological model. Employing a limited data set it was established that the transition between laminar and non-laminar flow in circular pipes was suitably represented by $\mathrm{N}_{\mathrm{Re,G,cr}} \approx 3470-1370N$. For non-laminar to fully turbulent flow it is suggested that the transition occurs at about $\mathrm{N}_{\mathrm{Re,G,cr}} \approx 4270 - 1370N$.

8. The need for tractability in laminar flow functions is essentially redundant in the presence of sufficient computational resources at the rig-site. It has been shown that the new parameter can be utilised within a general laminar pressure loss flow function that makes no assumptions concerning conduit geometry, the presence on an unsheared region in the fluid body or the form of the rheological model. The model furnishes good agreement when compared to actual pressure loss data.

9. Confidence intervals for laminar flow pressure losses were calculated from a fitted nonlinear rheological model with good agreement against measured data. The approach can be applied to *any* fitted nonlinear function and it is suggested that eventual ECD estimates may benefit from such a representation thereby providing the driller with more realistic operating margins, particularly when operating in region of tight pore- and fracture-pressure tolerances.

10. An explicit, hybrid, non-Newtonian turbulent flow friction factor utilising the generalised flow behaviour index was able to provide adequate results when compared to a limited set of measured data and a number of published non-Newtonian and a purely Newtonian friction factor correlation. Linear interpolation between laminar and fully-turbulent flow friction factors was found to provide the most representative approach of modelling transitional flow.

11. A purely theoretical model for accommodating a more realistic spread of drill cuttings sizes and shapes, along with the velocity profile of the fluid, has been proposed. While the lack of any suitable data restricts the proposal to a conjecture, the generality of the methodology appears to be suitable for handling the multivariate nature of the cuttings concentration calculation while retaining accepted single-value cuttings transportation expressions.

12. ECD's calculated using contemporary drilling hydraulics procedures appear to be somewhat different from those calculated using the alternative procedures proposed in this document. While the lack of data severely limits the confidence one can place in these findings, the noticeable differences appear to be sufficient to warrant closer examination once suitable data is made available.

5.2 Recommendations for Further Work

Several aspects of the drilling hydraulics calculation procedure would benefit from further:

- investigation of the conjecture concerning multivariate treatment of single-value particle slip correlations (RMSPT);
- investigation of drilled particle size and shape distributions from actual field tests to develop functional relationships for approximating such distributions for well planning activities;
- recording and interpretation of downhole pressures and temperatures (from TPL logs) in the annulus, thereby providing a means to more accurately calibrate drilling hydraulics calculations and to establish the degree of accuracy provided by the proposed models;
- detailed investigation of different PDM/turbine pressure losses, under realistic operating conditions (representative drilling fluids, WOB, torque etc.) and the construction of related pressure loss function(s);
- detailed studies of MWD tool pressure losses under realistic operating conditions;
- detailed studies of drill bit/core barrel pressure losses under realistic operating conditions;
- investigation of slimhole losses and the application of the proposed models to such high aspect ratio systems;
- investigation of the sensitivity of the generalised flow behaviour index, N, to temperature and pressure;
- experimental investigation of annulus friction losses obtained from different pseudoplastic drilling fluids for a variety of aspect ratios for all flow regimes, thus providing data suitable for more rigorous calculation of the constants of the proposed turbulent flow friction factor correlation;
- evaluation of more realistic flow regime transition criteria from the aforementioned experimental studies;

- investigation of the effect of pipe rotation on annulus pressure losses due to helical flow and Taylor vortices;
- detailed studies of thermal expansion and compressibility behaviour for a wide range of base-oils.

5.3 Closing Remarks

During the course of this work it was evident that drilling hydraulics programs have undergone little fundamental development since their first widespread implementation at the rig-site using PC-based platforms. It is hoped, therefore, that this work will encourage providers of such programs to continue their development and to question contemporary procedures. It is further hoped that the status of the drilling hydraulics calculation be returned to prominance, a status that has been somewhat eroded since the deployment, and often blind application, of commercial drilling hydraulics packages in the field.

Nomenclature

A	Inverse ln-cosh and Prandtl-Eyring constants, Pa *or* Robertson-Stiff and Robertson-Stiff* consistency factors, Pa·s^B
A_{1-5}	Turbulent flow friction factor constants, dimensionless
a	Herschel-Bulkley/linear constant, Pa *or* Hyperbolic and Hyperbolic* constants, s^{-1} *or* Sisko and Sisko* constants, Pa·s
a_j	polynomial coefficients for PDM/turbine and MWD pressure losses *or* 'Toms phenomenon' factor polynomials *or* regression coefficients for fluid compressibility and thermal expansion models
B	Inverse ln-cosh, Prandtl-Eyring and Prandtl-Eyring* constants, s^{-1} *or* Robertson-Stiff and Robertson-Stiff* flow behaviour indices, dimensionless
b	Herschel-Bulkley/linear constant, Pa·s^c *or* Hyperbolic and Hyperbolic* constants, Pa *or* Sisko and Sisko* constants, Pa·s^c
c	Herschel-Bulkley/linear, Sisko and Sisko* exponents, dimensionless *or* Power Law/linear constant, Pa·s^n *or* ratio of the square of inner and outer radii of coaxial rotational viscometer cylinders, dimensionless
D	diameter at the contact surface of the conduit, m
d	Herschel-Bulkley/linear constant, s^c
F	F-distribution value
$\hat{F}$	$n \times p$ matrix of partial derivatives of the rheological model evaluated at $\hat{\phi}$ and the n data points $\dot{\gamma}_i$
f	friction factor, dimensionless
$f_{v,x}$	volume fraction of fluid constituent x, dimensionless
G_N	modified Fredrickson & Bird hydraulic diameter correlation factor calculated from a function using N, dimensionless
G_v	correction factor to the API Power Law consistency factor, dimensionless
H	perpendicular distance between parallel plates used in the slot-flow assumption, m
$\hat{H}$	row vector of partial derivatives of $h\left(\hat{\phi}\right)$ with respect to the rheological model parameters
h_0	true value of the nonlinear function
k	Collins-Graves, Collins-Graves*, Herschel-Bulkley, Power Law and Power Law/linear consistency factors, Pa·s^x where x refers to the flow behaviour index of the appropriate model
L	length, m

m Herschel-Bulkley (yield-Power Law) flow behaviour index, dimensionless, *or* rotational shear rate decay rate term, dimensionless

N generalised flow behaviour index, dimensionless

$\mathrm{N_{He}}$ Hedtröm number (Hedström, 1952), dimensionless

$\mathrm{N_{Re}}$ Reynolds number (Reynolds, 1884), dimensionless

$\mathrm{N_Y}$ Yield number, dimensionless

n' Metzner & Reed pseudo-shear flow behaviour index, dimensionless

n Power Law and Power Law/linear flow behaviour indices, dimensionless *or* number of Fann viscometer readings

p number of parameters in the rheological model *or* pressure, Pa

Q volumetric flowrate, $\mathrm{m^3/s}$

R radius of conduit at the contact surface, m

R ratio of eccentric and concentric frictional pressure losses, dimensionless

RMS residual mean square, $\mathrm{Pa^2}$

RSS residual sum of squares, $\mathrm{Pa^2}$

r *in situ* radius, m

S intermediate Hyperbolic model constant, Pa *or* marginal for governing parameter indicated by subscript, units of parameter

s^2 estimated error variance, $\mathrm{Pa^2}$

T 'Toms phenomenon' factor, dimensionless

T temperature, Kelvin or °C

t t-distribution value

$U_{1,2}$ (pseudo) random numbers with values between 0 and 1, dimensionless

v *in situ* fluid velocity, m/s

$\bar{v}$ average velocity of the fluid in the conduit (Q/A), m/s

v_p free-fall particle slip velocity, m/s

v_t net particle transport velocity, m/s

w width of parallel plates used in the slot-flow assumption, m

x dimensionless quantity derived from manipulation of the Buckingham equation, dimensionless **or** polymer concentration, ppm (parts per million)

Y yield number ('plasticity'), dimensionless *or* intermediate parameter required in the solution of G_N, dimensionless

y radial fraction such that $Ry = r$, dimensionless

Z intermediate parameter required in the solution of G_N

z radial fraction such that $Rz = r$, dimensionless

Greek

α Ellis *et al.* exponent, dimensionless *or* Cross constant, $\mathrm{s^{2/3}}$ *or* Collins-Graves* yield stress, Pa *or* intermediate Hyperbolic constant, Pa·s *or* significance level

β intermediate Hyperbolic constant, Pa·s *or* Collins-Graves and Collins-Graves* constants, s

γ specific gravity, dimensionless

$\dot{\gamma}$ shear rate, s^{-1}

$\dot{\gamma}_1, \dot{\gamma}_2$ reparameterised Sisko constants, s^{-1}

$\dot{\gamma}_{cp}$ Hyperbolic and Hyperbolic* constants, s^{-1}

$\dot{\gamma}_\circ$ Robertson-Stiff and Robertson-Stiff* constants, s^{-1}

γ_1 Hougaard skewness statistic

δ distance between the centres of inner- and outer-pipes, m

Δp pressure drop over conduit length L, Pa

ϵ random shear stress error term, Pa *or* annular eccentricity, dimensionless *or* error (usually given as a percentage), dimensionless

ε contact-wall roughness of conduit, m

θ_x Fann viscometer dial reading at rotation speed x, $(\text{lb}_\text{f}/100\ \text{ft}^2)/1.0678$

κ ratio of $(\dot{\gamma}_w)_{MR}/\dot{\gamma}_w$, dimensionless

λ radial fraction, dimensionless

$\lambda_{[+]}$ outer boundary of plug flow region nearest casing/open-hole wall, dimensionless

$\lambda_{[-]}$ inner boundary of plug flow region nearest drillpipe outer wall, dimensionless

$\mu_{w,\text{app}}$ apparent viscosity of non-Newtonian fluid at the conduit wall, Pa·s

$\mu_\circ$ Cross and Reiner-Philippoff low shear rate limiting viscosity, Pa·s

μ_∞ Bingham Plastic, Casson, Cross and Reiner-Philippoff high shear limiting (plastic) viscosities, Pa·s

ξ *in site* aspect (diameter) ratio (r/D_o), dimensionless

ρ fluid density, kg/m^3

σ^2 variance, Pa^2

τ measured shear stress, Pa

τ_1, τ_2 reparameterised Sisko parameters, Pa

τ_b $M/(2\pi R_1^2 L)$ shear stress at the inner cylinder of the coaxial rotational viscometer where M = torque on inner cylinder, R_1 = radius of inner cylinder and L = effective length of the inner cylinder of the rotational viscometer

τ_{cp} Hyperbolic constant, Pa

$\tau_\circ$ Bingham Plastic, Casson, Collins-Graves, Collins-Graves*, Herschel-Bulkley, Inverse ln-cosh, Prandtl-Eyring*, Robertson-Stiff* and Sisko* yield stresses (at $\dot{\gamma} = 0$), Pa

τ_s Reiner-Philippoff constant, Pa

τ_w shear stress at the conduit wall, Pa

τ_y yield stress of the fluid, Pa

ϕ rheological model parameter set

ϕ_0 Ellis *et al.* constant, $(\text{s·Pa})^{-1}$

ϕ_1 Ellis *et al.* constant, $(\text{s·Pa})^{-\alpha}$

$\hat{\phi}$ estimated rheological model parameter set

Ψ sphericity of particle (drill cutting), dimensionless

ψ aspect (or diameter) ratio (D_i/D_o), dimensionless

Ω reactive torque factor, dimensionless *or* relative angular velocity of the rotational viscometer, 2π/s; (refer to Yang & Krieger, 1978, for a thorough review of the different approaches of how this parameter may be used to furnish corrected shear rates)

ω angular velocity (rotation speed), 2π/s

Subscripts

- ann annulus
- app apparent
- conc concentric conditions
- c centraliser or stabiliser component of drillstring *or* chemical additive phase of the fluid
- cp centre point of the hyperbola
- cr critical
- ecc eccentric conditions
- ecd equivalent circulating density
- eff effective
- equiv equivalent
- f circulating fluid
- G generalised
- hel helical
- hy hydraulic
- i inner
- L lower
- lam laminar
- lower point defining change from laminar to transitional flow
- M middle
- MR Metzner & Reed defined quantity
- mod modified
- mwc mud with cuttings
- nl no-load (off-bottom)
- o outer *or* base-oil-phase of the fluid
- p particle
- plug plug flow
- r *in situ* radial position
- s solid weighting material phase of the fluid *or* slip/transport
- tan tangential direction, perpendicular to axial and radial directions and positive in the direction of pipe rotation
- trans transitional
- turb turbulent
- U upper
- upper point defining change from transitional to fully turbulent flow
- w at the wall
- w water-phase of the fluid
- x axial direction (parallel to conduit walls)
- z radial direction, perpendicular to conduit wall

Superscripts

*	indicates published rheological model is modified by the inclusion or omission of an explicit shear stress term
R	reparameterised model

Abbreviations

ANSI	American National Standards Institute
ASCII	American Standard Code for Information Interchange
Bi-Pl	Bingham Plastic model
BHA	bottom hole assembly
Co-Gr	Collins-Graves model
DC	drill collar
DP	drill pipe
ECD	equivalent circulating density
EDA	exploratory data analysis
Ellis	Ellis, Lanham & Pankhurst/Ellis *et al.*
FIT	formation integrity test
GRN	generalised Reynolds number
HB/lin	Herschel-Bulkley/linear model
He-Bu	Herschel-Bulkley model
HW	heavy weight (often associated with drill pipe, DP)
Hyper	Hyperbolic model
IN	intrinsic nonlinearity
Inv-lc	Inverse ln-cosh model
LOT	leak-off test
MP-Law	API (Modified) Power Law
MWD	measurement while drilling (tool)
NM	nonmagnetic
PDC	polycrystaline diamond compact (drill bit)
PDM	positive displacement (drilling) motor
PE	parameter effects nonlinearity
P-Law	Power Law model
PL/lin	Power Law/linear model
POV	pop-off valve
Pr-Ey	Prandtl-Eyring model
PV	plastic viscosity
Re-Ph	Reiner-Philippoff model
RMSPT	rejection method of simulation for particle transport
ROP	rate of penetration
Ro-St	Robertson-Stiff model

SPP	stand-pipe pressure
Stab	stabiliser
TFA	total flow area of bit nozzles, usually cited in square inches or in 1/32nd in^2
WOB	weight on bit
XO	cross-over
YP	yield point

References

Aadnøy, B.S. and Ravnøy, J.M.: "Improved Pressure Drop/Flow Rate Equation for Non-Newtonian Fluids in Laminar Flow," *J. Pet. Sci. & Eng.* (1994) **11**, 261-266.

Alderman, N.J., Gavignet, A., Guillot, D. and Maitland, G.C.: "High-Temperature, High-Pressure Rheology of Water-Based Muds," paper SPE 18035, *Proc.* 63rd Annual Technical Conference and Exhibition of the Soc. Pet. Eng., Houston, Texas (Oct. 2-5, 1988), 187-195.

Alves, G.E., Boucher, D.F. and Pigford, R.L.: "Pipe-Line Design for Non-Newtonian Solutions and Suspensions," *Chem. Eng. Progress* (Aug. 1952) **48**, No. 8, 385-393.

Anadrill Drilling Services MWD Tool Catalogue, Anadrill Drilling Services brochure AMP-7006 (1993).

Annis, M.R.: "High Temperature Flow Properties of Water-Base Drilling Fluids," *J. Pet. Tech.* (Aug. 1967), 1074-1080; *Trans.*, AIME.

Ansley, R.W. and Smith, T.N.: "Motion of Spherical Particles in a Bingham Plastic," *AIChE J.* (Nov. 1967) **13**, No. 6, 1193-1196.

Babu, D.R.: "Effects of p-ρ-T Behavior of Muds on Static Pressures During Deep Well Drilling," paper SPE 27419, *SPE Drilling & Completion* (June 1996), 91-97.

Bailey, W.J.: "Compressibility and Expansion of Drilling Fluids," Nordic Offshore Systems AS external document EXT 92/35, Rev. 1.0 (1992).

Bannister, C.E.: "Rheological Evaluation of Cement Slurries: Methods and Models," paper SPE 9284, *Proc.* 55th Annual Fall Technical Conference and Exhibition of the Soc. Pet. Eng. of AIME, Dallas, Texas (Sept. 21-24, 1980).

Barnes, H.A., Hutton, J.F. and Walters, K.: *An Introduction to Rheology*, Elsevier Science Publishers B.V., Amsterdam, The Netherlands (1989).

Bartlett, L.E.: "Effect of Temperature on the Flow Properties of Drilling Fluids," paper SPE 1861, *Proc.* Annual Fall Technical Conference and Exhibition of the Soc. Pet. Eng. of AIME, Houston, Texas (Oct. 1-4, 1967).

Bates, D.M. and Watts, D.G.: "Relative Curvature Measures of Nonlinearity," *J. Royal Statistical Soc.* (1980) **B 42**, No. 1, 1-25.

Becker, T.E.: *Correlation for Drill-Cutting Transport in Directional-Well Drilling*, Ph.D. thesis, University of Tulsa, Tulsa, Oklahoma (1987).

Becker, T.E., Azar, J.J. and Okrajni, S.S.: "Correlations of Mud Rheological Properties with Cuttings-Transport Performance in Directional Drilling," paper SPE 19535, *Soc. Pet. Eng. Drilling Eng.* (March, 1991), 16-24; first presented at the Annual Technical Conference and Exhibition of the Soc. Pet. Eng., San Antonio, New Mexico (Oct. 8-11, 1989).

Beirute, R.M. and Flumerfelt, R.W.: "An Evaluation of the Robertson-Stiff Model Describing Rheological Properties of Drilling Fluids and Cement Slurries," paper SPE 6505, *Soc. Pet. Eng. J.* (April, 1977), 97-100.

Beirute, R.M.: "A Circulating and Shut-In Well-Temperature-Profile Simulator," paper SPE 17591, *J. Pet. Tech.* (Sept. 1991), 1140-1146; first presented at the 1988 Soc. Pet. Eng. Intl. Meeting on Petroleum Engineering, Tianjin, China (Nov. 1-4, 1988).

Bingham, E.C.: "An Investigation of the Laws of Plastic Flow," *Scientific Papers of the Bureau of Standards*, Dept. of Commerce, Washington DC, Paper 278 (June 5, 1916) **13**, 309-353; recapitulated in *Fluidity and Plasticity*, (also by Eugene C. Bingham) McGraw-Hill Book Co. Inc., New York (1922).

Bin-Haddah, A.S.: *Development of Models for Drill Cuttings Transport in Inclined Wells Based on Deposition Critical Velocity Concept*, M.Sc. dissertation, University of Tulsa, Tulsa, Oklahoma (1988).

Bird, R.B., Armstrong, R.C. and Hassager, O.: *Dynamics of Polymeric Liquids, Volume 1: Fluid Mechanics*, John Wiley & Sons Inc., New York (1977), 226-229.

Bizanti, M.S. and Robinson, S.: "PC Program Speeds Slip-Velocity Calculations," *Oil & Gas J.* (Nov. 7, 1988), 44-46.

Bjørge, E., Kvalvaag, T. and Vefring, E.: *GasKick User Manual*, Rogaland Research (Petroleum) document, Rogaland Research Institute, Stavanger/Bergen, Norway (1990).

Bourgoyne *Jr.*, A.T., Chenevert, M.E., Millheim, K.K. and Young *Jr.*, F.S.: *Applied Drilling Engineering*, SPE Textbook Series, Vol. 2, Society of Petroleum Engineers, Richardson, Texas (1986), Chapter 4.

Buckingham, E.: "On Plastic Flow Through Capillary Tubed," *Proc.* 24th Annual Meeting of the Am. Soc. Testing Materials, Asbury Park, New Jersey (June 21-24, 1921) **21**, 1154-1161.

Caldwell, D.H. and Babbitt, H.E.: "Flow of Muds, Sludges, and Suspensions in Circular Pipe," *Ind. Eng. Chem.* (1941) **33**, No. 2, 249-256.

Cartalos, U. and Dupuis, D.: "An Analysis Accounting for the Combined Effect of Drillstring Rotation and Eccentricity on Pressure Losses in Slimhole Drilling," paper SPE/IADC 25769, *Proc.* SPE/IADC Drilling Conference, Amsterdam, The Netherlands (Feb. 23-25, 1993), 871-881.

Casson, N.: "A Flow Equation for Pigment-Oil Suspensions of the Printing Ink Type," presented at the conference organised by the British Society of Rheology, University College, Swansea, UK (Sept. 1957), proceedings published as *Rheology of Disperse Systems*, Mill, C.C. (*ed.*), Pergamon Press, London (1959).

Chilingarian, G.V. and Vorabutr, P.: *Drilling and Drilling Fluids*, Developments in Petroleum Science, **11**, updated textbook edition, Elsevier Publishing Company Inc., New York (1983).

Churchill, S.W.: "Friction Factor Equation Spans All Fluid-Flow Regimes," *Chemical Engineer* (Nov. 7, 1977), 91-92.

Clapp, R.M.: "Turbulent Heat Transfer in Pseudoplastic Non-Newtonian Fluids," *Proc.* of the Conference on International Developments in Heat Transfer, University of Colorado, Boulder, Colorado (1961), 652-661.

Clark, P.E.: "Drilling Mud Rheology and the API Recommended Measurements," paper SPE 29543, *Proc.* Production Operations Symposium, Oklahoma City, Oklahoma (Apr. 2-4, 1995), 933-941.

Clarke, G.P.Y.: "Approximate Confidence Limits for a Parameter Function in a Nonlinear Regression," JASA - *J. Amer. Statist. Assoc.* (Mar. 1987) **82**, No. 397, 221-230.

Cloud, J.E. and Clark, P.E.: "Stimulation Fluid Rheology III. Alternatives to the Power Law Fluid Model for Cross-Linked Fluids," paper SPE 9332, *Proc.* 55th Annual Fall Technical Conference and Exhibition of the Soc. Pet. Eng. of AIME, Dallas, Texas (Sept. 21-24, 1980).

Code, R.K. and Raal, J.D.: "Rates of Shear in Coaxial Cylinder Viscometers," *Rheologica Acta* (1973) **12**, 578-587.

Colebrook, C.F.: "Turbulent Flow in Pipes with Particular Reference to the Transition Region Between Smooth and Rough Pipe Laws," *J. Inst. Civil Eng.*, London (1938/39) **11**, 133-156.

Comité des Techniciens: *Drilling Mud and Cement Slurry Rheology Manual*, Éditions Technip, Paris, France (1982); sometimes referred to as the Association Recherche Technip Ecole du Pétrole (ARTEP).

Crittendon, B.C.: "The Mechanics of Design and Interpretation of Hydraulic Fracture Treatment," *J. Pet. Tech.* (Oct. 1959) 21-29; *Trans.*, AIME.

Cross, M.M.: "Rheology of Non-Newtonian Fluids: A New Flow Equation for Pseudoplastic Systems," *J. Colloid Sci.* (June 1965) **20**, No. 5, 417-437.

Crowley, P.R. and Kitzes, A.S.: "Rheological Behavior of Thorium Oxide Slurries in Laminar Flow," *Ind. Eng. Chem.* (May 1957) **49**, No. 5, 888-892.

Daniel, C. and Wood, F.S.: *Fitting Equations to Data*, Wiley-Interscience, New York (1971) App. 3A.

Davies, S.J. and White, C.M.: "A Review of Flow in Pipes and Channels," article split into three successive unnumbered parts, *Engineering* (July 19, 1929) **128**, No. 71, 69-72; continued July 26, 98-100 and Aug. 2, 131-132.

De Sá, C.H.M., Martins, A.L. and Amaral, M.S.: "A Computer Programme for Drilling Hydraulics Optimisation Considering Realistic Rheological Models," paper SPE 27554, *Proc.* European Petroleum Computer Conference, Aberdeen, UK (Mar. 15-17, 1994), 137-146.

Deissler, R.G.: "Investigation of Turbulent Flow and Heat Transfer in Smooth Tubes, Including the Effect of Variable Fluid Properties," *Trans.*, ASME (Feb. 1951) **73**, 101-107.

Delwiche, R.A., Lejeune, M.W.D., Mawet, P.F.B.N. and Vighetto, R.: "Slimhole Drilling Hydraulics," paper SPE 24596, *Proc.* 67th Annual Technical Conference and Exhibition of the Soc. Pet. Eng., Washington, DC (Oct. 4-7, 1992), 527-541.

Dodge, D.W. and Metzner, A.B.: "Turbulent Flow of Non-Newtonian Systems," *AIChE J.* (June 1959) **5**, No. 2, 189-204.

Draper, N.R.: "The Box-Wetz Criterion versus R^2," *J. Royal Statistical Soc.* (1984) **A 147**, 100-103.

Drazin, P.G., and Reid, W.H.: *Hydrodynamic Stability,* Cambridge University Press, Cambridge, UK (1981).

Eisenschitz, R., Rabinowitsch, B. and Weissenberg, K.: "Zur Analyse des Formänderungswiderstandes," (*transl.* Analysis of Resistance to Strain) *Mitteilungen der deutschen Materialprüfungs-Austalten*, Berlin-Dahlen (1929) sonder heft No. 9, 91-94.

Ellis, S.C., Lanham, A.F. and Pankhurst, K.G.A.: "A Rotational Viscometer for Surface Films," *J. Scientific Instruments* (Feb. 1955) **32**, 70-73.

Exlog staff: *Theory and Application of Drilling Fluid Hydraulics*, Whittaker, A. (*ed.*), International Human Resources Development Corp., Boston, Massachusettes (1985).

Eyring, H.J.: "Viscosity, Plasticity and Diffusion as Examples of Absolute Reaction Rates," *J. Chemical Phys.* (Apr. 1936) **4**, 283-291.

Fisk, J.V. and Jamison, D.E.: "Physical Properties of Drilling Fluids at High Temperatures and Pressures," paper SPE 17200, *Soc. Pet. Eng. Drilling Eng.* (Dec. 1989) 341-346; first presented at the 1988 IADC/SPE Drilling Conference, Dallas, Texas, Feb. 28 - Mar. 2.

Franco, V. and Verduzco, M.B.: "Transition Critical Velocity in Pipes Transporting Slurries with Non-Newtonian Behavior," *Proc.* 4th Miami Univ. Intl. Symposium on Multiphase Transport & Particulate Phenomena, Coral Gables, Miami Beach, Florida (Dec. 15-17, 1988); published as *Particulate Phenomena and Multiphase Transport,* **4**, 289-299.

Fredrickson, A.G. and Bird, R.B.: "Non-Newtonian Flow in Annuli," *Ind. Eng. Chem.* (Mar. 1958) **50**, No. 3, 347-352.

Fredrickson, A.G. and Bird, R.B.: "Transport Phenomena in Multicomponent Systems," *Handbook of Fluid Dynamics*, Streeter, V.L. (*ed.*), Section 6, McGraw-Hill Book Co. Inc., New York (1961).

Gallant, A.R.: *Nonlinear Statistical Models*, John Wiley & Sons Inc., New York (1987).

Gavignet, A.A. and Wick, C.J.: "Computer Processing Improves Hydraulics Optimization with New Methods," paper SPE 14774, *Soc. Pet. Eng. Drilling Eng.* (Dec. 1987), 309-315; first presented at the IADC/SPE Drilling Conference, Dallas, Texas (Feb. 10-12, 1986).

Gavignet, A.A. and Sobey, I.J.: "Model Aids Cuttings Transport Prediction," paper SPE 15417, *J. Pet. Tech.* (Sept. 1989), 916-921; first presented as "A Model for the Transport of Cuttings in Highly Deviated Wells," *Proc.* Annual Technical Conference and Exhibition of the Soc. Pet. Eng., New Orleans, Louisiana (Oct. 5-9, 1986).

Geoservices Ltd.: *ALS-2 Application Hydraulics*, Geoservices Ltd operations manual for proprietary drilling hydraulics program HYDRAULIC, 3rd edition (May 1995).

Gill, P.E., Hammarling, S.J., Murray, W., Saunders, M.A. and Wright, M.H.: *User's Guide for LSSOL (Version 1.0)*, Report SOL 86-1, Department of Operations Research, Stanford University, California (1986).

Govier, G.W.: "For Laminar Flow of Bingham Plastics Use Chart to Find Friction Factors," *Chem. Eng.* (Aug. 24, 1959) **66**, 139-142.

Govier, G.W. and Aziz, K.: *The Flow of Complex Mixtures in Pipes*, Van Norstrand Reinhold Co., New York (1972).

Graves, W.G. and Collins, R.E.: "A New Rheological Model for Non-Newtonian Fluids," paper SPE 7654 *unsolicited* (June 1978); maniscript submitted for review to *J. Pet. Tech.* in 1978 and to *Soc. Pet. Eng. J.* in 1980 but remained unpublished.

Guckes, T.L.: "Laminar Flow of Non-Newtonian Fluids in an Eccentric Annulus," *J. Engineering for Industry* (May 1975) **97**, 498-506; *Trans.*, ASME; first presented at the Petroleum Mechanical Engineering Conference, Dallas, Texas (Sept. 15-18, 1974), paper No. 74-Pet-57.

Gücüyener, H.I. and Mehmetoğlu, T.: "Flow of Yield-Pseudo-Plastic Fluids Through a Concentric Annulus," *AIChE J.* (July 1992) **38**, No. 7, 1139-1143.

Guillot, D.: "Rheology of Well Cement Slurries," in *Well Cementing*, Nelson E.B. (*ed.*), Elsevier Science Publishing B.V., Amsterdam, The Netherlands (1990), Chapter 4.

Haciislamoglu, M.: *Non-Newtonian Fluid Flow in Eccentric Annuli and Its Application to Petroleum Engineering Problems*, Ph.D. thesis, Louisiana State University and Agricultural and Mechanical College, Louisiana (1989).

Haciislamoglu, M. and Langlinais, J.: "Non-Newtonian Fluid Flow in Eccentric Annuli," *J. Energy Res. Tech.* (Sept. 1990) **112**, No. 3, 163-169; *Trans.*, ASME.

Hall, H.N., Thompson, H. and Nuss, F.: "Ability of Drilling Mud to Lift Bit Cuttings," *Petroleum Transactions* (1950) **189**, T.P. 2782, 35-46; *Trans.*, AIME. First presented at the Petroleum Branch meeting, Columbus, Ohio (Sept. 25-28, 1949).

Hanks, R.W. and Christiansen, E.B.: "The Laminar-Turbulent Transition in Nonisothermal Flow of Pseudoplastic Fluids in Tubes," *AIChE J.* (Sept. 1962) **8**, No. 4, 467-471.

Hanks, R.W.: "The Laminar-Turbulent Transition for Fluids with a Yield Stress," *AIChE J.* (May 1963) **9**, No. 3, 306-309.

Hanks, R.W. and Pratt, D.R.: "On the Flow of Bingham Plastic Slurries in Pipes and Between Parallel Plates," *Soc. Pet. Eng. J.* (Dec. 1967) **7**, 342-346.

Hanks, R.W.: "Critical Reynolds Numbers for Newtonian Flow in Concentric Annuli," *AIChE J.* (Jan. 1980) **26**, No. 1, 152-154.

Hanks, R.W. and Peterson, J.M.: "Complex Transitional Flows in Concentric Annuli," *AIChE J.* (Sept. 1982) **28**, No. 5, 800-806.

Haut, R.C., Collins, R.E. and Graves, W.G.: "Application of a Computer Simulator to Primary Cementing," paper SPE 7588, *Proc.* 53rd Annual Fall Technical Conference and Exhibition of the Soc. Pet. Eng. of AIME, Houston, Texas (Oct. 1-3, 1978).

Healy, M.J.R.: "The Use of R^2 as a Measure of Goodness of Fit," *J. Royal Statistical Soc.* (1984) **A 147**, Part 4, 608-609.

Hedström, B.O.A.: "Flow of Plastics Materials in Pipes," *Ind. Eng. Chem.* (Mar. 1952) **44**, No. 3, 651-656.

Helland, I.S.: "On the Interpretation and Use of R^2 in Regression Analysis," *Biometrics* (Mar. 1987) **43**, No. 1, 61-69.

Hemphill, T., Campos, W. and Pilehvari, A.: "Yield-Power Law Model More Accurately Predicts Mud Rheology," *Oil & Gas J.* (Aug. 23, 1993), 45-50.

Herschel, W.H. and Bulkley, R.: "Measurement of Consistency as Applied to Rubber-Benzene Solutions," *Proc.* 29th Annual Meeting of the Am. Soc. Testing Materials, Atlantic City, NJ (June 21-25, 1926) **26**, No. 82, 621-629.

Hersey, M.D.: "Future Problems of Theoretical Rheology," *J. Rheology* (Apr. 1932) **3**, No. 2, 196-204.

Herzog, R.O. and Weissenberg, K.: "Ueber die thermische, mechanische und röntgenoptische Analyse der Quelling," (*transl.* The Thermal, Mechanical, and X-Ray Analysis of Swelling) *Kolloid-Zeit.* (Sept. - Dec. 1928) **46**, 277-289.

Hoberock, L.L., Thomas, D.C. and Nickens, H.V.: "Here's How Compressibility and Temperature Affect Bottom-Hole Mud Pressure," *Oil & Gas J.* (Mar. 22, 1982) 159-164.

Hougaard, P.: "The Appropriateness of the Asymptotic Distribution in a Nonlinear Regression Model in Relation to Curvature," *J. Royal Statistical Soc.* (1985) **B 47**, No. 1, 103-114.

Houwen, O.H. and Geehan, T.: "Rheology of Oil-Base Muds," paper SPE 15416, *Proc.* 61st Annual Technical Conference and Exhibition of the Soc. Pet. Eng., New Orleans, Louisiana (Oct. 5-8, 1986).

Hoyt, J.W.: "Effect of Additives on Fluid Friction," *J. Basic Eng.* Series D (June 1972) **94**, No. 2, 258-285, *Trans.*, ASME; First presented as a John R. Freeman scholar lecture, Winter Annual Meeting of the Fluids Engineering Division of the ASME, Washington, DC (Nov. 28 - Dec. 2, 1971).

Hussaini, S.M.M.: *A Study on the Applicability of Zeidler's Transport Model to the Prediction of Actual Drilling Mud Carrying Capacity*, M.Sc. dissertation, University of Tulsa, Tulsa, Oklahoma (1977).

Iyoho, A.W. and Azar, J.J.: "An Accurate Slot-Flow Model for Non-Newtonian Fluid Flow Through Eccentric Annuli," paper SPE 9447, *Soc. Pet. Eng. J.* (Oct. 1981), 565-572; first presented at the 55th Annual Technical Conference and Exhibition of the Soc. Pet. Eng. of AIME, Dallas, Texas (Sept. 21-24, 1980).

Iyoho, A.W., Horeth II, J.M. and Veenkant, R.L.: "A Computer Model for Hole-Cleaning Analysis," paper SPE 16694, *J. Pet. Tech.* (Sept. 1988) 1183-1192; first presented at the Annual Technical Conference and Exhibition of the Soc. Pet. Eng., Dallas, Texas (Sept. 27-30, 1987).

Jensen, T.B. and Sharma, M.P.: "Study of Friction Factor and Equivalent Diameter Correlations for Annular Flow of Non-Newtonian Drilling Fluids," *J. Energy Res. Tech.* (Dec. 1987) **109**, 200-205; *Trans.*, ASME.

Jones *Jr.*, O.C. and Leung, J.C.M.: "An Improvement in the Calculation of Turbulent Friction in Smooth Concentric Annuli," *J. Fluids Eng.* (Dec. 1981) **103**, 615-623; *Trans.*, ASME.

Khataniar, S., Chukwu, G.A. and Hua Xu: "Evaluation of Rheological Models and Application to Flow Regime Determination," *J. Pet. Sci. & Eng.* (1994) **11**, 155-164.

Knudsen, J.G. and Katz, D.L.: *Fluid Dynamics and Heat Transfer*, McGraw-Hill Book Co. Inc., New York (1958).

Krieger, I.M. and Elrod, H.: "Direct Determination of the Flow Curves of Non-Newtonian Fluids. II: Shearing Rate in the Concentric Cylindrical Viscometer," *J. Appl. Phys.* (Feb. 1953) **24**, Part 2, 134-136.

Krieger, I.M.: "Computation of Shear Rate in the Couette Viscometer," *Proc.* Fifth Int. Congress of Rheology held at Kyoto Int. Conf. Hall, Kyoto, Japan (Oct. 7-11, 1968) proceedings published by U. of Tokyo Press, Japan and U. Park Press, Manchester, UK (1969) **1**, 511-516.

Kutasov, I.M.: "Empirical Correlation Determines Downhole Mud Density," *Oil & Gas J.* (Dec. 12, 1988), 61-63.

Kutasov, I.M.: "Water FV Factors at Higher Pressures and Temperatures," *Oil & Gas J.* (Mar. 20, 1989), 102-104.

Kutasov, I.M.: "Correlation Simplifies Obtaining Downhole Brine Density," *Oil & Gas J.* (Aug. 5, 1991), 48-49.

Lamb, H.: *Hydrodynamics*, 6th edition, Dover Publications, New York (1932).

Langlinais, J.P., Bourgoyne *Jr.*, A.T. and Holden, W.R.: "Frictional Pressure Losses for Annular Flow of Drilling Mud and Mud-Gas Mixtures," *J. Energy Res. Tech.* (Mar. 1985) **107**, 142-151; *Trans.*, ASME.

Lauzon, R.V. and Reid, K.I.G.: "New Rheological Model Offers Field Alternative," *Oil & Gas J.* (May 21, 1979), 47-57.

Lenchow, J.R.: "Pressure Drop Calculations for Non-Newtonian Fluids," *Proc.* 3rd Lerkendal Petroleum Engineering Workshop, Trondheim, Norway (Jan. 20-21, 1993), 99-110.

Lohrenz, J. and Kurata, F.: "A Friction Factor Plot for Smooth Circular Conduits, Concentric Annuli, and Parallel Plates," *Ind. Eng. Chem.* (1960) **52**, No. 8, 703-706.

Lyness, J.N. and Moler, C.B.: "Numerical Differentiation of Analytic Functions," *SIAM J. Numerical Analysis* (June 1967) **4**, No. 2, 202-210.

Marken, C.D., Xiaojun He and Saasen, A.: "The Influence of Drilling Conditions on Annular Pressure Losses," paper SPE 24598, *Proc.* 67th Annual Technical Conference and Exhibition of the Soc. Pet. Eng., Washington, DC (Oct. 4-7, 1992), 553-567.

Martin, M., Georges, C., Bisson, P. and Konirsch, O.: "Transport of Cuttings in Directional Wells," paper SPE/IADC 16083, *Proc.* SPE/IADC Drilling Conference, New Orleans, Louisiana (Mar. 15-18, 1987), 293-303.

McCann, R.C., Quigley, M.S., Zamora, M. and Slater, K.S.: "Effects of High-Speed Pipe Rotation on Pressure in Narrow Annuli," paper SPE 26343, *Proc.* 68th Annual Technical Conference and Exhibition of the Soc. Pet. Eng., Houston, Texas (Oct. 3-6, 1993), 295-307.

McMordie *Jr.*, W.C., Bennett, R.B. and Bland, R.G.: "The Effect of Temperature and Pressure on the Viscosity of Oil-Base Muds," *J. Pet. Tech.* (July 1975), 884-886; *Trans.*, AIME.

McMordie *Jr.*, W.C., Bland, R.G. and Hauser, J.M.: "Effect of Temperature and Pressure on the Density of Drilling Fluids," paper SPE 11114, *Proc.* 57th Annual Fall Technical Conference and Exhibition of the Soc. Pet. Eng. of AIME, New Orleans, Louisiana (Sept. 26-29, 1982).

Melbouci, M.: *Modélisation de la Rhéologie, de la Compressibilité et de L'Ecoulement des Boues de Forage à Emulsion Inverse*, *Thèse de Doctorat*, Institut de Mécanique des Fluides, Université Louis Pasteur, Strasbourg, France (Jan. 1991).

Melrose, J.C., Savins, J.G., Foster, W.R. and Parish, E.R.: "Practical Utilization of the Theory of Bingham Plastic Flow in Stationary Pipes and Annuli," paper 876-G, *Proc.* 32nd Annual Fall Meeting of the SPE of the AIME, Dallas, Texas (Oct. 6-9, 1957); manuscript revised as paper TP8043, *Petroleum Development & Technology* (1958), 316-324; *Trans.*, AIME, **213**.

Metzner, A.B. and Reed, J.C.: "Flow of Non-Newtonian Fluids - Correlation of the Laminar, Transition and Turbulent Flow Regions," *AIChE J.* (Dec. 1955) **1**, No. 4, 434-440.

Metzner, A.B.: *Advances in Chemical Engineering*, Drew, T.B. and Hoopes, J.W. (*eds.*), Academic Press, New York (1956) **1**.

Millikan, C.B.: "A Critical Discussion of Turbulent Flows in Channels and Circular Tubes," paper presented at the 5th Intl. Congress for Applied Mechanics, held at Harvard University and the Massachusettes Institute of Technology, Cambridge, Massachusettes (Sept. 12-16, 1938); *Proc.* published by John Wiley & Sons Inc., New York (1939), 386-392.

Mitsuishi, N. and Aoyagi, Y.: "Non-Newtonian Fluid Flow in an Eccentric Annulus," *J. Chem. Eng. of Japan* (1973) **6**, No. 5, 402-408; first presented at the American Rheology Meeting, Cincinnati, Ohio (Jan. 31, 1973).

Mooney, M.: "Explicit Formulas for Slip and Fluidity," *J. Rheology* (Apr. 1931) **2**, No. 2, 210-222.

Moore, P.L.: *Drilling Practices Manual*, Petroleum Publishing Co., Tulsa, Oklahoma (1974).

NAG FORTRAN *Library Manual - Mark 13*, The Numerical Algorithms Group Limited, Oxford, UK (1988).

NOS staff: HYCAT *Drilling Hydraulics Simulator Instruction Manual*, Nordic Offshore Systems AS instruction manual for proprietary drilling hydraulics program, Bailey, W.J. (*ed.*) (1993).

Okafor, M.N.: *Experimental Verification of the Robertson-Stiff Rheology Model for Drilling Fluids*, M.Sc. dissertation, University of Wyoming, Laramie, Wyoming (May 1982).

Okafor, M.N. and Evers, J.F.: "Experimental Comparison of Rheology Models for Drilling Fluids," paper SPE 24086, *Proc.* Western Regional Meeting of the Soc. Pet. Eng., Bakersfield, California (March 30 - April 1, 1992), 575-581.

Okrajni, S.S. and Azar, J.J.: "The Effect of Mud Rheology on Annular Hole Cleaning in Directional Wells," paper SPE 10960, *Soc. Pet. Eng. Drilling Eng.* (Aug. 1986), 297-276; first presented at the Soc. Pet. Eng. Annual Technical Conference and Exhibition, New Orleans, Louisiana (Sept. 26-29, 1985).

Ostwald, W.: "Ueber die Geschwindigkeitsfunktion der Viskosität Disperser Systeme. I.," (*transl.* The Velocity Function of Viscosity of Disperse Systems) *Kolloid-Zeit.* (Jan. 1925) **36**, 99-117.

Parigot, P.: "Surface Recorder Can Signal Downhole Drilling Problems," *World Oil* (Nov. 1985), 71-79.

Paul, J.M.: "ECD Graphs from Power Law Equation for Laminar Flow," paper SPE 7156 *unsolicited* (1978) - unpublished.

Pawlowski, J.: "Bestimming des Reibungsgesetzes der nicht-Newtonschen Flüssigkeiten aus den Viskositätsmessungen mit Hilfe eines Rotationsviskosimeters," *Kolliod-Zeit.* (Mar. 1953) **130**, Part 3, 129-135.

Peden, J.M. and Yuejin Luo: "Settling Velocity of Variously Shaped Particles in Drilling and Fracturing Fluids," paper SPE 16243, *Soc. Pet. Eng. Drilling Eng.* (Dec. 1987), 337-343.

Peden, J.M., Ford, J.T. and Oyeneyin, M.B.: "Comprehensive Experimental Investigation of Drilled Cuttings Transport in Inclined Wells Including the Effects of Rotation and Eccentricity," paper SPE 20925, *Proc.* European Petroleum Conference (Europec 90), The Hague, The Netherlands (Oct. 22-24, 1990) Vol. 1, 393-404.

Peters, E.J., Chenevert, M.E. and Chunhai Zhang: "A Model for Predicting the Density of Oil-Based Muds at High Pressures and Temperatures," paper SPE 18036, *Soc. Pet. Eng. Drilling Eng.* (June 1990) **5**, No. 2, 141-148; first presented at the Soc. Pet. Eng. Annual Technical Conference and Exhibition, Houston, Texas (Oct. 2-5, 1988).

Philippoff, W.: "Zur Theorie der Strukturviskosität. I.," *Kolloid-Zeit.* (Apr. 1935) **71**, Part 1, 1-16.

Pigott, R.J.S.: "Mud Flow in Drilling," *Drilling and Production Practice*, (1941), 91-103; *Trans.*, API.

Politte, M.D.: "Invert Oil Mud Rheology as a Function of Temperature and Pressure," paper SPE/IADC 13458, *Proc.* SPE/IADC Drilling Conference, New Orleans, Louisiana (Mar. 6-8, 1985), 305-323.

Prandtl, L.: "Ein Gedenkenmodell zur Kinetischen Theorie der festen Körper," *Zeit. angew. Math. Mech.* (1928) **8**, 85-106.

Press, W.H., Flannery, B.P., Teukolsky, S.A. and Vetterling, W.T.: *Numerical Recipes in C*, Cambridge University Press, Cambridge, UK (1988).

Rabinowitsch, B.: "Über die Viskosität und Elastizatät von Solen," (*transl.* The Viscosity and Elasticity of Brines) *Zeit. für Physikalische Chem.* (1929) **A145**, 1-26.

Randall, B.V. and Anderson, D.B.: "Flow of Mud During Drilling Operations," paper SPE 9444, *J. Pet. Tech.* (July 1982), 1414-1420.

Ratkowsky, D.A.: *Nonlinear Regression Modelling*, Statistics: Textbooks and Monographs, Owens, D.B. (*ed.*), Marcel Dekker Inc., New York (1983) **48**.

Ratkowsky, D.A.: *Handbook of Nonlinear Regression Models*, Statistics: Textbooks and Monographs, Owens, D.B. (*ed.*), Marcel Dekker Inc., New York (1990) **107**.

Reed, T.D. and Pilehvari, A.A.: "A New Model for Laminar, Transitional, and Turbulent Flow of Drilling Fluids," paper SPE 25456, *Proc.* Production Operations Symposium, Oklahoma City, Oklahoma (Mar. 21-23, 1993), 469-482.

Reiner, M. and Rivlin, R.S.: "Zur Hydrodynamik von Systemen veränderlicher Viskosität, II. Die Strömung in der Kapillare," *Kolloid-Zeit.* (1928) **44**, 9-10.

Reiner, M.: "In Search for a General Law of the Flow of Matter," *J. Rheology* (Apr. 1930) **1**, No. 3, 250-260.

Reiner, M.: *Deformation, Strain and Flow*, Interscience, New York (1960).

Reynolds, O.: "An Experimental Investigation of the Circumstances Which Determine Whether the Motion of Water Shall be Direct or Sinuous, and the Laws of Resistance in Parallel Channels," *Phil. Trans. Royal Soc.*, London (1884) **174**, 935-982; first part of paper originally published in the *Proc. Royal Soc.* (1883) **35**, 84-99.

Ribeiro, P.R., Podio, A.L. and Sepehrnoori, K.: "The Effect of Rotational Speed and Eccentricity on Annular Flows with Application to Slim Hole Drilling Hydraulics," paper SPE 26958, *Proc.* 3rd Latin American/Caribbean Petroleum Engineering Conference, Buenos Aires, Argentina (Oct. 3-6, 1993), 669-677.

Robertson, R.E. and Stiff, H.H.: "An Improved Mathematical Model for Relating Shear Stress to Shear Rate in Drilling Fluids and Cement Slurries," paper SPE 5333 *Soc. Pet. Eng. J.* (Feb. 1976) **16**, No. 1, 31-36; first presented at the SPE-AIME Rocky Mountain Regional Meeting, Denver, Colorado (Apr. 7-9, 1975).

Rommetveit, R.: *A Numerical Simulation Model for Gas Kicks in Oil Based Drilling Fluids*, Doctor Scientiarum thesis, University of Bergen, Norway (1988).

Rommetveit, R. and Olsen, T.L.: "Gas Kick Experiments in Oil-Based Drilling Muds in a Full-Scale, Inclined Research Well," paper SPE 19561, *Proc.* 64th Annual Technical Conference and Exhibition of the Soc. Pet. Eng., San Antonio, New Mexico (Oct. 8-11, 1989), 433-446.

Ross, G.J.S.: "Simple Non-linear Modelling for the General User," *Proc.* 40th Session of the Intl. Stats. Inst., Warsaw, Poland, *Bulletin of the Int. Stats. Inst.* (Sept. 1-9, 1975) **46**, Book 2: *The Invited Papers*, 585-593.

Rothfus, R.R.: *Velocity Distribution and Fluid Friction in Concentric Annuli*, D.Sc. thesis, Carnegie Institute of Technology, Pittsburgh (1948).

Rothfus, R.R., Monrad, C.C. and Senecal, V.E.: "Velocity Distribution and Fluid Friction in Smooth Concentric Annuli," *Ind. Eng. Chem.* (1955) **42**, 2511-2520.

Ryan, N.W. and Johnson, M.M.: "Transition From Laminar to Turbulent Flow in Pipes," *AIChE J.* (Dec. 1959) **5**, No. 4, 433-435.

Saffman, P.G.: "The Lift on a Small Sphere in a Slow Shear Flow," *J. Fluid Mech.* (1965) **22**, part 2, 385-400.

Savins, J.G.: "Generalized Newtonian (Pseudoplastic) Flow in Stationary Pipes and Annuli," *J. Pet. Tech.* (1958) **213**, 325-332; *Trans.*, AIME.

Savins, J.G., Wallick, G.C. and Foster, W.R.: "The Differentiation Method in Rheology: I. Poiseuille-Type Flow," *Soc. Pet. Eng. J.* (Sept. 1962*a*) **2**, 211-215; an outline of the paper was presented at the 31st Annual Meeting of the Society of Rheology, Pittsburgh, Pensylvania (Oct. 31 - Nov. 2, 1960).

Savins, J.G., Wallick, G.C. and Foster, W.R.: "The Differentiation Method in Rheology: II. Characteristic Derivatives of Ideal Models in Poiseuille Flow," *Soc. Pet. Eng. J.* (Dec. 1962*b*) **2**, 309-316; an outline of the paper was presented at the 31st Annual Meeting of the Society of Rheology, Pittsburgh, Pensylvania (Oct. 31 - Nov. 2, 1960).

Schuh, F.J.: "Computer Makes Surge Pressure Calculations Useful," *Oil & Gas J.* (Aug. 3, 1964), 96-104.

Seber, G.A.F. and Wild, C.J.: *Nonlinear Regression*, John Wiley & Sons Inc., New York (1989).

Sifferman, T.R., Myers, G.M., Haden, E.L. and Wahl, H.A.: "Drill Cutting Transport in Full Scale vertical Annuli," paper SPE 4514, *J. Pet. Tech.* (Nov. 1976), 1295-1302, *Trans.*, AIME; first presented at the 48th Annual Fall Meeting of the Soc. Pet. Eng. of AIME, Las Vegas, Nevada (Sept. 30 - Oct. 3, 1973).

Silva, M.G.P. and Martins, A.L.: "Pressure Drop Estimate for the Turbulent Annular Flow of Drilling Fluids," *Proc.* 10th Brazilian Congress of Mechanical Engineers, Rio de Janeiro, Brazil (1989).

Sisko, A.W.: "The Flow of Lubricating Greases," *Ind. Eng. Chem.* (Dec. 1958) **50**, No. 12, 1789-1792.

Skelland, A.H.P.: *Non-Newtonian Flow and Heat Transfer*, John Wiley & Sons Inc., New York (1967).

Skjetne, E.: "Hyperbolic Rheological Model for Pseudoplastic Fluid Characterisation," IPT/NTNU Technical Note, Institute for Petroleum Technology and Applied Geophysics, University of Trondheim, Norway (1996).

Spencer, R.S.: "Flow of Linear Amorphous Polymers," *J. Polymer Sci.* (1950) **5**, 591-608.

Spencer, R.S. and Dillon, R.E.: "The Viscous Flow of Molten Polystyrene," *J. Colloid Sci.* (1948) **3**, 168-180; plus notes by Dienes, G.L. and Dexter, F.D., 181-183.

Sperry-Sun Drilling Services MWD Technical Information Manual, Sperry-Sun Inc. document M00052 - Revision A, (May 1989).

Strømnes, E. and Lydvo, A.: *Drilling Hydraulics*, document EXT 93/02, Rev. 1.0 NSD 109.93, part of a series of tutorials produced for the joint development project between the North Sea Drilltrainer foundation, Norsk Agip A/S and Nordic Offshore Systems AS (1993).

Symonds, F.L., Rosenthal, A.J. and Shaw, E.H.: "Sizing Pipe for Flow of Cellulose Acetate Solution," *Ind. Eng. Chem.* (1955) **47**, 2463-2466.

Sze-Foo Chien: "Annular Velocity for Rotary Drilling Operations," *Intl. J. Rock Mech. Min. Sci.* (1972) **9**, 403-416.

Taylor, R. and Smalling, D.: "A New and Practical Application of Annular Hydraulics," paper SPE 4518, *Proc.* 48th Annual Fall Meeting of the Soc. Pet. Eng. of AIME, Las Vagas, Nevada (Sept. 30 - Oct. 3, 1973).

Thomas, R.P.: *Drill Pipe Eccentricity Effect on Drilled Cuttings Behavior*, M.Sc. dissertation, University of Tulsa, Tulsa, Oklahoma (1978).

Thonhauser, G., Millheim, K.K. and Spörker, H.F.: "The Applicability of Current Slimhole Hydraulics Algorithms Under Field Conditions - A Critical Review," paper SPE 30489, *Proc.* Annual Technical Conference and Exhibition of the Soc. Pet. Eng., Dallas, Texas (Oct. 22-25, 1995).

Tomita, Y.: "On the Fundamental Formula of Non-Newtonian Flow," *Bulletin Jap. Soc. Mech. Eng.* (Aug. 1959) **2**, No. 7, 469-474.

Toms, B.A.: "Some Observations on the Flow of Linear Polymer Solutions Through Straight Tubes at Large Reynolds Number," *Proc.* 1st International Congress on Rheology, Part 2, North-Holland Publishing Co., Amsterdam, The Netherlands (1948), 135-141.

Torrance, B. McK.: "Friction Factors for Turbulent Non-Newtonian Fluid Flow in Circular Pipes," *South African Mechanical Engineer* (Nov. 1963) **13**, 89-91.

Tukey, J.W.: *Exploratory Data Analysis*, Behavioral Science: Quantitative Methods Series, Addison-Wesley Publishing Company Inc., New York (1977), 39-43.

Üner, D., Özgen, C. and Tosun, İ.: "An Approximate Solution for Non-Newtonian Flow in Eccentric Annuli," *Ind. Eng. Chem. Res.* (1988) **27**, No. 4, 698-701.

Üner, D., Özgen, C. and Tosun, İ.: "Flow of a Power-Law Fluid in an Eccentric Annulus," paper SPE 17002, *Soc. Pet. Eng. Drilling Eng.* (Sept. 1989), 269-272.

Valentic, L. and Whitmore, R.L.: "The Terminal Velocity of Spheres in Bingham Plastics," *British J. Appl. Phys.* (1965) **16**, 1197-1203.

Vaughn, R.D.: "Axial laminar Flow of Non-Newtonian Fluids in Narrow Eccentric Annuli," *Soc. Pet. Eng. J.* (1965) **5**, 277-280.

de Waele, A.: "Viscometry and Plastometry," *J. Oil and Colour Chemists' Assoc.* (Feb. 1923) **6**, No. 38, 33-88.

Walker, R.E. and Al-Rawi, O.: "Helical Flow of Bentonite Slurries," paper SPE 3108, *Proc.* 45th Annual Fall Meeting of the Soc. Pet. Eng. of AIME, Houston, Texas (Oct. 4-7, 1970).

Walker, R.E. and Mayes, T.M.: "Design of Muds for Carrying Capacity," paper SPE 4975 *J. Pet. Tech.* (July 1975), 893-900, *Trans.*, AIME; first presented at the SPE-AIME 49th Annual Fall Meeting, Houston, Texas (Oct. 6-9, 1974).

Wallick, G.C. and Savins, J.G.: "A Comparison of Differential and Integral Descriptions of the Annular Flow of a Power-Law Fluid," *Soc. Pet. Eng. J.* (Sept. 1969), 311-315.

Wang Zhongying and Tang Songren: "Casson Rheological Model in Drilling Fluid Mechanics," paper SPE 10564, *Proc.* International Meeting on Petroleum Engineering presented by the Chinese Party, China (1982), 397-435.

Wani. G.A., Sarkar, M.K. and Mani, B.P.: "Critical Velocity in Multisize Particle Transportation Through Horizontal Pipes," *J. Pipelines*, Elsevier Scientific Publishing Company, Amsterdam, The Netherlands (1982) **2**, 57-62.

Warren, T.M.: "Evaluation of Jet-Bit Pressure Losses," paper SPE 17916, *Soc. Pet. Eng. Drilling Eng.* (Dec. 1989), 335-340.

Wetherill, G.B.: *Elementary Statistical Methods*, Chapman & Hall, London (1972).

White, D.B. and Walton, I.C.: "A Computer Model for Kicks in Water- and Oil-Based Muds," paper IADC/SPE 19975, *Proc.* 1990 IADC/SPE Drilling Conference, Houston, Texas (Feb. 27 - Mar. 2, 1990), 541-550.

Wilhelm, R.H., Wroughton, D.M. and Loeffel, W.F.: "Flow of Suspensions Through Pipes," *Ind. Eng. Chem.* (May 1939) **31**, No. 5, 622-629.

Williams *Jr.*, C.E. and Bruce, G.H.: "Carrying Capacity of Drilling Muds," *Petroleum Transactions* (1951) **192**, T.P. 3026, 111-120, *Trans.*, AIME; first presented at the Fall Meeting of the Petroleum Branch of the AIME, New Orleans, Louisiana (Oct. 4-6, 1950).

Williamson, R.V.: "The Flow of Pseudoplastic Materials," *Ind. Eng. Chem.* (Nov. 1929) **21**, 1108-1111.

Wilson, N.W. and Azad, R.S.: "A Continuous Prediction Method for Fully Developed Laminar, Transitional, and Turbulent Flows in Pipes," *J. Applied Mechanics* (Mar. 1975), 51-54; *Trans.*, ASME.

de Wolf, R.C., Coffin, G.B. and Byrd, R.V.: "Effects of Temperature and Pressure on Rheology of Less Toxic Oil Muds," paper SPE 11892, *Proc.* Offshore Europe Conference, Aberdeen, UK (Sept. 6-9, 1983).

Yang, T.M.T. and Krieger, I.M.: "Comparison of Methods for Calculating Shear Rates in Coaxial Viscometers," *J. Rheology*, John Wiley & Sons, Interscience, New York (1978) **22**, No. 4, 413-421; *Trans.*, Soc. of Rheology.

Yuejin Luo and Peden, J.M.: "Flow of Non-Newtonian Fluids Through Eccentric Annuli," paper SPE 16692, *Soc. Pet. Eng. Production Eng.* (Feb. 1990), 91-96; first presented at the Soc. Pet. Eng. Annual Technical Conference and Exhibition, Dallas, Texas (Sept. 27-30, 1987).

Zandi, I. and Govatos, G.: "Hetergeneous Flow of Solids in Pipelines," *J. of the Hydraulics Division of the ASCE* (May 1967) **HY3**, 145-159, *Proc.*, ASCE.

Zeidler, H.U.: *Fluid and Drilled Particle Dynamics Related to Drilling Mud Carrying Capacity*, Ph.D. thesis, University of Tulsa, Tulsa, Oklahoma (1974).

Zigrang, D.J. and Sylvester, N.D.: "Explicit Approximations to the Solution of Colebrook's Friction Factor Equation," *AIChE J.* (May 1982) **28**, No. 3, 514-515.

Appendix A

Drilling Fluid Data Tables

Fluid Type	Characteristic	Value/Range
Bentonite/ polymer (22 data sets)	Mud Weight [g/cm^3]:	$1.60 \rightarrow 1.68$
	Solids [vol.%]:	$18.0 \rightarrow 22.0$
	Gel @ 10sec [Pa]:	$4.4 \rightarrow 18.0$
	Gel @ 10min [Pa]:	$9.0 \rightarrow 40.0$
	pH:	$7.8 \rightarrow 9.5$
Sea water/ pac (23 data sets)	Mud Weight [g/cm^3]:	$1.05 \rightarrow 1.25$
	Solids [vol.%]:	$2.9 \rightarrow 13.5$
	Gel @ 10sec [Pa]:	$0.5 \rightarrow 2.5$
	Gel @ 10min [Pa]:	$1.0 \rightarrow 15.0$
	pH:	$7.7 \rightarrow 10.1$
KCl/ pac (83 data sets)	Mud Weight [g/cm^3]:	$1.30 \rightarrow 1.54$
	Solids [vol.%]:	$13.0 \rightarrow 23.0$
	Gel @ 10sec [Pa]:	$2.0 \rightarrow 4.0$
	Gel @ 10min [Pa]:	$3.0 \rightarrow 12.5$
	pH:	$7.7 \rightarrow 9.0$
	Polymer [kg/m^3]:	$14.7 \rightarrow 18.4$
Oil Based Muds (286 data sets)	Mud Weight [g/cm^3]:	$1.3 \rightarrow 1.7$
	Solids [vol.%]:	$16.0 \rightarrow 29.0$
	Gel @ 10sec [Pa]:	$3.5 \rightarrow 17.0$
	Gel @ 10min [Pa]:	$5.5 \rightarrow 27.0$
	Oil/Water Ratio:	$75/25 \rightarrow 84/16$

Table A.1: General drilling fluid data set characteristics with value ranges. All samples are from mud pits with measurements taken at 50°C.

Data	Fann Viscometer Readings:								Mud	Gel Str.		Solids
Set	θ_{600}	θ_{300}	θ_{200}	θ_{100}	θ_{60}	θ_{30}	θ_{6}	θ_{3}	Weight	[10s]	[10m]	[vol.%]
1	54	39	33	30	27	25	21	20	1.65	18.0	40.0	21.00
2	107	64	48	35	27	21	16	9	1.65	12.0	25.5	18.00
3	50	35	29	23	20	15	11	9	1.65	11.5	22.5	19.00
4	119	67	49	30	23	17	12	11	1.65	9.0	21.0	19.50
5	68	45	37	27	21	17	12	11	1.65	6.5	14.0	22.00
6	69	46	37	27	22	17	12	11	1.65	7.0	14.5	22.00
7	80	56	47	35	27	22	14	13	1.65	8.0	18.0	22.50
8	64	44	32	24	18	14	9	8	1.68	5.0	9.0	22.00
9	79	54	43	30	24	18	11	10	1.66	6.5	16.0	22.50
10	64	44	36	27	23	19	14	13	1.65	7.0	20.0	22.50
11	60	42	35	25	21	18	12	10	1.65	6.0	18.5	22.50
12	58	41	34	25	21	17	11	10	1.65	6.0	18.0	22.50
13	58	42	34	24	21	16	11	10	1.65	6.0	17.5	22.50
14	59	43	34	24	21	16	11	10	1.65	6.0	17.0	22.50
15	67	49	40	30	25	20	14	13	1.65	7.5	17.0	22.50
16	65	47	41	32	27	23	18	17	1.65	11.0	18.0	22.50
17	61	44	38	30	27	22	14	13	1.65	8.5	17.0	22.50
18	86	63	53	41	36	29	20	18	1.65	10.0	19.0	22.50
19	60	43	38	29	26	20	13	12	1.65	7.5	16.0	22.50
20	69	49	41	31	27	22	16	15	1.60	14.5	22.0	22.50
21	72	53	45	36	32	27	20	19	1.65	12.0	25.0	22.00
22	72	53	45	36	32	27	20	19	1.65	12.0	25.0	22.00

Table A.2: Bentonite/polymer drilling fluid data sets.

Data Set	Fann Viscometer Readings:								Mud Weight	Gel Str.		Solids
	θ_{600}	θ_{300}	θ_{200}	θ_{100}	θ_{60}	θ_{30}	θ_6	θ_3		[10s]	[10m]	[vol.%]
1	48	33	27	18	13	8	2	1	1.05	1.0	1.0	2.90
2	50	35	28	18	13	8	2	1	1.06	0.5	1.0	3.50
3	51	35	28	18	14	9	3	2	1.09	1.0	1.5	5.40
4	48	33	26	18	13	9	3	2	1.11	1.5	5.0	6.70
5	68	48	38	26	19	13	4	3	1.12	1.5	6.0	7.30
6	62	43	34	23	17	12	4	3	1.12	1.5	6.0	7.30
7	55	36	29	19	14	9	3	2	1.15	1.5	5.5	9.20
8	59	39	31	20	15	10	4	3	1.17	1.7	7.0	10.40
9	65	44	34	23	17	11	5	4	1.19	2.0	9.0	11.70
10	60	40	32	21	16	11	4	3	1.20	2.0	10.0	11.70
11	52	36	28	19	14	10	4	3	1.18	2.0	10.0	11.10
12	53	36	28	18	14	9	4	3	1.18	1.5	7.0	11.10
13	66	44	35	23	17	11	4	3	1.20	1.5	8.0	11.70
14	62	43	34	21	15	10	4	3	1.21	2.0	7.5	12.00
15	65	43	34	22	16	11	4	3	1.21	2.0	11.0	12.00
16	68	45	36	23	17	11	4	3	1.22	1.5	12.0	13.00
17	72	47	37	24	18	12	5	4	1.22	2.0	15.0	13.00
18	60	40	31	19	14	9	4	3	1.22	2.0	8.5	13.00
19	61	40	31	20	15	10	4	3	1.21	1.5	9.0	12.50
20	61	40	31	19	15	10	4	3	1.23	1.5	9.0	13.50
21	57	38	28	17	13	9	4	3	1.23	1.5	8.5	13.50
22	77	53	41	31	25	21	18	16	1.76	12.0	32.0	25.50
23	76	51	39	29	23	20	16	10	1.78	14.0	30.0	29.00

Table A.3: Seawater/pac drilling fluid data sets.

Data Set	Fann Viscometer Readings: θ_{600}	θ_{300}	θ_{200}	θ_{100}	θ_{60}	θ_{30}	θ_6	θ_3	Mud Weight	Gel Str. [10s]	[10m]	Solids [vol.%]
1	90	61	48	33	25	17	7	5	1.25	2.5	3.0	10.00
2	95	66	53	33	25	17	7	5	1.25	2.5	3.0	10.50
3	78	52	41	28	21	15	7	5	1.30	2.0	3.0	14.00
4	90	61	49	33	25	18	7	5	1.31	2.5	4.0	14.50
5	94	64	51	35	26	18	8	6	1.32	3.0	4.0	14.50
6	83	57	45	31	24	17	7	5	1.30	2.5	3.5	13.00
7	92	63	51	35	27	19	8	6	1.35	3.0	4.5	17.00
8	94	66	53	37	29	20	8	6	1.36	3.5	5.0	18.00
9	97	67	54	37	29	20	9	6	1.36	3.5	5.0	18.00
10	102	70	57	39	30	21	9	6	1.35	3.5	4.5	16.50
11	105	72	58	40	31	21	9	7	1.45	3.5	7.0	21.50
12	104	71	57	40	31	21	9	7	1.45	3.5	7.0	21.50
13	106	73	60	40	31	21	9	7	1.45	3.5	6.0	21.50
14	121	83	67	47	37	26	12	8	1.45	4.0	8.0	21.50
15	105	72	58	40	30	20	8	6	1.45	3.0	4.0	20.00
16	98	67	53	37	28	19	8	6	1.45	3.0	5.0	20.00
17	95	65	53	36	27	19	8	5	1.45	2.5	5.0	20.00
18	104	72	58	40	31	21	9	6	1.45	3.0	6.0	21.50
19	85	58	47	33	25	17	7	5	1.45	2.5	4.0	20.00
20	86	58	47	33	25	17	7	5	1.45	2.5	4.0	20.00
21	99	68	55	32	28	19	8	6	1.45	3.0	5.0	20.00
22	91	62	50	34	26	18	8	6	1.46	3.0	5.0	20.00
23	89	60	48	33	25	17	7	5	1.45	2.5	4.5	20.00
24	93	64	51	36	28	20	9	7	1.48	3.5	6.0	21.50
25	88	59	48	33	25	18	7	5	1.45	2.5	4.0	20.00
26	116	79	63	43	33	24	10	7	1.50	4.0	7.0	22.50
27	115	78	62	42	33	23	10	7	1.50	4.0	6.0	21.50
28	107	72	58	40	29	20	8	6	1.50	3.0	4.5	21.50
29	98	67	54	37	29	20	9	6	1.50	3.5	5.0	21.50
30	114	77	62	42	32	22	9	7	1.50	3.5	5.5	21.50
31	105	72	57	39	30	21	8	6	1.50	3.5	5.0	21.50
32	110	75	61	41	31	22	9	6	1.50	3.5	5.5	21.00
33	113	77	63	43	34	23	10	7	1.50	4.0	6.0	21.00
34	110	75	60	42	33	23	10	7	1.50	4.0	6.0	21.00
35	108	73	58	40	31	22	9	6	1.50	3.5	5.0	21.00
36	106	72	59	41	31	22	10	7	1.50	3.5	5.5	21.00
37	101	70	56	39	30	21	9	6	1.50	3.5	5.5	21.00
38	109	74	58	40	31	22	9	6	1.50	3.5	5.5	21.50
39	116	80	64	44	34	23	10	7	1.50	3.5	5.5	21.50
40	120	81	67	45	35	24	10	7	1.53	4.0	6.0	22.50
41	117	79	63	44	33	23	9	6	1.53	3.5	5.5	23.00
42	110	74	59	40	31	22	9	6	1.53	3.5	5.5	22.50

Table A.4*a*: KCl/pac drilling fluid data (sets 1-42).

Data Set	Fann Viscometer Readings: θ_{600}	θ_{300}	θ_{200}	θ_{100}	θ_{60}	θ_{30}	θ_6	θ_3	Mud Weight	Gel Str. [10s]	[10m]	Solids [vol.%]
43	117	80	65	45	35	24	11	7	1.53	4.0	5.5	22.50
44	127	86	70	48	37	26	12	8	1.53	4.0	7.5	23.00
45	122	82	66	45	35	24	10	7	1.53	4.0	7.0	22.00
46	118	79	64	44	34	24	10	7	1.53	4.0	6.5	22.00
47	116	78	62	43	33	23	10	7	1.53	4.0	6.0	22.00
48	112	76	60	41	32	22	9	7	1.53	4.0	6.0	22.00
49	111	75	60	41	32	22	9	7	1.53	4.0	6.0	22.00
50	116	78	62	42	33	23	10	7	1.53	4.0	6.0	22.00
51	117	80	65	45	34	25	11	8	1.53	4.0	6.5	22.50
52	109	74	59	41	31	22	9	7	1.53	4.0	6.0	22.00
53	108	74	58	40	31	22	10	7	1.53	4.0	7.0	22.00
54	109	75	60	41	34	25	11	8	1.53	4.5	10.0	22.50
55	109	74	60	41	32	23	10	7	1.53	4.5	12.0	23.00
56	100	68	53	37	29	21	9	7	1.53	4.0	9.0	22.50
57	96	65	51	35	27	20	9	7	1.53	4.0	8.0	22.00
58	103	69	55	37	29	20	9	7	1.53	4.0	9.5	22.50
59	105	71	56	39	30	20	10	7	1.53	4.0	10.5	22.50
60	99	67	53	36	28	20	9	7	1.53	4.0	8.5	22.00
61	98	66	53	36	28	20	9	7	1.53	4.0	8.5	22.00
62	97	66	52	36	28	20	9	7	1.53	4.0	8.5	22.00
63	109	73	58	40	30	21	9	7	1.53	4.0	10.0	22.50
64	100	67	52	36	28	20	9	7	1.53	4.0	8.5	22.00
65	87	58	46	31	24	17	8	6	1.53	3.0	7.5	22.00
66	88	59	47	32	25	18	8	6	1.53	3.0	7.5	22.00
67	90	60	48	33	26	18	8	6	1.53	3.5	8.0	22.00
68	93	63	48	33	26	18	8	6	1.53	3.5	7.0	22.00
69	91	61	48	33	26	18	8	6	1.53	3.0	7.0	22.00
70	92	62	48	33	26	18	8	6	1.53	3.5	7.0	22.00
71	89	60	47	33	25	18	8	6	1.53	3.5	7.5	22.00
72	91	62	48	33	26	18	8	6	1.53	3.5	12.0	22.00
73	44	29	21	15	11	9	4	2	1.53	1.0	2.0	23.70
74	42	28	21	15	12	9	4	2	1.53	1.0	2.0	23.70
75	50	32	24	16	12	9	4	3	1.57	1.5	2.5	23.40
76	52	34	26	17	13	10	5	4	1.57	2.0	3.5	23.40
77	61	37	27	17	12	9	4	2	1.65	0.5	1.5	24.00
78	79	48	38	24	17	13	5	3	1.65	0.5	2.0	24.00
79	83	51	40	26	19	13	6	4	1.65	0.5	1.5	24.00
80	101	67	53	39	29	21	11	8	1.74	4.5	11.0	28.50
81	97	65	51	36	28	21	11	8	1.72	4.5	11.5	28.50
82	105	62	46	28	21	15	11	10	1.30	13.0	21.0	16.00
83	126	73	52	31	23	16	12	11	1.31	14.0	22.0	16.00

Table A.4*b*: KCl/pac drilling fluid data (sets 43-83).

Data Set	Fann Viscometer Readings: θ_{600}	θ_{300}	θ_{200}	θ_{100}	θ_{60}	θ_{30}	θ_{6}	θ_{3}	Mud Weight	Gel Str. [10s]	[10m]	Solids [vol.%]	Oil/Water Ratio
1	82	48	34	22	16	12	6	5	1.64	3.5	5.5	24.00	80/20
2	89	51	37	23	17	11	6	5	1.65	3.5	6.0	24.00	80/20
3	90	51	37	23	13	12	5	4	1.65	3.5	5.5	25.00	79/21
4	93	54	40	25	19	14	8	7	1.65	4.5	7.5	25.50	80/20
5	92	53	39	24	18	13	8	7	1.65	4.5	7.5	25.00	79/21
6	99	57	42	27	20	14	8	7	1.65	5.5	9.0	25.50	79/21
7	97	55	41	26	20	14	8	7	1.65	5.0	8.0	25.50	79/21
8	94	54	39	25	18	13	8	7	1.66	4.5	7.5	26.00	80/20
9	96	55	41	26	19	14	8	7	1.65	5.0	9.0	26.00	82/18
10	98	56	41	26	20	15	8	7	1.65	5.5	9.5	26.50	82/18
11	104	62	45	29	23	17	10	9	1.65	7.5	13.0	26.50	83/17
12	106	63	46	30	23	17	10	9	1.65	7.5	13.0	26.50	83/17
13	95	56	42	27	22	16	10	8	1.65	6.5	13.0	26.50	83/17
14	91	53	40	26	20	15	9	7	1.65	5.0	10.5	26.50	83/17
15	94	55	43	27	21	15	9	7	1.65	5.0	10.5	26.50	84/16
16	107	63	47	30	23	17	10	9	1.65	7.0	13.0	26.50	83/17
17	102	60	45	29	23	16	10	8	1.65	6.0	13.5	26.50	84/16
18	105	63	47	30	24	17	11	9	1.65	7.0	14.0	26.00	83/17
19	102	60	45	29	23	17	10	9	1.65	6.5	12.5	26.00	83/17
20	104	62	46	29	23	17	10	9	1.65	6.5	13.0	26.00	83/17
21	104	61	45	29	23	16	9	8	1.65	6.5	12.5	26.00	83/17
22	105	62	46	30	23	17	10	9	1.65	7.5	13.5	26.00	84/16
23	100	59	43	28	22	15	9	8	1.65	6.0	12.5	26.00	83/17
24	106	59	43	26	20	14	8	7	1.65	5.5	9.5	25.00	79/21
25	100	58	44	29	23	17	10	9	1.65	6.5	13.0	24.50	78/22
26	104	59	43	26	23	15	9	8	1.65	5.5	9.5	25.00	79/21
27	93	53	38	24	18	13	7	6	1.65	5.0	9.0	26.00	77/23
28	119	67	48	30	23	16	9	7	1.65	5.0	10.0	26.00	75/25
29	104	61	46	30	23	18	11	10	1.65	7.5	12.0	25.00	75/25
30	99	58	43	29	23	17	11	9	1.65	7.5	15.0	26.00	74/26
31	101	58	44	31	23	17	11	10	1.65	7.0	14.0	26.00	74/26
32	104	58	43	27	22	15	9	8	1.65	5.5	11.0	25.50	74/26
33	100	58	42	28	20	15	9	8	1.65	5.0	9.5	25.50	74/26
34	99	58	43	27	21	15	9	8	1.65	5.5	9.5	25.00	75/25
35	110	64	47	30	25	17	11	10	1.65	6.5	12.0	26.50	77/23
36	102	60	45	29	23	17	11	10	1.65	6.5	13.0	25.50	78/22
37	98	58	44	29	23	17	11	10	1.65	6.0	12.0	26.00	77/23
38	95	56	42	28	22	16	10	9	1.65	6.0	9.5	25.50	79/21
39	102	60	46	30	23	18	11	10	1.65	6.0	10.5	26.25	78/22
40	98	58	44	28	22	16	10	9	1.65	5.5	9.5	26.00	78/22
41	100	60	45	30	24	18	11	10	1.65	7.0	13.0	26.00	80/20
42	108	63	47	31	25	18	12	10	1.65	7.0	13.0	26.50	80/20
43	100	59	45	29	23	17	11	10	1.65	7.0	14.0	26.00	80/20
44	102	60	46	30	24	17	11	10	1.65	7.0	13.0	26.25	78/22
45	104	62	46	30	24	17	11	10	1.65	6.5	13.5	26.00	80/20
46	120	70	53	34	27	20	14	12	1.65	8.5	18.0	26.25	80/20
47	124	72	54	35	27	19	13	11	1.65	8.0	17.0	26.50	80/20
48	116	68	51	33	26	19	12	11	1.65	8.0	16.0	26.00	81/19
49	115	68	51	34	27	20	14	12	1.65	9.5	19.0	26.00	80/20
50	116	68	50	32	25	18	12	10	1.66	7.0	14.5	26.25	81/19
51	118	69	52	33	29	18	13	11	1.65	7.5	16.0	26.00	81/19
52	116	68	51	34	26	20	13	12	1.65	8.5	18.0	26.10	81/19
53	115	67	50	32	25	18	12	10	1.65	7.5	15.0	26.25	81/19
54	120	69	52	33	26	18	12	11	1.65	8.0	17.0	26.00	80/20
55	119	70	52	35	27	21	14	13	1.65	8.5	18.0	26.00	80/20
56	126	73	55	37	29	21	13	12	1.65	8.5	19.0	26.00	80/20
57	119	69	52	33	25	18	12	10	1.64	8.0	16.0	26.00	80/20
58	121	70	53	33	25	18	12	10	1.65	8.5	17.5	26.00	80/20
59	129	74	55	34	27	20	11	10	1.65	8.0	17.5	26.00	80/20
60	120	70	52	33	25	18	12	10	1.65	7.5	17.0	26.50	78/22
61	118	68	50	32	25	18	11	10	1.65	8.0	16.5	26.00	78/22
62	120	70	52	33	26	19	11	10	1.65	8.0	16.5	26.50	78/22

Table A.5*a*: Oil-based drilling fluid data (sets 1-62).

Data Set	Fann Viscometer Readings: θ_{600}	θ_{300}	θ_{200}	θ_{100}	θ_{60}	θ_{30}	θ_{6}	θ_{3}	Mud Weight	Gel Str. [10s]	[10m]	Solids [vol.%]	Oil/Water Ratio
63	114	66	49	31	24	18	11	10	1.65	7.5	16.5	26.00	78/22
64	111	64	48	30	24	18	11	10	1.65	7.0	16.0	26.00	78/22
65	122	70	51	33	25	19	12	10	1.66	8.0	16.5	26.00	78/22
66	112	64	48	31	24	18	11	10	1.65	7.5	15.0	26.00	80/20
67	115	67	50	32	25	18	11	10	1.65	7.5	15.0	26.00	81/19
68	112	65	48	30	24	17	10	9	1.64	6.5	14.0	26.00	81/19
69	108	63	46	30	23	17	10	9	1.65	6.5	15.0	26.00	80/20
70	117	68	51	31	24	18	11	10	1.65	7.5	17.0	25.50	80/20
71	117	68	50	32	26	19	12	11	1.65	8.0	18.0	26.00	80/20
72	127	73	54	34	27	19	12	11	1.65	8.5	17.5	26.00	80/20
73	122	71	52	33	27	19	12	10	1.64	8.5	20.0	26.50	79/21
74	114	66	48	30	25	18	11	9	1.65	7.5	18.0	26.00	80/20
75	116	67	49	31	25	18	11	9	1.64	7.5	18.0	26.00	80/20
76	118	69	51	33	27	20	13	12	1.65	10.0	19.0	26.50	81/19
77	114	67	51	33	27	20	13	12	1.66	10.0	20.0	26.50	80/20
78	130	75	56	35	28	20	13	11	1.62	9.5	20.0	25.50	80/20
79	129	74	55	34	28	20	13	11	1.65	9.5	20.5	26.50	80/20
80	132	76	58	36	28	20	12	11	1.69	10.0	20.0	27.00	79/21
81	107	64	50	32	26	18	11	10	1.64	8.5	18.5	27.00	79/21
82	105	62	49	31	25	18	11	10	1.65	8.5	20.0	26.00	78/22
83	108	64	48	31	25	18	11	9	1.65	8.0	20.0	26.00	78/22
84	133	79	65	46	39	30	23	20	1.65	17.0	27.0	26.00	78/22
85	130	77	63	43	38	29	22	20	1.65	16.0	26.0	25.50	79/21
86	128	75	60	40	36	28	20	18	1.66	15.0	25.0	25.50	79/21
87	116	68	52	33	27	20	13	12	1.65	10.0	20.0	26.00	77/23
88	115	67	50	31	25	18	12	11	1.64	8.0	17.5	25.00	77/23
89	106	62	46	29	23	17	11	10	1.65	8.0	19.0	25.50	77/23
90	104	61	45	29	23	17	11	10	1.65	7.5	19.0	25.50	77/23
91	105	61	46	29	23	18	11	10	1.65	8.0	18.5	25.50	77/23
92	113	65	48	30	23	17	11	10	1.65	8.0	18.5	25.50	77/23
93	110	64	47	30	23	17	11	9	1.65	8.0	18.0	25.50	77/23
94	107	62	45	29	23	17	10	9	1.65	7.5	17.0	26.00	77/23
95	110	64	47	30	23	17	11	10	1.65	8.0	18.0	25.50	76/24
96	103	59	44	28	22	16	10	9	1.64	7.5	17.5	26.00	77/23
97	112	63	47	30	23	18	10	9	1.65	8.0	17.0	26.50	78/22
98	116	66	49	31	24	18	11	10	1.65	8.0	17.0	27.00	77/23
99	107	61	44	28	22	16	9	8	1.65	7.5	15.0	26.50	78/22
100	114	65	49	30	23	17	11	9	1.66	7.0	17.0	26.50	79/21
101	119	70	50	32	25	19	12	11	1.65	8.5	20.0	27.00	78/22
102	114	67	48	31	25	18	12	10	1.65	8.5	20.0	26.50	78/22
103	107	61	45	29	23	16	10	8	1.65	7.0	17.0	26.50	78/22
104	118	68	51	32	25	18	13	11	1.65	8.0	19.0	26.50	79/21
105	114	65	49	31	24	18	12	10	1.65	8.0	18.5	26.50	79/21
106	108	62	45	29	23	17	11	9	1.65	8.0	17.0	26.50	80/20
107	111	65	48	31	24	18	11	10	1.65	8.0	17.0	26.50	80/20
108	105	61	44	28	22	16	10	9	1.65	7.0	15.0	27.00	80/20
109	114	66	49	32	25	18	11	10	1.65	7.5	16.0	26.50	80/20
110	109	63	47	31	24	18	11	9	1.65	7.5	16.0	26.00	80/20
111	110	63	48	31	25	18	11	9	1.65	7.5	16.0	26.00	80/20
112	108	63	44	29	23	17	10	9	1.65	7.0	13.0	26.00	80/20
113	116	70	52	33	27	20	12	11	1.65	8.0	17.0	26.00	80/20
114	117	69	52	33	27	20	13	11	1.65	8.5	18.0	26.00	80/20
115	119	70	53	34	28	20	12	10	1.65	10.0	19.5	26.00	80/20
116	123	72	55	36	29	21	13	12	1.65	10.0	20.0	26.50	81/19
117	122	72	55	35	29	21	12	10	1.65	9.5	19.0	26.00	80/20
118	123	73	55	36	29	21	14	12	1.64	9.0	20.0	26.50	80/20
119	116	68	51	33	26	19	12	10	1.65	8.0	17.0	26.00	80/20
120	119	71	53	34	28	20	13	11	1.65	8.5	19.0	26.00	81/19
121	115	69	52	33	27	20	13	11	1.65	8.0	16.5	26.50	81/19
122	113	68	51	34	26	19	12	11	1.65	8.0	14.5	26.50	81/19
123	122	72	53	35	28	21	13	12	1.65	9.5	18.5	26.50	81/19
124	114	67	50	33	26	19	12	11	1.65	8.5	14.5	26.50	81/19

Table A.5*b*: Oil-based drilling fluid data (sets 63-124).

Data Set	Fann Viscometer Readings: θ_{600}	θ_{300}	θ_{200}	θ_{100}	θ_{60}	θ_{30}	θ_{6}	θ_{3}	Mud Weight	Gel Str. [10s]	[10m]	Solids [vol.%]	Oil/Water Ratio
125	117	70	53	34	28	20	12	11	1.65	8.0	15.0	26.50	80/20
126	124	73	54	35	28	20	12	11	1.65	8.0	16.0	26.50	80/20
127	110	65	49	32	25	18	11	10	1.65	8.0	14.0	26.50	81/19
128	115	68	51	34	27	20	12	11	1.65	8.5	15.0	26.00	80/20
129	121	72	55	36	29	21	13	12	1.65	9.5	16.0	26.00	80/20
130	106	62	47	30	23	17	10	7	1.65	7.0	12.0	26.00	80/20
131	124	72	56	35	28	20	12	11	1.64	8.0	14.0	26.50	80/20
132	104	60	45	28	23	16	10	9	1.64	6.5	12.0	26.00	80/20
133	112	66	49	31	25	18	11	9	1.65	6.5	12.0	26.50	80/20
134	121	72	55	36	27	20	12	11	1.65	8.0	16.0	26.00	80/20
135	103	60	45	29	23	16	9	8	1.65	6.0	11.0	26.50	81/19
136	106	62	46	30	24	17	10	9	1.66	6.5	11.5	26.50	81/19
137	110	65	48	31	24	18	10	9	1.66	6.5	11.0	26.50	81/19
138	100	58	43	28	21	16	9	8	1.65	6.0	10.5	26.50	81/19
139	110	64	48	31	25	18	11	10	1.69	7.0	12.0	27.00	81/19
140	104	61	47	31	25	18	11	10	1.65	7.0	12.0	26.50	81/19
141	116	69	51	34	26	20	12	11	1.65	8.0	14.0	26.50	81/19
142	108	65	49	33	26	19	13	11	1.65	7.5	12.5	26.75	81/19
143	112	66	51	32	26	19	12	11	1.65	8.0	13.0	26.50	81/19
144	105	63	48	32	25	19	12	11	1.65	8.0	13.0	26.50	81/19
145	113	66	51	32	26	19	12	11	1.65	8.0	13.5	26.50	81/19
146	107	64	49	33	26	19	13	11	1.65	7.5	13.0	26.50	81/19
147	122	72	54	36	28	20	12	11	1.65	8.0	15.0	25.50	81/19
148	115	69	52	34	27	20	12	10	1.64	7.5	14.5	26.50	81/19
149	112	65	49	32	25	18	11	10	1.65	7.0	14.0	26.50	82/18
150	107	62	46	30	23	17	10	9	1.65	6.5	13.5	26.25	82/18
151	116	69	51	33	25	19	11	10	1.65	7.5	14.0	26.50	82/18
152	123	71	53	34	26	19	11	10	1.65	7.0	14.0	26.50	82/18
153	116	69	52	34	26	19	12	11	1.65	7.5	16.0	26.50	82/18
154	112	65	49	31	24	17	10	9	1.65	6.5	12.0	26.50	82/18
155	120	71	54	35	28	21	14	13	1.67	8.5	17.0	26.50	81/19
156	122	71	54	34	27	19	13	11	1.65	8.0	16.0	26.50	82/18
157	116	68	51	33	26	19	13	12	1.65	8.0	17.0	26.50	81/19
158	117	70	55	36	29	21	14	13	1.65	8.5	17.0	26.50	82/18
159	116	71	54	36	28	21	14	13	1.65	8.0	18.0	26.50	81/19
160	123	73	55	36	29	21	14	13	1.65	8.5	17.0	26.50	82/18
161	120	70	53	35	27	20	13	11	1.65	8.0	16.5	26.50	81/19
162	121	71	53	35	27	20	13	12	1.65	8.5	17.0	26.50	81/19
163	121	73	55	36	28	21	14	13	1.65	8.5	17.0	27.00	81/19
164	118	70	52	34	28	21	14	13	1.65	8.0	16.5	26.50	81/19
165	117	69	51	34	28	20	13	12	1.65	8.5	17.0	26.50	81/19
166	119	70	53	34	28	20	14	12	1.68	8.5	17.0	26.50	81/19
167	129	76	57	37	30	22	14	12	1.67	7.5	16.0	26.50	77/23
168	126	74	55	35	28	20	12	10	1.64	7.5	15.0	26.50	76/24
169	125	73	55	35	28	20	14	12	1.66	8.0	16.0	27.00	78/22
170	142	83	63	41	32	24	16	14	1.67	8.5	17.0	27.50	82/18
171	129	77	58	38	31	23	15	13	1.66	9.0	19.0	27.00	78/22
172	148	87	64	41	31	21	13	11	1.62	8.5	16.5	25.00	81/19
173	140	82	61	38	30	22	13	11	1.64	7.0	15.5	27.00	78/22
174	130	76	58	37	30	21	13	11	1.66	7.5	16.5	26.50	79/21
175	145	85	64	42	33	24	15	14	1.65	8.5	19.0	26.50	76/24
176	136	79	59	38	30	22	13	11	1.65	7.5	16.0	26.00	76/24
177	136	78	58	37	28	21	12	11	1.65	7.0	16.0	26.00	74/26
178	134	76	56	35	27	19	11	9	1.65	6.5	13.5	25.50	77/23
179	135	76	56	35	28	19	11	9	1.65	6.5	14.0	25.50	77/23
180	127	75	56	36	29	22	14	12	1.65	7.5	17.0	26.00	74/26
181	134	79	60	38	30	22	13	12	1.64	8.0	16.5	26.00	74/26
182	136	79	60	38	34	22	14	12	1.64	8.5	16.0	26.00	76/24
183	132	77	58	37	33	22	13	12	1.65	8.0	16.0	26.50	76/24
184	131	78	58	38	30	22	14	12	1.65	8.5	16.0	26.00	76/24
185	129	75	56	36	28	20	12	11	1.65	7.5	14.0	26.00	76/24
186	114	67	49	31	25	18	11	10	1.68	7.0	12.0	26.50	77/23

Table A.5c: Oil-based drilling fluid data (sets 125-186).

Data	Fann Viscometer Readings:								Mud	Gel Str.		Solids	Oil/Water
Set	θ_{600}	θ_{300}	θ_{200}	θ_{100}	θ_{60}	θ_{30}	θ_{6}	θ_{3}	Weight	[10s]	[10m]	[vol.%]	Ratio
187	118	70	52	34	27	20	12	10	1.65	7.0	14.0	26.50	78/22
188	115	67	51	33	26	19	12	10	1.65	7.0	13.0	26.00	78/22
189	120	71	52	34	27	20	12	11	1.65	7.5	13.0	26.50	78/22
190	116	68	52	34	27	20	12	10	1.65	7.0	13.0	26.00	78/22
191	119	70	52	34	26	19	11	9	1.65	6.5	12.0	26.50	79/21
192	120	70	53	34	27	20	12	10	1.65	6.5	12.0	26.50	80/20
193	122	71	53	35	28	20	12	10	1.65	7.0	13.0	26.50	79/21
194	124	73	54	35	27	20	12	10	1.65	6.5	12.0	26.50	80/20
195	120	70	53	34	26	19	11	9	1.65	6.0	11.5	26.50	80/20
196	119	70	52	33	25	18	10	9	1.65	8.0	14.5	26.50	80/20
197	123	72	54	34	27	19	11	9	1.65	6.0	11.0	26.50	80/20
198	127	75	57	37	28	21	13	11	1.65	8.0	14.5	26.50	80/20
199	126	75	56	36	27	20	12	11	1.65	7.5	14.5	26.50	80/20
200	121	71	53	34	26	19	11	10	1.65	7.0	13.0	26.50	80/20
201	119	69	52	33	25	19	11	9	1.65	7.0	13.0	26.50	81/19
202	109	63	47	30	24	17	10	9	1.65	6.0	12.0	26.50	82/18
203	111	64	48	30	23	17	10	9	1.65	6.5	12.5	26.00	81/19
204	114	66	49	31	24	17	11	10	1.65	6.5	12.5	26.00	81/19
205	105	60	45	29	22	16	10	9	1.69	6.0	12.0	26.00	81/19
206	109	63	47	31	24	18	11	10	1.66	8.0	15.0	26.50	82/18
207	113	65	48	31	24	18	12	10	1.65	7.5	14.5	26.00	82/18
208	113	65	49	31	24	17	11	9	1.65	6.5	12.5	26.00	82/18
209	112	65	48	31	24	18	9	8	1.64	6.5	13.5	26.00	82/18
210	109	63	47	30	23	17	10	9	1.65	6.5	13.5	26.50	83/17
211	112	65	48	31	23	17	10	9	1.68	7.0	14.0	26.50	83/17
212	110	63	47	30	23	17	10	9	1.65	6.5	13.0	26.50	82/18
213	105	61	45	29	22	16	10	9	1.66	6.0	11.5	26.50	82/18
214	113	65	49	31	24	18	11	9	1.66	7.0	13.5	25.50	83/17
215	102	59	44	28	21	16	9	8	1.67	5.5	11.0	26.00	82/18
216	105	60	44	28	21	15	9	8	1.66	6.0	11.5	26.50	82/18
217	111	64	48	31	24	18	10	9	1.65	7.5	14.0	26.50	82/18
218	108	63	47	30	23	17	10	9	1.65	7.0	14.0	26.00	82/18
219	117	68	50	32	25	18	11	10	1.68	7.0	14.0	26.50	82/18
220	114	65	49	31	24	18	11	10	1.66	7.0	14.0	26.50	83/17
221	112	65	49	31	25	18	12	10	1.65	8.0	16.0	26.50	82/18
222	108	63	48	30	23	17	11	10	1.66	7.0	14.5	26.50	82/18
223	104	61	46	30	24	17	11	10	1.65	7.0	15.0	26.50	82/18
224	113	65	49	31	24	18	11	10	1.63	6.5	14.0	26.00	82/18
225	111	65	48	31	24	17	10	9	1.71	6.5	14.0	26.50	82/18
226	112	64	48	30	23	17	11	9	1.65	6.5	14.0	26.50	82/18
227	116	68	50	32	25	19	11	10	1.65	8.0	17.5	26.50	81/19
228	120	70	52	33	26	19	12	11	1.65	7.5	17.0	26.50	81/19
229	113	66	49	32	25	18	12	11	1.65	7.5	15.5	26.50	81/19
230	110	64	48	31	24	18	11	10	1.65	7.5	15.0	26.50	81/19
231	114	67	50	32	25	18	12	10	1.65	7.0	16.0	26.50	81/19
232	118	69	52	33	26	19	12	11	1.65	7.0	16.5	27.00	81/19
233	114	66	49	31	25	18	11	10	1.65	7.5	16.0	27.00	82/18
234	116	68	50	32	25	18	11	10	1.66	7.0	15.5	27.00	82/18
235	118	69	51	32	25	18	12	10	1.65	7.0	15.5	27.00	82/18
236	117	68	51	32	25	18	12	10	1.65	7.0	15.5	27.00	82/18
237	108	63	47	30	23	18	11	10	1.65	7.0	15.0	26.50	82/18
238	111	65	48	30	24	18	11	10	1.65	6.5	15.0	26.50	82/18
239	111	64	48	31	25	18	12	10	1.66	7.5	17.0	27.00	82/18
240	112	67	50	32	25	19	13	12	1.65	8.0	17.5	27.00	82/18
241	116	67	50	32	25	19	12	10	1.64	7.5	17.0	27.00	82/18
242	109	64	48	32	25	19	12	11	1.63	8.0	18.0	27.00	82/18
243	120	70	52	33	26	19	13	11	1.65	7.5	17.5	27.25	82/18
244	118	69	51	33	25	19	12	11	1.62	7.5	18.0	27.00	82/18
245	116	70	50	33	24	19	13	11	1.62	8.0	18.0	27.50	82/18
246	112	67	51	33	27	20	13	12	1.61	8.0	18.0	27.25	82/18
247	115	68	51	33	26	19	13	11	1.61	8.0	18.0	27.25	82/18
248	117	69	52	33	26	19	12	11	1.62	8.0	18.0	27.50	82/18

Table A.5*d*: Oil-based drilling fluid data (sets 187-248).

Data Set	Fann Viscometer Readings: θ_{600}	θ_{300}	θ_{200}	θ_{100}	θ_{60}	θ_{30}	θ_{6}	θ_{3}	Mud Weight	Gel Str. [10s]	Gel Str. [10m]	Solids [vol.%]	Oil/Water Ratio
249	114	68	51	33	26	20	13	11	1.64	8.0	18.0	27.50	82/18
250	112	67	50	32	26	20	12	11	1.65	8.0	17.5	27.50	82/18
251	108	64	47	31	25	19	12	11	1.65	7.5	17.0	27.50	82/18
252	120	70	52	33	27	21	14	13	1.75	9.0	20.0	27.50	80/20
253	121	71	53	33	28	21	14	13	1.65	9.5	21.0	27.00	82/18
254	122	71	53	34	29	21	14	13	1.65	9.0	21.0	27.00	82/18
255	101	59	44	29	23	17	10	9	1.65	7.5	16.0	26.50	82/18
256	118	69	51	32	25	19	13	11	1.65	8.0	18.0	27.50	81/19
257	114	67	50	32	25	18	11	10	1.65	7.5	14.0	26.50	82/18
258	115	66	48	30	24	18	13	12	1.68	15.0	22.0	27.75	80/20
259	120	68	51	31	24	18	14	13	1.67	14.5	19.5	27.75	80/20
260	125	72	54	35	28	22	16	15	1.69	16.0	21.0	27.75	81/19
261	118	68	50	32	25	19	15	14	1.67	15.5	19.0	27.75	80/20
262	120	69	51	32	25	19	15	14	1.68	15.0	19.5	27.75	80/20
263	130	74	54	35	26	18	14	13	1.68	13.0	19.0	28.00	79/21
264	125	71	52	32	25	18	13	12	1.68	13.0	18.5	27.50	80/20
265	118	68	49	30	23	17	13	12	1.67	12.0	18.0	27.75	80/20
266	119	69	50	32	25	18	13	12	1.68	13.0	19.0	27.75	80/20
267	128	74	54	34	25	18	12	11	1.70	11.5	17.0	28.00	79/21
268	124	71	52	32	24	18	12	11	1.68	11.0	16.5	28.00	79/21
269	132	76	56	35	27	20	14	13	1.68	13.0	19.0	28.00	79/21
270	131	75	55	35	26	19	14	13	1.68	13.0	19.0	28.00	79/21
271	125	71	52	32	25	18	13	11	1.70	11.0	16.5	29.00	79/21
272	126	72	53	33	24	18	12	11	1.70	11.0	17.0	29.00	80/20
273	125	71	52	33	24	17	13	12	1.70	11.5	18.0	28.50	79/21
274	128	73	53	33	25	18	12	11	1.70	11.5	17.0	28.50	79/21
275	110	63	45	28	21	15	11	10	1.72	8.5	14.5	28.00	80/20
276	116	66	48	30	22	17	12	10	1.71	9.5	15.0	28.50	80/20
277	119	68	50	31	23	17	12	11	1.70	11.0	16.0	28.50	80/20
278	123	70	51	32	24	17	12	11	1.70	11.5	17.0	28.00	79/21
279	132	77	61	37	28	20	13	12	1.71	11.5	19.0	28.00	76/24
280	111	63	46	29	21	15	11	10	1.70	10.0	13.0	28.00	79/21
281	137	80	59	37	28	20	14	13	1.72	12.0	20.0	28.00	76/24
282	136	79	59	37	28	20	14	13	1.70	12.0	19.0	28.00	76/24
283	118	68	50	31	23	17	13	12	1.71	12.5	17.0	28.00	80/20
284	93	54	40	25	19	13	10	9	1.73	8.5	13.0	27.00	75/25
285	127	74	54	34	26	18	13	12	1.73	11.0	18.5	27.00	75/25
286	120	69	51	32	25	18	13	12	1.70	13.0	19.0	28.50	80/20

Table A.5*e*: Oil-based drilling fluid data (sets 249-286).

Characteristic/ Observed Data	Bentonite/ polymer	Sea water/ pac	KCl/pac	Oil Based Mud
Mud Weight [g/cm^3]	1.65	1.19	1.53	1.65
Solids [vol.%]	21.0	11.7	22.5	26.0
Gel @ 10sec [Pa]	18.0	2.0	4.0	5.0
Gel @ 10min [Pa]	40.0	10.0	5.5	9.0
pH	9.5	8.0	7.9	-
PV [mPa·s]	15.0	20.0	37.0	41.0
YP [Pa]	12.0	10.0	21.5	7.0
Chlorides [1000 mg/l]	-	22	79	104
Calcium [mg/l]	80	600	580	-
Magnesium [mg/l]	-	1094	680	-
Oil/Water Ratio	n/a	n/a	n/a	82/18
θ_{600}/τ_{600} [Pa]	54/27.60	60/30.66	117/59.79	96/49.06
θ_{300}/τ_{300} [Pa]	39/19.93	40/20.44	80/40.88	55/28.11
θ_{200}/τ_{200} [Pa]	33/16.86	32/16.35	65/33.22	41/20.95
θ_{100}/τ_{100} [Pa]	30/15.33	21/10.73	45/23.00	26/13.29
θ_{60}/τ_{60} [Pa]	27/13.80	16/ 8.18	35/17.89	19/ 9.71
θ_{30}/τ_{30} [Pa]	25/12.78	11/ 5.62	24/12.26	14/ 7.15
θ_{6}/τ_{6} [Pa]	21/10.73	4/ 2.04	11/ 5.62	8/ 4.09
θ_{3}/τ_{3} [Pa]	20/10.22	3/ 1.53	7/ 3.58	7/ 3.58

Table A.6: Fluid characteristics and observed Fann viscometer readings for an example of each of the four different drilling fluids. θ_x and τ_x are Fann viscometer dial readings and equivalent shear stresses at x rpm respectively.

Appendix B

Rheological Models Considered, Partial Derivatives and Direct Parameter Solutions

B.1 Bingham Plastic

This 2-parameter model (Bingham, 1916; with industry application specified by Melrose *et al.*, 1957) has the following form:

$$\tau = \tau_\circ + \mu_\infty \dot{\gamma},$$

or in terms of shear stress,

$$\dot{\gamma} = \frac{\tau - \tau_\circ}{\mu_\infty},$$

where $\tau_\circ$ (the yield stress of the fluid) and μ_∞ (the fluid's plastic viscosity) are model parameters. Direct parameter solution is possible from the following expressions:

$$\tau_\circ = \tau_1 - \mu_\infty \dot{\gamma}_1,$$

and

$$\mu_\infty = \frac{\tau_2 - \tau_1}{\dot{\gamma}_2 - \dot{\gamma}_1}.$$

First order partial derivatives are:

$$\frac{\partial \tau}{\partial \tau_\circ} = 1 \quad ; \quad \frac{\partial \tau}{\partial \mu_\infty} = \dot{\gamma}.$$

B.2 Casson

Although first published back in 1959 (Casson), the model was not proposed for industry application until 1979 (Lauzon & Reid), and has the form

$$\tau = \left(\sqrt{\tau_\circ} + \sqrt{\mu_\infty \dot{\gamma}}\right)^2,$$

or in terms of shear stress,

$$\dot{\gamma} = \frac{\left(\sqrt{\tau_\circ} - \sqrt{\tau_\circ}\right)^2}{\mu_\infty},$$

where $\tau_\circ$ and μ_∞ are model parameters. Direct parameter solution is possible from the following expressions:

$$\mu_\infty = \left(\frac{\sqrt{\tau_2} - \sqrt{\tau_1}}{\sqrt{\dot{\gamma}_1} - \sqrt{\dot{\gamma}_2}}\right)^2,$$

and

$$\tau_\circ = \left(\sqrt{\tau_1} - \sqrt{\mu_\infty \dot{\gamma}_1}\right)^2.$$

First-order partial derivatives are:

$$\frac{\partial \tau}{\partial \tau_\circ} = \frac{\sqrt{\tau_\circ} + \sqrt{\mu_\infty \dot{\gamma}}}{\sqrt{\tau_\circ}} \quad ; \quad \frac{\partial \tau}{\partial \mu_\infty} = \frac{\left(\sqrt{\tau_\circ} + \sqrt{\mu_\infty \dot{\gamma}}\right) \dot{\gamma}}{\sqrt{\mu_\infty \dot{\gamma}}}.$$

B.3 Collins-Graves

First published in 1978 (Graves & Collins), this model is little-used in the industry due to the implicit form of the function for shear rate (the prerequisiste for analytical solution). The 3-parameter model has the form:

$$\tau = (\tau_\circ + k\dot{\gamma})\left[1 - \exp(-\beta\dot{\gamma})\right],$$

or in terms of τ:

$$0 = (\tau_\circ + k\dot{\gamma})\left[1 - \exp(-\beta\dot{\gamma})\right] - \tau,$$

where β, k and $\tau_\circ$ are model parameters. Direct parameter solution can be obtained from evaluation of the following relationships:

$$0 = \left(\frac{\tau_1 - k\dot{\gamma}_1\left[1 - \exp(-\beta\dot{\gamma}_1)\right]}{1 - \exp(-\beta\dot{\gamma}_1)}\right)\left[1 - \exp(-\beta\dot{\gamma}_3)\right] + k\left[\dot{\gamma}_3 - \dot{\gamma}_3\exp(-\beta\dot{\gamma}_3)\right] - \tau_3,$$

which represents an implicit expression for β when Eq.(B.1) is substituted for k

$$k = \frac{\tau_1\left[1 - \exp(-\beta\dot{\gamma}_2)\right] - \tau_2\left[1 - \exp(-\beta\dot{\gamma}_1)\right]}{(\dot{\gamma}_1 - \dot{\gamma}_2)\left[1 - \exp(-\beta\dot{\gamma}_1)\right]\left[1 - \exp(-\beta\dot{\gamma}_2)\right]}, \tag{B.1}$$

with $\tau_\circ$ being given by:

$$\tau_\circ = \frac{\tau_1 - k\dot{\gamma}_1\left[1 - \exp(-\beta\dot{\gamma}_1)\right]}{\left[1 - \exp(-\beta\dot{\gamma}_1)\right]}.$$

First-order partial derivatives are:

$$\frac{\partial\tau}{\partial\tau_\circ} = 1 - \exp(-\beta\dot{\gamma}) \quad ; \quad \frac{\partial\tau}{\partial k} = \dot{\gamma}\left[1 - \exp(-\beta\dot{\gamma})\right] \quad ; \quad \frac{\partial\tau}{\partial\beta} = (\tau_\circ + k\dot{\gamma})\,\dot{\gamma}\exp(-\beta\dot{\gamma}).$$

B.4 Collins-Graves* (Modified Collins-Graves)

Constructed specifically for solution using nonlinear least squares, the modification to the basic Collins-Graves model involves the addition of an explicit yield stress component, α, nemaly:

$$\tau = \alpha + (\tau_\circ + k\dot{\gamma})\left[1 - \exp(-\beta\dot{\gamma})\right],$$

with $\dot{\gamma}$ as a function of τ being given by the implicit expression:

$$0 = \alpha + (\tau_\circ + k\dot{\gamma})\left[1 - \exp(-\beta\dot{\gamma})\right] - \tau.$$

First-order partial derivatives are the same as those given in section B.3 but with the extra partial:

$$\frac{\partial\tau}{\partial\alpha} = 1.$$

B.5 Cross

This 3-parameter model (Cross, 1965) is empirical in nature being derived from observations taken from a number rubber solutions and has the form:

$$\tau = \dot{\gamma}\left(\mu_\infty + \frac{\mu_\circ - \mu_\infty}{1 + \alpha\dot{\gamma}^{2/3}}\right),$$

and for $\dot{\gamma}$ has the following implicit form:

$$0 = \dot{\gamma}\left(\mu_\infty + \frac{\mu_\circ - \mu_\infty}{1 + \alpha\dot{\gamma}^{2/3}}\right) - \tau,$$

where μ_∞, $\mu_\circ$ and α are model parameters. Direct parameter solution is obtained from the following functions:

$$\mu_\infty = -\left\{\tau_3\left[1 - \frac{\left(\tau_1 + \frac{\dot{\gamma}_1\Omega}{\Phi}\right)\dot{\gamma}_3^{2/3}}{\left(\tau_1 - \mu_\infty\dot{\gamma}_1\right)\dot{\gamma}_1^{2/3}} + \frac{\dot{\gamma}_3\Omega}{\Phi}\right]\left(\tau_1 - \mu_\infty\dot{\gamma}_1\right)\dot{\gamma}_1^{2/3}\right\} \times \left[\left(\tau_1 + \frac{\dot{\gamma}_1\Omega}{\Phi}\right)\dot{\gamma}_3^{5/3}\right]^{-1}, \quad \text{(B.2)}$$

where

$$\Phi = 1 - \frac{\tau_2\dot{\gamma}_1^{1/3}}{\left(\tau_1 - \mu_\infty\dot{\gamma}_1\right)\dot{\gamma}_2^{1/3}} + \frac{\mu_\infty\dot{\gamma}_1^{1/3}\dot{\gamma}_2^{2/3}}{\tau_1 - \mu_\infty\dot{\gamma}_1},$$

and

$$\Omega = -\frac{\tau_2}{\dot{\gamma}_2} + \frac{\tau_2\tau_1}{\left(\tau_1 - \mu_\infty\dot{\gamma}_1\right)\dot{\gamma}_2^{1/3}\dot{\gamma}_1^{2/3}} - \frac{\mu_\infty\tau_1\dot{\gamma}_2^{2/3}}{\left(\tau_1 - \mu_\infty\dot{\gamma}_1\right)\dot{\gamma}_1^{2/3}}.$$

Finally,

$$\begin{aligned}\mu_\circ \;=\;& \left(\frac{\tau_2}{\dot{\gamma}_2} - \frac{\tau_2\tau_1}{\dot{\gamma}_2^{1/3}\left(\tau_1 - \mu_\infty\dot{\gamma}_1\right)\dot{\gamma}_1^{2/3}} + \frac{\mu_\infty\dot{\gamma}_2^{2/3}\tau_1}{\left(\tau_1 - \mu_\infty\dot{\gamma}_1\right)\dot{\gamma}_1^{2/3}}\right) \times \\ & \left(1 - \frac{\tau_2\dot{\gamma}_1^{1/3}}{\dot{\gamma}_2^{1/3}\left(\tau_1 - \mu_\infty\dot{\gamma}_1\right)} + \frac{\mu_\infty\dot{\gamma}_2^{2/3}\dot{\gamma}_1^{1/3}}{\tau_1 - \mu_\infty\dot{\gamma}_1}\right)^{-1}, \qquad \text{(B.3)}\end{aligned}$$

and

$$\alpha = -\frac{\tau_1 - \mu_\circ\dot{\gamma}_1}{\left(\tau_1 - \mu_\infty\dot{\gamma}_1\right)\dot{\gamma}_1^{2/3}}. \qquad \text{(B.4)}$$

Model first-order partial derivatives are:

$$\frac{\partial\tau}{\partial\mu_\infty} = \dot{\gamma}\left(1 - \frac{1}{1 + \alpha\dot{\gamma}^{2/3}}\right) \quad ; \quad \frac{\partial\tau}{\partial\mu_\circ} = \frac{\dot{\gamma}}{1 + \alpha\dot{\gamma}^{2/3}} \quad ; \quad \frac{\partial\tau}{\partial\alpha} = -\frac{\left(\mu_\circ - \mu_\infty\right)\dot{\gamma}^{5/3}}{\left(1 + \alpha\dot{\gamma}^{2/3}\right)^2}.$$

B.6 Ellis, Lanham & Pankhurst

This 3-parameter expression (Ellis, Lanham, & Pankhurst, 1955) was first developed specifically for Newtonian fluid surface films but found wider applicability after slight modifications to the original were presented in the seminal work by Reiner (1960). The Reiner-modified expression yields an implicit function about shear stress and has the form:

$$\dot{\gamma} = \left(\phi_0 + \phi_1 \tau^{(\alpha-1)}\right)\tau,$$

and in terms of shear rate,

$$0 = \left(\phi_0 + \phi_1 \tau^{(\alpha-1)}\right)\tau - \dot{\gamma}.$$

Model parameters are: ϕ_0, ϕ_1 and α. Direct parameter solution is given by the following three expressions:

$$\phi_0 = \left[\frac{\dot{\gamma}_1}{\tau_1} - \phi_1 \tau_1^{(\alpha-1)}\right]\tau_1,$$

and

$$\phi_1 = \frac{\dot{\gamma}_2 \tau_2^{-\alpha} - \left[\frac{\dot{\gamma}_1}{\tau_1}\right]\tau_2^{(1-\alpha)}}{1 - \left(\tau_1^{(\alpha-1)} \cdot \tau_2^{(1-\alpha)}\right)},$$

which are utilised in the following iterative solution about α:

$$0 = \left[\phi_0 + \phi_1 \tau_3^{(\alpha-1)}\right]\tau_3 - \dot{\gamma}_3.$$

Model first-order partial derivatives are:

$$\frac{\partial \dot{\gamma}}{\partial \phi_0} = \tau \quad ; \quad \frac{\partial \dot{\gamma}}{\partial \phi_1} = \tau^{(\alpha-1)}\tau \quad ; \quad \frac{\partial \dot{\gamma}}{\partial \alpha} = \phi_1 \tau^{(\alpha-1)} \ln(\tau)\tau.$$

B.7 Herschel-Bulkley

This 3-parameter model (Herschel & Bulkley, 1926) is essentialy a Power Law with a yield stress component and has the form,

$$\tau = \tau_\circ + k\dot{\gamma}^m,$$

and in terms of shear stress,

$$\dot{\gamma} = \left(\frac{\tau - \tau_\circ}{k}\right)^{1/m},$$

where $\tau_\circ$, k and m are model parameters. For direct parameter solution, m is obtained through the following implicit function:

$$0 = (\tau_1 - \tau_3) + \dot{\gamma}_3^m \left(\frac{\tau_2 - \tau_1}{\dot{\gamma}_2^m - \dot{\gamma}_1^m} \right) - \dot{\gamma}_1^m \left(\frac{\tau_2 - \tau_1}{\dot{\gamma}_2^m - \dot{\gamma}_1^m} \right),$$

with the Herschel-Bulkley consistency factor being given by:

$$k = \frac{\tau_2 - \tau_1}{\dot{\gamma}_2^m - \dot{\gamma}_1^m},$$

and $\tau_\circ$ by

$$\tau_\circ = \tau_1 - k\dot{\gamma}_1^m.$$

Model first-order partial derivatives are:

$$\frac{\partial \tau}{\partial \tau_\circ} = 1 \quad ; \quad \frac{\partial \tau}{\partial k} = \dot{\gamma}^m \quad ; \quad \frac{\partial \tau}{\partial m} = k\dot{\gamma}^m \ln(\dot{\gamma}).$$

B.8 Herschel-Bulkley/Linear (Hybrid Yield-Power Law)

Constructed specifically for solution using nonlinear least squares, the hybrid segmented model comprises Herschel-Bulkley and linear forms joined at a constant shear rate value (itself a parameter requiring determination) forming a continuous and smooth function:

$$\tau = \begin{cases} a + bd^c(c-1) + b\dot{\gamma}^c, & \text{if } \dot{\gamma} \le d, \\ a + bcd^{(c-1)}\dot{\gamma}, & \text{otherwise.} \end{cases}$$

Model constants are a, b, c and d. The inverse of the above are:

$$\dot{\gamma} = \begin{cases} \left[\frac{\tau - a - bd^c(c-1)}{b}\right]^{1/c}, & \text{if } \dot{\gamma} \le d, \\ \frac{\tau - a}{bcd^{(c-1)}}, & \text{otherwise.} \end{cases}$$

First-order partial derivatives for expressions used when $\dot{\gamma} \le d$:

$$\frac{\partial \tau}{\partial a} = 1 \; ; \; \frac{\partial \tau}{\partial b} = d^c(c-1) + \dot{\gamma}^c \; ; \; \frac{\partial \tau}{\partial c} = bd^c \ln(d)(c-1) + bd^c + b\dot{\gamma}^c \ln \dot{\gamma} \; ; \; \frac{\partial \tau}{\partial d} = \frac{bd^c c(c-1)}{d},$$

and for the function applicable when $\dot{\gamma} > d$:

$$\frac{\partial \tau}{\partial a} = 1 \quad ; \quad \frac{\partial \tau}{\partial b} = cd^{c-1}\dot{\gamma} \quad ; \quad \frac{\partial \tau}{\partial c} = bd^{(c-1)}\dot{\gamma} + bcd^{(c-1)} \ln(d)\dot{\gamma} \quad ; \quad \frac{\partial \tau}{\partial d} = \frac{bcd^{(c-1)}(c-1)\dot{\gamma}}{d}.$$

B.9 Hyperbolic

This 4-parameter model is given by

$$\tau = \tau_{cp} + b\sqrt{\left(\frac{\dot{\gamma} - \dot{\gamma}_{cp}}{a}\right)^2 - 1},$$

and in terms of shear stress,

$$\dot{\gamma} = \dot{\gamma}_{cp} + a\sqrt{\left(\frac{\tau - \tau_{cp}}{b}\right)^2 + 1},$$

where a, b, τ_{cp} and $\dot{\gamma}_{cp}$ are model parameters which can be determined from specific Fann viscometer measurements, (refer to section 2.3.3 on page 14, for definition and solution methodology of model parameters). Direct parameter solution functions generated from successive substitution of this model are unwieldy and unuseable. For purposes of nonlinear least squares model first-order partial derivarives are:

$$\frac{\partial \tau}{\partial a} = -\frac{b\,(\dot{\gamma} - \dot{\gamma}_{cp})^2}{a^3\sqrt{\left(\frac{\dot{\gamma}-\dot{\gamma}_{cp}}{a}\right)^2 - 1}} \quad ; \quad \frac{\partial \tau}{\partial b} = \sqrt{\left(\frac{\dot{\gamma} - \dot{\gamma}_{cp}}{a}\right)^2 - 1},$$

and

$$\frac{\partial \tau}{\partial \dot{\gamma}_{cp}} = -\frac{b\,(\dot{\gamma} - \dot{\gamma}_{cp})}{a^2\sqrt{\left(\frac{\dot{\gamma}-\dot{\gamma}_{cp}}{a}\right)^2 - 1}} \quad ; \quad \frac{\partial \tau}{\partial \tau_{cp}} = 1.$$

B.10 Hyperbolic* (Modified Hyperbolic)

Constructed specifically for solution using nonlinear least squares, the modification to the basic Hyperbolic model involves the removal of the shear stress at the centre-point of the hyperbola, τ_{cp}, namely:

$$\tau = b\sqrt{\left(\frac{\dot{\gamma} - \dot{\gamma}_{cp}}{a}\right)^2 - 1},$$

and for $\dot{\gamma}$,

$$\dot{\gamma} = \dot{\gamma}_{cp} + a\sqrt{\left(\frac{\tau}{b}\right)^2 + 1}.$$

First-order partial derivatives are given in section B.9 but excluding the τ_{cp} partial derivative.

B.11 Inverse ln-cosh

Constructed specifically for solution using nonlinear least squares, this new 3-parameter model was formulated after observations of the large data set and has the form:

$$\tau = \tau_\circ + A\cosh^{-1}\left[\exp\left(\frac{\dot\gamma}{B}\right)\right],$$

and the inverse:

$$\dot\gamma = B\ln\left[\cosh\left(\frac{\tau-\tau_\circ}{A}\right)\right],$$

where A, B and $\tau_\circ$ are model parameters. Model first-order partial derivatives are:

$$\frac{\partial\tau}{\partial\tau_\circ}=1 \quad ; \quad \frac{\partial\tau}{\partial A}=\cosh^{-1}\left[\exp\left(\frac{\dot\gamma}{B}\right)\right] \quad ; \quad \frac{\partial\tau}{\partial B}=-\frac{A\dot\gamma\exp\left(\frac{\dot\gamma}{B}\right)}{B^2\sqrt{\left[\exp\left(\frac{\dot\gamma}{B}\right)\right]^2-1}}.$$

B.12 Power Law (Ostwald – de Waele)

This 2-parameter model (Ostwald, 1925 and de Waele, 1923) can be represented in simplified notation (applicable for the region of positive shear rates) as

$$\tau = k\dot\gamma^n$$

and

$$\dot\gamma = (\tau/k)^{1/n},$$

where n is the flow behaviour index and k defined as the consistency factor. Direct parameter solution expressions are:

$$k=\frac{\tau_1}{\dot\gamma_1^n},$$

and

$$n=\frac{\log(\tau_2/\tau_1)}{\log(\dot\gamma_2/\dot\gamma_1)}.$$

The API 'modified' Power Law is applicable only when the Power Law consistency factor, k, is calculated from the conventional oilfield procedure employing Fann viscoemeter dial readings at 300 rpm only (i.e, $k=\tau_{300}/511^n$). The modified Power Law is given by $\tau = k_{\mathbf{mod}}\dot\gamma^n$ where $k_{\mathbf{mod}} = k\cdot G_v$. The correction term, G_v, accounts for the Fann viscometer dial factor of 1.0678 which is missing from the expression for k when readings at 300 rpm are employed. The correction factor is given by:

$$G_v = 1.0678\left[8.1328n\left(1-1.0678^{-2/n}\right)\right]^n.$$

Standard Power Law first-order partial derivatives are:

$$\frac{\partial\tau}{\partial k}=\dot\gamma^n \quad ; \quad \frac{\partial\tau}{\partial n}=k\dot\gamma^n\ln(\dot\gamma).$$

B.13 Power Law/Linear (Hybrid Power Law)

Constructed specifically for solution using nonlinear least squares, the hybrid segmented model comprises Power Law and linear forms joined at a constant shear rate value (itself a parameter requiring determination) forming a continuous and smooth function:

$$\tau = \begin{cases} k\dot{\gamma}^n, & \text{if } \dot{\gamma} \le c, \\ kc^n(1-n) + knc^{n-1}\dot{\gamma}, & \text{otherwise,} \end{cases}$$

where c is the new model parameter. The inverse functions are:

$$\dot{\gamma} = \begin{cases} \left(\frac{\tau}{k}\right)^{1/n}, & \text{if } \dot{\gamma} \le c, \\ \frac{\tau - kc^n(1-n)}{knc^{n-1}}, & \text{otherwise.} \end{cases}$$

Model first-order partial derivatives for the function applicable when $\dot{\gamma} \le c$:

$$\frac{\partial \tau}{\partial k} = c^n(1-n) + nc^{(n-1)}\dot{\gamma} \quad ; \quad \frac{\partial \tau}{\partial n} = kc^n \ln(c)(1-n) - kc^n + kc^{(n-1)}\dot{\gamma} + knc^{(n-1)}\ln(c)\dot{\gamma},$$

and

$$\frac{\partial \tau}{\partial c} = \frac{kn}{c}\left[c^n(1-n) + c^{(n-1)}(n-1)\dot{\gamma}\right].$$

Partial derivatives for the function applicable when $\dot{\gamma} > c$ are identical to those presented in section B.12.

B.14 Prandtl-Eyring

This 2-parameter model (Prandtl, 1928; with modifications later proposed by Eyring, 1936) has the form,

$$\tau = A\sinh^{-1}(\dot{\gamma}/B),$$

and for $\dot{\gamma}$,

$$\dot{\gamma} = B\sinh\left(\frac{\tau}{A}\right),$$

where A and B are model parameters. Expressions for direct parameter solution are:

$$A = \tau_1\left(\ln\left[\left(\frac{\dot{\gamma}_1}{B}\right) + \sqrt{\left(\frac{\dot{\gamma}_1}{B}\right)^2 + 1}\right]\right)^{-1},$$

and

$$0 = \tau_1 \cdot \left(\ln\left[\left(\frac{\dot{\gamma}_1}{B}\right) + \sqrt{\left(\frac{\dot{\gamma}_1}{B}\right)^2 + 1}\right]\right)^{-1} \cdot \sinh^{-1}\left(\frac{\dot{\gamma}_2}{B}\right) - \tau_2.$$

Model first-order partial derivatives are:

$$\frac{\partial \tau}{\partial A} = \sinh^{-1}\left(\frac{\dot{\gamma}}{B}\right) \quad ; \quad \frac{\partial \tau}{\partial B} = -\frac{A\dot{\gamma}}{B^2\sqrt{1 + \frac{\dot{\gamma}^2}{B^2}}}.$$

B.15 Prandtl-Eyring* (Modified Prandtl-Eyring)

Constructed specifically for solution using nonlinear least squares, the modification to the basic Prandtl-Eyring model involves the addition of an explicit yield stress component, $\tau_\circ$, namely:

$$\tau = \tau_\circ + A \sinh^{-1}\left(\frac{\dot{\gamma}}{B}\right),$$

and in terms of τ:

$$\dot{\gamma} = B \sinh\left(\frac{\tau - \tau_\circ}{A}\right),$$

where $\tau_\circ$ is the new model parameter. This expression is reminiscent of the Powell-Eyring (1944) model with the yield-stress term corresponding to the linear velocity gradient except here it is written as a constant and not as a gradient term. Model first-order partial derivatives are the same as those provided in section B.14 but with:

$$\frac{\partial \tau}{\partial \tau_\circ} = 1.$$

B.16 Reiner-Philippoff

This 3-parameter model (Reiner, 1929/30; Philippoff, 1935) is an explicit function for $\dot{\gamma}$ and has the form:

$$\dot{\gamma} = \frac{\tau}{\mu_\infty + \frac{\mu_\circ - \mu_\infty}{1+(\tau/\tau_s)^2}},$$

and an implicit function for τ,

$$0 = \frac{\tau}{\mu_\infty + \frac{\mu_\circ - \mu_\infty}{1+(\tau/\tau_s)^2}} - \dot{\gamma},$$

where μ_∞, $\mu_\circ$ and τ_s are model parameters. Direct parameter solution may be obtained from:

$$\mu_\infty = \frac{\tau_1 \tau_s^2 + \tau_1^3 - \mu_\circ \dot{\gamma}_1 \tau_s^2}{\dot{\gamma}_1 \tau_1^2},$$

and

$$\mu_\circ = \frac{\tau_2 \tau_1 \left(\tau_2 \tau_1^2 \dot{\gamma}_2 + \tau_2 \dot{\gamma}_2 \tau_s^2 - \tau_1 \tau_2^2 \dot{\gamma}_1 - \tau_1 \dot{\gamma}_1 \tau_s^2\right)}{\dot{\gamma}_1 \dot{\gamma}_2 \tau_s^2 \left(\tau_2^2 - \tau_1^2\right)},$$

which is used in the following implicit expression about τ_s:

$$0 = \frac{\tau_3}{\mu_\infty + \frac{\mu_\circ - \mu_\infty}{1+(\tau_3/\tau_s)^2}} - \dot{\gamma}_3.$$

Model first-order partial derivatives are:

$$\frac{\partial\dot{\gamma}}{\partial\mu_\infty} = -\tau\left[1 - \frac{1}{1+(\tau/\tau_s)^2}\right]\cdot\left[\mu_\infty + \frac{\mu_\circ - \mu_\infty}{1+(\tau/\tau_s)^2}\right]^{-2},$$

$$\frac{\partial\dot{\gamma}}{\partial\mu_\circ} = -\tau\left\{\left[\mu_\infty + \frac{\mu_\circ - \mu_\infty}{1+(\tau/\tau_s)^2}\right]^2\left[1+(\tau/\tau_s)^2\right]\right\}^{-1},$$

and

$$\frac{\partial\dot{\gamma}}{\partial\tau_s} = -2\tau^3\left(\mu_\circ - \mu_\infty\right)\left\{\left[\mu_\infty + \frac{\mu_\circ - \mu_\infty}{1+(\tau/\tau_s)^2}\right]^2\left[1+(\tau/\tau_s)^2\right]^2{\tau_s}^3\right\}^{-1}.$$

B.17 Robertson-Stiff

This 3-parameter model (Robertson & Stiff, 1976) characterizes the yield stress by a shear rate intercept, $\dot{\gamma}_\circ$, that acts as a 'correction' to the shear rate, rather than the shear stress to obtain a pseudo-yield stress. The model is given by

$$\tau = A\left(\dot{\gamma}_\circ + \dot{\gamma}\right)^B,$$

and for $\dot{\gamma}$,

$$\dot{\gamma} = \left(\frac{\tau}{A}\right)^{1/B} - \dot{\gamma}_\circ,$$

where A, B and $\dot{\gamma}_\circ$ are model parameters. Direct parameter solution is obtained from the following relationship:

$$0 = \left[\frac{\tau_1}{\left(\dot{\gamma}_\circ + \dot{\gamma}_1\right)^B}\right]\left(\dot{\gamma}_\circ + \dot{\gamma}_3\right)^B - \tau_3,$$

which requires an iterative solution about B when Eq.(B.5) is used to substitute $\dot{\gamma}_\circ$:

$$\dot{\gamma}_\circ = \frac{\dot{\gamma}_2 - \dot{\gamma}_1\left(\tau_2/\tau_1\right)^{1/B}}{\left(\tau_2/\tau_1\right)^{1/B} - 1}, \tag{B.5}$$

with parameter A being determined from

$$A = \frac{\tau_1}{\left(\dot{\gamma}_\circ + \dot{\gamma}_1\right)^B}.$$

Model first-order partial derivatives are:

$$\frac{\partial\tau}{\partial A} = \left(\dot{\gamma}_\circ - \dot{\gamma}\right)^B \quad ; \quad \frac{\partial\tau}{\partial B} = A\left(\dot{\gamma}_\circ - \dot{\gamma}\right)^B\ln\left(\dot{\gamma}_\circ - \dot{\gamma}\right) \quad ; \quad \frac{\partial\tau}{\partial\dot{\gamma}_\circ} = \frac{A\left(\dot{\gamma}_\circ - \dot{\gamma}\right)^B B}{\dot{\gamma}_\circ - \dot{\gamma}}.$$

B.18 Robertson-Stiff* (Modified Robertson-Stiff)

Constructed specifically for solution using nonlinear least squares, the modification to the basic Robertson-Stiff model involves the addition of an explicit yield stress component, $\tau_\circ$, namely:

$$\tau = \tau_\circ + A\left(\dot{\gamma}_\circ + \dot{\gamma}\right)^B,$$

with the inverse:

$$\dot{\gamma} = \left(\frac{\tau - \tau_\circ}{A}\right)^{1/B} - \dot{\gamma}_\circ.$$

Model first-order partial derivatives are as presented in section B.17 with:

$$\frac{\partial \tau}{\partial \tau_\circ} = 1.$$

B.19 Sisko

This simple 3-parameter model (Sisko, 1958) model cannot be manipulated into tractable, analytic, flow relations. The model form is:

$$\tau = a\dot{\gamma} + b\dot{\gamma}^c,$$

and for $\dot{\gamma}$ by the implicit function

$$0 = a\dot{\gamma} + b\dot{\gamma}^c - \tau,$$

where a, b and c are model parameters. Direct parameter solution expressions are:

$$a = \frac{\tau_1 - b\dot{\gamma}_1^c}{\dot{\gamma}_1},$$

and

$$b = -\frac{\dot{\gamma}_2\tau_1 - \dot{\gamma}_1\tau_2}{\dot{\gamma}_1\dot{\gamma}_2^c - \dot{\gamma}_2\dot{\gamma}_1^c},$$

which allows solution of the following implicit expression about c:

$$0 = a\dot{\gamma}_3 + b\dot{\gamma}_3^c - \tau_3.$$

Model first-order partial derivatives are:

$$\frac{\partial \tau}{\partial a} = \dot{\gamma} \quad ; \quad \frac{\partial \tau}{\partial b} = \dot{\gamma}^c \quad ; \quad \frac{\partial \tau}{\partial c} = b\dot{\gamma}^c \ln\left(\dot{\gamma}\right).$$

B.20 Sisko* (Modified Sisko)

Constructed specifically for solution using nonlinear least squares, the modification to the basic Sisko model involves the addition of an explicit yield stress component, $\tau_\circ$, namely:

$$\tau = \tau_\circ + a\dot{\gamma} + b\dot{\gamma}^c,$$

with its inverse written as the following implicit function:

$$0 = \tau_\circ + a\dot{\gamma} + b\dot{\gamma}^c - \tau,$$

where $\tau_\circ$ is the new model parameter. Model first-order partial derivatives are as presented in section B.19 with:

$$\frac{\partial \tau}{\partial \tau_\circ} = 1.$$

Appendix C

Direct Parameter Estimation Results

Fann speeds	No. Sol's	Lower ext.	Lower q'tile	Med.	Upper q'tile	Upper ext.	Median 95% conf. limits	Max. RMS	No. outs
600/300	414	1.3220	7.633	11.71	26.16	53.76	(10.28 , 13.14)	159.4	76
600/200	414	0.7936	4.725	7.158	17.61	36.43	(6.162 , 8.155)	122.1	75
600/100	414	0.2856	2.543	3.700	8.168	16.60	(3.265 , 4.136)	55.59	77
600/60	414	0.2684	2.249	3.335	6.129	11.11	(3.035 , 3.635)	38.22	77
600/30	414	0.3402	1.671	2.347	5.130	9.400	(2.080 , 2.615)	31.97	76
600/6	414	0.3083	3.008	4.428	9.327	18.15	(3.939 , 4.917)	58.76	76
600/3	414	0.4622	4.067	5.788	11.17	20.26	(5.238 , 6.338)	77.44	77
300/200	414	0.7025	3.309	5.374	16.19	33.99	(4.377 , 6.370)	110.4	60
300/100	414	0.5867	2.557	3.575	8.400	16.78	(3.123 , 4.027)	49.91	75
300/60	414	0.4985	2.602	3.638	7.672	13.84	(3.245 , 4.030)	41.99	76
300/30	414	0.5841	2.186	3.270	7.594	15.38	(2.852 , 3.689)	43.65	75
300/6	414	0.5196	3.897	5.639	12.65	23.98	(4.962 , 6.317)	71.11	76
300/3	414	0.6679	4.879	6.902	14.86	27.28	(6.130 , 7.674)	90.13	76
200/100	414	0.6342	3.178	4.942	12.26	25.60	(4.239 , 5.645)	107.1	70
200/60	414	0.5518	3.076	4.549	12.45	25.81	(3.824 , 5.274)	85.21	75
200/30	414	0.6849	3.738	6.195	16.36	35.14	(5.218 , 7.171)	114.8	73
200/6	414	0.7720	8.370	12.40	29.71	59.85	(10.75 , 14.05)	199.8	75
200/3	414	1.1610	10.01	15.02	33.08	62.80	(13.24 , 16.81)	230.6	76
100/60	414	0.2357	3.533	7.963	40.55	95.32	(5.099 , 10.83)	247.3	49
100/30	414	0.3301	8.340	15.54	43.43	95.83	(12.83 , 18.26)	302.4	73
100/6	414	0.2946	27.01	43.55	88.26	173.1	(38.82 , 48.29)	641.7	78
100/3	414	0.7307	37.25	53.35	112.9	213.1	(47.50 , 59.20)	810.2	77
60/30	414	1.6460	31.63	72.20	143.5	302.2	(63.55 , 80.85)	730.1	59
60/6	414	0.7797	89.10	139.0	247.2	371.4	(126.8 , 151.3)	1441	80
60/3	414	3.2000	115.4	171.4	297.6	556.5	(157.3 , 185.5)	1915	76
30/6	414	0.6445	184.9	306.0	535.8	944.4	(278.8 , 333.1)	3400	78
30/3	414	0.6679	274.5	381.5	692.3	1316	(349.2 , 413.9)	4454	76
6/3	414	2470.0	530.2	1108	5098	7572	(754.4 , 1461)	100900	35

Table C.1: Bingham Plastic: RMS values for various Fann speed combinations.

Fann Speeds	No. Sol's	Lower ext.	Lower q'tile	Med	Upper q'tile	Upper ext.	Median 95% conf. limits	Max. RMS	No. outs
600/300	414	0.02882	0.8897	1.785	5.722	12.30	(1.411 , 2.159)	37.33	74
600/200	414	0.01039	0.8399	1.568	4.072	8.273	(1.318 , 1.818)	30.64	65
600/100	414	0.01339	0.5734	1.059	2.543	5.477	(0.906 , 1.211)	13.42	60
600/60	414	0.01492	0.4305	0.746	2.057	4.417	(0.620 , 0.872)	10.03	59
600/30	414	0.01276	0.4758	0.819	1.916	3.942	(0.708 , 0.931)	9.316	60
600/6	414	0.01016	0.7248	1.516	5.144	11.74	(1.174 , 1.858)	23.76	55
600/3	414	0.00916	0.9726	1.809	5.768	12.84	(1.438 , 2.180)	32.84	62
300/200	414	0.05507	0.9936	1.974	4.665	10.17	(1.690 , 2.258)	36.86	50
300/100	414	0.03211	0.6437	1.139	2.659	5.621	(0.983 , 1.295)	15.06	61
300/60	414	0.01597	0.5989	1.080	2.736	5.910	(0.915 , 1.246)	10.94	53
300/30	414	0.01510	0.6408	1.129	2.405	4.983	(0.993 , 1.266)	13.09	69
300/6	414	0.01633	0.9063	1.754	5.801	13.07	(1.376 , 2.133)	26.20	57
300/3	414	0.01487	1.0680	1.977	6.686	15.11	(1.542 , 2.412)	34.86	61
200/100	414	0.01455	0.9958	1.746	4.156	8.642	(1.501 , 1.990)	77.90	51
200/60	414	0.04812	1.6270	2.892	5.828	12.12	(2.567 , 3.217)	29.76	31
200/30	414	0.03567	1.5550	2.977	6.078	12.13	(2.627 , 3.327)	35.34	56
200/6	414	0.01029	2.0520	4.164	12.53	27.45	(3.353 , 4.974)	75.52	59
200/3	414	0.00991	2.3530	4.539	14.76	33.11	(3.579 , 5.498)	94.03	59
100/60	414	0.19640	6.1030	15.49	27.17	57.12	(13.86 , 17.12)	466.8	21
100/30	414	0.14540	5.1380	10.89	21.08	43.33	(9.652 , 12.12)	101.5	39
100/6	414	0.01562	5.8770	13.96	39.73	86.78	(11.34 , 16.58)	234.1	58
100/3	414	0.01718	6.6050	15.06	45.38	101.7	(12.06 , 18.06)	308.1	60
60/30	414	0.02091	2.3640	8.617	31.14	71.94	(6.391 , 10.84)	313.6	50
60/6	414	0.05253	3.0760	11.14	70.47	171.3	(5.928 , 16.36)	461.5	69
60/3	414	0.08619	4.3640	12.79	75.80	179.6	(7.264 , 18.32)	623.1	71
30/6	414	0.07889	5.3330	26.10	167.3	401.8	(13.57 , 38.63)	1094	62
30/3	414	0.12290	8.1340	26.95	174.0	422.7	(14.12 , 39.78)	1446	67
6/3	414	0.12940	94.230	156.9	291.9	580.0	(141.7 , 172.2)	73290	69

Table C.2: Casson: RMS values for various Fann speed combinations.

Fann Speeds	No. Sol's	Lower ext.	Lower q'tile	Med.	Upper q'tile	Upper ext.	Median 95% conf. limits	Max. RMS	No. outs
600/300/200	376	0.05462	8.827	13.37	17.10	27.14	(12.70 , 14.05)	56.34	5
600/300/100	409	0.07334	5.722	9.511	12.01	20.79	(9.021 , 10.00)	33.40	6
600/300/60	408	0.03678	3.952	6.459	8.645	15.27	(6.093 , 6.825)	25.57	6
600/300/30	413	0.10320	4.062	5.428	7.168	11.81	(5.187 , 5.668)	19.99	7
600/300/6	414	0.29650	2.631	3.880	6.882	13.18	(3.551 , 4.209)	23.64	65
600/300/3	414	0.24350	2.960	4.277	8.868	17.43	(3.820 , 4.734)	34.69	66
600/200/100	408	0.07754	5.035	8.662	10.86	19.29	(8.207 , 9.116)	41.21	10
600/200/60	400	0.03358	3.387	5.977	7.971	14.16	(5.616 , 6.337)	25.32	8
600/200/30	412	0.07754	3.011	4.575	6.287	10.61	(4.321 , 4.829)	21.66	9
600/200/6	414	0.20830	1.433	2.125	4.028	7.582	(1.924 , 2.326)	16.34	48
600/200/3	414	0.16890	1.534	2.304	5.110	10.43	(2.027 , 2.580)	23.19	56
600/100/60	325	0.17580	3.188	4.367	6.007	10.05	(4.121 , 4.614)	25.35	21
600/100/30	411	0.31500	3.130	4.110	5.286	8.343	(3.943 , 4.278)	19.22	18
600/100/6	414	0.31980	0.881	1.182	2.088	3.810	(1.088 , 1.275)	9.689	57
600/100/3	412	0.24280	0.815	1.155	2.209	4.231	(1.047 , 1.263)	10.12	68
600/60/30	411	0.46780	3.347	4.608	5.897	9.710	(4.410 , 4.806)	19.98	12
600/60/6	414	0.34630	0.885	1.165	2.393	4.607	(1.049 , 1.282)	10.84	66
600/60/3	412	0.24240	0.791	1.111	2.481	4.837	(0.980 , 1.242)	11.53	71
600/30/6	403	0.41970	1.279	1.888	4.100	8.317	(1.667 , 2.110)	22.62	71
600/30/3	400	0.28740	1.119	1.715	4.363	8.796	(1.460 , 1.970)	24.14	72
600/6/3	212	0.58670	3.506	7.480	33.90	61.19	(4.194 , 10.77)	61.19	0
300/200/100	345	0.09426	5.156	8.811	11.23	20.11	(8.296 , 9.326)	60.70	8
300/200/60	344	0.06124	4.655	6.282	8.330	13.45	(5.970 , 6.594)	37.59	10
300/200/30	387	0.20460	4.156	5.362	6.974	10.72	(5.136 , 5.587)	32.20	12
300/200/6	405	0.39750	1.546	2.262	4.592	9.079	(2.024 , 2.500)	20.10	43
300/200/3	402	0.34290	1.546	2.308	5.471	11.12	(2.000 , 2.617)	23.62	48
300/100/60	270	0.64700	4.011	6.398	9.998	18.97	(5.824 , 6.971)	25.89	4
300/100/30	403	1.40200	4.048	5.554	8.057	14.07	(5.240 , 5.868)	29.57	20
300/100/6	410	0.44860	1.464	2.109	4.613	8.739	(1.864 , 2.354)	29.58	64
300/100/3	408	0.39310	1.362	1.981	4.571	9.083	(1.731 , 2.231)	29.66	65
300/60/30	408	1.00600	4.262	5.777	8.729	15.40	(5.429 , 6.125)	24.63	30
300/60/6	410	0.45170	1.442	2.050	5.188	10.37	(1.758 , 2.341)	26.81	70
300/60/3	406	0.38780	1.350	1.995	5.605	11.98	(1.662 , 2.327)	27.24	67
300/30/6	400	0.46270	2.187	3.109	7.359	14.94	(2.702 , 3.516)	41.64	74
300/30/3	396	0.39340	2.027	2.999	8.451	17.80	(2.491 , 3.507)	43.10	69
300/6/3	208	1.24800	4.665	9.314	45.80	76.81	(4.825 , 13.80)	76.81	0
200/100/60	223	0.44110	5.318	9.601	18.26	37.39	(8.237 , 10.97)	79.83	8
200/100/30	379	0.42850	4.935	7.358	14.11	27.82	(6.616 , 8.100)	78.12	34
200/100/6	410	0.30140	2.103	4.310	11.65	24.86	(3.568 , 5.052)	127.5	49
200/100/3	403	0.25130	2.058	4.252	11.85	26.34	(3.484 , 5.020)	127.5	49
200/60/30	405	0.93090	5.007	7.066	14.31	27.72	(6.339 , 7.793)	73.58	56
200/60/6	407	0.32670	2.007	3.405	12.47	26.52	(2.589 , 4.222)	80.44	65
200/60/3	406	0.31890	1.939	3.346	12.25	27.23	(2.541 , 4.152)	81.97	65
200/30/6	400	0.62280	3.939	6.791	19.41	41.04	(5.573 , 8.009)	122.7	62
200/30/3	394	0.57110	3.758	6.847	19.19	42.05	(5.623 , 8.071)	127.4	64
200/6/3	206	1.71700	11.30	22.00	112.0	221.5	(10.95 , 33.05)	221.5	0
100/60/30	375	1.34700	5.669	12.92	38.23	86.58	(10.28 , 15.57)	287.5	36
100/60/6	404	0.38160	1.939	6.816	40.20	96.81	(3.820 , 9.813)	291.3	52
100/60/3	399	0.51750	1.924	6.685	41.08	96.50	(3.600 , 9.771)	292.2	54
100/30/6	397	0.46700	9.606	18.59	51.25	113.0	(15.30 , 21.88)	347.2	70
100/30/3	391	0.28550	9.550	18.56	55.30	123.0	(14.91 , 22.20)	354.1	70
100/6/3	199	2.59300	33.46	74.11	392.0	684.4	(34.10 , 114.1)	684.4	0
60/30/6	378	0.44290	38.41	85.91	169.1	362.7	(75.33 , 96.49)	857.9	51
60/30/3	362	0.39300	37.68	86.63	181.1	393.4	(74.77 , 98.50)	870.2	44
60/6/3	194	0.68470	120.3	246.1	865.8	1569	(161.8 , 330.3)	1569	0
30/6/3	181	2.34800	200.3	483.1	1820	3832	(293.6 , 672.5)	3832	0

Table C.3: Collins-Graves: RMS values for various Fann speed combinations.

Fann Speeds	No. Sol's	Lower ext.	Lower q'tile	Med.	Upper q'tile	Upper ext.	Median 95% conf. limits	Max. RMS	No. outs
600/300/200	414	0.01680	0.8811	3.2640	7.8230	17.00	(2.727 , 3.801)	95.90	30
600/300/100	414	0.01298	0.2342	0.4947	1.2940	2.849	(0.413 , 0.577)	14.47	33
600/300/60	414	0.01302	0.2694	0.7181	1.5010	3.285	(0.623 , 0.813)	15.13	23
600/300/30	414	0.00898	0.1675	0.3913	0.6234	1.235	(0.356 , 0.427)	3.721	20
600/300/6	414	0.01114	0.1095	0.2068	0.3334	0.666	(0.189 , 0.224)	3.846	34
600/300/3	414	0.00920	0.1168	0.2588	0.4550	0.958	(0.233 , 0.285)	5.752	25
600/200/100	414	0.02334	0.2978	0.6687	1.6300	3.625	(0.566 , 0.772)	22.87	28
600/200/60	414	0.01142	0.3250	0.8604	1.8420	4.085	(0.743 , 0.978)	15.46	21
600/200/30	414	0.01158	0.1568	0.3878	0.6612	1.382	(0.349 , 0.427)	3.241	19
600/200/6	414	0.01208	0.1011	0.1856	0.3328	0.658	(0.168 , 0.204)	2.717	18
600/200/3	414	0.01420	0.1075	0.2191	0.4061	0.846	(0.196 , 0.242)	4.916	16
600/100/60	413	0.01766	0.6494	1.8110	3.8710	8.302	(1.561 , 2.060)	43.38	24
600/100/30	414	0.01306	0.2033	0.4183	0.7931	1.665	(0.373 , 0.464)	9.387	17
600/100/6	414	0.01184	0.1048	0.1605	0.2885	0.548	(0.146 , 0.175)	4.555	23
600/100/3	414	0.01194	0.1043	0.1937	0.3332	0.671	(0.176 , 0.211)	4.523	20
600/60/30	414	0.01122	0.2983	0.5252	0.9887	2.018	(0.472 , 0.579)	21.52	28
600/60/6	414	0.00784	0.1393	0.3311	0.7609	1.689	(0.283 , 0.379)	8.468	19
600/60/3	414	0.00760	0.1457	0.3781	0.8318	1.832	(0.325 , 0.431)	8.644	21
600/30/6	414	0.00740	0.2294	0.6420	1.2580	2.796	(0.562 , 0.722)	6.194	13
600/30/3	414	0.01044	0.2489	0.7233	1.4380	3.113	(0.631 , 0.815)	9.033	11
600/6/3	412	0.01702	0.4174	1.0510	5.7440	13.48	(0.638 , 1.465)	144.6	73
300/200/100	414	0.04854	0.7699	2.4890	5.1740	11.62	(2.148 , 2.830)	72.11	40
300/200/60	414	0.02120	0.8320	1.9390	4.1050	8.717	(1.686 , 2.192)	31.34	29
300/200/30	414	0.01860	0.4385	0.8507	1.6890	3.526	(0.754 , 0.948)	23.54	43
300/200/6	414	0.01784	0.2531	0.5402	1.0780	2.227	(0.476 , 0.604)	21.73	41
300/200/3	414	0.01850	0.2749	0.5784	1.1300	2.373	(0.512 , 0.645)	22.46	40
300/100/60	413	0.01926	1.1780	3.0330	7.2330	14.82	(2.564 , 3.502)	100.9	23
300/100/30	414	0.01390	0.3986	0.6917	1.3020	2.638	(0.622 , 0.762)	32.63	40
300/100/6	414	0.01170	0.1644	0.3239	0.7191	1.501	(0.281 , 0.367)	13.62	27
300/100/3	414	0.01166	0.1792	0.3784	0.7359	1.549	(0.335 , 0.421)	14.47	29
300/60/30	414	0.01606	0.4545	1.0290	2.4560	5.248	(0.874 , 1.184)	49.23	36
300/60/6	414	0.01526	0.2656	0.8408	2.0550	4.235	(0.702 , 0.979)	21.20	23
300/60/3	414	0.01030	0.2897	0.9563	2.3500	5.428	(0.797 , 1.116)	23.00	17
300/30/6	414	0.01170	0.4151	1.3800	2.7520	6.239	(1.199 , 1.560)	18.23	12
300/30/3	414	0.00990	0.5356	1.4800	3.1800	6.864	(1.275 , 1.684)	21.08	11
300/6/3	412	0.02308	0.6728	1.7520	7.0050	16.34	(1.261 , 2.243)	84.86	79
200/100/60	412	0.03634	2.3570	6.5530	17.870	39.90	(5.350 , 7.756)	273.6	36
200/100/30	414	0.03026	0.6568	1.6010	3.3380	7.254	(1.394 , 1.809)	186.2	47
200/100/6	414	0.02632	0.3617	0.9543	2.3820	5.146	(0.798 , 1.111)	104.9	30
200/100/3	414	0.02344	0.3837	0.9615	2.4010	5.297	(0.805 , 1.118)	96.06	33
200/60/30	414	0.01120	1.0880	3.2720	10.210	23.67	(2.566 , 3.978)	118.7	22
200/60/6	414	0.01662	0.7736	3.0600	8.0530	18.92	(2.497 , 3.623)	60.07	15
200/60/3	414	0.01446	0.8643	3.4510	8.3660	18.35	(2.871 , 4.031)	56.06	17
200/30/6	414	0.02386	1.0860	4.1650	9.2740	21.10	(3.532 , 4.799)	32.33	6
200/30/3	414	0.01758	1.2430	4.7210	10.240	23.22	(4.025 , 5.417)	43.92	5
200/6/3	409	0.04110	1.8310	5.1740	17.730	40.63	(3.936 , 6.411)	133.0	71
100/60/30	410	0.06558	13.400	36.130	106.60	244.9	(28.88 , 43.37)	448.9	12
100/60/6	413	0.01694	6.4070	27.020	69.190	159.2	(22.16 , 31.88)	419.4	15
100/60/3	413	0.04822	6.5950	27.280	65.630	151.0	(22.71 , 31.85)	409.8	16
100/30/6	414	0.03098	4.7140	19.020	43.350	101.1	(16.03 , 22.01)	220.6	11
100/30/3	414	0.01764	4.8800	21.590	44.350	103.4	(18.54 , 24.65)	176.7	9
100/6/3	409	0.08476	4.8810	15.090	87.840	211.5	(8.638 , 21.55)	246.0	2
60/30/6	413	0.01648	3.4980	22.730	65.300	157.0	(17.94 , 27.51)	1729	31
60/30/3	413	0.02094	3.1440	16.450	54.430	126.1	(12.48 , 20.43)	1466	20
60/6/3	409	0.09630	6.2310	25.350	142.90	347.2	(14.71 , 35.99)	994.2	3
30/6/3	407	0.18740	29.960	111.20	380.10	668.9	(83.83 , 138.5)	1941	15

Table C.4: Ellis *et al.*: RMS values for various Fann speed combinations.

Fann Speeds	No. Sol's	Lower ext.	Lower q'tile	Med.	Upper q'tile	Upper ext.	Median 95% conf. limits	Max. RMS	No. outs
600/300/200	414	0.01930	0.8825	3.0400	8.5860	19.98	(2.444 , 3.636)	97.44	36
600/300/100	414	0.01066	0.2546	0.5926	1.3130	2.831	(0.511 , 0.675)	18.56	32
600/300/60	414	0.01622	0.3066	0.8419	1.6140	3.560	(0.741 , 0.943)	15.14	18
600/300/30	414	0.01006	0.1772	0.4011	0.6496	1.330	(0.365 , 0.438)	3.714	19
600/300/6	414	0.01214	0.1240	0.2383	0.3923	0.776	(0.218 , 0.259)	3.849	34
600/300/3	414	0.00976	0.1369	0.3034	0.5557	1.181	(0.271 , 0.336)	5.763	20
600/200/100	414	0.01752	0.3134	0.6563	1.6170	3.230	(0.555 , 0.757)	30.56	28
600/200/60	414	0.01166	0.3803	0.9318	1.9210	4.217	(0.813 , 1.051)	15.53	17
600/200/30	414	0.01130	0.1709	0.3931	0.6643	1.327	(0.355 , 0.431)	3.182	17
600/200/6	414	0.01086	0.1150	0.2070	0.3679	0.740	(0.187 , 0.227)	2.692	17
600/200/3	414	0.01118	0.1225	0.2465	0.4578	0.926	(0.221 , 0.272)	5.106	15
600/100/60	414	0.01796	0.6501	1.7710	3.7770	8.261	(1.530 , 2.013)	46.64	24
600/100/30	414	0.01354	0.2023	0.4064	0.7125	1.466	(0.367 , 0.446)	8.968	22
600/100/6	414	0.01136	0.1085	0.1817	0.3028	0.584	(0.167 , 0.197)	4.442	23
600/100/3	414	0.01118	0.1119	0.2108	0.3488	0.702	(0.192 , 0.229)	4.423	22
600/60/30	414	0.01022	0.3164	0.5914	1.0200	2.058	(0.537 , 0.646)	31.86	31
600/60/6	414	0.00788	0.1447	0.3846	0.8684	1.942	(0.329 , 0.441)	8.810	18
600/60/3	414	0.00722	0.1638	0.4421	0.9154	1.895	(0.384 , 0.500)	8.903	22
600/30/6	414	0.00730	0.2232	0.7216	1.4620	3.303	(0.626 , 0.817)	5.851	10
600/30/3	414	0.00868	0.2855	0.7947	1.5190	3.332	(0.699 , 0.890)	8.950	10
600/6/3	414	0.01806	0.3742	0.8216	4.1280	9.608	(0.535 , 1.112)	138.2	90
300/200/100	414	0.01916	0.8027	2.5330	5.2720	11.88	(2.187 , 2.878)	91.34	49
300/200/60	414	0.06644	0.8625	1.9910	4.1260	8.774	(1.738 , 2.243)	39.75	31
300/200/30	414	0.01886	0.4326	0.8662	1.7210	3.638	(0.766 , 0.966)	23.78	43
300/200/6	414	0.01788	0.2714	0.5437	1.0940	2.240	(0.480 , 0.607)	20.84	40
300/200/3	414	0.01822	0.2928	0.6043	1.1890	2.469	(0.535 , 0.674)	21.42	36
300/100/60	414	0.01932	1.1670	3.2020	8.0000	17.85	(2.673 , 3.730)	234.1	38
300/100/30	414	0.01404	0.3596	0.6793	1.2080	2.405	(0.614 , 0.745)	31.87	43
300/100/6	414	0.01156	0.1848	0.3682	0.7890	1.668	(0.321 , 0.415)	12.06	27
300/100/3	414	0.01092	0.2008	0.4244	0.8560	1.801	(0.374 , 0.475)	12.95	26
300/60/30	414	0.01468	0.5070	1.1650	2.7020	5.925	(0.995 , 1.335)	457.7	35
300/60/6	414	0.01504	0.3027	1.0420	2.3740	5.366	(0.882 , 1.202)	21.08	20
300/60/3	414	0.01146	0.2934	1.1560	2.6350	5.918	(0.975 , 1.337)	20.69	16
300/30/6	414	0.01348	0.4003	1.5070	3.0540	6.852	(1.302 , 1.713)	18.28	14
300/30/3	414	0.00926	0.4887	1.5330	3.3180	7.389	(1.314 , 1.752)	16.95	10
300/6/3	414	0.02272	0.5328	1.2910	4.9790	11.00	(0.947 , 1.635)	92.67	92
200/100/60	414	0.13150	2.2980	7.5520	25.590	60.43	(5.757 , 9.354)	4640	51
200/100/30	414	0.02978	0.6612	1.5070	3.3360	7.271	(1.377 , 1.714)	294.6	45
200/100/6	414	0.02504	0.3977	1.0230	2.6470	5.998	(0.849 , 1.197)	94.03	26
200/100/3	414	0.01758	0.4214	1.0750	2.7860	5.952	(0.892 , 1.258)	83.74	28
200/60/30	414	0.01170	1.1750	3.5880	11.210	26.00	(2.812 , 4.365)	5549	18
200/60/6	414	0.02302	0.9172	3.5850	8.3240	19.01	(3.012 , 4.158)	58.96	15
200/60/3	414	0.01162	0.8958	3.6840	8.6010	20.11	(3.088 , 4.280)	53.57	15
200/30/6	414	0.02232	0.9755	4.0810	9.4390	21.61	(3.427 , 4.736)	37.03	8
200/30/3	414	0.01136	1.1580	4.5980	9.6280	22.18	(3.943 , 5.254)	42.33	5
200/6/3	414	0.04092	1.2330	3.6160	13.760	32.39	(2.647 , 4.585)	153.3	81
100/60/30	414	0.13870	14.300	41.970	115.10	257.0	(34.17 , 49.77)	98630	23
100/60/6	414	0.08012	6.1220	27.130	66.080	147.5	(22.49 , 31.77)	2518	17
100/60/3	414	0.03288	5.9770	26.340	60.440	141.7	(22.12 , 30.55)	1653	18
100/30/6	414	0.03082	4.4100	17.810	39.710	91.50	(15.08 , 20.54)	575.4	15
100/30/3	414	0.02224	4.0360	17.480	37.600	86.34	(14.89 , 20.08)	286.9	11
100/6/3	414	0.06076	2.5050	10.220	56.180	135.4	(6.071 , 14.38)	262.2	33
60/30/6	414	0.01802	2.8080	20.590	58.170	141.0	(16.30 , 24.87)	17350	43
60/30/3	414	0.01102	2.5900	13.580	47.770	112.4	(10.09 , 17.08)	4580	24
60/6/3	414	0.10410	5.7730	24.650	113.30	265.6	(16.33 , 32.97)	1076	7
30/6/3	414	0.13130	44.020	105.10	343.90	787.8	(81.85 , 128.3)	3038	14

Table C.5: Herschel-Bulkley: RMS values for various Fann speed combinations.

Fann Speeds	No. Sol's	Lower ext.	Lower q'tile	Med.	Upper q'tile	Upper ext.	Median 95% conf. limits	Max. RMS	No. outs
600/300/200/100	409	0.5059	2.677	4.171	8.345	16.24	(3.730 , 4.612)	56.60	78
600/300/200/60	406	0.4698	2.850	4.304	8.204	13.91	(3.886 , 4.723)	47.30	76
600/300/200/30	412	0.4695	2.239	3.210	7.713	15.69	(2.785 , 3.634)	45.05	75
600/300/200/6	414	0.3882	3.522	5.231	12.39	25.55	(4.545 , 5.918)	75.06	76
600/300/200/3	414	0.4721	4.537	6.603	14.68	28.12	(5.818 , 7.387)	98.49	76
600/300/100/60	350	0.6090	2.765	4.310	10.13	21.13	(3.690 , 4.929)	40.92	51
600/300/100/30	413	0.5426	1.931	2.729	6.752	13.35	(2.355 , 3.102)	38.78	76
600/300/100/6	414	0.5026	2.419	3.549	9.976	20.88	(2.964 , 4.133)	57.88	75
600/300/100/3	414	0.5504	2.961	4.331	11.25	21.19	(3.690 , 4.972)	73.77	76
600/300/60/30	413	0.2896	1.347	2.007	6.174	12.60	(1.633 , 2.381)	36.51	75
600/300/60/6	414	0.2913	1.490	2.271	7.694	16.27	(1.791 , 2.751)	49.34	77
600/300/60/3	414	0.3435	1.847	2.655	8.962	18.30	(2.104 , 3.205)	61.26	76
600/300/30/6	408	0.1966	1.124	1.740	7.355	16.70	(1.255 , 2.226)	44.13	72
600/300/30/3	413	0.2208	1.230	1.934	7.568	16.19	(1.444 , 2.425)	52.12	75
600/300/6/3	414	0.0877	0.685	1.145	5.945	12.71	(0.738 , 1.552)	44.88	77
600/200/100/60	340	0.3952	2.529	4.100	9.295	19.35	(3.522 , 4.678)	38.49	51
600/200/100/30	413	0.4218	1.809	2.466	5.983	12.21	(2.143 , 2.790)	36.20	75
600/200/100/6	414	0.3424	2.338	3.426	8.435	17.54	(2.954 , 3.897)	56.56	76
600/200/100/3	414	0.4178	2.907	4.188	10.06	18.85	(3.635 , 4.742)	69.70	76
600/200/60/30	411	0.2772	1.381	2.007	5.544	11.64	(1.684 , 2.331)	33.83	74
600/200/60/6	414	0.2763	1.586	2.377	6.996	14.87	(1.959 , 2.796)	48.21	77
600/200/60/3	414	0.3034	1.960	2.760	8.097	16.31	(2.285 , 3.235)	58.76	76
600/200/30/6	405	0.2331	1.314	1.946	6.430	13.89	(1.546 , 2.346)	42.92	75
600/200/30/3	413	0.2517	1.451	2.148	6.725	13.59	(1.740 , 2.556)	49.98	76
600/200/6/3	414	0.1053	0.938	1.542	5.384	11.09	(1.198 , 1.886)	44.19	79
600/100/60/30	412	0.3805	1.596	2.276	5.713	11.74	(1.956 , 2.595)	33.22	74
600/100/60/6	414	0.3147	1.902	2.801	7.298	15.07	(2.384 , 3.219)	46.73	76
600/100/60/3	414	0.3704	2.286	3.247	8.237	16.03	(2.786 , 3.707)	57.50	76
600/100/30/6	405	0.3889	1.692	2.450	6.859	13.77	(2.046 , 2.855)	43.50	76
600/100/30/3	412	0.4377	1.862	2.689	7.257	13.77	(2.271 , 3.108)	50.97	76
600/100/6/3	414	0.2719	1.496	2.292	6.602	13.77	(1.897 , 2.687)	47.67	77
600/60/30/6	404	0.3692	1.760	2.624	7.624	16.36	(2.165 , 3.083)	46.74	75
600/60/30/3	411	0.4211	1.969	2.790	8.352	15.45	(2.295 , 3.286)	54.98	76
600/60/6/3	414	0.2970	1.599	2.415	7.566	15.12	(1.953 , 2.877)	52.85	77
600/30/6/3	414	0.5059	2.507	3.689	9.249	17.84	(3.168 , 4.211)	64.98	77
300/200/100/60	290	0.6280	2.657	4.448	13.21	28.76	(3.472 , 5.423)	392.2	5
300/200/100/30	392	0.3388	1.786	2.872	6.155	12.61	(2.525 , 3.219)	266.5	63
300/200/100/6	406	0.3411	2.075	3.151	7.332	14.82	(2.741 , 3.562)	47.04	72
300/200/100/3	408	0.4356	2.633	3.774	8.415	16.82	(3.324 , 4.225)	56.54	78
300/200/60/30	398	0.2780	1.457	2.378	5.487	11.37	(2.060 , 2.696)	217.0	63
300/200/60/6	406	0.2768	1.545	2.506	6.428	13.52	(2.124 , 2.887)	39.38	71
300/200/60/3	409	0.3198	1.860	3.048	7.325	14.99	(2.623 , 3.474)	46.23	74
300/200/30/6	398	0.1964	1.353	2.328	6.021	12.99	(1.960 , 2.696)	34.58	68
300/200/30/3	406	0.2356	1.490	2.537	6.227	13.23	(2.167 , 2.907)	38.96	73
300/200/6/3	412	0.1309	1.163	2.253	5.716	12.54	(1.900 , 2.606)	32.70	66
300/100/60/30	407	0.7052	1.902	2.765	6.622	13.68	(2.397 , 3.133)	40.10	65
300/100/60/6	412	0.5886	1.957	2.959	6.666	13.50	(2.594 , 3.325)	40.93	74
300/100/60/3	413	0.6016	2.161	3.283	7.193	14.73	(2.893 , 3.672)	42.05	74
300/100/30/6	402	0.5865	1.821	2.776	6.784	13.70	(2.387 , 3.166)	40.67	69
300/100/30/3	410	0.6324	1.931	2.914	6.784	13.83	(2.537 , 3.292)	41.37	74
300/100/6/3	412	0.5731	1.743	2.740	6.492	13.57	(2.372 , 3.109)	40.96	72
300/60/30/6	402	0.4046	1.770	2.624	8.132	17.60	(2.125 , 3.124)	40.72	71
300/60/30/3	409	0.4478	1.908	2.826	8.050	16.79	(2.348 , 3.304)	45.13	75
300/60/6/3	414	0.3732	1.669	2.564	7.857	16.67	(2.085 , 3.043)	43.61	74
300/30/6/3	411	0.5987	2.950	4.467	11.54	23.50	(3.800 , 5.134)	64.18	74
200/100/60/30	391	0.7293	2.737	5.113	14.95	31.70	(4.141 , 6.086)	97.68	49
200/100/60/6	409	0.6457	2.801	5.102	14.68	32.44	(4.178 , 6.027)	159.7	51
200/100/60/3	411	0.6795	3.099	5.676	15.05	31.41	(4.747 , 6.604)	159.8	52
200/100/30/6	402	0.6225	2.676	5.077	14.84	33.06	(4.122 , 6.032)	159.7	48
200/100/30/3	406	0.7073	2.802	5.343	14.93	32.08	(4.395 , 6.291)	159.9	51
200/100/6/3	411	0.4082	2.665	4.849	14.75	32.73	(3.911 , 5.787)	159.9	50
200/60/30/6	401	0.3108	2.445	4.034	16.15	34.01	(2.956 , 5.112)	100.3	65
200/60/30/3	405	0.3482	2.522	4.202	15.88	34.60	(3.158 , 5.247)	101.3	65
200/60/6/3	413	0.2743	2.380	4.117	15.80	34.12	(3.078 , 5.156)	100.9	65
200/30/6/3	411	0.9364	4.962	8.586	23.18	49.98	(7.172 , 10.00)	162.8	72
100/60/30/6	397	0.8387	3.099	9.750	57.48	135.4	(5.454 , 14.05)	357.4	39
100/60/30/3	406	0.3344	3.224	9.895	57.75	136.4	(5.636 , 14.15)	356.9	39
100/60/6/3	410	0.2633	2.921	9.369	54.35	128.5	(5.371 , 13.37)	358.1	45
100/30/6/3	408	0.4496	11.69	22.45	67.43	148.7	(18.11 , 26.80)	439.0	71
60/30/6/3	396	1.1680	46.93	107.6	220.0	473.2	(93.91 , 121.3)	1081	47

Table C.6: Hyperbolic: RMS values for various Fann speed combinations.

Fann Speeds	No. Sol's	Lower ext.	Lower q'tile	Med.	Upper q'tile	Upper ext.	Median 95% conf. limits	Max. RMS	No. outs
600/300	414	0.01213	1.991	9.380	11.69	23.46	(8.630 , 10.13)	57.93	4
600/200	414	0.01157	2.720	8.017	10.12	19.90	(7.445 , 8.590)	34.05	4
600/100	414	0.01554	1.479	6.107	7.639	15.98	(5.631 , 6.584)	27.04	3
600/60	414	0.01975	1.621	6.233	7.847	15.68	(5.751 , 6.715)	25.06	3
600/30	414	0.01924	1.722	9.374	11.65	23.05	(8.607 , 10.14)	30.32	3
600/6	414	0.01152	4.292	32.60	42.75	83.47	(29.62 , 35.57)	83.47	0
600/3	414	0.02732	5.445	50.36	63.04	114.5	(45.90 , 54.81)	114.5	0
300/200	414	0.01386	2.914	7.715	9.646	18.62	(7.194 , 8.235)	34.34	5
300/100	414	0.01885	2.138	7.241	9.108	18.38	(6.701 , 7.780)	34.01	3
300/60	414	0.01901	1.590	9.093	11.62	26.14	(8.317 , 9.869)	37.04	3
300/30	414	0.02037	1.711	12.62	15.63	28.94	(11.54 , 13.69)	39.00	3
300/6	414	0.01165	3.219	28.09	35.77	63.74	(25.58 , 30.61)	63.74	0
300/3	414	0.02787	4.294	37.12	46.28	78.83	(33.88 , 40.37)	78.83	0
200/100	414	0.02812	3.363	11.19	14.50	29.63	(10.33 , 12.05)	48.89	3
200/60	414	0.02619	3.434	19.35	25.12	57.28	(17.67 , 21.03)	58.21	1
200/30	414	0.02430	3.817	27.73	34.24	57.91	(25.38 , 30.08)	57.91	0
200/6	414	0.01162	6.624	53.32	67.06	111.2	(48.65 , 58.00)	111.2	0
200/3	414	0.03623	7.658	65.56	79.36	134.1	(60.02 , 71.11)	134.1	0
100/60	414	0.02161	10.93	57.88	88.87	202.4	(51.85 , 63.91)	335.2	6
100/30	414	0.02101	10.30	73.17	93.91	179.6	(66.71 , 79.64)	179.6	0
100/6	414	0.02455	17.13	121.7	157.9	251.8	(110.9 , 132.6)	251.8	0
100/3	414	0.03929	18.98	146.3	179.6	284.3	(133.9 , 158.7)	284.3	0
60/30	414	0.03904	13.40	76.60	108.4	223.1	(69.26 , 83.95)	313.7	1
60/6	414	0.04437	23.70	160.3	201.4	369.0	(146.6 , 174.1)	369.0	0
60/3	414	0.08326	25.51	189.8	233.0	408.4	(173.8 , 205.9)	408.4	0
30/6	414	0.02483	40.97	232.2	303.2	595.4	(211.9 , 252.5)	595.4	0
30/3	414	0.04343	37.56	271.4	343.1	612.5	(247.7 , 295.0)	612.5	0
6/3	414	0.36620	182.9	391.6	530.4	923.6	(364.7 , 418.5)	25970	6

Table C.7: Power Law: RMS values for various Fann speed combinations.

Fann Speeds	No. Sol's	Lower ext.	Lower q'tile	Med	Upper q'tile	Upper ext.	Median 95% conf. limits	Max. RMS	No. outs
600/300	414	5.5910	17.05	20.79	25.12	36.74	(20.17 , 21.41)	92.80	40
600/200	414	3.1710	13.77	17.30	20.86	31.32	(16.75 , 17.85)	70.68	31
600/100	414	0.4603	11.23	17.31	20.77	34.44	(16.57 , 18.05)	63.90	4
600/60	414	0.7607	15.01	28.33	33.70	60.66	(26.89 , 29.78)	78.84	3
600/30	414	1.8550	27.72	59.05	69.53	117.8	(55.82 , 62.28)	117.8	0
600/6	414	3.8840	86.59	204.5	241.7	361.3	(192.5 , 216.5)	361.3	0
600/3	413	3.8550	125.1	284.4	335.7	504.8	(268.1 , 300.7)	504.8	0
300/200	414	0.6462	14.64	22.49	27.41	44.87	(21.50 , 23.48)	83.68	5
300/100	414	0.6703	15.11	29.86	35.61	57.75	(28.28 , 31.45)	83.78	3
300/60	414	0.9605	16.30	38.63	45.71	86.78	(36.36 , 40.91)	86.78	0
300/30	414	1.6380	20.88	52.13	61.21	92.55	(49.01 , 55.25)	92.55	0
300/6	413	2.7950	43.14	92.43	109.7	166.6	(87.28 , 97.59)	166.6	0
300/3	410	2.7710	57.41	114.1	134.3	205.7	(108.1 , 120.1)	205.7	0
200/100	413	1.0530	23.48	53.46	63.12	99.94	(50.39 , 56.53)	99.94	0
200/60	414	2.0010	29.03	73.59	85.16	129.3	(69.24 , 77.93)	129.3	0
200/30	413	3.0480	38.44	91.92	106.0	156.1	(86.69 , 97.16)	156.1	0
200/6	413	4.2980	59.96	126.5	149.4	232.5	(119.6 , 133.4)	232.5	0
200/3	409	4.2610	71.63	142.1	164.6	259.1	(134.9 , 149.4)	259.1	0
100/60	413	5.3640	65.92	150.5	184.0	340.5	(141.3 , 159.6)	366.7	1
100/30	413	7.8650	83.70	177.9	208.2	310.5	(168.3 , 187.6)	310.5	0
100/6	409	10.840	125.6	225.8	266.4	409.6	(214.9 , 236.8)	409.6	0
100/3	394	10.700	145.2	243.4	283.4	438.6	(232.4 , 254.4)	438.6	0
60/30	412	11.170	115.8	209.1	248.8	376.0	(198.8 , 219.4)	376.0	0
60/6	401	17.470	174.4	279.0	327.1	532.0	(267.0 , 291.0)	532.0	0
60/3	353	17.080	197.1	290.9	340.1	514.8	(279.0 , 302.9)	566.6	1
30/6	319	26.680	225.4	329.9	391.3	617.8	(315.2 , 344.5)	735.5	1
30/3	156	25.300	193.1	262.8	331.8	520.0	(245.3 , 280.2)	616.2	4
6/3	100	100.30	279.7	368.1	458.5	625.9	(340.0 , 396.3)	625.9	0

Table C.8: Prandtl-Eyring: RMS values for various Fann speed combinations.

Fann Speeds	No. Sol's	Lower ext.	Lower q'tile	Med	Upper q'tile	Upper ext.	Median 95% conf. limits	Max. RMS	No. outs
600/300/200	387	0.10960	6.243	11.12	15.14	25.31	(10.41 , 11.83)	41.94	1
600/300/100	398	0.01778	4.196	8.036	10.55	19.74	(7.534 , 8.538)	19.74	0
600/300/60	397	0.01810	2.323	4.463	6.298	12.15	(4.149 , 4.777)	15.67	3
600/300/30	394	0.01370	1.630	2.837	4.072	7.713	(2.644 , 3.031)	9.567	10
600/300/6	209	0.04748	1.092	1.420	1.826	2.909	(1.340 , 1.500)	7.672	7
600/300/3	123	0.04286	1.486	1.901	2.716	4.111	(1.726 , 2.075)	6.845	3
600/200/100	395	0.05902	3.414	6.627	9.275	17.32	(6.163 , 7.091)	30.94	3
600/200/60	375	0.02912	1.493	2.901	4.613	9.200	(2.647 , 3.154)	11.70	10
600/200/30	373	0.02514	1.062	1.566	2.546	4.708	(1.445 , 1.687)	8.452	22
600/200/6	154	0.07306	0.495	0.696	0.997	1.655	(0.632 , 0.760)	4.360	6
600/200/3	110	0.06804	0.791	1.105	1.517	2.479	(0.996 , 1.214)	5.461	5
600/100/60	201	0.01788	0.955	1.406	2.891	5.428	(1.191 , 1.621)	11.32	21
600/100/30	232	0.02628	0.799	1.192	1.611	2.824	(1.108 , 1.276)	9.015	21
600/100/6	110	0.06400	0.563	0.804	1.026	1.646	(0.735 , 0.874)	8.010	4
600/100/3	108	0.05894	0.740	1.017	1.319	1.814	(0.930 , 1.105)	8.176	4
600/60/30	280	0.09560	1.059	1.494	2.228	3.973	(1.384 , 1.604)	15.63	20
600/60/6	112	0.11030	0.904	1.159	1.569	2.437	(1.060 , 1.258)	5.254	6
600/60/3	105	0.09954	1.161	1.515	1.963	3.164	(1.392 , 1.638)	5.930	4
600/30/6	107	0.10210	1.419	2.322	3.422	6.417	(2.017 , 2.627)	8.184	2
600/30/3	106	0.15790	2.191	3.191	4.419	7.599	(2.850 , 3.532)	9.616	3
600/6/3	100	0.30780	8.386	13.05	17.22	29.01	(11.65 , 14.44)	201.5	9
300/200/100	340	0.17400	3.944	6.895	9.854	18.47	(6.390 , 7.399)	71.66	7
300/200/60	278	0.09800	2.121	3.426	4.995	9.303	(3.154 , 3.697)	26.02	9
300/200/30	289	0.23130	1.593	2.544	3.694	6.502	(2.350 , 2.739)	20.43	19
300/200/6	119	0.19950	1.262	2.135	3.449	5.491	(1.819 , 2.451)	13.39	9
300/200/3	107	0.19890	1.750	2.735	4.190	7.843	(2.364 , 3.106)	13.59	5
300/100/60	163	0.01812	2.480	3.945	6.044	10.48	(3.506 , 4.385)	21.28	5
300/100/30	172	0.06150	2.347	3.302	4.716	8.235	(3.017 , 3.586)	20.57	10
300/100/6	108	0.21190	3.130	4.599	6.209	10.47	(4.133 , 5.066)	35.74	3
300/100/3	107	0.19180	3.888	5.487	7.184	11.64	(4.985 , 5.988)	36.09	2
300/60/30	264	0.32870	2.201	3.179	4.484	7.796	(2.958 , 3.400)	34.33	21
300/60/6	110	0.73360	4.193	5.863	7.977	11.68	(5.295 , 6.431)	23.55	2
300/60/3	104	0.58910	5.359	7.235	9.471	15.62	(6.600 , 7.870)	25.43	1
300/30/6	107	0.48780	6.375	9.351	12.77	19.71	(8.378 , 10.32)	29.24	3
300/30/3	106	0.26460	8.050	11.89	15.42	25.48	(10.76 , 13.02)	32.34	2
300/6/3	92	0.45350	16.86	28.40	36.28	64.05	(25.21 , 31.59)	147.8	1
200/100/60	149	0.31040	3.038	7.452	13.44	28.55	(6.111 , 8.793)	64.65	8
200/100/30	155	0.25320	2.844	6.379	12.94	24.51	(5.102 , 7.655)	93.10	5
200/100/6	107	0.29920	6.372	11.83	19.56	38.24	(9.822 , 13.84)	160.2	4
200/100/3	106	0.42870	8.432	13.82	21.64	40.73	(11.80 , 15.84)	160.0	4
200/60/30	257	0.30130	2.437	3.963	9.180	19.07	(3.301 , 4.626)	127.0	26
200/60/6	111	0.44510	8.514	14.65	20.76	34.22	(12.82 , 16.48)	79.62	10
200/60/3	102	0.55660	12.68	18.56	25.62	42.87	(16.54 , 20.57)	84.33	8
200/30/6	107	0.28220	12.76	23.14	35.17	64.22	(19.73 , 26.55)	90.65	3
200/30/3	106	1.44900	18.25	31.39	45.21	84.27	(27.27 , 35.51)	99.01	2
200/6/3	84	0.31102	45.91	69.10	100.7	181.1	(59.68 , 78.51)	201.4	1
100/60/30	279	0.36980	16.47	34.11	132.3	305.7	(23.20 , 45.02)	385.5	8
100/60/6	124	0.55560	12.88	32.85	72.61	158.7	(24.40 , 41.29)	492.6	9
100/60/3	110	0.66090	17.49	42.82	76.93	164.0	(33.90 , 51.74)	480.6	11
100/30/6	107	0.24640	23.55	54.33	112.5	219.4	(40.80 , 67.86)	289.0	3
100/30/3	106	0.44530	41.98	77.32	138.7	269.0	(62.53 , 92.11)	334.0	2
100/6/3	82	1.76000	133.6	247.1	358.2	624.4	(208.1 , 286.1)	726.7	2
60/30/6	106	0.61490	40.60	135.2	267.8	571.2	(100.4 , 169.9)	749.1	3
60/30/3	105	0.79820	80.95	172.2	334.3	697.0	(133.3 , 211.2)	795.8	3
60/6/3	73	4.72040	276.0	660.4	810.6	1513	(561.9 , 758.8)	1513	0
30/6/3	69	3.36000	302.7	1508	1776	3104	(1229 , 1787)	3104	0

Table C.9: Reiner-Philippoff: RMS values for various Fann speed combinations.

Fann Speeds	No. Sol's	Lower ext.	Lower q'tile	Med	Upper q'tile	Upper ext.	Median 95% conf. limits	Max. RMS	No. outs
600/300/200	409	0.00530	1.0560	3.6780	10.59	24.84	(2.936 , 4.420)	110.3	43
600/300/100	413	0.01428	0.4409	0.9634	2.125	4.451	(0.833 , 1.094)	31.68	40
600/300/60	414	0.01238	0.6721	1.3780	2.310	4.726	(1.251 , 1.505)	14.87	23
600/300/30	414	0.00554	0.3708	0.6768	1.013	1.960	(0.627 , 0.726)	4.623	20
600/300/6	414	0.01002	0.1868	0.3962	0.607	1.215	(0.364 , 0.429)	4.177	20
600/300/3	414	0.00720	0.2260	0.5109	0.838	1.736	(0.464 , 0.558)	6.554	14
600/200/100	413	0.01878	0.4777	1.0840	2.302	4.997	(0.942 , 1.225)	50.84	35
600/200/60	413	0.01442	0.7611	1.4380	2.583	5.293	(1.296 , 1.579)	15.15	19
600/200/30	414	0.00552	0.3201	0.6508	1.031	2.084	(0.596 , 0.706)	4.556	14
600/200/6	414	0.00722	0.1592	0.3312	0.538	1.095	(0.302 , 0.361)	2.839	10
600/200/3	414	0.00730	0.1969	0.4067	0.683	1.407	(0.369 , 0.444)	5.912	10
600/100/60	403	0.01628	0.9778	2.0910	4.272	9.074	(1.833 , 2.349)	21.75	15
600/100/30	414	0.00856	0.3433	0.6396	1.018	1.978	(0.587 , 0.692)	9.497	20
600/100/6	414	0.01092	0.1463	0.2941	0.438	0.871	(0.271 , 0.317)	4.324	17
600/100/3	414	0.00782	0.1662	0.3449	0.546	1.106	(0.316 , 0.374)	4.840	14
600/60/30	413	0.01020	0.4817	0.8752	1.483	2.984	(0.798 , 0.953)	26.80	23
600/60/6	414	0.00896	0.2426	0.7190	1.423	3.194	(0.628 , 0.810)	10.70	11
600/60/3	414	0.00834	0.2458	0.8792	1.613	3.533	(0.773 , 0.985)	11.07	12
600/30/6	414	0.00800	0.4196	1.3920	2.703	5.718	(1.215 , 1.568)	9.303	4
600/30/3	414	0.00836	0.4628	1.7380	3.099	6.502	(1.534 , 1.942)	11.69	4
600/6/3	414	0.01008	1.1150	2.8770	7.641	17.34	(2.372 , 3.381)	87.69	90
300/200/100	403	0.04102	1.1270	2.6210	6.456	14.42	(2.203 , 3.039)	100.6	37
300/200/60	410	0.02694	1.2730	2.4650	4.845	10.18	(2.188 , 2.743)	36.81	30
300/200/30	412	0.00550	0.6556	1.1860	2.128	4.222	(1.072 , 1.300)	24.54	41
300/200/6	414	0.01256	0.3539	0.6870	1.344	2.782	(0.610 , 0.764)	23.79	34
300/200/3	414	0.00804	0.4171	0.7946	1.465	3.023	(0.715 , 0.876)	24.51	30
300/100/60	371	0.01672	1.3460	3.2080	6.496	14.08	(2.787 , 3.629)	35.32	21
300/100/30	414	0.02386	0.5341	0.9431	1.527	2.989	(0.866 , 1.020)	31.14	29
300/100/6	414	0.01468	0.2686	0.6022	1.252	2.556	(0.526 , 0.678)	15.73	24
300/100/3	414	0.00976	0.3041	0.7356	1.443	3.144	(0.647 , 0.824)	18.28	19
300/60/30	413	0.01234	0.8329	1.8980	3.717	7.992	(1.675 , 2.122)	53.60	28
300/60/6	414	0.01396	0.4458	2.1110	4.205	9.803	(1.821 , 2.402)	25.32	9
300/60/3	414	0.01284	0.4489	2.4410	4.713	11.03	(2.111 , 2.771)	27.55	7
300/30/6	414	0.01048	0.7290	3.5170	6.100	13.63	(3.101 , 3.932)	36.26	8
300/30/3	414	0.01100	0.8170	3.8510	6.716	13.34	(3.395 , 4.308)	27.26	6
300/6/3	414	0.01522	1.7140	5.1660	11.31	25.48	(4.423 , 5.909)	62.71	62
200/100/60	332	0.02008	2.3530	5.7920	12.74	27.98	(4.895 , 6.689)	128.0	37
200/100/30	411	0.02632	0.9828	1.8610	4.313	9.298	(1.602 , 2.119)	57.90	40
200/100/6	414	0.02424	0.5431	1.6780	4.157	9.251	(1.399 , 1.958)	87.77	21
200/100/3	414	0.01896	0.6068	1.9770	4.533	10.16	(1.674 , 2.281)	77.10	22
200/60/30	413	0.01610	1.8120	5.4250	14.02	31.21	(4.479 , 6.371)	108.3	15
200/60/6	414	0.01548	1.5210	6.7870	13.66	30.26	(5.848 , 7.726)	63.96	10
200/60/3	414	0.01646	1.5440	7.8160	14.79	34.41	(6.792 , 8.841)	62.61	8
200/30/6	411	0.00770	1.9110	9.1090	17.76	38.32	(7.878 , 10.34)	82.91	4
200/30/3	414	0.00818	2.2800	10.940	18.85	41.36	(9.662 , 12.23)	46.70	1
200/6/3	414	0.01460	3.4260	13.170	32.63	75.71	(10.91 , 15.43)	105.4	5
100/60/30	400	0.43830	15.780	46.100	106.3	232.0	(38.97 , 53.22)	475.3	12
100/60/6	412	0.04026	8.8250	37.110	79.91	181.1	(31.59 , 42.62)	415.7	12
100/60/3	413	0.02634	9.1940	40.160	80.21	178.8	(34.66 , 45.66)	404.3	11
100/30/6	407	0.03046	6.3820	34.610	62.58	146.6	(30.22 , 38.99)	183.1	4
100/30/3	412	0.02002	6.8040	39.650	65.26	147.1	(35.12 , 44.18)	214.4	3
100/6/3	414	0.01116	10.360	33.640	107.4	229.9	(26.14 , 41.15)	258.8	1
60/30/6	391	0.02986	8.5020	20.990	73.47	160.3	(15.82 , 26.17)	626.4	20
60/30/3	408	0.01870	7.1490	21.820	72.76	164.0	(16.70 , 26.93)	1947	23
60/6/3	414	0.05766	7.3870	35.470	150.3	356.0	(24.42 , 46.53)	2116	2
30/6/3	409	0.17550	7.0320	86.980	351.8	659.0	(60.14 , 113.8)	6759	5

Table C.10: Robertson-Stiff: RMS values for various Fann speed combinations.

Fann Speeds	No. Sol's	Lower ext.	Lower q'tile	Med	Upper q'tile	Upper ext.	Median 95% conf. limits	Max. RMS	No. outs
600/300/200	414	0.02052	0.9153	3.4670	8.052	18.60	(2.915 , 4.019)	23380	27
600/300/100	414	0.01488	0.2147	0.7543	2.178	5.011	(0.602 , 0.906)	78.82	23
600/300/60	414	0.01018	0.1176	0.2461	0.613	1.356	(0.208 , 0.285)	34.15	50
600/300/30	414	0.00996	0.0849	0.1992	0.442	0.958	(0.172 , 0.227)	3.840	39
600/300/6	414	0.00996	0.0714	0.1589	0.309	0.646	(0.141 , 0.177)	3.129	35
600/300/3	414	0.01036	0.0884	0.1902	0.377	0.809	(0.168 , 0.213)	3.669	35
600/200/100	414	0.02098	0.2103	0.6201	1.905	4.428	(0.489 , 0.751)	83.05	28
600/200/60	414	0.01270	0.1011	0.2259	0.648	1.379	(0.184 , 0.268)	20.72	49
600/200/30	414	0.00912	0.0708	0.1484	0.332	0.714	(0.128 , 0.169)	3.285	44
600/200/6	414	0.01394	0.0630	0.1082	0.199	0.401	(0.098 , 0.119)	2.287	32
600/200/3	414	0.00824	0.0655	0.1160	0.213	0.431	(0.105 , 0.127)	2.992	43
600/100/60	413	0.01610	0.2436	0.8786	3.669	8.758	(0.613 , 1.144)	572.6	50
600/100/30	414	0.01440	0.0983	0.2156	0.399	0.836	(0.192 , 0.239)	7.909	42
600/100/6	414	0.01528	0.0708	0.1254	0.237	0.476	(0.113 , 0.138)	5.363	33
600/100/3	414	0.01500	0.0716	0.1347	0.250	0.505	(0.121 , 0.149)	5.403	34
600/60/30	414	0.00926	0.1667	0.4094	0.914	2.033	(0.352 , 0.467)	204.4	25
600/60/6	414	0.00966	0.0758	0.1496	0.282	0.578	(0.134 , 0.166)	4.592	32
600/60/3	414	0.00826	0.0794	0.1377	0.257	0.523	(0.124 , 0.151)	4.084	40
600/30/6	414	0.00996	0.0967	0.1863	0.512	1.085	(0.154 , 0.218)	3.938	40
600/30/3	414	0.00796	0.0988	0.1967	0.438	0.932	(0.171 , 0.223)	6.487	47
600/6/3	409	0.03342	0.8252	1.6750	3.189	6.722	(1.491 , 1.859)	1995	35
300/200/100	414	0.02470	0.9540	2.8980	5.225	11.15	(2.568 , 3.229)	97490	59
300/200/60	414	0.02438	0.4109	1.2910	3.486	7.955	(1.053 , 1.529)	1482	50
300/200/30	414	0.01750	0.2782	0.6497	1.635	3.654	(0.545 , 0.755)	55.72	40
300/200/6	414	0.01844	0.1999	0.5085	1.241	2.792	(0.428 , 0.589)	14.97	32
300/200/3	414	0.02118	0.2038	0.5122	1.257	2.787	(0.431 , 0.594)	14.91	31
300/100/60	413	0.01886	0.9008	2.7590	9.238	21.60	(2.113 , 3.404)	2613	54
300/100/30	414	0.02122	0.2380	0.6423	1.305	2.886	(0.560 , 0.725)	32.87	31
300/100/6	414	0.02212	0.1488	0.4247	0.882	1.950	(0.368 , 0.481)	19.23	28
300/100/3	414	0.01882	0.1663	0.4693	0.916	1.990	(0.411 , 0.527)	18.95	30
300/60/30	414	0.00964	0.3692	0.8302	1.806	3.941	(0.719 , 0.941)	966.7	41
300/60/6	414	0.00986	0.1434	0.2877	0.674	1.450	(0.247 , 0.329)	10.69	38
300/60/3	414	0.01032	0.1628	0.3049	0.669	1.324	(0.266 , 0.344)	17.12	46
300/30/6	414	0.00996	0.1739	0.3726	1.081	2.421	(0.303 , 0.443)	27.13	47
300/30/3	414	0.01168	0.1949	0.4769	0.983	2.021	(0.416 , 0.538)	47.64	50
300/6/3	408	0.03818	1.1810	2.4030	4.797	10.19	(2.122 , 2.685)	102.2	40
200/100/60	413	0.04478	2.3340	7.7660	25.72	60.10	(5.955 , 9.577)	99510	60
200/100/30	414	0.03230	0.5394	1.4700	3.800	8.615	(1.218 , 1.722)	192.3	43
200/100/6	414	0.02022	0.3001	0.9424	2.556	5.912	(0.768 , 1.117)	116.1	34
200/100/3	414	0.02298	0.3135	0.9327	2.406	5.544	(0.771 , 1.095)	112.3	38
200/60/30	414	0.01694	0.6993	2.1520	6.130	14.07	(1.732 , 2.572)	6350	40
200/60/6	414	0.02400	0.2426	0.7543	2.128	4.949	(0.608 , 0.900)	38.87	34
200/60/3	414	0.01514	0.2186	0.6297	1.678	3.855	(0.517 , 0.743)	42.42	44
200/30/6	414	0.02294	0.2968	0.9503	2.745	6.404	(0.761 , 1.140)	73.61	46
200/30/3	413	0.01648	0.2395	0.8573	2.529	5.864	(0.680 , 1.035)	108.8	35
200/6/3	408	0.05202	2.1560	5.4550	11.42	24.71	(4.733 , 6.177)	287.6	42
100/60/30	391	0.12370	6.0870	48.770	129.9	314.4	(38.91 , 58.62)	929.8	30
100/60/6	409	0.06216	2.6220	11.880	38.98	91.86	(9.052 , 14.71)	511.2	26
100/60/3	410	0.01572	1.9400	8.1930	29.45	70.22	(6.055 , 10.33)	829.2	27
100/30/6	412	0.03020	1.0870	4.5800	14.09	32.99	(3.571 , 5.588)	324.4	45
100/30/3	410	0.03392	0.8328	3.0530	9.724	23.03	(2.362 , 3.744)	210.2	39
100/6/3	404	0.06914	9.3660	22.600	44.20	96.17	(19.87 , 25.33)	541.4	38
60/30/6	404	0.01214	5.4490	27.020	69.13	163.3	(22.03 , 32.01)	1119	32
60/30/3	407	0.01574	5.6980	25.000	62.06	145.1	(20.61 , 29.40)	973.4	29
60/6/3	402	0.08498	27.340	74.560	139.5	306.1	(65.76 , 83.36)	801.0	26
30/6/3	384	0.09054	98.240	251.40	465.5	985.7	(221.9 , 280.9)	2355	19

Table C.11: Sisko: RMS values for various Fann speed combinations.

Appendix D

Box-and-Whisker Plots

Box-and-whisker plots (often referred to as simply 'boxplots') provide a visual impression of the empirical distribution of a data batch; the location, spread, skewness, tail length and outlying data points being easily identified. By arranging box-and-whisker plots for different data batches in parallel, it is possible to compare them with respect to location, spread, skewness and tail heaviness.

In order to construct the box-and-whisker plots presented in this work it was necessary to calculate the median and the lower- and upper-quartiles (Q_L and Q_U respectively). These are the three values that divide the ordered data batch into four groups of equal size. The inter-quartile range was then calculated ($IQ = Q_U - Q_L$), and from this the outlier cut-offs were determined from $Q_L - 1.5 \times IQ$ and $Q_U + 1.5 \times IQ$. Points outside of these cut-offs are considered to be outliers. The box is drawn with ends at the lower- and upper-quartiles and a crossbar at the median. A line is drawn from each box to the most remote point that is not an outlier (plot 'whiskers'). Finally, outliers are individually marked.

The median shows the location of the batch. The length (height) of the box shows the spread. The relative position of the median to the quartiles indicates skewness. The tail length is indicated by the lines and outliers. The number of observations in each data batch used to construct each individual box-and-whisker plot is reflected in the width of that box. If all plots were constructed from the same size of data batch (for example 414 in the analysis in sections 2.3 and 2.4) then all boxes would have the same width. Plots constructed from a smaller data batch will have their box widths correspondingly narrowed. With respect to the information presented in this work, one would prefer a model whose box-and-whisker plot indicates that the RMS values have a distribution that is located close to zero, has a small spread, is positively skewed (i.e., the median closer to the lower-quartile), has a short upper tail, and few large valued outliers.

Appendix E

Flow Regime Transition Data & Results

		Mud 'A'	Mud 'B'
Mud Density [kg/m^3]		1066.4	1036.5
$\dot{\gamma}_3/\tau_3$	$[s^{-1}]/[\mathrm{Pa}]$	5.1/ 0.958	5.1/ 9.819
$\dot{\gamma}_6/\tau_6$	$[s^{-1}]/[\mathrm{Pa}]$	10.2/ 1.437	10.2/11.016
$\dot{\gamma}_{100}/\tau_{100}$	$[s^{-1}]/[\mathrm{Pa}]$	170.3/ 6.226	170.3/15.327
$\dot{\gamma}_{200}/\tau_{200}$	$[s^{-1}]/[\mathrm{Pa}]$	340.7/10.537	340.7/17.961
$\dot{\gamma}_{300}/\tau_{300}$	$[s^{-1}]/[\mathrm{Pa}]$	511.0/13.890	511.0/20.835
$\dot{\gamma}_{600}/\tau_{600}$	$[s^{-1}]/[\mathrm{Pa}]$	1022.0/22.990	1022.0/26.104
Bingham Plastic:	$\tau_\circ$	1.94484	11.5244
	μ_∞	0.02155	0.01550
Casson:	$\tau_\circ$	0.84005	9.37423
	μ_∞	0.01497	4.177×10^{-3}
Collins-Graves:	$\tau_\circ$	3.55824	13.2578
	k	0.01928	0.01306
	β	0.05039	0.22715
Ellis *et al.*:	α	1.41257	5.25857
	ϕ_0	0.00000	5.49×10^{-8}
	ϕ_1	12.2674	5.54×10^{-5}
Herschel-Bulkley:	$\tau_\circ$	0.62201	9.43084
	k	0.11934	0.29647
	m	0.75534	0.58176
Hyperbolic:	a	2625.62	1923.28
	b	30.5556	14.7333
	τ_{cp}	-8.46613	9.07684
	$\dot{\gamma}_{cp}$	-2745.89	-1923.28
Power Law:	k	0.16953	6.44784
	n	0.70793	0.19017
Reiner-Philippoff:	τ_s	0.17235	1903.83
	$\mu_\circ$	2.65916	0.10140
	μ_∞	0.02684	0.00000
Robertson-Stiff:	$\dot{\gamma}_\circ$	10.6763	86.5450
	A	0.13841	1.91870
	B	0.73679	0.37222
Sisko:	a	0.01271	0.00940
	b	0.40278	8.49260
	c	0.46432	0.09701

Diameters of conduits used in the study		
Nominal Diameter [inches]	Internal Diameter [m]	External Diameter [m]
3″	0.0773913	n/a
2″	0.0515950	0.0607212
$1\frac{1}{2}$″	n/a	0.0482194
1″	0.0259944	0.0333375

Table E.1: Fluid data (per Okafor, 1982) and nonlinear least squares rheological model parameters for muds 'A' and 'B' flowing in PVC tubes.

Model	Fixed				N-criteria			
	$(Q_{cr})_L$	$\epsilon\%$	$(Q_{cr})_U$	$\epsilon\%$	$(Q_{cr})_L$	$\epsilon\%$	$(Q_{cr})_U$	$\epsilon\%$
Bi-Pl	63.98	23.03	88.35	10.44	69.84	34.31	94.21	17.76
Casson	68.10	30.96	94.04	17.55	78.73	51.41	104.68	30.85
Co-Gr	72.96	40.31	100.75	25.94	84.44	62.38	112.23	40.29
Ellis	79.16	52.23	109.32	36.65	94.24	81.23	124.40	55.50
He-Bu	69.83	34.29	96.43	20.54	82.41	58.47	109.01	36.27
Hyper	70.04	34.69	96.72	20.90	82.88	59.39	109.57	36.96
P-Law	70.51	35.60	97.37	21.71	83.94	61.42	110.80	38.50
Re-Ph	56.23	8.13	77.64	-2.94	58.20	11.91	79.61	-0.48
Ro-St	69.94	34.49	96.58	20.72	82.56	58.77	109.20	36.51
Sisko	69.55	33.76	96.05	20.06	82.01	57.72	108.51	35.64

	N	$D_{\text{eff,G}}$	**Correlation:** Eqs.(3.18 & 3.19)					
	[-]	[m]	$(Q_{cr})_L$	$\epsilon\%$	$(Q_{cr})_M$	$\epsilon\%$	$(Q_{cr})_U$	$\epsilon\%$
Bi-Pl	0.859219	0.02458	108.99	109.60	129.37	99.03	169.82	112.28
Casson	0.760988	0.02380	73.93	42.18	94.34	45.14	119.59	49.49
Co-Gr	0.758934	0.02332	78.03	50.05	100.04	53.91	126.93	58.66
Ellis	0.707930	0.02196	67.01	28.86	90.16	38.71	110.90	38.62
He-Bu	0.724183	0.02364	63.39	21.90	83.65	28.70	103.72	29.65
Hyper	0.719188	0.02370	62.01	19.25	82.21	26.48	101.56	26.95
P-Law	0.707927	0.02357	59.01	13.48	79.16	21.78	97.01	21.26
Re-Ph	0.946134	0.02535	137.59	164.60	156.01	140.02	207.36	159.20
Ro-St	0.723301	0.02364	63.20	21.54	83.47	28.42	103.43	29.29
Sisko	0.725450	0.02352	63.53	22.17	83.78	28.88	104.00	30.00

Table E.2: Critical volumetric flowrates (in lpm) calculated for mud type 'A' in a 1″ pipe (nominal). Mud density: 1066.4 kg/m^3. Pipe internal diameter: 0.0259944 m. Observed critical flowrates: $(Q_{cr})_L = 52$, $(Q_{cr})_M = 65$ and $(Q_{cr})_U = 80$ lpm.

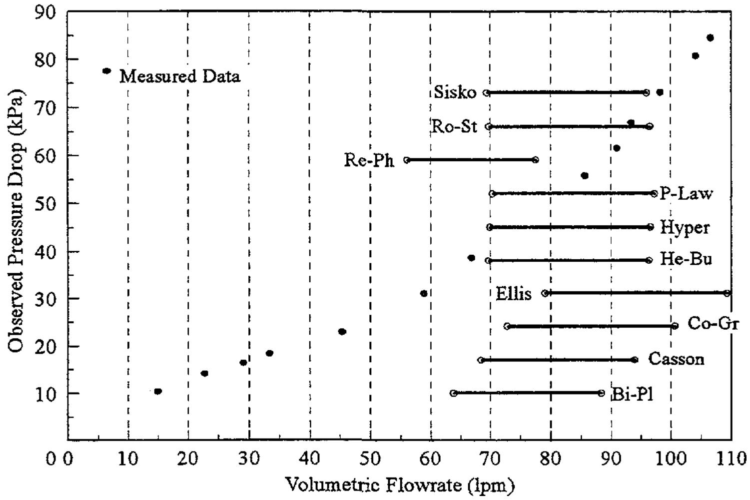

Figure E.1: Mud 'A', 1″ pipe: Fixed-transition results.

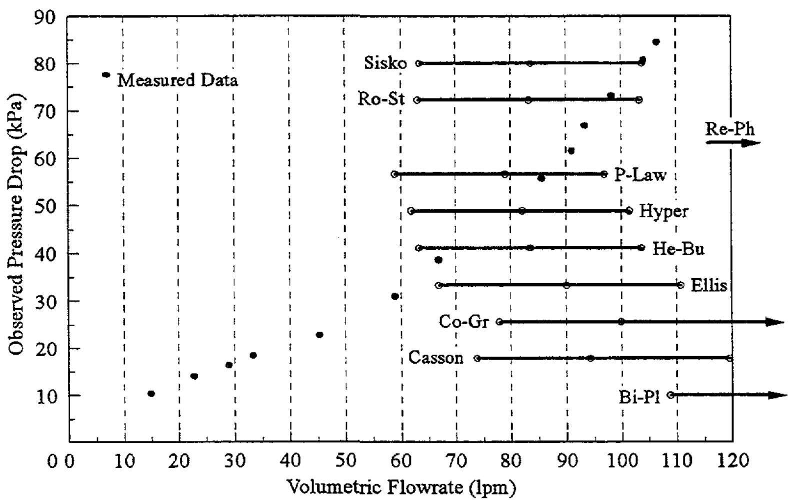

Figure E.2: Mud 'A', 1″ pipe: Correlation-transition results.

Model	Fixed				N-criteria			
	$(Q_{cr})_L$	$\epsilon\%$	$(Q_{cr})_U$	$\epsilon\%$	$(Q_{cr})_L$	$\epsilon\%$	$(Q_{cr})_U$	$\epsilon\%$
Bi-Pl	78.52	-14.65	108.43	10.65	98.43	6.99	128.35	30.97
Casson	77.63	-15.62	107.20	9.39	106.25	15.49	135.82	38.60
Co-Gr	83.41	-9.34	115.18	17.53	107.73	17.09	139.50	42.35
Ellis	76.84	-16.48	106.11	8.28	117.47	27.68	146.75	49.74
He-Bu	77.30	-15.98	106.74	8.92	107.88	17.26	137.34	40.14
Hyper	77.38	-15.89	106.86	9.04	105.98	15.19	135.46	38.22
P-Law	71.89	-21.86	99.27	1.30	109.88	19.44	137.27	40.07
Re-Ph	152.95	66.25	211.22	115.53	152.97	66.28	211.24	115.56
Ro-St	77.19	-16.10	106.59	8.77	109.90	19.46	139.31	42.16
Sisko	77.56	-15.70	107.10	9.29	104.12	13.17	133.67	36.40

	N	$D_{\text{eff},G}$	Correlation: Eqs.(3.18 & 3.19)					
	[-]	[m]	$(Q_{cr})_L$	$\epsilon\%$	$(Q_{cr})_M$	$\epsilon\%$	$(Q_{cr})_U$	$\epsilon\%$
Bi-Pl	0.611590	0.02082	45.00	-51.09	65.01	-31.57	72.34	-23.86
Casson	0.434710	0.01837	41.84	-54.52	56.39	-40.64	51.98	-45.28
Co-Gr	0.553146	0.01960	43.83	-52.36	63.42	-33.24	65.47	-31.08
Ellis	0.190166	0.01258	89.96	-2.21	95.88	0.93	99.50	4.74
He-Bu	0.393931	0.01783	45.59	-50.45	58.74	-38.17	53.72	-43.46
Hyper	0.433722	0.01823	42.33	-53.99	56.80	-40.21	52.41	-44.83
P-Law	0.190167	0.01265	83.92	-8.78	89.47	-5.83	92.84	-2.27
Re-Ph	0.999830	0.02602	450.32	389.48	498.98	425.25	663.85	598.78
Ro-St	0.350706	0.01727	51.07	-44.48	62.76	-33.94	57.91	-39.04
Sisko	0.475252	0.01866	40.39	-56.10	56.23	-40.81	53.28	-43.92

Table E.3: Critical volumetric flowrates (in lpm) calculated for mud type 'B' in a 1″ pipe (nominal). Mud density: 1036.5 kg/m^3. Pipe internal diameter: 0.0259944 m. Observed critical flowrates: $(Q_{cr})_L = 92$, $(Q_{cr})_M = 95$ and $(Q_{cr})_U = 98$ lpm.

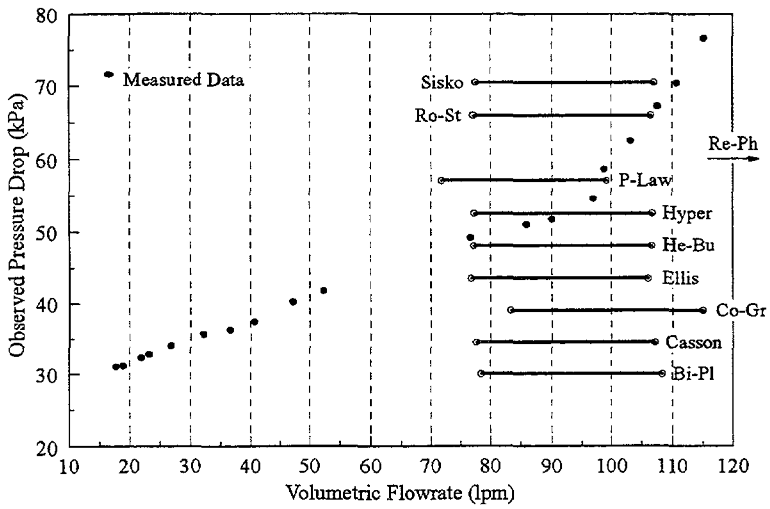

Figure E.3: Mud 'B', 1″ pipe: Fixed-transition results.

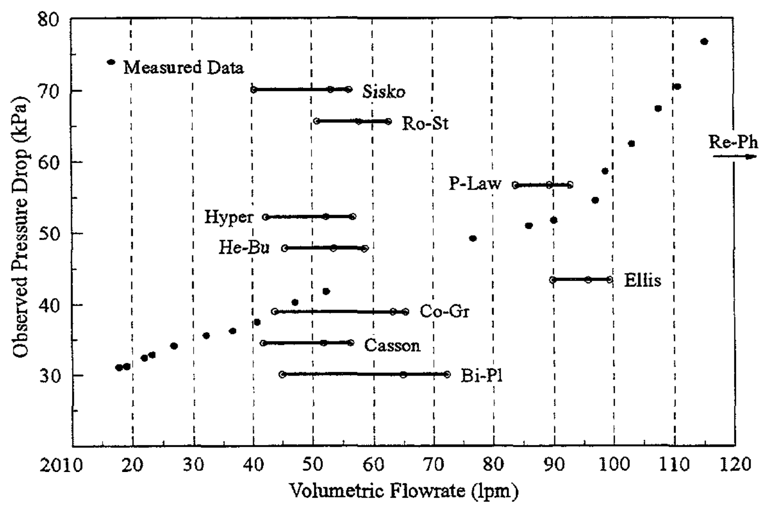

Figure E.4: Mud 'B', 1″ pipe: Correlation-transition results.

Model	Fixed				N-criteria			
	$(Q_{cr})_L$	$\epsilon\%$	$(Q_{cr})_U$	$\epsilon\%$	$(Q_{cr})_L$	$\epsilon\%$	$(Q_{cr})_U$	$\epsilon\%$
Bi-Pl	129.43	-15.41	178.74	2.14	142.26	-7.02	191.56	9.46
Casson	138.83	-9.26	191.72	9.55	161.25	5.39	214.13	22.36
Co-Gr	149.40	-2.35	206.32	17.90	174.49	14.05	231.40	32.23
Ellis	153.77	0.50	212.34	21.34	183.08	19.66	241.66	38.09
He-Bu	142.53	-6.84	196.83	12.47	168.39	10.06	222.69	27.25
Hyper	142.85	-6.63	197.27	12.73	168.94	10.42	223.36	27.63
P-Law	144.00	-5.88	198.86	13.63	171.45	12.06	226.30	29.32
Re-Ph	112.68	-26.35	155.61	-11.08	117.35	-23.30	160.28	-8.41
Ro-St	142.70	-6.73	197.07	12.61	168.60	10.20	222.97	27.41
Sisko	142.23	-7.04	196.42	12.24	168.34	10.02	222.52	27.16

	N	$D_{\text{eff,G}}$	Correlation: Eqs.(3.18 & 3.19)					
	[-]	[m]	$(Q_{cr})_L$	$\epsilon\%$	$(Q_{cr})_M$	$\epsilon\%$	$(Q_{cr})_U$	$\epsilon\%$
Bi-Pl	0.847710	0.04851	358.31	134.19	375.24	133.07	432.16	146.95
Casson	0.752362	0.04705	174.26	13.90	198.74	23.44	228.67	30.67
Co-Gr	0.742417	0.04586	166.91	9.09	194.56	20.85	224.63	28.36
Ellis	0.707930	0.04678	107.46	-29.76	136.54	-15.19	156.16	-10.76
He-Bu	0.721933	0.04686	123.36	-19.37	149.79	-6.96	171.75	-1.86
Hyper	0.719862	0.04706	119.97	-21.59	146.40	-9.07	167.67	-4.19
P-Law	0.707927	0.04678	100.63	-34.23	127.86	-20.58	146.24	-16.44
Re-Ph	0.936758	0.05011	521.93	241.13	529.43	228.84	607.99	247.42
Ro-St	0.721957	0.04689	123.55	-19.25	150.00	-6.83	171.97	-1.73
Sisko	0.718747	0.04651	117.73	-23.05	144.44	-10.29	165.74	-5.29

Table E.4: Critical volumetric flowrates (in lpm) calculated for mud type 'A' in a 2″ pipe (nominal). Mud density: 1066.4 kg/m^3. Pipe internal diameter: 0.051595 m. Observed critical flowrates: $(Q_{cr})_L = 153$, $(Q_{cr})_M = 161$ and $(Q_{cr})_U = 175$ lpm.

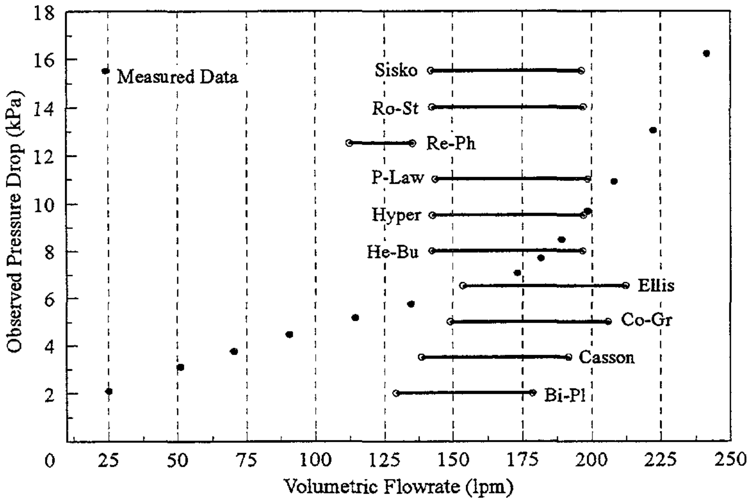

Figure E.5: Mud ‘A’, 2″ pipe: Fixed-transition results.

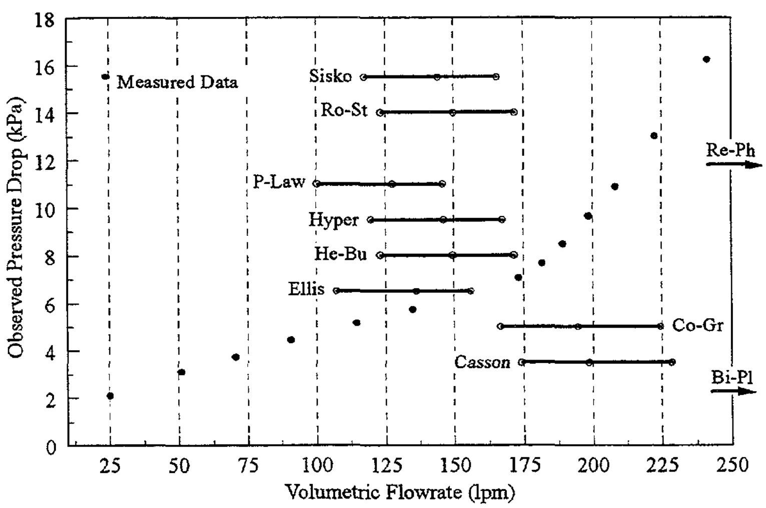

Figure E.6: Mud ‘A’, 2″ pipe: Correlation-transition results.

Model	Fixed				N-criteria			
	$(Q_{cr})_L$	$\epsilon\%$	$(Q_{cr})_U$	$\epsilon\%$	$(Q_{cr})_L$	$\epsilon\%$	$(Q_{cr})_U$	$\epsilon\%$
Bi-Pl	206.03	47.17	284.52	22.64	271.34	93.81	349.82	50.79
Casson	213.69	52.63	295.09	27.19	299.73	114.09	381.13	64.28
Co-Gr	225.68	61.20	311.65	34.33	305.88	118.49	391.85	68.90
Ellis	229.41	63.86	316.80	36.55	350.61	150.44	438.01	88.80
He-Bu	214.54	53.24	296.26	27.70	304.19	117.28	385.92	66.35
Hyper	213.87	52.76	295.34	27.30	301.24	115.17	382.72	64.97
P-Law	214.81	53.44	296.65	27.87	328.38	134.56	410.23	76.82
Re-Ph	303.69	116.92	419.38	80.77	303.70	116.93	419.40	80.77
Ro-St	215.59	53.99	297.72	28.33	308.54	120.39	390.67	68.39
Sisko	213.30	52.36	294.56	26.96	297.06	112.18	378.31	63.06

	N	$D_{\text{eff},G}$	**Correlation:** Eqs.(3.18 & 3.19)					
	[-]	[m]	$(Q_{cr})_L$	$\epsilon\%$	$(Q_{cr})_M$	$\epsilon\%$	$(Q_{cr})_U$	$\epsilon\%$
Bi-Pl	0.514061	0.03718	206.02	47.16	206.02	11.36	284.51	22.63
Casson	0.382657	0.03392	213.67	52.62	213.67	15.50	295.07	27.19
Co-Gr	0.455167	0.03451	225.67	61.19	225.67	21.98	311.64	34.33
Ellis	0.190166	0.02488	142.92	2.09	164.39	-11.14	171.70	-25.99
He-Bu	0.359590	0.03341	214.55	53.25	214.55	15.97	296.29	27.71
Hyper	0.373989	0.03353	213.89	52.78	213.89	15.62	295.37	27.32
P-Law	0.190167	0.02490	133.69	-4.51	153.80	-16.87	160.63	-30.76
Re-Ph	0.999938	0.05162	1907.66	1262.61	1908.62	931.68	2183.59	841.20
Ro-St	0.339008	0.03311	215.58	53.99	215.58	16.53	297.71	28.32
Sisko	0.397885	0.03362	213.28	52.34	213.28	15.29	294.53	26.95

Table E.5: Critical volumetric flowrates (in lpm) calculated for mud type 'B' in a 2″ pipe (nominal). Mud density: 1036.5 kg/m^3. Pipe internal diameter: 0.051595 m. Observed critical flowrates: $(Q_{cr})_L = 140$, $(Q_{cr})_M = 185$ and $(Q_{cr})_U = 232$ lpm.

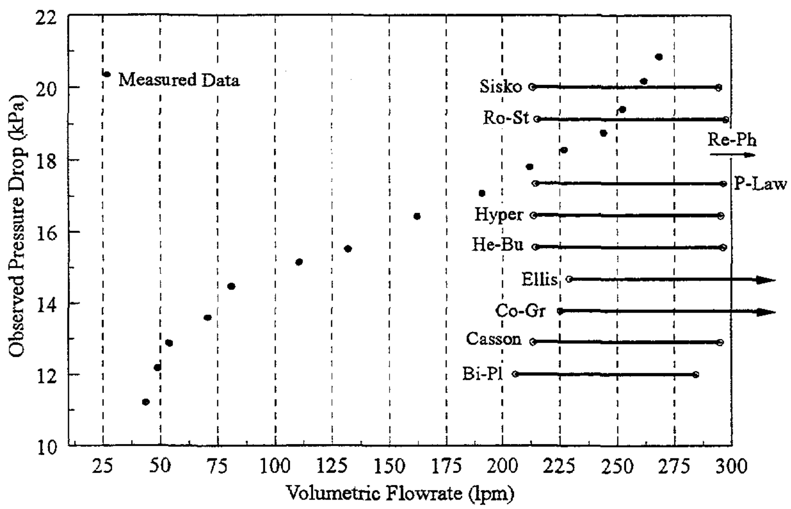

Figure E.7: Mud 'B', 2″ pipe: Fixed-transition results.

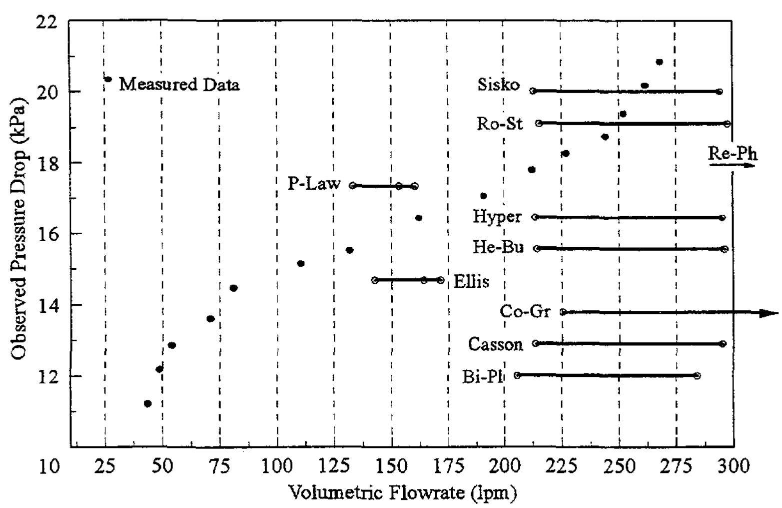

Figure E.8: Mud 'B', 2″ pipe: Correlation-transition results.

Model	Fixed				N-criteria			
	$(Q_{cr})_L$	ϵ%	$(Q_{cr})_U$	ϵ%	$(Q_{cr})_L$	ϵ%	$(Q_{cr})_U$	ϵ%
Bi-Pl	213.71	22.12	295.13	34.15	242.60	38.63	324.00	47.27
Casson	235.35	34.49	325.01	47.73	279.16	59.52	368.82	67.65
Co-Gr	260.75	49.00	360.08	63.67	317.14	81.22	416.46	89.30
Ellis	259.64	48.36	358.54	62.97	309.12	76.64	408.03	85.47
He-Bu	240.78	37.59	332.50	51.14	286.16	63.52	377.88	71.76
Hyper	239.77	37.01	331.11	50.50	283.01	61.72	374.36	70.16
P-Law	243.14	38.94	335.76	52.62	289.49	65.42	382.12	73.69
Re-Ph	178.92	2.24	247.07	12.31	192.40	9.95	260.55	18.43
Ro-St	240.65	37.51	332.32	51.06	285.46	63.12	377.15	71.43
Sisko	242.70	38.69	335.16	52.34	291.66	66.66	384.13	74.60

	N	$D_{\text{eff},G}$	Correlation: Eqs.(3.18 & 3.19)					
	[-]	[m]	$(Q_{cr})_L$	ϵ%	$(Q_{cr})_M$	ϵ%	$(Q_{cr})_U$	ϵ%
Bi-Pl	0.792494	0.07070	213.68	22.10	213.68	6.84	295.08	34.13
Casson	0.714718	0.06919	235.36	34.49	235.36	17.68	325.02	47.74
Co-Gr	0.668389	0.06570	260.73	48.99	260.73	30.37	360.06	63.66
Ellis	0.707930	0.07017	145.31	-16.96	169.11	-15.44	169.38	-23.01
He-Bu	0.710847	0.06991	240.75	37.57	240.75	20.37	332.46	51.12
Hyper	0.723780	0.07063	239.79	37.03	239.79	19.90	331.14	50.52
P-Law	0.707927	0.07017	136.07	-22.25	158.35	-20.82	158.60	-27.91
Re-Ph	0.884157	0.07342	903.22	416.12	884.09	342.05	950.52	332.06
Ro-St	0.714854	0.07004	240.69	37.53	240.69	20.34	332.38	51.08
Sisko	0.691057	0.06885	242.74	38.71	242.74	21.37	335.21	52.37

Table E.6: Critical volumetric flowrates (in lpm) calculated for mud type 'A' in a 3″ pipe (nominal). Mud density: 1066.4 kg/m^3. Pipe internal diameter: 0.0773913 m. Observed critical flowrates: $(Q_{cr})_L = 175$, $(Q_{cr})_M = 200$ and $(Q_{cr})_U = 220$ lpm.

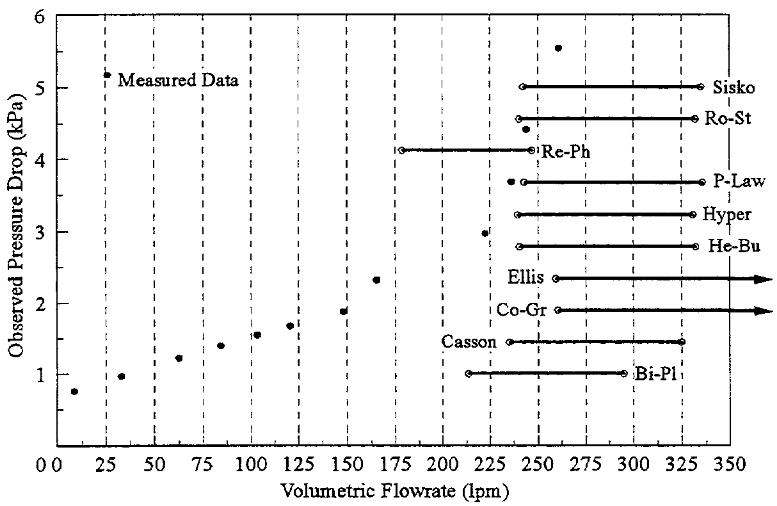

Figure E.9: Mud 'A', 3″ pipe: Fixed-transition results.

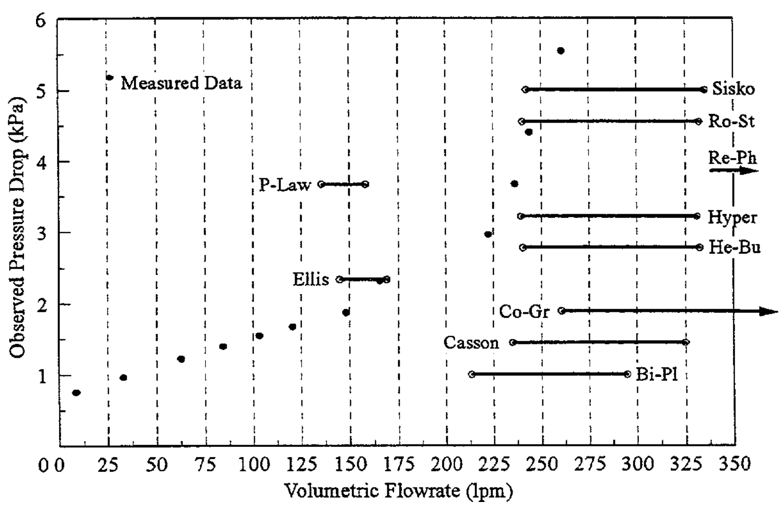

Figure E.10: Mud 'A', 3″ pipe: Correlation-transition results.

Model	Fixed				N-criteria			
	$(Q_{cr})_L$	ϵ%	$(Q_{cr})_U$	ϵ%	$(Q_{cr})_L$	ϵ%	$(Q_{cr})_U$	ϵ%
Bi-Pl	456.11	160.64	629.87	179.94	632.38	261.36	806.11	258.27
Casson	485.10	177.20	669.91	197.74	698.12	298.92	882.91	292.40
Co-Gr	515.00	194.28	711.19	216.08	731.35	317.91	927.52	312.23
Ellis	553.80	216.46	764.77	239.90	846.30	383.60	1057.25	369.89
He-Bu	488.67	179.24	674.83	199.92	705.97	303.41	892.13	296.50
P-Law	518.16	196.09	715.56	218.03	791.92	352.53	989.32	339.70
Re-Ph	455.64	160.36	629.21	179.65	455.63	160.36	629.20	179.64
Ro-St	490.53	180.30	677.40	201.07	708.33	304.76	895.22	297.88
Sisko	487.51	178.58	673.23	199.21	703.77	302.15	889.50	295.33

	N	$D_{\text{eff,G}}$	Correlation: Eqs.(3.18 & 3.19)					
	[-]	[m]	$(Q_{cr})_L$	ϵ%	$(Q_{cr})_M$	ϵ%	$(Q_{cr})_U$	ϵ%
Bi-Pl	0.407376	0.04769	456.06	160.60	456.06	128.03	629.79	179.91
Casson	0.326765	0.04611	485.07	177.18	485.07	142.54	669.86	197.72
Co-Gr	0.355804	0.04357	514.94	194.25	514.94	157.47	711.11	216.05
Ellis	0.190166	0.03735	18.72	-89.30	78.59	-60.70	86.94	-61.36
He-Bu	0.318423	0.04595	488.68	179.24	488.68	144.34	674.84	199.93
P-Law	0.190167	0.03753	13.09	-92.52	69.22	-65.39	76.90	-65.82
Re-Ph	0.999981	0.07741	4355.14	2388.65	4207.75	2003.87	4526.77	1911.90
Ro-St	0.319631	0.04633	490.58	180.33	490.58	145.29	677.47	201.10
Sisko	0.320203	0.04462	487.55	178.60	487.55	143.77	673.28	199.23

Table E.7: Critical volumetric flowrates (in lpm) calculated for mud type 'B' in a 3″ pipe (nominal). Mud density: 1036.5 kg/m^3. Pipe internal diameter: 0.0773913 m. Observed critical flowrates: $(Q_{cr})_L = 175$, $(Q_{cr})_M = 200$ and $(Q_{cr})_U = 225$ lpm.

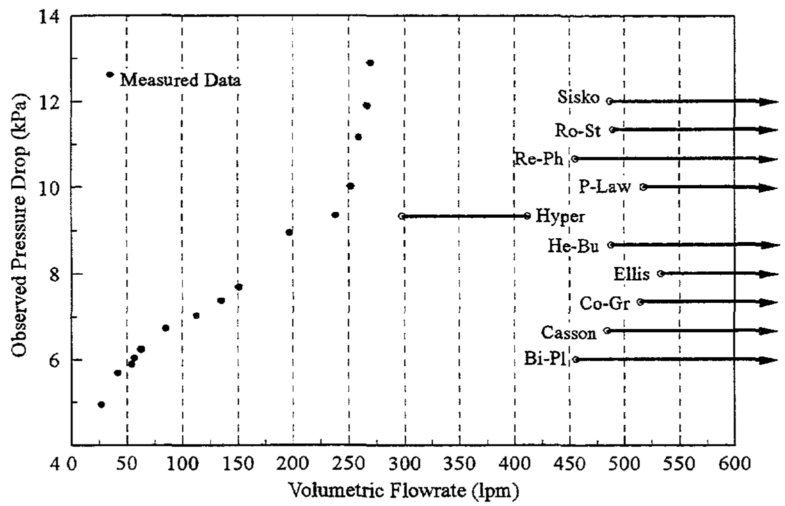

Figure E.11: Mud 'B', 3″ pipe: Fixed-transition results.

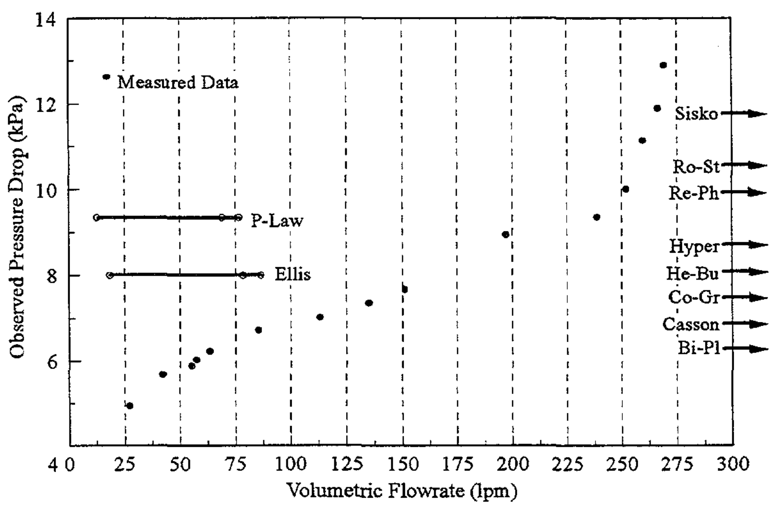

Figure E.12: Mud 'B', 3″ pipe: Correlation-transition results.

Appendix F

Derivation of a General Expression for Wall Shear Stress in an Annulus

From the derivation for the well documented general expression for laminar flow in a cylindrical tube (see Chapter 3 section 3.2.1, page 45), the general equation relating Q and τ_w for laminar flow of time-independent fluids in a concentric annulus is obtained using similar principals. The volumetric flow rate through the differential annulus between r and $r + \mathrm{d}r$ is given by $\mathrm{d}Q = v2\pi r\,\mathrm{d}r$. Volumetric flow rate, Q, is given by

$$\begin{aligned} Q &= \int_0^Q \mathrm{d}Q = 2\pi \int_{R\psi}^{R} vr\,\mathrm{d}r \\ &= 2\pi \left[v_p \frac{r^2}{2} - \frac{1}{2} \int_{R\psi}^{R} r^2 \frac{\mathrm{d}v}{\mathrm{d}r}\,\mathrm{d}r \right], \end{aligned} \tag{F.1}$$

where ψ is the radial fraction corresponding to the outer wall of the inner pipe and R is the radius of the outer pipe. As $\frac{\mathrm{d}v}{\mathrm{d}r} = \dot{\gamma}_r = -f^{-1}(\tau_r;\phi)$ and assuming no slippage at the inner pipe wall (no axial motion), τ_w would have the same value at both conduit contact surfaces then Eq.(F.1) can be written as:

$$Q = \pi \int_{R\psi}^{R} r^2 f^{-1}(\tau_r;\phi)\,\mathrm{d}r. \tag{F.2}$$

From Eq.(3.29) it can be shown that the shear stress at the outer conduit wall may be described by:

$$\tau_w = \frac{\Delta p R}{2L} \left| \lambda^2 - 1 \right|. \tag{F.3}$$

Combining Eq.(F.3) with Eq.(3.29) one obtains the relationship for *in situ* shear stress as a function of radial fraction and τ_w thus:

$$\tau_r = \tau_w \left| \frac{\lambda^2 - z^2}{z(\lambda^2 - 1)} \right|. \tag{F.4}$$

The radial fraction modulus reflects the fact that shear stresses have the same sign either side of the point of maximum velocity. Writing Eq.(F.2) in terms of the dimensionless radial fraction z where $r = Rz$ and $\mathrm{d}r = R\mathrm{d}z$, and substituting Eq.(F.4) for τ_r, the following general equation relating Q and τ_w for laminar flow of time independent fluids in a concentric annulus is constructed:

$$Q = \pi R^3 \int_{\psi}^{1.0} z^2 f^{-1} \left(\tau_w \left| \frac{\lambda^2 - z^2}{z(\lambda^2 - 1)} \right| ; \phi \right) \mathrm{d}z. \tag{F.5}$$

During tripping, inner pipe wall slippage may be non-negligible and Eq.(F.5) can be reconstructed to accommodate inner pipe motion for a fluid possessing no yield stress by considering that flowrate may be separated about two separate regions delimited axialy about λ hence $Q = Q_{[\psi \to \lambda]} + Q_{[\lambda \to 1.0]}$.

$$Q_{[\psi \to \lambda]} = 2\pi R^3 \left[v_p \, \frac{z^3}{3} \Big[_{\psi}^{\lambda} + \frac{1}{2} \int_{\psi}^{\lambda} z^2 f^{-1} \left(\tau_{w,1} \left| \frac{\lambda^2 - z^2}{z\,(\lambda^2 - 1)} \right| ; \phi \right) \, \mathrm{d}z \right] , \tag{F.6}$$

where v_p is the axial velocity of the drillstring and is positive when tripping-out (upward motion) and negative tripping-in (downward motion). The portion of volumetric flowrate occupying the annulus region defined between λ and 1.0 is given by:

$$Q_{[\lambda \to 1.0]} = \pi R^3 \left[\int_{\lambda}^{1.0} z^2 f^{-1} \left(\tau_{w,2} \left| \frac{\lambda^2 - z^2}{z\,(\lambda^2 - 1)} \right| ; \phi \right) \, \mathrm{d}z \right] . \tag{F.7}$$

Solution of the simultaneous equations, Eqs.(F.6 & F.7), requires knowledge of the dimensionless radial fraction, λ, with initial values being provided by the simple expressions presented in section 3.3.7, page 63. For fluids possessing a yield stress, the above procedure may be modified to include the third region of volumetric flowrate defined by the geometry of plug flow (bounded by radial fractions $\lambda_{[-]}$ and $\lambda_{[+]}$) hence solving the three expressions for the regions: $Q = Q_{[\psi \to \lambda_{[-]}]} + Q_{[\lambda_{[-]} \to \lambda_{[+]}]} + Q_{[\lambda_{[+]} \to 1.0]}$. These expressions accommodating axial inner-pipe motion assume (1) pure laminar flow, (2) no cross-over between laminar fluid shells (i.e., no Taylor vortices), (3) identical flow regimes within each region (as distinct from the Rothfus conjecture) and (4) the volume of fluid flowing within each section is proportional to the area of flow.

Appendix G

Pipe Flow Pressure Loss: Tables & Results

Velocity [m/s]	Pressure Drop, [kPa] Meas.	Calc.	ϵ%	N [-]	$D_{\text{eff},G}$ [m]	$N_{Re,G}$ [-]	τ_w [Pa]	$\dot{\gamma}_w$ [1/s]	$\mu_{w,\text{app}}$ [Pa.s]	Type
1″ pipe: Total RMS = 521.21, $\sigma = 28.78$.										
0.471	10.377	9.615	-7.34	0.65838	0.02166	332.7	5.695	174.038	0.03272	Lam
0.717	14.024	12.407	-11.53	0.73494	0.02291	597.9	7.340	250.398	0.02931	Lam
0.914	16.347	14.630	-10.50	0.77546	0.02345	823.3	8.665	311.888	0.02778	Lam
1.049	18.312	16.120	-11.97	0.79612	0.02379	983.5	9.542	352.629	0.02706	Lam
1.428	22.760	20.366	-10.52	0.83870	0.02433	1442.3	12.062	469.564	0.02569	Lam
1.853	31.033	25.120	-19.05	0.86922	0.02469	1968.2	14.877	600.234	0.02479	Lam
2.104	38.631	37.716	-2.37	0.88240	0.02484	2282.9	16.545	677.623	0.02442	Trans
2.692	55.758	89.869	61.18	0.90482	0.02508	3023.9	20.441	858.479	0.02381	Turb
2.861	61.487	95.404	55.16	0.90976	0.02514	3237.9	21.561	910.447	0.02368	Turb
2.935	66.838	97.855	46.41	0.91178	0.02516	3332.6	22.056	933.429	0.02363	Turb
3.088	73.140	102.874	40.65	0.91566	0.02520	3526.5	23.069	980.425	0.02353	Turb
3.272	80.738	108.933	34.92	0.91990	0.02524	3760.5	24.290	1037.083	0.02342	Turb
3.349	84.523	111.463	31.87	0.92154	0.02526	3858.2	24.799	1060.722	0.02338	Turb
2″ pipe: Total RMS = 19.38, $\sigma = 27.24$.										
0.202	2.082	2.644	26.99	0.37419	0.02990	111.8	3.108	53.991	0.05757	Lam
0.409	3.110	3.295	5.95	0.49779	0.03653	368.0	3.873	89.504	0.04327	Lam
0.562	3.744	3.761	0.45	0.55915	0.03928	611.4	4.413	114.535	0.03853	Lam
0.724	4.447	4.231	-4.86	0.60887	0.04121	899.7	4.974	140.576	0.03538	Lam
0.914	5.157	4.785	-7.21	0.65412	0.04283	1268.3	5.624	170.782	0.03293	Lam
1.076	5.736	5.248	-8.51	0.68465	0.04392	1601.9	6.169	196.054	0.03147	Lam
1.382	7.067	8.188	15.86	0.72971	0.04535	2263.7	7.198	243.805	0.02952	Trans
1.448	7.681	10.414	35.58	0.73797	0.04556	2410.7	7.425	254.336	0.02919	Trans
1.509	8.487	12.613	48.62	0.74502	0.04574	2545.3	7.630	263.865	0.02892	Trans
1.584	9.660	15.584	61.33	0.75324	0.04596	2714.2	7.884	275.667	0.02860	Trans
1.662	10.894	19.094	75.27	0.76126	0.04617	2892.1	8.149	287.962	0.02830	Trans
1.775	13.024	20.296	55.84	0.77194	0.04646	3151.5	8.531	305.667	0.02791	Turb
1.926	16.216	21.827	34.60	0.78432	0.04692	3508.6	9.020	328.397	0.02747	Turb
3″ pipe: Total RMS = 1.48, $\sigma = 35.76$.										
0.031	0.758	1.267	67.15	0.13031	0.01838	3.7	2.236	13.528	0.16531	Lam
0.118	0.965	1.460	51.30	0.24541	0.03213	46.0	2.578	29.371	0.08776	Lam
0.223	1.220	1.640	34.43	0.32720	0.04059	146.5	2.891	43.914	0.06583	Lam
0.300	1.393	1.758	26.20	0.37255	0.04471	247.1	3.100	53.614	0.05782	Lam
0.366	1.544	1.856	20.21	0.40570	0.04755	349.9	3.273	61.643	0.05310	Lam
0.428	1.669	1.944	16.48	0.43247	0.04975	455.9	3.427	68.810	0.04981	Lam
0.525	1.868	2.079	11.30	0.46944	0.05262	642.6	3.666	79.897	0.04589	Lam
0.587	2.317	2.163	-6.65	0.48997	0.05411	770.1	3.814	86.749	0.04396	Lam
0.789	2.965	2.433	-17.94	0.54651	0.05799	1237.6	4.289	108.822	0.03942	Lam
0.838	3.675	2.500	-31.97	0.55788	0.05885	1362.3	4.400	113.947	0.03861	Lam
0.865	4.406	2.532	-42.53	0.56424	0.05920	1431.0	4.464	116.929	0.03818	Lam
0.925	5.543	2.611	-52.90	0.57744	0.05997	1585.9	4.604	123.400	0.03731	Lam

Table G.1: Bingham Plastic (no plug flow): Results for mud 'A' – 1″, 2″ & 3″ pipes.

Velocity	Pressure Drop, [kPa]			N	$D_{\text{eff},G}$	$N_{\text{Re},G}$	τ_w	$\dot{\gamma}_w$	$\mu_{w,\text{app}}$	Type
[m/s]	Meas.	Calc.	ϵ%	[-]	[m]	[-]	[Pa]	[1/s]	[Pa.s]	
1″ pipe: Total RMS $= 8.93$, $\sigma = 3.94$.										
0.562	31.006	28.390	-8.44	0.31411	0.01319	155.7	16.804	340.667	0.04933	Lam
0.600	31.171	28.763	-7.73	0.32392	0.01346	174.8	17.048	356.385	0.04783	Lam
0.693	32.350	29.701	-8.19	0.34455	0.01418	226.5	17.585	391.036	0.04497	Lam
0.732	32.798	30.115	-8.18	0.35318	0.01443	249.6	17.819	406.181	0.04387	Lam
0.843	34.026	31.168	-8.40	0.37527	0.01509	319.4	18.450	446.849	0.04129	Lam
1.010	35.605	32.703	-8.15	0.40514	0.01595	436.9	19.376	506.644	0.03824	Lam
1.151	36.218	33.992	-6.15	0.42737	0.01658	545.4	20.129	555.191	0.03626	Lam
1.280	37.418	35.122	-6.14	0.44672	0.01705	652.3	20.833	600.627	0.03468	Lam
1.484	40.196	36.947	-8.08	0.47327	0.01777	834.9	21.883	668.397	0.03274	Lam
1.645	41.720	38.313	-8.17	0.49235	0.01824	988.6	22.705	721.460	0.03147	Lam
2.410	49.118	44.805	-8.78	0.56552	0.01991	1814.9	26.531	968.285	0.02740	Lam
2.702	50.980	47.927	-5.99	0.58804	0.02035	2163.1	27.981	1061.880	0.02635	Trans
2.829	51.724	50.923	-1.55	0.59707	0.02053	2320.4	28.609	1102.381	0.02595	Trans
3.048	54.538	56.996	4.51	0.61161	0.02082	2596.1	29.680	1171.479	0.02534	Trans
3.101	58.592	58.661	0.12	0.61497	0.02088	2664.0	29.938	1188.180	0.02520	Trans
3.242	62.453	63.472	1.63	0.62359	0.02105	2846.1	30.625	1232.456	0.02485	Trans
3.381	67.293	66.567	-1.08	0.63164	0.02120	3028.1	31.294	1275.637	0.02453	Turb
3.480	70.437	68.128	-3.28	0.63705	0.02132	3161.1	31.760	1305.726	0.02432	Turb
3.621	76.663	70.797	-7.65	0.64525	0.02141	3345.3	32.494	1353.096	0.02401	Turb
2″ pipe: Total RMS $= 5.05$, $\sigma = 6.40$.										
0.349	11.204	12.006	7.16	0.18370	0.01668	71.5	14.118	167.384	0.08435	Lam
0.392	12.169	12.156	-0.11	0.19379	0.01754	89.1	14.295	178.801	0.07995	Lam
0.431	12.859	12.296	-4.38	0.20251	0.01826	106.6	14.451	188.854	0.07652	Lam
0.566	13.603	12.742	-6.33	0.22977	0.02039	177.3	14.964	221.919	0.06743	Lam
0.647	14.465	12.980	-10.27	0.24447	0.02150	227.4	15.255	240.708	0.06337	Lam
0.883	15.134	13.672	-9.66	0.28227	0.02415	402.9	16.058	292.565	0.05489	Lam
1.053	15.506	14.127	-8.89	0.30662	0.02560	552.9	16.623	328.972	0.05053	Lam
1.293	16.430	14.768	10.12	0.33556	0.02754	799.5	17.346	375.672	0.04617	Lam
1.522	17.065	15.334	10.14	0.36090	0.02898	1064.5	18.034	420.047	0.04293	Lam
1.692	17.788	15.740	11.51	0.37703	0.03006	1282.5	18.502	450.212	0.04110	Lam
1.811	18.264	16.018	12.30	0.38773	0.03075	1443.9	18.825	471.081	0.03996	Lam
1.947	18.747	16.346	12.81	0.40010	0.03139	1635.6	19.213	496.138	0.03873	Lam
2.012	19.395	16.498	14.94	0.40567	0.03170	1730.3	19.393	507.740	0.03820	Lam
2.088	20.174	16.692	17.26	0.41168	0.03209	1845.6	19.591	520.515	0.03764	Lam
2.141	20.857	16.808	19.41	0.41679	0.03222	1923.7	19.763	531.597	0.03718	Lam
3″ pipe: Total RMS $= 4.10$, $\sigma = 21.76$.										
0.098	4.937	7.110	44.01	0.08134	0.01185	6.3	12.545	65.869	0.19046	Lam
0.151	5.681	7.266	27.90	0.10013	0.01455	14.7	12.807	82.767	0.15474	Lam
0.196	5.888	7.371	25.19	0.11349	0.01644	24.4	13.000	95.204	0.13655	Lam
0.204	6.026	7.400	22.80	0.11609	0.01667	26.4	13.038	97.692	0.13346	Lam
0.225	6.226	7.443	19.55	0.12176	0.01745	32.0	13.123	103.123	0.12725	Lam
0.304	6.715	7.603	13.22	0.14165	0.01977	56.9	13.428	122.823	0.10933	Lam
0.402	7.019	7.790	10.98	0.16183	0.02241	97.6	13.750	143.610	0.09575	Lam
0.479	7.364	7.931	7.70	0.17570	0.02418	136.2	13.982	158.550	0.08818	Lam
0.536	7.681	8.021	4.43	0.18553	0.02533	168.6	14.150	169.436	0.08351	Lam
0.700	8.942	8.280	-7.40	0.21033	0.02826	278.2	14.595	198.126	0.07366	Lam
0.847	9.356	8.488	-9.28	0.22952	0.03058	397.7	14.959	221.605	0.06750	Lam
0.894	10.011	8.555	-14.54	0.23530	0.03126	440.0	15.071	228.855	0.06585	Lam
0.920	11.149	8.583	-23.02	0.23888	0.03154	464.0	15.143	233.469	0.06486	Lam
0.945	11.893	8.628	-27.45	0.24208	0.03182	486.8	15.206	237.589	0.06400	Lam
0.956	12.893	8.636	-33.02	0.24349	0.03192	496.9	15.235	239.457	0.06363	Lam

Table G.2: Bingham Plastic (no plug flow): Results for mud 'B' – 1″, 2″ & 3″ pipes.

Vel.	Pressure Drop, [kPa]			λ	Type
[m/s]	Meas.	Calc.	ε%	[-]	
1″ pipe, mud 'A': Total RMS = 519.53, $\sigma = 26.68$.					
0.471	10.377	10.591	2.06	0.3094	Lam
0.717	14.024	13.313	-5.07	0.2472	Lam
0.914	16.347	15.482	-5.29	0.2121	Lam
1.049	18.312	16.937	-7.51	0.1935	Lam
1.428	22.760	21.096	-7.31	0.1560	Lam
1.853	31.033	25.759	-17.00	0.1277	Lam
2.104	38.631	38.173	-1.18	0.1153	Trans
2.692	55.758	89.869	61.18	0.1153	Turb
2.861	61.487	95.404	55.16	0.1153	Turb
2.935	66.838	97.855	46.41	0.1153	Turb
3.088	73.140	102.874	40.65	0.1153	Turb
3.272	80.738	108.933	34.92	0.1153	Turb
3.349	84.523	111.463	31.87	0.1153	Turb

Vel.	Pressure Drop, [kPa]			λ	Type
[m/s]	Meas.	Calc.	ε%	[-]	
2″ pipe, mud 'A': Total RMS = 19.97, $\sigma = 23.45$.					
0.202	2.082	3.071	47.52	0.5376	Lam
0.409	3.110	3.776	21.41	0.4373	Lam
0.562	3.744	4.254	13.61	0.3897	Lam
0.724	4.447	4.725	6.25	0.3494	Lam
0.914	5.157	5.276	2.31	0.3129	Lam
1.076	5.736	5.735	-0.03	0.2885	Lam
1.382	7.067	8.553	21.03	0.2515	Trans
1.448	7.681	10.693	39.21	0.2446	Trans
1.509	8.487	12.813	50.98	0.2387	Trans
1.584	9.660	15.688	62.40	0.2313	Trans
1.662	10.894	19.094	75.27	0.2245	Trans
1.775	13.024	20.296	55.84	0.2245	Turb
1.926	16.216	21.827	34.60	0.2245	Turb

Vel.	Pressure Drop, [kPa]			λ	Type
[m/s]	Meas.	Calc.	ε%	[-]	
3″ pipe, mud 'A': Total RMS = 1.28, $\sigma = 41.49$.					
0.031	0.758	1.431	88.75	0.7709	Lam
0.118	0.965	1.691	75.20	0.6511	Lam
0.223	1.220	1.908	56.39	0.5769	Lam
0.300	1.393	2.042	46.60	0.5390	Lam
0.366	1.544	2.152	39.40	0.5114	Lam
0.428	1.669	2.248	34.70	0.4896	Lam
0.525	1.868	2.393	28.13	0.4599	Lam
0.587	2.317	2.483	7.16	0.4442	Lam
0.789	2.965	2.759	-6.95	0.3998	Lam
0.838	3.675	2.829	-23.03	0.3907	Lam
0.865	4.406	2.864	-34.99	0.3858	Lam
0.925	5.543	2.943	-46.91	0.3741	Lam

Vel.	Pressure Drop, [kPa]			λ	Type
[m/s]	Meas.	Calc.	ε%	[-]	
1″ pipe, mud 'B': Total RMS = 8.65, $\sigma = 4.18$.					
0.562	31.006	33.014	6.48	0.5894	Lam
0.600	31.171	33.452	7.32	0.5805	Lam
0.693	32.350	34.536	6.76	0.5623	Lam
0.732	32.798	34.990	6.68	0.5550	Lam
0.843	34.026	36.199	6.39	0.5375	Lam
1.010	35.605	37.941	6.56	0.5118	Lam
1.151	36.218	39.336	8.61	0.4937	Lam
1.280	37.418	40.636	8.60	0.4798	Lam
1.484	40.196	42.512	5.76	0.4568	Lam
1.645	41.720	43.947	5.34	0.4419	Lam
2.410	49.118	50.644	3.11	0.3835	Lam
2.702	50.980	53.107	4.17	0.3657	Trans
2.829	51.724	55.192	6.71	0.3590	Trans
3.048	54.538	59.212	8.57	0.3471	Trans
3.101	58.592	60.383	3.06	0.3444	Trans
3.242	62.453	64.321	2.99	0.3374	Trans
3.381	67.293	66.567	-1.08	0.3374	Turb
3.480	70.437	68.128	-3.28	0.3374	Turb
3.621	76.663	70.797	-7.65	0.3374	Turb

Vel.	Pressure Drop, [kPa]			λ	Type
[m/s]	Meas.	Calc.	ε%	[-]	
2″ pipe, mud 'B': Total RMS = 1.43, $\sigma = 7.03$.					
0.349	11.204	13.766	22.87	0.7122	Lam
0.392	12.169	13.960	14.72	0.7009	Lam
0.431	12.859	14.143	9.98	0.6918	Lam
0.566	13.603	14.723	8.23	0.6672	Lam
0.647	14.465	15.050	4.04	0.6514	Lam
0.883	15.134	15.877	4.91	0.6163	Lam
1.053	15.506	16.425	5.93	0.5969	Lam
1.293	16.430	17.164	4.47	0.5700	Lam
1.522	17.065	17.820	4.42	0.5491	Lam
1.692	17.788	18.286	2.80	0.5351	Lam
1.811	18.264	18.589	1.78	0.5274	Lam
1.947	18.747	18.959	1.13	0.5161	Lam
2.012	19.395	19.130	-1.36	0.5114	Lam
2.088	20.174	19.328	-4.19	0.5062	Lam
2.141	20.857	19.475	-6.63	0.5034	Lam

Vel.	Pressure Drop, [kPa]			λ	Type
[m/s]	Meas.	Calc.	ε%	[-]	
3″ pipe, mud 'B': Total RMS = 4.33, $\sigma = 23.06$.					
0.098	4.937	7.856	59.13	0.8319	Lam
0.151	5.681	8.098	42.55	0.8055	Lam
0.196	5.888	8.273	40.50	0.7885	Lam
0.204	6.026	8.302	37.76	0.7857	Lam
0.225	6.226	8.385	34.67	0.7795	Lam
0.304	6.715	8.613	28.27	0.7588	Lam
0.402	7.019	8.879	26.50	0.7346	Lam
0.479	7.364	9.073	23.21	0.7218	Lam
0.536	7.681	9.200	19.77	0.7119	Lam
0.700	8.942	9.533	6.61	0.6842	Lam
0.847	9.356	9.810	4.85	0.6663	Lam
0.894	10.011	9.894	-1.17	0.6606	Lam
0.920	11.149	9.939	-10.85	0.6576	Lam
0.945	11.893	9.979	-16.09	0.6536	Lam
0.956	12.893	9.998	-22.45	0.6537	Lam

Table G.3: Bingham Plastic (including plug flow): Results for 1″, 2″ & 3″ pipes.

Velocity [m/s]	Pressure Drop, [kPa] Meas.	Calc.	ϵ%	N [-]	$D_{\text{eff},G}$ [m]	$N_{\text{Re},G}$ [-]	τ_w [Pa]	$\dot{\gamma}_w$ [1/s]	$\mu_{w,\text{app}}$ [Pa.s]	Type
1″ pipe: Total RMS $= 36.57$, $\sigma = 10.61$.										
0.471	10.377	10.655	2.68	0.63537	0.02211	299.8	6.320	170.471	0.03707	Lam
0.717	14.024	13.800	-1.60	0.67934	0.02277	537.0	8.172	251.999	0.03243	Lam
0.914	16.347	16.163	-1.13	0.70375	0.02309	745.0	9.575	316.834	0.03022	Lam
1.049	18.312	17.747	-3.09	0.71703	0.02328	894.3	10.494	360.494	0.02911	Lam
1.428	22.760	21.968	-3.48	0.74581	0.02363	1337.6	13.006	483.373	0.02691	Lam
1.853	31.033	26.540	-14.48	0.76876	0.02388	1863.2	15.716	620.549	0.02533	Lam
2.104	38.631	31.988	-17.20	0.77946	0.02400	2185.9	17.278	701.374	0.02464	Trans
2.692	55.758	68.315	22.52	0.79920	0.02421	2965.7	20.843	889.463	0.02343	Turb
2.861	61.487	72.087	17.24	0.80388	0.02426	3195.2	21.849	943.349	0.02316	Turb
2.935	66.838	73.762	10.36	0.80584	0.02428	3297.3	22.292	967.161	0.02305	Turb
3.088	73.140	77.199	5.55	0.80965	0.02432	3507.5	23.194	1015.820	0.02283	Turb
3.272	80.738	81.364	0.78	0.81394	0.02436	3762.9	24.274	1074.427	0.02259	Turb
3.349	84.523	83.109	-1.67	0.81563	0.02438	3870.0	24.723	1098.863	0.02250	Turb
2″ pipe: Total RMS $= 3.67$, $\sigma = 10.55$.										
0.202	2.082	2.504	20.27	0.46569	0.03785	118.0	2.943	42.648	0.06901	Lam
0.409	3.110	3.435	10.45	0.54381	0.04099	353.0	4.038	79.782	0.05061	Lam
0.562	3.744	4.039	7.88	0.57968	0.04213	567.3	4.756	106.793	0.04454	Lam
0.724	4.447	4.638	4.30	0.60743	0.04310	820.7	5.452	134.422	0.04056	Lam
0.914	5.157	5.306	2.89	0.63290	0.04383	1144.0	6.235	166.884	0.03736	Lam
1.076	5.736	5.840	1.81	0.65012	0.04441	1439.6	6.865	193.859	0.03541	Lam
1.382	7.067	6.823	-3.45	0.67630	0.04511	2031.8	8.020	245.079	0.03272	Lam
1.448	7.681	7.730	0.64	0.68111	0.04524	2166.0	8.264	256.138	0.03226	Trans
1.509	8.487	9.293	9.50	0.68527	0.04535	2289.4	8.483	266.166	0.03187	Trans
1.584	9.660	11.374	17.74	0.69017	0.04548	2444.6	8.754	278.604	0.03142	Trans
1.662	10.894	13.717	25.91	0.69501	0.04560	2608.8	9.034	291.576	0.03098	Trans
1.775	13.024	17.414	33.71	0.70156	0.04577	2849.5	9.435	310.266	0.03041	Trans
1.926	16.216	19.224	18.55	0.70957	0.04597	3176.8	9.963	335.146	0.02973	Turb
3″ pipe: Total RMS $= 1.17$, $\sigma = 24.18$.										
0.031	0.758	0.854	12.66	0.25312	0.03857	5.5	1.506	6.449	0.23355	Lam
0.118	0.965	1.193	23.63	0.36814	0.04951	56.4	2.104	19.059	0.11042	Lam
0.223	1.220	1.481	21.39	0.43251	0.05465	162.3	2.609	32.614	0.08000	Lam
0.300	1.393	1.662	19.31	0.46458	0.05671	261.3	2.931	42.270	0.06934	Lam
0.366	1.544	1.808	17.10	0.48661	0.05811	359.2	3.188	50.441	0.06320	Lam
0.428	1.669	1.935	15.94	0.50361	0.05924	458.2	3.410	57.788	0.05901	Lam
0.525	1.868	2.127	13.87	0.52668	0.06047	628.1	3.751	69.518	0.05395	Lam
0.587	2.317	2.241	-3.28	0.53880	0.06125	743.5	3.950	76.630	0.05155	Lam
0.789	2.965	2.603	-12.21	0.57205	0.06290	1157.1	4.588	100.324	0.04573	Lam
0.838	3.675	2.684	-26.97	0.57896	0.06316	1264.6	4.740	106.166	0.04465	Lam
0.865	4.406	2.730	-38.04	0.58215	0.06352	1327.4	4.813	108.979	0.04416	Lam
0.925	5.543	2.830	-48.94	0.58964	0.06384	1463.1	4.990	115.920	0.04305	Lam

Table G.4: Casson (no plug flow): Results for mud ‘A’ – 1″, 2″ & 3″ pipes.

Velocity [m/s]	**Pressure Drop,** [kPa] Meas.	Calc.	ϵ%	N [-]	$D_{\text{eff,G}}$ [m]	$\text{N}_{\text{Re,G}}$ [-]	τ_w [Pa]	$\dot{\gamma}_w$ [1/s]	$\mu_{w,\text{app}}$ [Pa.s]	**Type**
1″ pipe: Total RMS $= 37.58$, $\sigma = 5.81$.										
0.562	31.006	30.208	-2.57	0.27575	0.01381	146.4	17.874	325.432	0.05492	Lam
0.600	31.171	30.645	-1.69	0.28091	0.01400	164.4	18.131	342.579	0.05292	Lam
0.693	32.350	31.668	-2.11	0.29289	0.01440	212.5	18.751	385.150	0.04868	Lam
0.732	32.798	32.070	-2.22	0.29761	0.01454	234.1	19.004	403.042	0.04715	Lam
0.843	34.026	33.208	-2.40	0.30967	0.01493	299.6	19.673	451.746	0.04355	Lam
1.010	35.605	34.823	-2.20	0.32546	0.01547	410.8	20.606	522.638	0.03943	Lam
1.151	36.218	36.059	-0.44	0.33743	0.01581	514.0	21.357	582.267	0.03668	Lam
1.280	37.418	37.185	-0.62	0.34739	0.01610	617.3	22.014	636.123	0.03461	Lam
1.484	40.196	38.825	-3.41	0.36157	0.01649	794.3	23.002	720.027	0.03195	Lam
1.645	41.720	40.095	-3.90	0.37158	0.01677	945.5	23.741	784.871	0.03025	Lam
2.410	49.118	45.468	-7.43	0.40985	0.01780	1788.6	26.921	1082.769	0.02486	Lam
2.702	50.980	47.387	-7.05	0.42201	0.01806	2156.6	28.065	1196.757	0.02345	Trans
2.829	51.724	49.089	-5.09	0.42667	0.01821	2327.3	28.524	1243.330	0.02294	Trans
3.048	54.538	52.296	-4.11	0.43472	0.01837	2625.9	29.342	1327.701	0.02210	Trans
3.101	58.592	53.209	-9.19	0.43656	0.01841	2700.4	29.534	1347.756	0.02191	Trans
3.242	62.453	55.882	-10.52	0.44131	0.01852	2901.7	30.039	1400.758	0.02144	Turb
3.381	67.293	57.255	-14.92	0.44578	0.01866	3107.4	30.495	1449.187	0.02104	Turb
3.480	70.437	58.418	-17.06	0.44872	0.01871	3254.1	30.852	1487.404	0.02074	Turb
3.621	76.663	60.067	-21.65	0.45309	0.01880	3467.8	31.347	1540.830	0.02034	Turb
2″ pipe: Total RMS $= 2.03$, $\sigma = 5.61$.										
0.349	11.204	12.296	9.75	0.19469	0.02128	69.9	14.456	131.210	0.11017	Lam
0.392	12.169	12.531	2.97	0.20198	0.02181	86.5	14.721	143.805	0.10237	Lam
0.431	12.859	12.714	-1.13	0.20760	0.02238	103.2	14.931	154.082	0.09690	Lam
0.566	13.603	13.298	-2.24	0.22559	0.02376	169.8	15.633	190.494	0.08206	Lam
0.647	14.465	13.650	-5.63	0.23506	0.02441	216.5	16.022	211.983	0.07558	Lam
0.883	15.134	14.483	-4.30	0.25779	0.02609	380.2	17.019	270.808	0.06284	Lam
1.053	15.506	15.019	-3.14	0.27118	0.02710	520.7	17.650	310.778	0.05679	Lam
1.293	16.430	15.725	-4.29	0.28758	0.02828	750.8	18.472	365.799	0.05050	Lam
1.522	17.065	16.338	-4.26	0.30119	0.02919	999.9	19.199	417.043	0.04604	Lam
1.692	17.788	16.781	-5.66	0.31063	0.02969	1202.8	19.728	455.810	0.04328	Lam
1.811	18.264	17.077	-6.50	0.31647	0.03010	1354.5	20.067	481.244	0.04170	Lam
1.947	18.747	17.420	-7.08	0.32313	0.03044	1535.7	20.464	511.629	0.04000	Lam
2.012	19.395	17.548	-9.52	0.32577	0.03071	1627.0	20.625	524.113	0.03935	Lam
2.088	20.174	17.731	-12.11	0.32935	0.03086	1734.6	20.845	541.398	0.03850	Lam
2.141	20.857	17.855	-14.39	0.33164	0.03100	1811.5	20.987	552.652	0.03798	Lam
3″ pipe: Total RMS $= 3.19$, $\sigma = 18.98$.										
0.098	4.937	6.788	37.49	0.11460	0.02075	6.6	11.958	37.606	0.31800	Lam
0.151	5.681	7.064	24.34	0.13197	0.02322	15.1	12.442	51.884	0.23980	Lam
0.196	5.888	7.245	23.05	0.14385	0.02470	24.8	12.790	63.370	0.20182	Lam
0.204	6.026	7.276	20.74	0.14486	0.02528	26.8	12.820	64.422	0.19900	Lam
0.225	6.226	7.356	18.15	0.14963	0.02589	32.4	12.964	69.502	0.18653	Lam
0.304	6.715	7.621	13.49	0.16461	0.02787	56.9	13.433	87.157	0.15413	Lam
0.402	7.019	7.901	12.57	0.17990	0.02980	96.3	13.939	108.015	0.12905	Lam
0.479	7.364	8.096	9.94	0.18971	0.03115	133.3	14.279	123.057	0.11603	Lam
0.536	7.681	8.231	7.16	0.19627	0.03206	164.4	14.513	133.872	0.10841	Lam
0.700	8.942	8.583	-4.01	0.21297	0.03406	268.3	15.135	164.371	0.09208	Lam
0.847	9.356	8.861	-5.29	0.22547	0.03562	380.7	15.628	190.234	0.08215	Lam
0.894	10.011	8.949	-10.61	0.22939	0.03597	420.1	15.787	198.913	0.07937	Lam
0.920	11.149	8.997	-19.30	0.23139	0.03620	442.7	15.869	203.451	0.07800	Lam
0.945	11.893	9.040	-23.99	0.23321	0.03640	464.3	15.945	207.651	0.07679	Lam
0.956	12.893	9.059	-29.74	0.23400	0.03649	473.9	15.978	209.481	0.07627	Lam

Table G.5: Casson (no plug flow): Results for mud 'B' – 1″, 2″ & 3″ pipes.

Vel. [m/s]	Pressure Drop, [kPa] Meas.	Calc.	ϵ%	λ [-]	Type
1″ pipe, mud 'A': Total RMS = 36.37, $\sigma = 10.50$.					
0.471	10.377	10.856	4.62	0.1307	Lam
0.717	14.024	13.958	-0.47	0.1014	Lam
0.914	16.347	16.310	-0.22	0.0870	Lam
1.049	18.312	17.848	-2.53	0.0795	Lam
1.428	22.760	22.082	-2.98	0.0641	Lam
1.853	31.033	26.639	-14.16	0.0531	Lam
2.104	38.631	32.071	-16.98	0.0484	Trans
2.692	55.758	68.315	22.52	0.0484	Turb
2.861	61.487	72.087	17.24	0.0484	Turb
2.935	66.838	73.762	10.36	0.0484	Turb
3.088	73.140	77.199	5.55	0.0484	Turb
3.272	80.738	81.364	0.78	0.0484	Turb
3.349	84.523	83.109	-1.67	0.0484	Turb
3″ pipe, mud 'A': Total RMS = 1.12, $\sigma = 26.44$.					
0.031	0.758	0.933	23.08	0.5117	Lam
0.118	0.965	1.279	32.51	0.3718	Lam
0.223	1.220	1.566	28.39	0.3036	Lam
0.300	1.393	1.745	25.28	0.2725	Lam
0.366	1.544	1.889	22.37	0.2516	Lam
0.428	1.669	2.016	20.82	0.2363	Lam
0.525	1.868	2.205	18.06	0.2156	Lam
0.587	2.317	2.320	0.11	0.2054	Lam
0.789	2.965	2.675	-9.79	0.1781	Lam
0.838	3.675	2.756	-24.99	0.1728	Lam
0.865	4.406	2.804	-36.37	0.1699	Lam
0.925	5.543	2.899	-47.71	0.1640	Lam
2″ pipe, mud 'B': Total RMS = 1.24, $\sigma = 6.64$.					
0.349	11.204	13.504	20.53	0.5905	Lam
0.392	12.169	13.733	12.85	0.5807	Lam
0.431	12.859	13.958	8.55	0.5725	Lam
0.566	13.603	14.579	7.18	0.5481	Lam
0.647	14.465	14.918	3.13	0.5335	Lam
0.883	15.134	15.799	4.40	0.5037	Lam
1.053	15.506	16.369	5.56	0.4862	Lam
1.293	16.430	17.089	4.01	0.4657	Lam
1.522	17.065	17.748	4.00	0.4493	Lam
1.692	17.788	18.181	2.21	0.4378	Lam
1.811	18.264	18.485	1.21	0.4305	Lam
1.947	18.747	18.820	0.39	0.4229	Lam
2.012	19.395	18.976	-2.16	0.4194	Lam
2.088	20.174	19.165	-5.00	0.4161	Lam
2.141	20.857	19.282	-7.55	0.4136	Lam

Vel. [m/s]	Pressure Drop, [kPa] Meas.	Calc.	ϵ%	λ [-]	Type
2″ pipe, mud 'A': Total RMS = 3.75, $\sigma = 10.45$.					
0.202	2.082	2.629	26.25	0.2713	Lam
0.409	3.110	3.555	14.29	0.2010	Lam
0.562	3.744	4.150	10.85	0.1722	Lam
0.724	4.447	4.739	6.56	0.1505	Lam
0.914	5.157	5.397	4.64	0.1324	Lam
1.076	5.736	5.928	3.35	0.1203	Lam
1.382	7.067	6.903	-2.32	0.1033	Lam
1.448	7.681	7.803	1.59	0.1003	Trans
1.509	8.487	9.352	10.19	0.0978	Trans
1.584	9.660	11.417	18.19	0.0948	Trans
1.662	10.894	13.744	26.16	0.0921	Trans
1.775	13.024	17.419	33.74	0.0882	Trans
1.926	16.216	19.224	18.55	0.0882	Turb
1″ pipe, mud 'B': Total RMS = 36.88, $\sigma = 8.87$.					
0.562	31.006	32.887	6.07	0.4803	Lam
0.600	31.171	33.339	6.95	0.4738	Lam
0.693	32.350	34.402	6.34	0.4592	Lam
0.732	32.798	34.829	6.19	0.4535	Lam
0.843	34.026	36.044	5.93	0.4391	Lam
1.010	35.605	37.633	5.70	0.4198	Lam
1.151	36.218	38.939	7.51	0.4065	Lam
1.280	37.418	40.005	6.91	0.3949	Lam
1.484	40.196	41.682	3.70	0.3797	Lam
1.645	41.720	42.929	2.90	0.3680	Lam
2.410	49.118	48.349	-1.57	0.3274	Lam
2.702	50.980	50.198	-1.53	0.3147	Trans
2.829	51.724	51.025	-1.35	0.3096	Trans
3.048	54.538	53.737	-1.47	0.3016	Trans
3.101	58.592	54.323	-7.29	0.2997	Trans
3.242	62.453	55.882	-10.52	0.2997	Turb
3.381	67.293	57.255	-14.92	0.2997	Turb
3.480	70.437	58.418	-17.06	0.2997	Turb
3.621	76.663	60.067	-21.65	0.2997	Turb
3″ pipe, mud 'B': Total RMS = 3.56, $\sigma = 20.76$.					
0.098	4.937	7.412	50.13	0.7159	Lam
0.151	5.681	7.728	36.03	0.6866	Lam
0.196	5.888	7.943	34.90	0.6693	Lam
0.204	6.026	7.978	32.40	0.6664	Lam
0.225	6.226	8.065	29.54	0.6592	Lam
0.304	6.715	8.366	24.59	0.6367	Lam
0.402	7.019	8.677	23.62	0.6140	Lam
0.479	7.364	8.890	20.72	0.5992	Lam
0.536	7.681	9.037	17.65	0.5883	Lam
0.700	8.942	9.414	5.28	0.5647	Lam
0.847	9.356	9.716	3.84	0.5472	Lam
0.894	10.011	9.806	-2.04	0.5421	Lam
0.920	11.149	9.856	-11.60	0.5394	Lam
0.945	11.893	9.901	-16.75	0.5370	Lam
0.956	12.893	9.920	-23.06	0.5359	Lam

Table G.6: Casson (including plug flow): Results for 1″, 2″ & 3″ pipes.

Velocity [m/s]	**Pressure Drop**, [kPa] Meas.	Calc.	ϵ%	N [-]	$D_{\text{eff},G}$ [m]	$N_{Re,G}$ [-]	τ_w [Pa]	$\dot{\gamma}_w$ [1/s]	$\mu_{w,app}$ [Pa.s]	**Type**
1″ pipe: Total RMS $= 15.55$, $\sigma = 13.57$.										
0.471	10.377	13.026	25.53	0.50813	0.01982	245.6	7.714	190.171	0.04056	Lam
0.717	14.024	15.915	13.48	0.59853	0.02099	465.7	9.424	273.407	0.03447	Lam
0.914	16.347	18.125	10.88	0.64685	0.02171	664.5	10.735	336.957	0.03186	Lam
1.049	18.312	19.623	7.16	0.67357	0.02208	807.5	11.622	380.036	0.03058	Lam
1.428	22.760	23.737	4.29	0.72984	0.02293	1237.5	14.058	498.292	0.02821	Lam
1.853	31.033	28.308	-8.78	0.77776	0.02356	1747.6	16.755	629.184	0.02663	Lam
2.104	38.631	31.085	-19.53	0.79638	0.02381	2056.8	18.363	706.867	0.02598	Lam
2.692	55.758	70.436	26.32	0.82977	0.02421	2796.8	22.101	889.464	0.02485	Trans
2.861	61.487	80.048	30.19	0.83745	0.02431	3012.6	23.174	941.481	0.02461	Turb
2.935	66.838	82.150	22.91	0.84063	0.02435	3108.3	23.648	964.484	0.02452	Turb
3.088	73.140	86.480	18.24	0.84678	0.02442	3304.7	24.617	1011.524	0.02434	Turb
3.272	80.738	91.740	13.63	0.85358	0.02451	3542.5	25.784	1068.154	0.02414	Turb
3.349	84.523	93.951	11.15	0.85624	0.02454	3642.0	26.271	1091.785	0.02406	Turb
2″ pipe: Total RMS $= 1.82$, $\sigma = 19.77$.										
0.202	2.082	3.254	56.29	0.53168	0.04432	90.8	3.825	36.424	0.10501	Lam
0.409	3.110	4.647	49.42	0.37492	0.03865	260.9	5.463	84.602	0.06458	Lam
0.562	3.744	5.304	41.67	0.40695	0.03780	432.8	6.234	119.027	0.05238	Lam
0.724	4.447	5.882	32.27	0.45449	0.03825	647.2	6.914	151.463	0.04565	Lam
0.914	5.157	6.496	25.96	0.50323	0.03925	934.2	7.636	186.386	0.04097	Lam
1.076	5.736	6.998	22.00	0.54168	0.04005	1201.4	8.226	214.956	0.03827	Lam
1.382	7.067	7.897	11.74	0.59250	0.04148	1755.4	9.282	266.515	0.03483	Lam
1.448	7.681	8.090	5.32	0.60204	0.04175	1882.3	9.509	277.515	0.03427	Lam
1.509	8.487	8.264	-2.63	0.61027	0.04199	1999.4	9.714	287.426	0.03379	Lam
1.584	9.660	8.936	-7.49	0.61997	0.04228	2147.3	9.966	299.651	0.03326	Trans
1.662	10.894	10.781	-1.04	0.62956	0.04257	2304.5	10.227	312.345	0.03274	Trans
1.775	13.024	13.764	5.68	0.64252	0.04296	2535.6	10.603	330.567	0.03208	Trans
1.926	16.216	18.363	13.24	0.65835	0.04344	2851.3	11.100	354.671	0.03130	Trans
3″ pipe: Total RMS $= 0.98$, $\sigma = 37.40$.										
0.031	0.758	0.332	-56.20	0.93796	0.07639	14.1	0.585	3.256	0.17971	Lam
0.118	0.965	1.100	13.99	0.77570	0.07334	61.2	1.939	12.867	0.15071	Lam
0.223	1.220	1.781	45.98	0.61118	0.06943	134.8	3.141	25.673	0.12235	Lam
0.300	1.393	2.156	54.77	0.53820	0.06656	201.5	3.802	36.014	0.10556	Lam
0.366	1.544	2.421	56.80	0.45127	0.06402	268.3	4.269	45.785	0.09324	Lam
0.428	1.669	2.627	57.40	0.41505	0.06204	337.4	4.631	55.183	0.08393	Lam
0.525	1.868	2.896	55.03	0.35975	0.05941	461.4	5.106	70.762	0.07216	Lam
0.587	2.317	3.041	31.25	0.37503	0.05835	547.9	5.361	80.446	0.06664	Lam
0.789	2.965	3.440	16.02	0.39656	0.05676	875.2	6.066	111.188	0.05456	Lam
0.838	3.675	3.526	-4.05	0.40589	0.05670	964.0	6.218	118.255	0.05258	Lam
0.865	4.406	3.574	-18.88	0.41135	0.05666	1013.9	6.301	122.172	0.05158	Lam
0.925	5.543	3.675	-33.70	0.42354	0.05667	1126.9	6.479	130.601	0.04961	Lam

Table G.7: Collins-Graves: Results for mud 'A' – 1″, 2″ & 3″ pipes.

Velocity [m/s]	Pressure Drop, [kPa] Meas.	Calc.	$\epsilon\%$	N [-]	$D_{\text{eff},G}$ [m]	$N_{\text{Re},G}$ [-]	τ_w [Pa]	$\dot{\gamma}_w$ [1/s]	$\mu_{w,\text{app}}$ [Pa.s]	Type
1″ pipe: Total RMS $= 7.82$, $\sigma = 4.50$.										
0.562	31.006	32.712	5.50	0.27061	0.01201	135.0	19.376	374.068	0.05180	Lam
0.600	31.171	33.118	6.25	0.27946	0.01226	151.9	19.617	391.217	0.05014	Lam
0.693	32.350	34.040	5.22	0.29885	0.01286	197.6	20.164	431.179	0.04677	Lam
0.732	32.798	34.427	4.97	0.30617	0.01312	218.3	20.379	446.530	0.04564	Lam
0.843	34.026	35.463	4.22	0.32641	0.01374	280.7	20.996	490.702	0.04279	Lam
1.010	35.605	36.994	3.90	0.35386	0.01456	386.7	21.894	554.992	0.03945	Lam
1.151	36.218	38.204	5.48	0.37440	0.01517	485.4	22.617	606.771	0.03727	Lam
1.280	37.418	39.290	5.00	0.39174	0.01568	584.1	23.265	653.181	0.03562	Lam
1.484	40.196	41.009	2.02	0.41750	0.01633	752.0	24.297	727.170	0.03341	Lam
1.645	41.720	42.309	1.41	0.43508	0.01684	895.9	25.056	781.542	0.03206	Lam
2.410	49.118	48.355	-1.55	0.50577	0.01856	1680.9	28.646	1038.924	0.02757	Lam
2.702	50.980	50.583	-0.78	0.53041	0.01908	2020.3	29.960	1132.555	0.02645	Lam
2.829	51.724	52.090	0.71	0.53900	0.01929	2174.2	30.533	1173.442	0.02602	Trans
3.048	54.538	56.259	3.16	0.55317	0.01960	2444.0	31.526	1244.263	0.02534	Trans
3.101	58.592	57.435	-1.97	0.55657	0.01966	2510.0	31.774	1261.951	0.02518	Trans
3.242	62.453	60.722	-2.77	0.56441	0.01986	2693.6	32.359	1306.270	0.02477	Trans
3.381	67.293	64.840	-3.65	0.57253	0.02002	2872.8	32.986	1351.122	0.02441	Trans
3.480	70.437	66.284	-5.90	0.57811	0.02013	3003.1	33.431	1382.940	0.02417	Turb
3.621	76.663	68.357	-10.83	0.58577	0.02028	3191.6	34.060	1427.982	0.02385	Turb
2″ pipe: Total RMS $= 2.15$, $\sigma = 8.92$.										
0.349	11.204	14.128	26.10	0.14762	0.01588	60.8	16.608	175.789	0.09448	Lam
0.392	12.169	14.307	17.57	0.15825	0.01643	75.8	16.818	190.824	0.08813	Lam
0.431	12.859	14.453	12.40	0.16678	0.01697	90.7	16.990	203.175	0.08362	Lam
0.566	13.603	14.918	9.67	0.19273	0.01867	151.3	17.537	242.357	0.07236	Lam
0.647	14.465	15.174	4.90	0.20631	0.01961	194.5	17.837	263.889	0.06759	Lam
0.883	15.134	15.859	4.79	0.24071	0.02196	347.0	18.645	321.855	0.05793	Lam
1.053	15.506	16.335	5.35	0.26397	0.02330	478.7	19.200	361.483	0.05311	Lam
1.293	16.430	16.945	3.13	0.29020	0.02507	696.4	19.916	412.608	0.04827	Lam
1.522	17.065	17.506	2.58	0.31285	0.02641	932.9	20.579	460.823	0.04466	Lam
1.692	17.788	17.907	0.67	0.32805	0.02737	1127.4	21.048	494.404	0.04257	Lam
1.811	18.264	18.169	-0.52	0.33885	0.02790	1270.5	21.394	519.197	0.04121	Lam
1.947	18.747	18.492	-1.36	0.34922	0.02864	1445.7	21.737	543.744	0.03998	Lam
2.012	19.395	18.633	-3.93	0.35434	0.02894	1531.5	21.910	556.162	0.03940	Lam
2.088	20.174	18.821	-6.71	0.36072	0.02921	1633.9	22.130	571.899	0.03870	Lam
2.141	20.857	18.920	-9.29	0.36439	0.02948	1708.0	22.259	581.104	0.03830	Lam
3″ pipe: Total RMS $= 5.76$, $\sigma = 25.02$.										
0.098	4.937	8.044	62.93	0.08401	0.04270	5.6	14.184	18.274	0.77620	Lam
0.151	5.681	8.502	49.66	0.05590	0.02012	12.5	14.992	59.877	0.25038	Lam
0.196	5.888	8.678	47.38	0.07500	0.01908	20.8	15.302	82.040	0.18652	Lam
0.204	6.026	8.694	44.27	0.07666	0.01938	22.4	15.330	84.059	0.18237	Lam
0.225	6.226	8.766	40.80	0.08390	0.01929	27.1	15.457	93.297	0.16567	Lam
0.304	6.715	8.985	33.80	0.10562	0.02009	48.2	15.842	120.914	0.13102	Lam
0.402	7.019	9.187	30.89	0.12607	0.02198	82.9	16.198	146.432	0.11062	Lam
0.479	7.364	9.341	26.85	0.14055	0.02309	115.6	16.471	165.978	0.09924	Lam
0.536	7.681	9.445	22.97	0.15000	0.02396	143.3	16.654	179.113	0.09298	Lam
0.700	8.942	9.719	8.69	0.17394	0.02619	237.0	17.137	213.739	0.08018	Lam
0.847	9.356	9.943	6.27	0.19256	0.02799	339.3	17.533	242.088	0.07242	Lam
0.894	10.011	10.009	-0.02	0.19779	0.02858	375.8	17.648	250.323	0.07050	Lam
0.920	11.149	10.047	-9.88	0.20087	0.02886	396.6	17.715	255.164	0.06943	Lam
0.945	11.893	10.090	-15.16	0.20431	0.02900	416.1	17.792	260.641	0.06826	Lam
0.956	12.893	10.097	-21.69	0.20487	0.02923	425.3	17.804	261.519	0.06808	Lam

Table G.8: Collins-Graves: Results for mud 'B' – 1″, 2″ & 3″ pipes.

Velocity [m/s]	Pressure Drop, [kPa] Meas.	Calc.	ϵ%	N [-]	$D_{\text{eff,G}}$ [m]	$N_{\text{Re,G}}$ [-]	τ_w [Pa]	$\dot{\gamma}_w$ [1/s]	$\mu_{w,\text{app}}$ [Pa.s]	Type
1″ pipe: Total RMS = 80.14, $\sigma = 8.74$.										
0.471	10.377	10.406	0.28	0.70793	0.02357	307.6	6.158	159.913	0.03851	Lam
0.717	14.024	14.015	-0.06	0.70793	0.02357	529.3	8.292	243.445	0.03406	Lam
0.914	16.347	16.615	1.64	0.70793	0.02357	724.4	9.847	310.372	0.03173	Lam
1.049	18.312	18.311	-0.01	0.70793	0.02357	864.9	10.851	355.995	0.03048	Lam
1.428	22.760	22.786	0.11	0.70793	0.02357	1288.6	13.501	484.705	0.02785	Lam
1.853	31.033	27.401	-11.70	0.70793	0.02357	1803.7	16.233	628.842	0.02581	Lam
2.104	38.631	30.579	-20.84	0.70793	0.02357	2126.1	17.764	714.209	0.02487	Trans
2.692	55.758	56.801	1.87	0.70793	0.02357	2922.8	21.149	913.710	0.02315	Turb
2.861	61.487	59.281	-3.59	0.70793	0.02357	3161.8	22.080	971.036	0.02274	Turb
2.935	66.838	60.377	-9.67	0.70793	0.02357	3268.9	22.486	996.388	0.02257	Turb
3.088	73.140	62.617	-14.39	0.70793	0.02357	3490.3	23.308	1048.230	0.02224	Turb
3.272	80.738	65.315	-19.10	0.70793	0.02357	3761.4	24.284	1110.731	0.02186	Turb
3.349	84.523	66.440	-21.39	0.70793	0.02357	3875.9	24.686	1136.807	0.02172	Turb
2″ pipe: Total RMS = 2.68, $\sigma = 11.41$.										
0.202	2.082	1.769	-15.03	0.70793	0.04661	166.6	2.085	34.635	0.06020	Lam
0.409	3.110	2.917	-6.21	0.70793	0.04677	415.8	3.428	69.908	0.04904	Lam
0.562	3.744	3.655	-2.38	0.70793	0.04677	628.0	4.297	96.182	0.04467	Lam
0.724	4.447	4.372	-1.69	0.70793	0.04678	870.7	5.139	123.861	0.04149	Lam
0.914	5.157	5.157	0.00	0.70793	0.04678	1176.9	6.061	156.386	0.03876	Lam
1.076	5.736	5.787	0.89	0.70793	0.04678	1452.7	6.803	184.063	0.03696	Lam
1.382	7.067	6.908	-2.25	0.70793	0.04678	2006.7	8.120	236.338	0.03436	Lam
1.448	7.681	7.497	-2.40	0.70793	0.04678	2132.3	8.394	247.700	0.03389	Trans
1.509	8.487	9.009	6.15	0.70793	0.04678	2247.8	8.640	258.019	0.03349	Trans
1.584	9.660	10.979	13.65	0.70793	0.04678	2393.2	8.942	270.840	0.03302	Trans
1.662	10.894	13.146	20.67	0.70793	0.04678	2547.2	9.253	284.233	0.03255	Trans
1.775	13.024	16.473	26.48	0.70793	0.04678	2773.3	9.694	303.568	0.03193	Trans
1.926	16.216	18.966	16.96	0.70793	0.04678	3081.6	10.270	329.367	0.03118	Turb
3″ pipe: Total RMS = 1.69, $\sigma = 19.37$.										
0.031	0.758	0.192	-74.67	0.70793	0.07010	19.9	0.416	3.548	0.11711	Lam
0.118	0.965	0.603	-37.51	0.70793	0.07051	111.6	1.064	13.383	0.07947	Lam
0.223	1.220	0.949	-22.21	0.70793	0.07020	253.1	1.674	25.393	0.06591	Lam
0.300	1.393	1.171	-15.94	0.70793	0.07016	370.9	2.065	34.165	0.06044	Lam
0.366	1.544	1.351	-12.50	0.70793	0.07010	480.7	2.382	41.811	0.05698	Lam
0.428	1.669	1.508	-9.65	0.70793	0.07013	587.7	2.658	48.818	0.05446	Lam
0.525	1.868	1.744	-6.64	0.70793	0.07016	766.5	3.073	59.917	0.05129	Lam
0.587	2.317	1.885	-18.64	0.70793	0.07016	883.9	3.323	66.903	0.04967	Lam
0.789	2.965	2.324	-21.62	0.70793	0.07016	1295.6	4.098	89.945	0.04556	Lam
0.838	3.675	2.426	-33.99	0.70793	0.07016	1401.3	4.277	95.575	0.04475	Lam
0.865	4.406	2.481	-43.69	0.70793	0.07016	1460.2	4.375	98.668	0.04434	Lam
0.925	5.543	2.601	-53.08	0.70793	0.07016	1591.8	4.587	105.480	0.04348	Lam

Table G.9: Ellis *et al.*: Results for mud 'A' – 1″, 2″ & 3″ pipes.

Velocity [m/s]	Pressure Drop, [kPa] Meas.	Calc.	ϵ%	N [-]	$D_{\text{eff},G}$ [m]	$N_{Re,G}$ [-]	τ_w [Pa]	$\dot{\gamma}_w$ [1/s]	$\mu_{w,app}$ [Pa.s]	Type
1″ pipe: Total RMS = 36.57, σ = 10.61.										
0.562	31.006	35.528	14.58	0.19017	0.01258	124.3	21.058	357.369	0.05893	Lam
0.600	31.171	35.964	15.38	0.19017	0.01262	139.9	21.306	380.044	0.05606	Lam
0.693	32.350	36.961	14.25	0.19017	0.01263	181.9	21.900	439.183	0.04987	Lam
0.732	32.798	37.348	13.87	0.19017	0.01261	201.0	22.136	464.601	0.04764	Lam
0.843	34.026	38.429	12.94	0.19017	0.01260	259.2	22.741	535.469	0.04247	Lam
1.010	35.605	39.770	11.70	0.19017	0.01255	359.4	23.554	644.016	0.03657	Lam
1.151	36.218	40.765	12.55	0.19017	0.01265	455.4	24.107	727.613	0.03313	Lam
1.280	37.418	41.604	11.19	0.19017	0.01256	551.6	24.634	815.209	0.03022	Lam
1.484	40.196	42.800	6.48	0.19017	0.01259	721.4	25.326	943.130	0.02685	Lam
1.645	41.720	43.567	4.43	0.19017	0.01266	870.0	25.801	1039.899	0.02481	Lam
2.410	49.118	46.894	-4.53	0.19017	0.01255	1732.8	27.789	1536.323	0.01809	Lam
2.702	50.980	48.405	-5.05	0.19017	0.01265	2134.5	28.357	1708.874	0.01659	Trans
2.829	51.724	51.817	0.18	0.19017	0.01262	2319.6	28.618	1793.424	0.01596	Trans
3.048	54.538	59.583	9.25	0.19017	0.01258	2652.7	29.047	1939.120	0.01498	Trans
3.101	58.592	61.763	5.41	0.19017	0.01259	2737.3	29.137	1970.982	0.01478	Trans
3.242	62.453	66.789	6.94	0.19017	0.01261	2967.5	29.372	2056.221	0.01428	Turb
3.381	67.293	68.550	1.87	0.19017	0.01264	3202.1	29.593	2138.804	0.01384	Turb
3.480	70.437	70.356	-0.11	0.19017	0.01259	3371.2	29.781	2211.178	0.01347	Turb
3.621	76.663	72.581	-5.32	0.19017	0.01256	3621.3	30.018	2305.353	0.01302	Turb
2″ pipe: Total RMS = 3.67, σ = 10.55.										
0.349	11.204	14.349	28.07	0.19017	0.02499	59.8	16.881	111.739	0.15108	Lam
0.392	12.169	14.673	20.58	0.19017	0.02506	73.9	17.248	125.108	0.13786	Lam
0.431	12.859	14.925	16.07	0.19017	0.02520	87.8	17.544	136.832	0.12822	Lam
0.566	13.603	15.722	15.58	0.19017	0.02516	143.6	18.482	179.907	0.10273	Lam
0.647	14.465	16.127	11.49	0.19017	0.02516	183.0	18.957	205.615	0.09220	Lam
0.883	15.134	17.139	13.25	0.19017	0.02495	321.1	20.147	283.178	0.07114	Lam
1.053	15.506	17.703	14.17	0.19017	0.02509	441.6	20.810	335.745	0.06198	Lam
1.293	16.430	18.425	12.14	0.19017	0.02497	640.3	21.659	414.327	0.05227	Lam
1.522	17.065	18.985	11.25	0.19017	0.02510	860.2	22.317	484.923	0.04602	Lam
1.692	17.788	19.386	8.98	0.19017	0.02500	1041.2	22.789	541.369	0.04209	Lam
1.811	18.264	19.624	7.45	0.19017	0.02509	1178.3	23.068	577.206	0.03997	Lam
1.947	18.747	19.927	6.29	0.19017	0.02490	1341.6	23.424	625.554	0.03745	Lam
2.012	19.395	20.049	3.37	0.19017	0.02491	1423.9	23.567	645.967	0.03648	Lam
2.088	20.174	20.191	0.08	0.19017	0.02492	1523.4	23.735	670.472	0.03540	Lam
2.141	20.857	20.288	-2.73	0.19017	0.02491	1594.0	23.850	687.773	0.03468	Lam
3″ pipe: Total RMS = 1.17, σ = 24.18.										
0.098	4.937	6.777	37.27	0.19017	0.03734	6.4	12.272	20.895	0.58735	Lam
0.151	5.681	7.462	31.35	0.19017	0.03996	14.3	13.158	30.142	0.43653	Lam
0.196	5.888	7.879	33.81	0.19017	0.03903	22.9	13.893	40.113	0.34634	Lam
0.204	6.026	7.936	31.70	0.19017	0.03911	24.6	13.992	41.647	0.33598	Lam
0.225	6.226	8.106	30.20	0.19017	0.03863	29.4	14.294	46.581	0.30685	Lam
0.304	6.715	8.603	28.12	0.19017	0.03815	50.4	15.169	63.667	0.23825	Lam
0.402	7.019	9.079	29.35	0.19017	0.03805	83.8	16.011	84.586	0.18928	Lam
0.479	7.364	9.391	27.53	0.19017	0.03796	115.0	16.559	100.975	0.16399	Lam
0.536	7.681	9.610	25.11	0.19017	0.03766	140.8	16.945	113.961	0.14869	Lam
0.700	8.942	10.108	13.04	0.19017	0.03766	227.9	17.823	148.674	0.11988	Lam
0.847	9.356	10.477	11.98	0.19017	0.03776	322.1	18.473	179.479	0.10293	Lam
0.894	10.011	10.594	5.82	0.19017	0.03760	355.0	18.679	190.253	0.09818	Lam
0.920	11.149	10.650	-4.48	0.19017	0.03764	374.1	18.779	195.649	0.09598	Lam
0.945	11.893	10.701	-10.02	0.19017	0.03768	392.4	18.869	200.635	0.09405	Lam
0.956	12.893	10.723	-16.83	0.19017	0.03770	400.5	18.907	202.763	0.09325	Lam

Table G.10: Ellis *et al.*: Results for mud 'B' – 1″, 2″ & 3″ pipes.

Velocity [m/s]	Pressure Drop, [kPa] Meas.	Calc.	ϵ%	N [-]	$D_{\text{eff},G}$ [m]	$N_{Re,G}$ [-]	τ_w [Pa]	$\dot{\gamma}_w$ [1/s]	$\mu_{w,\text{app}}$ [Pa.s]	Type
1″ pipe: Total RMS $= 50.48$, $\sigma = 8.10$.										
0.471	10.377	10.536	1.53	0.68002	0.02301	303.6	6.240	163.845	0.03808	Lam
0.717	14.024	13.967	-0.41	0.69850	0.02328	530.7	8.269	246.436	0.03355	Lam
0.914	16.347	16.489	0.87	0.70727	0.02339	729.6	9.777	312.782	0.03126	Lam
1.049	18.312	18.145	-0.91	0.71160	0.02349	873.5	10.744	357.236	0.03008	Lam
1.428	22.760	22.557	-0.89	0.72016	0.02359	1302.2	13.360	484.312	0.02759	Lam
1.853	31.033	27.165	-12.46	0.72613	0.02367	1819.9	16.089	626.241	0.02569	Lam
2.104	38.631	30.834	-20.18	0.72868	0.02370	2142.1	17.632	710.228	0.02483	Trans
2.692	55.758	59.470	6.66	0.73304	0.02376	2933.3	21.073	906.428	0.02325	Turb
2.861	61.487	62.205	1.17	0.73401	0.02376	3168.9	22.031	963.052	0.02288	Turb
2.935	66.838	63.412	-5.13	0.73440	0.02376	3274.2	22.450	988.084	0.02272	Turb
3.088	73.140	65.876	-9.93	0.73517	0.02377	3491.8	23.298	1039.256	0.02242	Turb
3.272	80.738	68.842	-14.73	0.73600	0.02378	3757.7	24.308	1100.926	0.02208	Turb
3.349	84.523	70.078	-17.09	0.73633	0.02378	3869.9	24.724	1126.650	0.02195	Turb
2″ pipe: Total RMS $= 3.06$, $\sigma = 9.63$.										
0.202	2.082	2.135	2.55	0.56786	0.04183	138.6	2.507	38.590	0.06496	Lam
0.409	3.110	3.157	1.51	0.62884	0.04398	383.7	3.715	74.355	0.04996	Lam
0.562	3.744	3.830	2.30	0.65104	0.04476	598.8	4.506	100.506	0.04483	Lam
0.724	4.447	4.496	1.10	0.66648	0.04520	846.0	5.289	128.175	0.04126	Lam
0.914	5.157	5.236	1.53	0.67889	0.04564	1160.4	6.148	160.296	0.03835	Lam
1.076	5.736	5.824	1.53	0.68671	0.04586	1443.0	6.848	187.740	0.03648	Lam
1.382	7.067	6.894	-2.45	0.69733	0.04619	2011.0	8.103	239.375	0.03385	Lam
1.448	7.681	7.544	-1.78	0.69917	0.04623	2139.1	8.367	250.654	0.03338	Trans
1.509	8.487	9.070	6.87	0.70072	0.04626	2256.9	8.605	260.894	0.03298	Trans
1.584	9.660	11.078	14.68	0.70251	0.04632	2405.5	8.896	273.554	0.03252	Trans
1.662	10.894	13.305	22.13	0.70423	0.04637	2562.8	9.196	286.780	0.03207	Trans
1.775	13.024	16.753	28.63	0.70652	0.04641	2792.9	9.626	305.963	0.03146	Trans
1.926	16.216	19.126	17.95	0.70923	0.04645	3104.7	10.194	331.752	0.03073	Turb
3″ pipe: Total RMS $= 1.44$, $\sigma = 17.78$.										
0.031	0.758	0.607	-19.92	0.31649	0.04309	7.7	1.071	5.772	0.18550	Lam
0.118	0.965	0.923	-4.35	0.46677	0.05611	72.9	1.628	16.818	0.09683	Lam
0.223	1.220	1.222	0.16	0.53699	0.06086	196.8	2.152	29.286	0.07349	Lam
0.300	1.393	1.414	1.51	0.56688	0.06269	307.1	2.494	38.234	0.06522	Lam
0.366	1.544	1.572	1.81	0.58587	0.06376	413.0	2.773	45.969	0.06032	Lam
0.428	1.669	1.712	2.58	0.59964	0.06455	517.6	3.018	53.035	0.05691	Lam
0.525	1.868	1.923	2.94	0.61675	0.06546	694.7	3.391	64.220	0.05280	Lam
0.587	2.317	2.052	-11.44	0.62542	0.06587	812.0	3.617	71.260	0.05076	Lam
0.789	2.965	2.452	-17.30	0.64662	0.06693	1228.1	4.323	94.284	0.04585	Lam
0.838	3.675	2.545	-30.75	0.65062	0.06712	1335.6	4.488	99.900	0.04493	Lam
0.865	4.406	2.596	-41.08	0.65277	0.06712	1394.2	4.582	103.135	0.04443	Lam
0.925	5.543	2.708	-51.15	0.65687	0.06743	1529.8	4.773	109.747	0.04349	Lam

Table G.11: Herschel-Bulkley (no plug flow): Results for mud 'A' – 1″, 2″ & 3″ pipes.

Velocity [m/s]	Pressure Drop, [kPa] Meas.	Calc.	ϵ%	N [-]	$D_{\text{eff},G}$ [m]	$N_{Re,G}$ [-]	τ_w [Pa]	$\dot{\gamma}_w$ [1/s]	$\mu_{w,app}$ [Pa.s]	Type
1″ pipe: Total RMS $= 47.48$, $\sigma = 6.60$.										
0.562	31.006	30.310	-2.24	0.27597	0.01400	145.8	17.945	320.974	0.05591	Lam
0.600	31.171	30.735	-1.40	0.28058	0.01415	163.6	18.219	338.926	0.05375	Lam
0.693	32.350	31.829	-1.61	0.29064	0.01453	211.4	18.849	381.733	0.04938	Lam
0.732	32.798	32.258	-1.65	0.29449	0.01467	232.9	19.101	399.498	0.04781	Lam
0.843	34.026	33.408	-1.82	0.30436	0.01502	298.0	19.780	448.952	0.04406	Lam
1.010	35.605	34.998	-1.70	0.31745	0.01541	407.8	20.761	524.495	0.03958	Lam
1.151	36.218	36.315	0.27	0.32639	0.01577	510.9	21.488	583.705	0.03681	Lam
1.280	37.418	37.416	-0.01	0.33401	0.01601	613.5	22.148	639.753	0.03462	Lam
1.484	40.196	39.058	-2.83	0.34464	0.01631	789.5	23.142	728.027	0.03179	Lam
1.645	41.720	40.285	-3.44	0.35157	0.01660	941.6	23.838	792.777	0.03007	Lam
2.410	49.118	45.513	-7.34	0.37818	0.01737	1786.3	26.955	1110.044	0.02428	Lam
2.702	50.980	47.275	-7.27	0.38578	0.01763	2161.7	28.000	1226.229	0.02283	Trans
2.829	51.724	48.754	-5.74	0.38893	0.01770	2332.8	28.457	1278.630	0.02226	Trans
3.048	54.538	51.632	-5.33	0.39394	0.01783	2637.3	29.216	1367.542	0.02136	Trans
3.101	58.592	52.452	-10.48	0.39509	0.01786	2713.1	29.396	1388.967	0.02116	Trans
3.242	62.453	54.787	-12.27	0.39802	0.01794	2918.4	29.866	1445.674	0.02066	Turb
3.381	67.293	56.246	-16.42	0.40077	0.01802	3125.5	30.319	1501.191	0.02020	Turb
3.480	70.437	57.293	-18.66	0.40265	0.01807	3276.9	30.638	1540.775	0.01988	Turb
3.621	76.663	58.800	-23.30	0.40524	0.01814	3496.9	31.086	1597.208	0.01946	Turb
2″ pipe: Total RMS $= 1.98$, $\sigma = 5.38$.										
0.349	11.204	12.272	9.53	0.20140	0.02176	70.0	14.425	128.318	0.11242	Lam
0.392	12.169	12.491	2.65	0.20810	0.02240	86.8	14.684	139.959	0.10492	Lam
0.431	12.859	12.706	-1.19	0.21369	0.02293	103.3	14.907	150.337	0.09916	Lam
0.566	13.603	13.311	-2.15	0.23105	0.02423	169.6	15.645	186.814	0.08375	Lam
0.647	14.465	13.642	-5.69	0.23960	0.02494	216.3	16.036	207.482	0.07729	Lam
0.883	15.134	14.510	-4.12	0.26011	0.02659	379.3	17.059	265.747	0.06419	Lam
1.053	15.506	15.077	-2.77	0.27214	0.02746	518.6	17.722	306.660	0.05779	Lam
1.293	16.430	15.807	-3.79	0.28635	0.02852	746.7	18.574	362.829	0.05119	Lam
1.522	17.065	16.434	-3.70	0.29768	0.02934	993.9	19.315	414.842	0.04656	Lam
1.692	17.788	16.878	-5.12	0.30512	0.02987	1196.3	19.835	453.032	0.04378	Lam
1.811	18.264	17.190	-5.88	0.30991	0.03021	1346.6	20.184	479.497	0.04210	Lam
1.947	18.747	17.498	-6.66	0.31521	0.03050	1526.5	20.586	510.694	0.04031	Lam
2.012	19.395	17.656	-8.97	0.31768	0.03060	1615.0	20.778	525.926	0.03951	Lam
2.088	20.174	17.837	-11.58	0.31991	0.03093	1725.4	20.956	540.111	0.03880	Lam
2.141	20.857	17.960	-13.89	0.32174	0.03103	1801.5	21.103	552.057	0.03823	Lam
3″ pipe: Total RMS $= 3.36$, $\sigma = 18.56$.										
0.098	4.937	6.731	36.34	0.11962	0.02081	6.6	11.872	37.494	0.31664	Lam
0.151	5.681	7.004	23.29	0.13727	0.02371	15.2	12.344	50.797	0.24301	Lam
0.196	5.888	7.192	22.15	0.14932	0.02544	25.0	12.688	61.538	0.20618	Lam
0.204	6.026	7.224	19.88	0.15121	0.02571	27.0	12.744	63.356	0.20114	Lam
0.225	6.226	7.307	17.36	0.15613	0.02636	32.6	12.891	68.276	0.18881	Lam
0.304	6.715	7.579	12.87	0.17090	0.02866	57.2	13.355	84.754	0.15757	Lam
0.402	7.019	7.866	12.07	0.18629	0.03067	96.7	13.874	104.961	0.13219	Lam
0.479	7.364	8.076	9.67	0.19624	0.03197	133.8	14.232	119.911	0.11869	Lam
0.536	7.681	8.214	6.94	0.20283	0.03283	164.8	14.480	130.732	0.11076	Lam
0.700	8.942	8.576	-4.09	0.21919	0.03474	268.3	15.134	161.170	0.09390	Lam
0.847	9.356	8.869	-5.21	0.23093	0.03632	380.4	15.640	186.556	0.08384	Lam
0.894	10.011	8.958	-10.52	0.23437	0.03676	419.9	15.795	194.620	0.08116	Lam
0.920	11.149	9.007	-19.21	0.23622	0.03699	442.5	15.879	199.076	0.07977	Lam
0.945	11.893	9.052	-23.89	0.23790	0.03720	463.9	15.957	203.209	0.07852	Lam
0.956	12.893	9.071	-29.64	0.23862	0.03729	473.5	15.991	205.014	0.07800	Lam

Table G.12: Herschel-Bulkley (no plug flow): Results for mud 'B' – 1″, 2″ & 3″ pipes.

1″ pipe, mud 'A': Total RMS = 50.38, $\sigma = 8.26$.

Vel.	Pressure Drop, [kPa]			λ	Type
[m/s]	Meas.	Calc.	ϵ%	[-]	
0.471	10.377	10.653	2.66	0.0984	Lam
0.717	14.024	14.059	0.25	0.0746	Lam
0.914	16.347	16.599	1.54	0.0633	Lam
1.049	18.312	18.218	-0.52	0.0575	Lam
1.428	22.760	22.619	-0.62	0.0463	Lam
1.853	31.033	27.217	-12.30	0.0385	Lam
2.104	38.631	30.880	-20.06	0.0352	Trans
2.692	55.758	59.470	6.66	0.0352	Turb
2.861	61.487	62.205	1.17	0.0352	Turb
2.935	66.838	63.412	-5.13	0.0352	Turb
3.088	73.140	65.876	-9.93	0.0352	Turb
3.272	80.738	68.842	-14.73	0.0352	Turb
3.349	84.523	70.078	-17.09	0.0352	Turb

2″ pipe, mud 'A': Total RMS = 3.09, $\sigma = 9.07$.

Vel.	Pressure Drop, [kPa]			λ	Type
[m/s]	Meas.	Calc.	ϵ%	[-]	
0.202	2.082	2.239	7.56	0.2358	Lam
0.409	3.110	3.247	4.41	0.1630	Lam
0.562	3.744	3.910	4.43	0.1351	Lam
0.724	4.447	4.563	2.60	0.1157	Lam
0.914	5.157	5.292	2.61	0.1000	Lam
1.076	5.736	5.877	2.46	0.0899	Lam
1.382	7.067	6.942	-1.76	0.0761	Lam
1.448	7.681	7.588	-1.21	0.0737	Trans
1.509	8.487	9.107	7.31	0.0717	Trans
1.584	9.660	11.106	14.97	0.0694	Trans
1.662	10.894	13.323	22.30	0.0671	Trans
1.775	13.024	16.759	28.68	0.0642	Trans
1.926	16.216	19.126	17.94	0.0642	Turb

3″ pipe, mud 'A': Total RMS = 1.37, $\sigma = 19.29$.

Vel.	Pressure Drop, [kPa]			λ	Type
[m/s]	Meas.	Calc.	ϵ%	[-]	
0.031	0.758	0.683	-9.85	0.5162	Lam
0.118	0.965	1.004	4.05	0.3506	Lam
0.223	1.220	1.296	6.19	0.2717	Lam
0.300	1.393	1.486	6.68	0.2369	Lam
0.366	1.544	1.641	6.28	0.2150	Lam
0.428	1.669	1.777	6.47	0.1981	Lam
0.525	1.868	1.985	6.27	0.1773	Lam
0.587	2.317	2.110	-8.93	0.1668	Lam
0.789	2.965	2.503	-15.57	0.1406	Lam
0.838	3.675	2.596	-29.35	0.1356	Lam
0.865	4.406	2.647	-39.93	0.1330	Lam
0.925	5.543	2.756	-50.28	0.1277	Lam

1″ pipe, mud 'B': Total RMS = 47.35, $\sigma = 9.77$.

Vel.	Pressure Drop, [kPa]			λ	Type
[m/s]	Meas.	Calc.	ϵ%	[-]	
0.562	31.006	33.076	6.68	0.4805	Lam
0.600	31.171	33.544	7.61	0.4738	Lam
0.693	32.350	34.634	7.06	0.4598	Lam
0.732	32.798	35.069	6.92	0.4541	Lam
0.843	34.026	36.209	6.41	0.4398	Lam
1.010	35.605	37.882	6.39	0.4212	Lam
1.151	36.218	39.137	8.06	0.4077	Lam
1.280	37.418	40.237	7.53	0.3965	Lam
1.484	40.196	41.874	4.17	0.3810	Lam
1.645	41.720	43.092	3.29	0.3703	Lam
2.410	49.118	48.252	-1.76	0.3300	Lam
2.702	50.980	50.031	-1.86	0.3183	Trans
2.829	51.724	50.812	-1.76	0.3134	Trans
3.048	54.538	52.755	-3.27	0.3057	Trans
3.101	58.592	53.310	-9.01	0.3039	Trans
3.242	62.453	54.787	-12.27	0.3039	Turb
3.381	67.293	56.246	-16.42	0.3039	Turb
3.480	70.437	57.293	-18.66	0.3039	Turb
3.621	76.663	58.800	-23.30	0.3039	Turb

2″ pipe, mud 'B': Total RMS = 1.41, $\sigma = 6.58$.

Vel.	Pressure Drop, [kPa]			λ	Type
[m/s]	Meas.	Calc.	ϵ%	[-]	
0.349	11.204	13.549	20.93	0.5921	Lam
0.392	12.169	13.796	13.37	0.5815	Lam
0.431	12.859	13.978	8.70	0.5728	Lam
0.566	13.603	14.631	7.56	0.5472	Lam
0.647	14.465	14.984	3.58	0.5344	Lam
0.883	15.134	15.911	5.14	0.5042	Lam
1.053	15.506	16.462	6.17	0.4864	Lam
1.293	16.430	17.211	4.75	0.4652	Lam
1.522	17.065	17.854	4.62	0.4494	Lam
1.692	17.788	18.289	2.82	0.4387	Lam
1.811	18.264	18.620	1.95	0.4317	Lam
1.947	18.747	18.948	1.07	0.4243	Lam
2.012	19.395	19.100	-1.52	0.4209	Lam
2.088	20.174	19.278	-4.44	0.4170	Lam
2.141	20.857	19.399	-6.99	0.4144	Lam

3″ pipe, mud 'B': Total RMS = 3.81, $\sigma = 20.55$.

Vel.	Pressure Drop, [kPa]			λ	Type
[m/s]	Meas.	Calc.	ϵ%	[-]	
0.098	4.937	7.395	49.79	0.7218	Lam
0.151	5.681	7.718	35.85	0.6930	Lam
0.196	5.888	7.940	34.86	0.6749	Lam
0.204	6.026	7.976	32.36	0.6719	Lam
0.225	6.226	8.068	29.58	0.6630	Lam
0.304	6.715	8.367	24.60	0.6380	Lam
0.402	7.019	8.682	23.70	0.6148	Lam
0.479	7.364	8.909	20.97	0.5992	Lam
0.536	7.681	9.053	17.86	0.5908	Lam
0.700	8.942	9.448	5.66	0.5650	Lam
0.847	9.356	9.757	4.29	0.5471	Lam
0.894	10.011	9.850	-1.61	0.5419	Lam
0.920	11.149	9.901	-11.20	0.5391	Lam
0.945	11.893	9.948	-16.36	0.5377	Lam
0.956	12.893	9.969	-22.68	0.5365	Lam

Table G.13: Herschel-Bulkley (including plug flow): Results for 1″, 2″ & 3″ pipes.

Velocity	**Pressure Drop,** [kPa]			N	$D_{\text{eff},G}$	$N_{\text{Re},G}$	τ_w	$\dot{\gamma}_w$	$\mu_{w,\text{app}}$	**Type**
[m/s]	Meas.	Calc.	ϵ%	[-]	[m]	[-]	[Pa]	[1/s]	[Pa.s]	
1″ pipe: Total RMS $= 70.71$, $\sigma = 7.88$.										
0.471	10.377	10.190	-1.80	0.72141	0.02351	314.0	6.034	160.353	0.03763	Lam
0.717	14.024	13.740	-2.03	0.72583	0.02368	539.3	8.137	242.305	0.03358	Lam
0.914	16.347	16.369	0.13	0.72476	0.02372	735.9	9.694	308.454	0.03143	Lam
1.049	18.312	18.075	-1.29	0.72355	0.02372	876.7	10.704	353.697	0.03026	Lam
1.428	22.760	22.592	-0.74	0.72048	0.02371	1300.3	13.380	481.753	0.02777	Lam
1.853	31.033	27.259	-12.16	0.71877	0.02370	1813.8	16.143	625.418	0.02581	Lam
2.104	38.631	30.701	-20.53	0.71858	0.02369	2134.7	17.693	710.512	0.02490	Trans
2.692	55.758	57.969	3.97	0.71993	0.02369	2926.1	21.125	909.129	0.02324	Turb
2.861	61.487	60.603	-1.44	0.72066	0.02369	3163.2	22.070	966.102	0.02284	Turb
2.935	66.838	61.773	-7.58	0.72102	0.02369	3269.3	22.483	991.282	0.02268	Turb
3.088	73.140	64.177	-12.25	0.72183	0.02369	3488.6	23.319	1042.738	0.02236	Turb
3.272	80.738	67.112	-16.88	0.72291	0.02369	3756.5	24.315	1104.904	0.02201	Turb
3.349	84.523	68.346	-19.14	0.72339	0.02369	3869.5	24.727	1130.847	0.02187	Turb
2″ pipe: Total RMS $= 4.87$, $\sigma = 13.20$.										
0.202	2.082	1.998	-4.03	0.58404	0.04103	147.9	2.349	39.338	0.05971	Lam
0.409	3.110	2.963	-4.73	0.67264	0.04468	409.9	3.478	73.180	0.04752	Lam
0.562	3.744	3.628	-3.10	0.69887	0.04567	632.6	4.265	98.511	0.04329	Lam
0.724	4.447	4.296	-3.40	0.71291	0.04619	884.5	5.059	125.437	0.04033	Lam
0.914	5.157	5.053	-2.02	0.72085	0.04664	1201.2	5.939	156.860	0.03786	Lam
1.076	5.736	5.668	-1.19	0.72404	0.04681	1483.2	6.663	183.937	0.03622	Lam
1.382	7.067	6.777	-4.10	0.72582	0.04699	2045.5	7.966	235.302	0.03385	Lam
1.448	7.681	7.859	2.32	0.72582	0.04701	2172.4	8.239	246.501	0.03342	Trans
1.509	8.487	9.480	11.70	0.72574	0.04702	2289.0	8.485	256.682	0.03306	Trans
1.584	9.660	11.587	19.95	0.72558	0.04704	2435.5	8.786	269.342	0.03262	Trans
1.662	10.894	13.899	27.58	0.72535	0.04705	2590.6	9.098	282.582	0.03219	Trans
1.775	13.024	17.436	33.88	0.72492	0.04707	2818.0	9.540	301.715	0.03162	Trans
1.926	16.216	19.447	19.92	0.72427	0.04708	3127.6	10.119	327.279	0.03092	Turb
3″ pipe: Total RMS $= 1.85$, $\sigma = 16.68$.										
0.031	0.758	0.673	-11.21	0.24785	0.03268	7.0	1.186	7.611	0.15585	Lam
0.118	0.965	0.912	-5.49	0.43274	0.05045	73.9	1.606	18.706	0.08588	Lam
0.223	1.220	1.156	-5.25	0.53642	0.05834	207.8	2.039	30.553	0.06672	Lam
0.300	1.393	1.326	-4.81	0.58252	0.06146	327.7	2.337	39.001	0.05993	Lam
0.366	1.544	1.468	-4.92	0.61182	0.06319	441.8	2.592	46.380	0.05589	Lam
0.428	1.669	1.599	-4.19	0.63226	0.06455	554.5	2.818	53.040	0.05313	Lam
0.525	1.868	1.798	-3.75	0.65673	0.06601	743.1	3.170	63.680	0.04979	Lam
0.587	2.317	1.920	-17.13	0.66840	0.06670	867.1	3.387	70.372	0.04814	Lam
0.789	2.965	2.315	-21.92	0.69415	0.06824	1300.8	4.081	92.475	0.04413	Lam
0.838	3.675	2.409	-34.45	0.69845	0.06848	1411.3	4.247	97.924	0.04337	Lam
0.865	4.406	2.460	-44.17	0.70055	0.06860	1472.8	4.337	100.915	0.04298	Lam
0.925	5.543	2.572	-53.60	0.70466	0.06884	1610.1	4.534	107.499	0.04218	Lam

Table G.14: Hyperbolic (no plug flow): Results for mud 'A' – 1″, 2″ & 3″ pipes.

Vel. [m/s]	Pressure Drop, [kPa] Meas.	Calc.	ϵ%	λ [-]	Type
1″ pipe, mud 'A': Total RMS = 70.43, $\sigma = 8.22$.					
0.471	10.377	10.452	0.72	0.1432	Lam
0.717	14.024	13.948	-0.54	0.1073	Lam
0.914	16.347	16.547	1.22	0.0906	Lam
1.049	18.312	18.237	-0.41	0.0822	Lam
1.428	22.760	22.722	-0.17	0.0660	Lam
1.853	31.033	27.367	-11.81	0.0548	Lam
2.104	38.631	30.796	-20.28	0.5000	Trans
2.692	55.758	57.969	3.97	0.5000	Turb
2.861	61.487	60.603	-1.44	0.5000	Turb
2.935	66.838	61.773	-7.58	0.5000	Turb
3.088	73.140	64.177	-12.25	0.5000	Turb
3.272	80.738	67.112	-16.88	0.5000	Turb
3.349	84.523	68.346	-19.14	0.5000	Turb
2″ pipe, mud 'A': Total RMS = 4.94, $\sigma = 11.55$.					
0.202	2.082	2.215	6.40	0.3403	Lam
0.409	3.110	3.153	1.37	0.2391	Lam
0.562	3.744	3.804	1.60	0.1986	Lam
0.724	4.447	4.454	0.17	0.1692	Lam
0.914	5.157	5.195	0.74	0.1454	Lam
1.076	5.736	5.792	0.97	0.1302	Lam
1.382	7.067	6.883	-2.60	0.1095	Lam
1.448	7.681	7.953	3.54	0.1060	Trans
1.509	8.487	9.557	12.61	0.1030	Trans
1.584	9.660	11.644	20.54	0.0995	Trans
1.662	10.894	13.935	27.92	0.0962	Trans
1.775	13.024	17.446	33.95	0.0918	Trans
1.926	16.216	19.447	19.92	0.0918	Turb
3″ pipe, mud 'A': Total RMS = 1.66, $\sigma = 20.12$.					
0.031	0.758	0.778	2.59	0.6462	Lam
0.118	0.965	1.049	8.66	0.4793	Lam
0.223	1.220	1.301	6.68	0.3861	Lam
0.300	1.393	1.470	5.54	0.3418	Lam
0.366	1.544	1.611	4.32	0.3120	Lam
0.428	1.669	1.738	4.15	0.2897	Lam
0.525	1.868	1.932	3.44	0.2606	Lam
0.587	2.317	2.050	-11.50	0.2451	Lam
0.789	2.965	2.432	-17.99	0.2071	Lam
0.838	3.675	2.526	-31.27	0.1994	Lam
0.865	4.406	2.577	-41.52	0.1954	Lam
0.925	5.543	2.681	-51.63	0.1874	Lam

Table G.15: Hyperbolic (including plug flow): Results for 1″, 2″ & 3″ pipes.

Velocity [m/s]	Pressure Drop, [kPa] Meas.	Calc.	$\epsilon\%$	N [-]	$D_{\mathrm{eff},G}$ [m]	$N_{\mathrm{Re},G}$ [-]	τ_w [Pa]	$\dot{\gamma}_w$ [1/s]	$\mu_{w,\mathrm{app}}$ [Pa.s]	Type
1″ pipe: Total RMS $= 72.85$, $\sigma = 8.73$.										
0.471	10.377	10.405	0.27	0.70793	0.02357	307.7	6.158	159.913	0.03851	Lam
0.717	14.024	14.015	-0.06	0.70793	0.02357	529.3	8.291	243.409	0.03406	Lam
0.914	16.347	16.615	1.64	0.70793	0.02357	724.5	9.847	310.353	0.03173	Lam
1.049	18.312	18.311	-0.01	0.70793	0.02357	864.9	10.851	355.983	0.03048	Lam
1.428	22.760	22.786	0.11	0.70793	0.02357	1288.6	13.501	484.702	0.02785	Lam
1.853	31.033	27.401	-11.70	0.70793	0.02357	1803.8	16.233	628.841	0.02581	Lam
2.104	38.631	30.580	-20.84	0.70793	0.02357	2126.2	17.764	714.209	0.02487	Trans
2.692	55.758	56.801	1.87	0.70793	0.02357	2922.8	21.148	913.711	0.02315	Turb
2.861	61.487	59.281	-3.59	0.70793	0.02357	3161.9	22.079	971.037	0.02274	Turb
2.935	66.838	60.377	-9.67	0.70793	0.02357	3268.9	22.486	996.389	0.02257	Turb
3.088	73.140	62.617	-14.39	0.70793	0.02357	3490.3	23.308	1048.231	0.02224	Turb
3.272	80.738	65.315	-19.10	0.70793	0.02357	3761.5	24.283	1110.732	0.02186	Turb
3.349	84.523	66.440	-21.39	0.70793	0.02357	3875.9	24.686	1136.808	0.02171	Turb
2″ pipe: Total RMS $= 2.43$, $\sigma = 11.42$.										
0.202	2.082	1.769	-15.03	0.70793	0.04681	167.1	2.078	34.482	0.06028	Lam
0.409	3.110	2.916	-6.24	0.70793	0.04680	416.0	3.427	69.868	0.04904	Lam
0.562	3.744	3.655	-2.38	0.70793	0.04680	628.2	4.295	96.136	0.04468	Lam
0.724	4.447	4.372	-1.69	0.70793	0.04679	870.9	5.138	123.813	0.04150	Lam
0.914	5.157	5.157	0.00	0.70793	0.04679	1177.1	6.060	156.339	0.03876	Lam
1.076	5.736	5.787	0.89	0.70793	0.04679	1453.0	6.801	184.017	0.03696	Lam
1.382	7.067	6.908	-2.25	0.70793	0.04679	2007.0	8.119	236.301	0.03436	Lam
1.448	7.681	7.499	-2.37	0.70793	0.04679	2132.5	8.393	247.665	0.03389	Trans
1.509	8.487	9.011	6.17	0.70793	0.04679	2248.0	8.639	257.986	0.03349	Trans
1.584	9.660	10.981	13.67	0.70793	0.04679	2393.4	8.941	270.810	0.03302	Trans
1.662	10.894	13.147	20.68	0.70793	0.04678	2547.4	9.252	284.207	0.03255	Trans
1.775	13.024	16.474	26.49	0.70793	0.04678	2773.5	9.693	303.547	0.03193	Trans
1.926	16.216	18.965	16.95	0.70793	0.04678	3081.8	10.270	329.351	0.03118	Turb
3″ pipe: Total RMS $= 1.51$, $\sigma = 18.27$.										
0.031	0.758	0.235	-69.00	0.70793	0.07010	19.9	0.416	3.548	0.11711	Lam
0.118	0.965	0.605	-37.31	0.70793	0.07025	111.3	1.066	13.433	0.07938	Lam
0.223	1.220	0.949	-22.21	0.70793	0.07023	253.1	1.673	25.382	0.06592	Lam
0.300	1.393	1.171	-15.94	0.70793	0.07022	371.1	2.064	34.136	0.06046	Lam
0.366	1.544	1.350	-12.56	0.70793	0.07021	481.3	2.380	41.744	0.05700	Lam
0.428	1.669	1.507	-9.71	0.70793	0.07021	588.2	2.656	48.762	0.05448	Lam
0.525	1.868	1.743	-6.69	0.70793	0.07020	766.9	3.072	59.880	0.05130	Lam
0.587	2.317	1.884	-18.69	0.70793	0.07020	884.3	3.322	66.863	0.04968	Lam
0.789	2.965	2.324	-21.62	0.70793	0.07020	1296.1	4.096	89.900	0.04556	Lam
0.838	3.675	2.426	-33.99	0.70793	0.07019	1401.8	4.276	95.529	0.04476	Lam
0.865	4.406	2.481	-43.69	0.70793	0.07019	1460.7	4.374	98.622	0.04435	Lam
0.925	5.543	2.601	-53.08	0.70793	0.07019	1592.3	4.585	105.433	0.04349	Lam

Table G.16: Power Law: Results for mud 'A' – 1″, 2″ & 3″ pipes.

Velocity [m/s]	Pressure Drop, [kPa] Meas.	Calc.	$\epsilon\%$	N [-]	$D_{\mathrm{eff},G}$ [m]	$N_{\mathrm{Re},G}$ [-]	τ_w [Pa]	$\dot{\gamma}_w$ [1/s]	$\mu_{w,\mathrm{app}}$ [Pa.s]	Type
1″ pipe: Total RMS $= 11.28$, $\sigma = 5.91$.										
0.562	31.006	33.294	7.38	0.19017	0.01260	132.7	19.714	356.676	0.05527	Lam
0.600	31.171	33.714	8.16	0.19017	0.01264	149.4	19.948	379.492	0.05256	Lam
0.693	32.350	34.629	7.04	0.19017	0.01255	194.0	20.532	441.710	0.04648	Lam
0.732	32.798	35.010	6.74	0.19017	0.01259	214.5	20.738	465.500	0.04455	Lam
0.843	34.026	35.946	5.64	0.19017	0.01255	276.6	21.311	537.264	0.03967	Lam
1.010	35.605	37.191	4.45	0.19017	0.01260	384.1	22.041	641.304	0.03437	Lam
1.151	36.218	38.189	5.44	0.19017	0.01263	486.1	22.584	728.962	0.03098	Lam
1.280	37.418	38.966	4.14	0.19017	0.01264	589.7	23.042	810.112	0.02844	Lam
1.484	40.196	40.075	-0.30	0.19017	0.01253	769.6	23.741	947.868	0.02505	Lam
1.645	41.720	40.867	-2.04	0.19017	0.01254	927.3	24.206	1049.791	0.02306	Lam
2.410	49.118	43.877	-10.67	0.19017	0.01254	1850.0	26.027	1537.146	0.01693	Lam
2.702	50.980	47.942	-5.96	0.19017	0.01253	2275.2	26.603	1724.683	0.01542	Trans
2.829	51.724	52.492	1.48	0.19017	0.01253	2473.4	26.840	1806.876	0.01485	Trans
3.048	54.538	61.692	13.12	0.19017	0.01265	2835.7	27.171	1927.542	0.01410	Trans
3.101	58.592	63.827	8.93	0.19017	0.01265	2925.6	27.262	1961.387	0.01390	Turb
3.242	62.453	65.855	5.45	0.19017	0.01264	3170.1	27.495	2051.290	0.01340	Turb
3.381	67.293	67.867	0.85	0.19017	0.01264	3419.0	27.716	2139.677	0.01295	Turb
3.480	70.437	69.318	-1.59	0.19017	0.01264	3602.2	27.870	2202.966	0.01265	Turb
3.621	76.663	71.400	-6.87	0.19017	0.01263	3870.7	28.084	2293.145	0.01225	Turb
2″ pipe: Total RMS $= 1.49$, $\sigma = 7.10$.										
0.349	11.204	13.447	20.02	0.19017	0.02488	63.8	15.822	112.206	0.14101	Lam
0.392	12.169	13.751	13.00	0.19017	0.02507	78.9	16.152	125.082	0.12913	Lam
0.431	12.859	14.008	8.94	0.19017	0.02503	93.6	16.451	137.747	0.11943	Lam
0.566	13.603	14.746	8.40	0.19017	0.02487	153.0	17.346	181.991	0.09531	Lam
0.647	14.465	15.123	4.55	0.19017	0.02501	195.2	17.775	206.921	0.08590	Lam
0.883	15.134	16.042	6.00	0.19017	0.02498	343.0	18.863	282.837	0.06669	Lam
1.053	15.506	16.591	7.00	0.19017	0.02505	471.5	19.494	336.226	0.05798	Lam
1.293	16.430	17.238	4.92	0.19017	0.02501	683.9	20.278	413.747	0.04901	Lam
1.522	17.065	17.788	4.24	0.19017	0.02497	917.7	20.920	487.412	0.04292	Lam
1.692	17.788	18.146	2.01	0.19017	0.02491	1111.1	21.357	543.355	0.03931	Lam
1.811	18.264	18.379	0.63	0.19017	0.02508	1258.0	21.606	577.525	0.03741	Lam
1.947	18.747	18.632	-0.61	0.19017	0.02501	1433.8	21.918	622.712	0.03520	Lam
2.012	19.395	18.747	-3.34	0.19017	0.02502	1521.6	22.053	643.251	0.03428	Lam
2.088	20.174	18.917	-6.23	0.19017	0.02503	1628.1	22.208	667.359	0.03328	Lam
2.141	20.857	19.007	-8.87	0.19017	0.02504	1703.9	22.313	684.003	0.03262	Lam
3″ pipe: Total RMS $= 2.48$, $\sigma = 16.18$.										
0.098	4.937	6.511	31.88	0.19017	0.03763	6.9	11.477	20.736	0.55346	Lam
0.151	5.681	7.073	24.50	0.19017	0.03735	15.1	12.482	32.247	0.38707	Lam
0.196	5.888	7.437	26.31	0.19017	0.03733	24.2	13.121	41.936	0.31289	Lam
0.204	6.026	7.493	24.34	0.19017	0.03732	26.0	13.221	43.646	0.30292	Lam
0.225	6.226	7.636	22.65	0.19017	0.03729	31.1	13.476	48.258	0.27926	Lam
0.304	6.715	8.076	20.27	0.19017	0.03758	53.6	14.246	64.622	0.22045	Lam
0.402	7.019	8.533	21.57	0.19017	0.03748	89.3	15.038	85.886	0.17509	Lam
0.479	7.364	8.814	19.69	0.19017	0.03745	122.4	15.548	102.367	0.15189	Lam
0.536	7.681	9.003	17.21	0.19017	0.03730	150.1	15.898	115.070	0.13816	Lam
0.700	8.942	9.484	6.06	0.19017	0.03751	243.1	16.704	149.237	0.11193	Lam
0.847	9.356	9.832	5.09	0.19017	0.03731	343.1	17.340	181.639	0.09546	Lam
0.894	10.011	9.934	-0.77	0.19017	0.03735	378.6	17.516	191.557	0.09144	Lam
0.920	11.149	9.988	-10.41	0.19017	0.03753	399.3	17.596	196.196	0.08968	Lam
0.945	11.893	10.038	-15.60	0.19017	0.03752	418.6	17.685	201.471	0.08778	Lam
0.956	12.893	10.059	-21.98	0.19017	0.03751	427.2	17.723	203.773	0.08697	Lam

Table G.17: Power Law: Results for mud 'B' – 1″, 2″ & 3″ pipes.

Velocity [m/s]	Pressure Drop, [kPa] Meas.	Calc.	ϵ%	N [-]	$D_{\mathrm{eff,G}}$ [m]	$N_{\mathrm{Re,G}}$ [-]	τ_w [Pa]	$\dot{\gamma}_w$ [1/s]	$\mu_{w,\mathrm{app}}$ [Pa.s]	Type
1″ pipe: Total RMS = 1889.55, $\sigma = 51.11$.										
0.471	10.377	7.457	-28.14	0.73437	0.02302	429.0	4.417	163.758	0.02697	Lam
0.717	14.024	10.026	-28.51	0.82086	0.02397	739.4	5.935	239.408	0.02479	Lam
0.914	16.347	12.099	-25.99	0.86560	0.02446	996.0	7.162	299.118	0.02394	Lam
1.049	18.312	13.522	-26.16	0.88792	0.02470	1172.1	8.007	339.670	0.02357	Lam
1.428	22.760	17.607	-22.64	0.92898	0.02516	1668.5	10.427	454.078	0.02296	Lam
1.853	31.033	30.800	-0.75	0.95373	0.02544	2220.5	13.187	582.588	0.02263	Trans
2.104	38.631	60.815	57.43	0.96292	0.02555	2545.4	14.838	658.917	0.02252	Trans
2.692	55.758	112.420	101.62	0.97619	0.02573	3302.9	18.715	837.043	0.02236	Turb
2.861	61.487	119.234	93.92	0.97880	0.02571	3512.7	19.875	890.129	0.02233	Turb
2.935	66.838	122.069	82.63	0.97979	0.02572	3608.2	20.372	912.868	0.02232	Turb
3.088	73.140	127.827	74.77	0.98162	0.02575	3803.3	21.390	959.403	0.02229	Turb
3.272	80.738	134.705	66.84	0.98351	0.02578	4038.2	22.619	1015.563	0.02227	Turb
3.349	84.523	137.555	62.74	0.98422	0.02578	4136.1	23.133	1039.009	0.02226	Turb
2″ pipe: Total RMS = 79.43, $\sigma = 70.75$.										
0.202	2.082	1.645	-20.99	0.48587	0.03954	179.6	1.934	40.824	0.04737	Lam
0.409	3.110	2.313	-25.63	0.57724	0.04201	524.2	2.719	77.841	0.03493	Lam
0.562	3.744	2.753	-26.47	0.63240	0.04334	833.9	3.236	103.802	0.03117	Lam
0.724	4.447	3.195	-28.15	0.68160	0.04448	1191.3	3.756	130.264	0.02883	Lam
0.914	5.157	3.702	-28.21	0.72963	0.04559	1639.4	4.351	160.469	0.02712	Lam
1.076	5.736	4.127	-28.05	0.76362	0.04638	2037.0	4.851	185.631	0.02613	Lam
1.382	7.067	16.367	131.60	0.81503	0.04744	2806.5	5.806	233.033	0.02491	Trans
1.448	7.681	18.815	144.96	0.82424	0.04764	2976.6	6.013	243.220	0.02472	Turb
1.509	8.487	19.678	131.86	0.83209	0.04781	3131.7	6.202	252.453	0.02457	Turb
1.584	9.660	20.764	114.95	0.84123	0.04801	3324.9	6.436	263.904	0.02439	Turb
1.662	10.894	21.916	101.17	0.85009	0.04820	3527.4	6.682	275.847	0.02422	Turb
1.775	13.024	23.605	81.24	0.86177	0.04846	3820.5	7.037	293.065	0.02401	Turb
1.926	16.216	25.900	59.72	0.87555	0.04876	4212.4	7.513	316.008	0.02378	Turb
3″ pipe: Total RMS = 2.68, $\sigma = 14.21$.										
0.031	0.758	0.441	-41.82	0.37738	0.05471	10.6	0.778	4.546	0.17122	Lam
0.118	0.965	0.737	-23.63	0.41631	0.05629	91.4	1.299	16.764	0.07750	Lam
0.223	1.220	0.958	-21.48	0.45764	0.05820	250.8	1.689	30.625	0.05515	Lam
0.300	1.393	1.092	-21.61	0.48484	0.05927	397.9	1.925	40.443	0.04760	Lam
0.366	1.544	1.196	-22.54	0.50654	0.06024	542.8	2.110	48.652	0.04336	Lam
0.428	1.669	1.288	-22.83	0.52564	0.06097	687.8	2.272	56.153	0.04046	Lam
0.525	1.868	1.427	-23.61	0.55405	0.06198	936.6	2.515	67.823	0.03709	Lam
0.587	2.317	1.507	-34.96	0.57028	0.06276	1105.3	2.657	74.786	0.03553	Lam
0.789	2.965	1.767	-40.40	0.62014	0.06457	1703.8	3.116	97.736	0.03188	Lam
0.838	3.675	1.828	-50.26	0.63123	0.06497	1859.2	3.224	103.214	0.03124	Lam
0.865	4.406	1.861	-57.76	0.63708	0.06521	1946.4	3.282	106.162	0.03092	Lam
0.925	5.543	2.165	-60.94	0.64952	0.06573	2141.9	3.409	112.594	0.03027	Trans

Table G.18: Reiner-Philippoff: Results for mud 'A' – 1″, 2″ & 3″ pipes.

Velocity [m/s]	Pressure Drop, [kPa] Meas.	Calc.	$\epsilon\%$	N [-]	$D_{\text{eff},G}$ [m]	$N_{\text{Re},G}$ [-]	τ_w [Pa]	$\dot{\gamma}_w$ [1/s]	$\mu_{w,\text{app}}$ [Pa.s]	Type
1″ pipe: Total RMS = 906.22, $\sigma = 42.24$.										
0.562	31.006	18.006	-41.93	0.99999	0.02600	245.4	10.662	172.856	0.06168	Lam
0.600	31.171	19.217	-38.35	0.99999	0.02600	261.9	11.379	184.484	0.06168	Lam
0.693	32.350	22.216	-31.33	0.99999	0.02600	302.8	13.155	213.272	0.06168	Lam
0.732	32.798	23.477	-28.42	0.99999	0.02600	320.0	13.901	225.368	0.06168	Lam
0.843	34.026	27.023	-20.58	0.99999	0.02600	368.4	16.001	259.405	0.06168	Lam
1.010	35.605	32.386	-9.04	0.99998	0.02600	441.5	19.175	310.878	0.06168	Lam
1.151	36.218	36.880	1.83	0.99998	0.02600	502.8	21.835	354.004	0.06168	Lam
1.280	37.418	41.032	9.66	0.99997	0.02600	559.4	24.293	393.845	0.06168	Lam
1.484	40.196	47.578	18.37	0.99996	0.02600	648.7	28.167	456.649	0.06168	Lam
1.645	41.720	52.736	26.40	0.99995	0.02601	719.0	31.219	506.138	0.06168	Lam
2.410	49.118	77.237	57.25	0.99989	0.02601	1053.3	45.714	741.158	0.06168	Lam
2.702	50.980	86.595	69.86	0.99987	0.02601	1181.0	51.249	830.910	0.06168	Lam
2.829	51.724	90.688	75.33	0.99985	0.02601	1236.9	53.670	870.161	0.06168	Lam
3.048	54.538	97.701	79.14	0.99983	0.02601	1332.7	57.817	937.417	0.06168	Lam
3.101	58.592	99.401	69.65	0.99982	0.02601	1355.9	58.822	953.715	0.06168	Lam
3.242	62.453	103.914	66.39	0.99981	0.02602	1417.5	61.490	996.987	0.06168	Lam
3.381	67.293	108.348	61.01	0.99979	0.02602	1478.1	64.112	1039.507	0.06168	Lam
3.480	70.437	111.523	58.33	0.99978	0.02602	1521.4	65.989	1069.944	0.06168	Lam
3.621	76.663	116.045	51.37	0.99976	0.02602	1583.2	68.663	1113.303	0.06167	Lam
2″ pipe: Total RMS = 53.35, $\sigma = 23.17$.										
0.349	11.204	2.839	-74.66	1.00000	0.05160	302.6	3.338	54.111	0.06168	Lam
0.392	12.169	3.189	-73.79	1.00000	0.05160	339.9	3.749	60.774	0.06168	Lam
0.431	12.859	3.507	-72.73	1.00000	0.05160	373.7	4.122	66.822	0.06168	Lam
0.566	13.603	4.603	-66.16	1.00000	0.05160	490.5	5.410	87.708	0.06168	Lam
0.647	14.465	5.262	-63.62	1.00000	0.05160	560.8	6.185	100.278	0.06168	Lam
0.883	15.134	7.187	-52.51	1.00000	0.05160	765.9	8.447	136.944	0.06168	Lam
1.053	15.506	8.565	-44.76	0.99999	0.05160	912.9	10.067	163.214	0.06168	Lam
1.293	16.430	10.522	-35.96	0.99999	0.05160	1121.5	12.367	200.490	0.06168	Lam
1.522	17.065	12.379	-27.46	0.99999	0.05161	1319.5	14.549	235.875	0.06168	Lam
1.692	17.788	13.763	-22.63	0.99999	0.05161	1467.0	16.175	262.234	0.06168	Lam
1.811	18.264	14.730	-19.35	0.99998	0.05161	1570.1	17.311	280.657	0.06168	Lam
1.947	18.747	15.839	-15.51	0.99998	0.05161	1688.3	18.614	301.772	0.06168	Lam
2.012	19.395	16.367	-15.61	0.99998	0.05161	1744.6	19.234	311.833	0.06168	Lam
2.088	20.174	16.989	-15.79	0.99998	0.05161	1811.0	19.966	323.689	0.06168	Lam
2.141	20.857	17.421	-16.47	0.99998	0.05161	1857.0	20.473	331.908	0.06168	Lam
3″ pipe: Total RMS = 50.62, $\sigma = 8.48$.										
0.098	4.937	0.353	-92.85	1.00000	0.07739	126.8	0.622	10.082	0.06168	Lam
0.151	5.681	0.544	-90.42	1.00000	0.07739	195.8	0.960	15.564	0.06168	Lam
0.196	5.888	0.708	-87.98	1.00000	0.07739	254.5	1.248	20.227	0.06168	Lam
0.204	6.026	0.736	-87.79	1.00000	0.07739	264.8	1.298	21.047	0.06168	Lam
0.225	6.226	0.813	-86.94	1.00000	0.07739	292.5	1.434	23.252	0.06168	Lam
0.304	6.715	1.098	-83.65	1.00000	0.07739	394.8	1.936	31.380	0.06168	Lam
0.402	7.019	1.455	-79.27	1.00000	0.07739	523.3	2.565	41.588	0.06168	Lam
0.479	7.364	1.733	-76.47	1.00000	0.07739	623.1	3.055	49.527	0.06168	Lam
0.536	7.681	1.940	-74.74	1.00000	0.07740	697.7	3.420	55.450	0.06168	Lam
0.700	8.942	2.531	-71.70	1.00000	0.07740	910.2	4.462	72.336	0.06168	Lam
0.847	9.356	3.063	-67.26	1.00000	0.07740	1101.6	5.400	87.552	0.06168	Lam
0.894	10.011	3.234	-67.70	1.00000	0.07740	1163.1	5.702	92.435	0.06168	Lam
0.920	11.149	3.329	-70.14	1.00000	0.07740	1197.2	5.869	95.144	0.06168	Lam
0.945	11.893	3.417	-71.27	1.00000	0.07740	1228.9	6.024	97.664	0.06168	Lam
0.956	12.893	3.455	-73.20	1.00000	0.07740	1242.8	6.092	98.767	0.06168	Lam

Table G.19: Reiner-Philippoff: Results for mud 'B' – 1″, 2″ & 3″ pipes.

Velocity [m/s]	Pressure Drop, [kPa] Meas.	Calc.	ϵ%	N [-]	$D_{\text{eff},G}$ [m]	$N_{Re,G}$ [-]	τ_w [Pa]	$\dot{\gamma}_w$ [1/s]	$\mu_{w,\text{app}}$ [Pa.s]	Type
1″ pipe: Total RMS $= 56.24$, $\sigma = 8.11$.										
0.471	10.377	10.433	0.54	0.69142	0.02316	306.5	6.180	162.799	0.03796	Lam
0.717	14.024	13.895	-0.92	0.70604	0.02339	533.2	8.231	245.260	0.03356	Lam
0.914	16.347	16.459	0.68	0.71235	0.02349	731.6	9.750	311.431	0.03131	Lam
1.049	18.312	18.127	-1.01	0.71536	0.02353	873.9	10.739	356.555	0.03012	Lam
1.428	22.760	22.567	-0.85	0.72087	0.02361	1301.0	13.373	483.863	0.02764	Lam
1.853	31.033	27.194	-12.37	0.72443	0.02366	1816.8	16.117	626.447	0.02573	Lam
2.104	38.631	30.754	-20.39	0.72588	0.02368	2138.1	17.665	710.902	0.02485	Trans
2.692	55.758	58.985	5.79	0.72822	0.02371	2928.2	21.110	908.291	0.02324	Turb
2.861	61.487	61.624	0.22	0.72872	0.02371	3164.3	22.062	965.014	0.02286	Turb
2.935	66.838	62.789	-6.06	0.72892	0.02372	3270.0	22.479	990.100	0.02270	Turb
3.088	73.140	65.170	-10.90	0.72931	0.02372	3488.2	23.322	1041.398	0.02239	Turb
3.272	80.738	68.037	-15.73	0.72972	0.02373	3755.1	24.325	1103.245	0.02205	Turb
3.349	84.523	69.232	-18.09	0.72988	0.02373	3867.7	24.738	1129.049	0.02191	Turb
2″ pipe: Total RMS $= 3.39$, $\sigma = 10.60$.										
0.202	2.082	2.091	0.43	0.57809	0.04149	141.4	2.456	38.908	0.06313	Lam
0.409	3.110	3.093	-0.55	0.64370	0.04427	391.6	3.639	73.863	0.04927	Lam
0.562	3.744	3.768	0.64	0.66556	0.04507	608.7	4.432	99.809	0.04441	Lam
0.724	4.447	4.435	-0.27	0.67969	0.04557	857.7	5.217	127.145	0.04103	Lam
0.914	5.157	5.176	0.37	0.69048	0.04593	1171.8	6.087	159.269	0.03822	Lam
1.076	5.736	5.777	0.72	0.69690	0.04614	1454.4	6.794	186.605	0.03641	Lam
1.382	7.067	6.857	-2.97	0.70517	0.04641	2020.6	8.064	238.241	0.03385	Lam
1.448	7.681	7.624	-0.74	0.70653	0.04645	2148.6	8.330	249.463	0.03339	Trans
1.509	8.487	9.179	8.15	0.70767	0.04648	2266.3	8.569	259.657	0.03300	Trans
1.584	9.660	11.214	16.09	0.70898	0.04652	2414.2	8.864	272.331	0.03255	Trans
1.662	10.894	13.466	23.61	0.71022	0.04656	2570.9	9.168	285.578	0.03210	Trans
1.775	13.024	16.946	30.11	0.71183	0.04661	2800.5	9.600	304.702	0.03151	Trans
1.926	16.216	19.203	18.42	0.71370	0.04666	3113.1	10.166	330.218	0.03079	Turb
3″ pipe: Total RMS $= 1.50$, $\sigma = 17.49$.										
0.031	0.758	0.687	-9.37	0.32285	0.02986	6.8	1.212	8.329	0.14549	Lam
0.118	0.965	0.933	-3.32	0.46346	0.05211	72.1	1.645	18.110	0.09086	Lam
0.223	1.220	1.203	-1.39	0.54294	0.05958	199.8	2.120	29.916	0.07085	Lam
0.300	1.393	1.387	-0.43	0.57698	0.06215	313.4	2.444	38.565	0.06337	Lam
0.366	1.544	1.540	-0.26	0.59814	0.06360	422.0	2.713	46.081	0.05888	Lam
0.428	1.669	1.676	0.42	0.61323	0.06458	528.9	2.954	53.014	0.05572	Lam
0.525	1.868	1.885	0.91	0.63140	0.06569	709.3	3.321	63.997	0.05190	Lam
0.587	2.317	2.012	-13.16	0.64031	0.06621	828.6	3.545	70.895	0.05000	Lam
0.789	2.965	2.412	-18.65	0.66135	0.06738	1249.4	4.249	93.650	0.04537	Lam
0.838	3.675	2.501	-31.95	0.66517	0.06759	1357.8	4.415	99.210	0.04450	Lam
0.865	4.406	2.552	-42.08	0.66711	0.06769	1418.1	4.505	102.264	0.04405	Lam
0.925	5.543	2.664	-51.94	0.67102	0.06790	1553.1	4.701	108.991	0.04313	Lam

Table G.20: Robertson-Stiff (no plug flow): Results for mud 'A' – 1″, 2″ & 3″ pipes.

Velocity [m/s]	Pressure Drop, [kPa] Meas.	Calc.	ϵ%	N [-]	$D_{\mathrm{eff,G}}$ [m]	$\mathrm{N_{Re,G}}$ [-]	τ_w [Pa]	$\dot\gamma_w$ [1/s]	$\mu_{w,\mathrm{app}}$ [Pa.s]	Type
1″ pipe: Total RMS $= 54.25$, $\sigma = 7.27$.										
0.562	31.006	30.395	-1.97	0.29340	0.01394	145.4	17.991	322.266	0.05583	Lam
0.600	31.171	30.838	-1.07	0.29649	0.01415	163.2	18.262	338.995	0.05387	Lam
0.693	32.350	31.957	-1.21	0.30321	0.01458	210.7	18.904	380.428	0.04969	Lam
0.732	32.798	32.386	-1.26	0.30562	0.01475	232.2	19.156	397.290	0.04822	Lam
0.843	34.026	33.545	-1.41	0.31191	0.01506	296.5	19.876	447.764	0.04439	Lam
1.010	35.605	35.184	-1.18	0.31913	0.01553	406.2	20.843	520.456	0.04005	Lam
1.151	36.218	36.465	0.68	0.32398	0.01583	508.2	21.600	581.532	0.03714	Lam
1.280	37.418	37.586	0.45	0.32774	0.01605	610.4	22.263	638.044	0.03489	Lam
1.484	40.196	39.248	-2.36	0.33262	0.01633	786.0	23.246	727.229	0.03197	Lam
1.645	41.720	40.479	-2.97	0.33577	0.01650	936.3	23.974	797.562	0.03006	Lam
2.410	49.118	45.613	-7.14	0.34577	0.01703	1782.4	27.014	1131.879	0.02387	Lam
2.702	50.980	47.355	-7.11	0.34828	0.01716	2158.9	28.036	1259.619	0.02226	Trans
2.829	51.724	48.541	-6.15	0.34923	0.01721	2332.3	28.463	1315.490	0.02164	Trans
3.048	54.538	51.103	-6.30	0.35071	0.01727	2640.2	29.176	1411.779	0.02067	Trans
3.101	58.592	51.859	-11.49	0.35104	0.01729	2717.8	29.345	1435.295	0.02045	Trans
3.242	62.453	53.841	-13.79	0.35182	0.01736	2928.8	29.760	1493.725	0.01992	Turb
3.381	67.293	55.295	-17.83	0.35258	0.01739	3139.6	30.183	1554.831	0.01941	Turb
3.480	70.437	56.338	-20.02	0.35309	0.01741	3293.9	30.479	1598.486	0.01907	Turb
3.621	76.663	57.829	-24.57	0.35377	0.01744	3518.8	30.893	1660.580	0.01860	Turb
2″ pipe: Total RMS $= 1.89$, $\sigma = 5.98$.										
0.349	11.204	12.570	12.19	0.23863	0.01806	68.3	14.783	154.632	0.09560	Lam
0.392	12.169	12.752	4.79	0.24341	0.01917	85.0	14.985	163.596	0.09160	Lam
0.431	12.859	12.915	0.43	0.24773	0.02001	101.5	15.176	172.266	0.08810	Lam
0.566	13.603	13.447	-1.15	0.26059	0.02239	167.9	15.805	202.103	0.07820	Lam
0.647	14.465	13.751	-4.94	0.26714	0.02351	214.6	16.165	220.105	0.07344	Lam
0.883	15.134	14.568	-3.74	0.28240	0.02596	377.5	17.138	272.220	0.06296	Lam
1.053	15.506	15.122	-2.48	0.29106	0.02713	516.4	17.796	310.484	0.05732	Lam
1.293	16.430	15.866	-3.43	0.30037	0.02858	744.7	18.623	361.962	0.05145	Lam
1.522	17.065	16.499	-3.32	0.30758	0.02955	991.1	19.370	411.963	0.04702	Lam
1.692	17.788	16.947	-4.73	0.31235	0.02996	1190.5	19.931	451.752	0.04412	Lam
1.811	18.264	17.249	-5.56	0.31511	0.03032	1340.0	20.284	477.742	0.04246	Lam
1.947	18.747	17.584	-6.20	0.31798	0.03068	1519.8	20.677	507.576	0.04074	Lam
2.012	19.395	17.740	-8.53	0.31925	0.03084	1608.6	20.860	521.807	0.03998	Lam
2.088	20.174	17.922	-11.16	0.32067	0.03102	1715.9	21.072	538.587	0.03913	Lam
2.141	20.857	18.045	-13.48	0.32161	0.03113	1791.8	21.218	550.224	0.03856	Lam
3″ pipe: Total RMS $= 4.18$, $\sigma = 22.52$.										
0.098	4.937	7.493	51.77	0.19163	0.00850	6.0	13.213	91.847	0.14386	Lam
0.151	5.681	7.611	33.97	0.19919	0.01209	14.0	13.425	99.640	0.13474	Lam
0.196	5.888	7.709	30.93	0.20513	0.01473	23.3	13.601	106.268	0.12799	Lam
0.204	6.026	7.726	28.21	0.20614	0.01516	25.2	13.632	107.432	0.12689	Lam
0.225	6.226	7.771	24.81	0.20878	0.01628	30.6	13.713	110.567	0.12403	Lam
0.304	6.715	7.952	18.42	0.21782	0.01989	54.6	14.007	122.122	0.11470	Lam
0.402	7.019	8.151	16.13	0.22786	0.02356	93.5	14.362	136.634	0.10511	Lam
0.479	7.364	8.301	12.72	0.23487	0.02589	130.1	14.631	148.030	0.09884	Lam
0.536	7.681	8.410	9.49	0.23969	0.02741	160.9	14.827	156.561	0.09470	Lam
0.700	8.942	8.709	-2.61	0.25141	0.03108	264.6	15.347	180.156	0.08519	Lam
0.847	9.356	8.964	-4.19	0.26051	0.03357	376.5	15.801	201.880	0.07827	Lam
0.894	10.011	9.044	-9.66	0.26314	0.03426	416.0	15.941	208.841	0.07633	Lam
0.920	11.149	9.087	-18.49	0.26458	0.03460	438.5	16.021	212.813	0.07528	Lam
0.945	11.893	9.127	-23.26	0.26586	0.03493	460.0	16.092	216.393	0.07436	Lam
0.956	12.893	9.145	-29.07	0.26640	0.03507	469.6	16.123	217.959	0.07397	Lam

Table G.21: Robertson-Stiff (no plug flow): Results for mud 'B' – 1″, 2″ & 3″ pipes.

Vel.	Pressure Drop, [kPa]			λ	Type
[m/s]	Meas.	Calc.	ϵ%	[-]	
1″ pipe, mud 'A': Total RMS = 56.06, $\sigma = 8.37$.					
0.471	10.377	10.643	2.56	0.1257	Lam
0.717	14.024	14.050	0.19	0.0950	Lam
0.914	16.347	16.593	1.51	0.0805	Lam
1.049	18.312	18.250	-0.34	0.0732	Lam
1.428	22.760	22.669	-0.40	0.0589	Lam
1.853	31.033	27.279	-12.10	0.0489	Lam
2.104	38.631	30.828	-20.20	0.0447	Trans
2.692	55.758	58.985	5.79	0.0447	Turb
2.861	61.487	61.624	0.22	0.0447	Turb
2.935	66.838	62.789	-6.06	0.0447	Turb
3.088	73.140	65.170	-10.90	0.0447	Turb
3.272	80.738	68.037	-15.73	0.0447	Turb
3.349	84.523	69.232	-18.09	0.0447	Turb

Vel.	Pressure Drop, [kPa]			λ	Type
[m/s]	Meas.	Calc.	ϵ%	[-]	
2″ pipe, mud 'A': Total RMS = 3.44, $\sigma = 9.52$.					
0.202	2.082	2.279	9.47	0.2951	Lam
0.409	3.110	3.246	4.38	0.2076	Lam
0.562	3.744	3.904	4.28	0.1726	Lam
0.724	4.447	4.558	2.50	0.1479	Lam
0.914	5.157	5.280	2.39	0.1274	Lam
1.076	5.736	5.874	2.40	0.1145	Lam
1.382	7.067	6.945	-1.72	0.0970	Lam
1.448	7.681	7.706	0.32	0.0940	Trans
1.509	8.487	9.247	8.95	0.0914	Trans
1.584	9.660	11.266	16.63	0.0884	Trans
1.662	10.894	13.494	23.87	0.0855	Trans
1.775	13.024	16.954	30.18	0.0817	Trans
1.926	16.216	19.203	18.42	0.0817	Turb

Vel.	Pressure Drop, [kPa]			λ	Type
[m/s]	Meas.	Calc.	ϵ%	[-]	
3″ pipe, mud 'A': Total RMS = 1.38, $\sigma = 21.48$.					
0.031	0.758	0.871	14.91	0.5169	Lam
0.118	0.965	1.088	12.74	0.4122	Lam
0.223	1.220	1.339	9.72	0.3350	Lam
0.300	1.393	1.513	8.59	0.2965	Lam
0.366	1.544	1.659	7.42	0.2704	Lam
0.428	1.669	1.789	7.20	0.2506	Lam
0.525	1.868	1.990	6.52	0.2254	Lam
0.587	2.317	2.112	-8.84	0.2123	Lam
0.789	2.965	2.500	-15.68	0.1797	Lam
0.838	3.675	2.592	-29.47	0.1734	Lam
0.865	4.406	2.642	-40.04	0.1701	Lam
0.925	5.543	2.751	-50.37	0.1634	Lam

Vel.	Pressure Drop, [kPa]			λ	Type
[m/s]	Meas.	Calc.	ϵ%	[-]	
1″ pipe, mud 'B': Total RMS = 58.62, $\sigma = 11.91$.					
0.562	31.006	34.708	11.94	0.4921	Lam
0.600	31.171	35.110	12.64	0.4864	Lam
0.693	32.350	36.070	11.50	0.4735	Lam
0.732	32.798	36.461	11.17	0.4684	Lam
0.843	34.026	37.521	10.27	0.4552	Lam
1.010	35.605	39.026	9.61	0.4367	Lam
1.151	36.218	40.212	11.03	0.4239	Lam
1.280	37.418	41.261	10.27	0.4131	Lam
1.484	40.196	42.829	6.55	0.3980	Lam
1.645	41.720	43.993	5.45	0.3874	Lam
2.410	49.118	48.772	-0.70	0.3488	Lam
2.702	50.980	50.413	-1.11	0.3374	Trans
2.829	51.724	51.101	-1.20	0.3329	Trans
3.048	54.538	52.242	-4.21	0.3256	Trans
3.101	58.592	52.512	-10.38	0.3239	Trans
3.242	62.453	53.841	-13.79	0.3239	Turb
3.381	67.293	55.295	-17.83	0.3239	Turb
3.480	70.437	56.338	-20.02	0.3239	Turb
3.621	76.663	57.829	-24.57	0.3239	Turb

Vel.	Pressure Drop, [kPa]			λ	Type
[m/s]	Meas.	Calc.	ϵ%	[-]	
2″ pipe, mud 'B': Total RMS = 4.50, $\sigma = 9.97$.					
0.349	11.204	15.130	35.04	0.5676	Lam
0.392	12.169	15.278	25.55	0.5621	Lam
0.431	12.859	15.410	19.83	0.5562	Lam
0.566	13.603	15.859	16.58	0.5426	Lam
0.647	14.465	16.118	11.43	0.5338	Lam
0.883	15.134	16.834	11.23	0.5111	Lam
1.053	15.506	17.315	11.67	0.4969	Lam
1.293	16.430	17.960	9.31	0.4791	Lam
1.522	17.065	18.537	8.63	0.4642	Lam
1.692	17.788	18.947	6.51	0.4541	Lam
1.811	18.264	19.223	5.25	0.4467	Lam
1.947	18.747	19.532	4.19	0.4397	Lam
2.012	19.395	19.676	1.45	0.4364	Lam
2.088	20.174	19.843	-1.64	0.4328	Lam
2.141	20.857	19.958	-4.31	0.4303	Lam

Vel.	Pressure Drop, [kPa]			λ	Type
[m/s]	Meas.	Calc.	ϵ%	[-]	
3″ pipe, mud 'B': Total RMS = 9.39, $\sigma = 30.40$.					
0.098	4.937	9.406	90.52	0.6087	Lam
0.151	5.681	9.495	67.14	0.6029	Lam
0.196	5.888	9.571	62.55	0.5982	Lam
0.204	6.026	9.584	59.04	0.5973	Lam
0.225	6.226	9.619	54.50	0.5951	Lam
0.304	6.715	9.749	45.18	0.5872	Lam
0.402	7.019	9.888	40.88	0.5778	Lam
0.479	7.364	10.009	35.92	0.5708	Lam
0.536	7.681	10.099	31.48	0.5658	Lam
0.700	8.942	10.346	15.71	0.5522	Lam
0.847	9.356	10.562	12.89	0.5409	Lam
0.894	10.011	10.630	6.18	0.5375	Lam
0.920	11.149	10.667	-4.32	0.5356	Lam
0.945	11.893	10.702	-10.02	0.5339	Lam
0.956	12.893	10.717	-16.88	0.5331	Lam

Table G.22: Robertson-Stiff (including plug flow): Results for 1″, 2″ & 3″ pipes.

Velocity [m/s]	Pressure Drop, [kPa] Meas.	Calc.	ϵ%	N [-]	$D_{\text{eff},G}$ [m]	$N_{\text{Re},G}$ [-]	τ_w [Pa]	$\dot{\gamma}_w$ [1/s]	$\mu_{w,\text{app}}$ [Pa.s]	Type
1″ pipe: Total RMS $= 27.45$, $\sigma = 8.44$.										
0.471	10.377	10.922	5.25	0.64117	0.02252	293.0	6.466	167.431	0.03862	Lam
0.717	14.024	14.230	1.47	0.66749	0.02286	520.8	8.426	250.935	0.03358	Lam
0.914	16.347	16.679	2.03	0.68348	0.02304	722.2	9.877	317.472	0.03111	Lam
1.049	18.312	18.274	-0.21	0.69269	0.02314	867.3	10.821	362.522	0.02985	Lam
1.428	22.760	22.532	-1.00	0.71374	0.02338	1303.2	13.350	488.667	0.02732	Lam
1.853	31.033	27.065	-12.79	0.73169	0.02357	1828.0	16.018	628.783	0.02547	Lam
2.104	38.631	31.012	-19.72	0.74060	0.02365	2152.1	17.550	711.843	0.02465	Trans
2.692	55.758	62.574	12.22	0.75750	0.02387	2949.1	20.960	902.270	0.02323	Turb
2.861	61.487	65.875	7.14	0.76169	0.02391	3184.3	21.924	957.282	0.02290	Turb
2.935	66.838	67.340	0.75	0.76346	0.02392	3289.2	22.347	981.581	0.02277	Turb
3.088	73.140	70.349	-3.82	0.76694	0.02396	3505.5	23.207	1031.215	0.02250	Turb
3.272	80.738	73.996	-8.35	0.77090	0.02399	3769.1	24.234	1090.966	0.02221	Turb
3.349	84.523	75.524	-10.65	0.77248	0.02401	3880.0	24.660	1115.870	0.02210	Turb
2″ pipe: Total RMS $= 1.83$, $\sigma = 6.92$.										
0.202	2.082	2.264	8.74	0.56145	0.04255	130.5	2.661	37.941	0.07014	Lam
0.409	3.110	3.357	7.94	0.59393	0.04355	361.2	3.946	75.082	0.05255	Lam
0.562	3.744	4.042	7.96	0.61081	0.04403	568.0	4.750	102.167	0.04649	Lam
0.724	4.447	4.704	5.78	0.62600	0.04439	809.2	5.530	130.520	0.04237	Lam
0.914	5.157	5.425	5.20	0.63980	0.04465	1118.7	6.377	163.823	0.03893	Lam
1.076	5.736	6.009	4.76	0.64983	0.04488	1399.6	7.061	191.858	0.03680	Lam
1.382	7.067	7.033	-0.48	0.66556	0.04534	1971.1	8.266	243.833	0.03390	Lam
1.448	7.681	7.250	-5.61	0.66861	0.04541	2100.5	8.521	255.185	0.03339	Trans
1.509	8.487	8.670	2.16	0.67128	0.04547	2219.6	8.750	265.477	0.03296	Trans
1.584	9.660	10.543	9.14	0.67446	0.04554	2369.6	9.031	278.243	0.03246	Trans
1.662	10.894	12.638	16.01	0.67764	0.04561	2528.6	9.321	291.556	0.03197	Trans
1.775	13.024	15.919	22.23	0.68201	0.04570	2762.1	9.733	310.733	0.03132	Trans
1.926	16.216	18.567	14.50	0.68746	0.04582	3080.5	10.274	336.254	0.03055	Turb
3″ pipe: Total RMS $= 1.26$, $\sigma = 19.05$.										
0.031	0.758	0.615	-18.87	0.50837	0.03540	7.6	1.085	7.026	0.15443	Lam
0.118	0.965	0.938	-2.80	0.52959	0.05950	71.7	1.655	15.859	0.10434	Lam
0.223	1.220	1.283	5.16	0.54961	0.06293	187.2	2.262	28.323	0.07987	Lam
0.300	1.393	1.501	7.75	0.56104	0.06380	289.4	2.647	37.571	0.07044	Lam
0.366	1.544	1.675	8.48	0.56955	0.06424	387.7	2.954	45.624	0.06474	Lam
0.428	1.669	1.824	9.29	0.57645	0.06467	485.8	3.216	52.938	0.06075	Lam
0.525	1.868	2.049	9.69	0.58622	0.06503	652.1	3.612	64.647	0.05588	Lam
0.587	2.317	2.182	-5.83	0.59171	0.06523	763.4	3.848	71.956	0.05347	Lam
0.789	2.965	2.590	-12.65	0.60711	0.06594	1163.0	4.565	95.695	0.04770	Lam
0.838	3.675	2.684	-26.97	0.61046	0.06604	1266.6	4.732	101.539	0.04661	Lam
0.865	4.406	2.736	-37.90	0.61223	0.06609	1324.6	4.823	104.738	0.04605	Lam
0.925	5.543	2.847	-48.64	0.61683	0.06626	1454.6	5.019	111.686	0.04494	Lam

Table G.23: Sisko: Results for mud 'A' – 1″, 2″ & 3″ pipes.

Velocity [m/s]	Pressure Drop, [kPa] Meas.	Calc.	ϵ%	N [-]	$D_{\mathrm{eff},G}$ [m]	$N_{Re,G}$ [-]	τ_w [Pa]	$\dot{\gamma}_w$ [1/s]	$\mu_{w,app}$ [Pa.s]	Type
1″ pipe: Total RMS $= 24.80$, $\sigma = 4.73$.										
0.562	31.006	30.599	-1.31	0.25551	0.01326	144.4	18.126	338.800	0.05350	Lam
0.600	31.171	31.016	-0.50	0.26171	0.01345	162.3	18.369	356.713	0.05150	Lam
0.693	32.350	32.020	-1.02	0.27669	0.01381	210.1	18.964	401.568	0.04723	Lam
0.732	32.798	32.391	-1.24	0.28211	0.01400	231.9	19.183	418.429	0.04585	Lam
0.843	34.026	33.461	-1.66	0.29753	0.01441	297.4	19.818	468.173	0.04233	Lam
1.010	35.605	34.983	-1.75	0.31862	0.01495	408.6	20.719	540.849	0.03831	Lam
1.151	36.218	36.156	-0.17	0.33503	0.01531	511.8	21.450	601.387	0.03567	Lam
1.280	37.418	37.240	-0.48	0.34811	0.01570	616.2	22.053	652.286	0.03381	Lam
1.484	40.196	38.823	-3.42	0.36747	0.01622	794.9	22.986	732.323	0.03139	Lam
1.645	41.720	40.050	-4.00	0.38195	0.01653	946.5	23.716	796.050	0.02979	Lam
2.410	49.118	45.384	-7.60	0.43807	0.01785	1791.9	26.871	1079.834	0.02488	Lam
2.702	50.980	47.332	-7.16	0.45610	0.01823	2160.5	28.015	1185.358	0.02363	Trans
2.829	51.724	49.587	-4.13	0.46376	0.01836	2327.4	28.524	1232.609	0.02314	Trans
3.048	54.538	53.612	-1.70	0.47527	0.01866	2628.3	29.315	1306.604	0.02244	Trans
3.101	58.592	54.759	-6.54	0.47811	0.01872	2702.1	29.516	1325.432	0.02227	Trans
3.242	62.453	58.106	-6.96	0.48542	0.01886	2901.3	30.042	1374.965	0.02185	Turb
3.381	67.293	59.818	-11.11	0.49232	0.01900	3101.6	30.553	1423.160	0.02147	Turb
3.480	70.437	61.297	-12.98	0.49993	0.01910	3247.5	30.915	1457.262	0.02121	Turb
3.621	76.663	63.055	-17.75	0.50636	0.01924	3459.0	31.427	1505.603	0.02087	Turb
2″ pipe: Total RMS $= 2.00$, $\sigma = 6.05$.										
0.349	11.204	12.493	11.50	0.16794	0.02287	68.8	14.684	122.077	0.12029	Lam
0.392	12.169	12.737	4.67	0.17448	0.02293	85.1	14.972	136.740	0.10949	Lam
0.431	12.859	12.932	0.57	0.17997	0.02313	101.3	15.202	149.039	0.10200	Lam
0.566	13.603	13.552	-0.37	0.19831	0.02369	166.6	15.932	191.028	0.08340	Lam
0.647	14.465	13.882	-4.03	0.20845	0.02413	212.7	16.311	214.465	0.07605	Lam
0.883	15.134	14.714	-2.78	0.23404	0.02525	374.0	17.298	279.889	0.06180	Lam
1.053	15.506	15.229	-1.79	0.24978	0.02610	513.3	17.903	322.648	0.05549	Lam
1.293	16.430	15.912	-3.15	0.27018	0.02710	741.5	18.704	381.766	0.04899	Lam
1.522	17.065	16.489	-3.38	0.28701	0.02805	990.4	19.383	433.921	0.04467	Lam
1.692	17.788	16.902	-4.98	0.29876	0.02866	1194.2	19.869	472.249	0.04207	Lam
1.811	18.264	17.182	-5.92	0.30655	0.02905	1345.7	20.198	498.554	0.04051	Lam
1.947	18.747	17.493	-6.69	0.31507	0.02948	1528.2	20.564	528.211	0.03893	Lam
2.012	19.395	17.639	-9.05	0.31899	0.02968	1618.4	20.735	542.169	0.03824	Lam
2.088	20.174	17.809	-11.72	0.32351	0.02991	1727.3	20.933	558.482	0.03748	Lam
2.141	20.857	17.930	-14.03	0.32667	0.03005	1804.0	21.074	570.102	0.03697	Lam
3″ pipe: Total RMS $= 3.04$, $\sigma = 18.17$.										
0.098	4.937	2.923	-40.79	1.00000	0.07739	15.3	5.154	10.082	0.51118	Lam
0.151	5.681	4.512	-20.58	1.00000	0.07739	23.6	7.956	15.564	0.51118	Lam
0.196	5.888	6.882	16.88	0.11850	0.05116	26.2	12.122	30.598	0.39618	Lam
0.204	6.026	6.956	15.43	0.12205	0.04803	28.0	12.271	33.916	0.36181	Lam
0.225	6.226	7.151	14.86	0.12434	0.04315	33.3	12.587	41.704	0.30182	Lam
0.304	6.715	7.586	12.97	0.13921	0.03669	57.1	13.377	66.201	0.20206	Lam
0.402	7.019	7.968	13.52	0.15311	0.03469	95.5	14.050	92.773	0.15144	Lam
0.479	7.364	8.202	11.38	0.16321	0.03443	131.6	14.462	111.327	0.12990	Lam
0.536	7.681	8.366	8.92	0.16945	0.03421	161.8	14.752	125.449	0.11759	Lam
0.700	8.942	8.744	-2.21	0.18527	0.03477	263.4	15.418	161.010	0.09576	Lam
0.847	9.356	9.033	-3.45	0.19820	0.03552	373.5	15.927	190.764	0.08349	Lam
0.894	10.011	9.125	-8.85	0.20239	0.03565	412.2	16.090	200.665	0.08018	Lam
0.920	11.149	9.170	-17.75	0.20442	0.03583	434.6	16.168	205.498	0.07868	Lam
0.945	11.893	9.204	-22.61	0.20596	0.03613	456.2	16.228	209.221	0.07756	Lam
0.956	12.893	9.228	-28.43	0.20709	0.03607	465.3	16.271	211.929	0.07677	Lam

Table G.24: Sisko: Results for mud 'B' – 1″, 2″ & 3″ pipes.

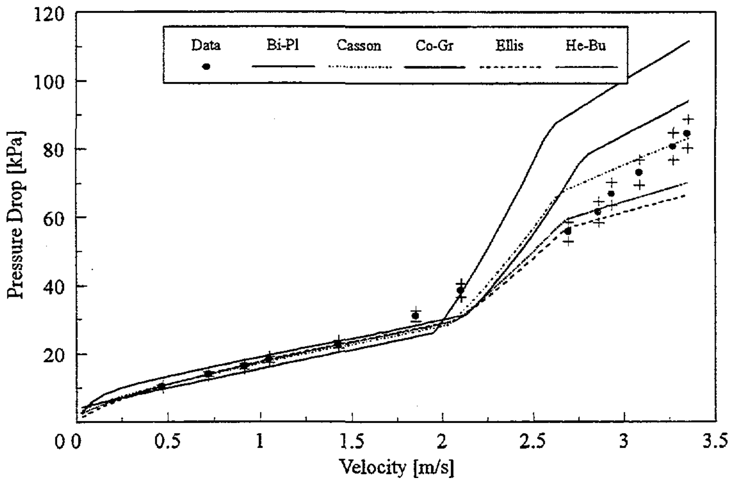

Figure G.1: Predicted and measured laminar, transitional and turbulent pressure losses for mud 'A', 1″ pipe for Bingham Plastic, Casson, Collins-Graves, Ellis *et al.* and Herschel-Bulkley rheological models. +'s represent ±5% data measurement accuracy.

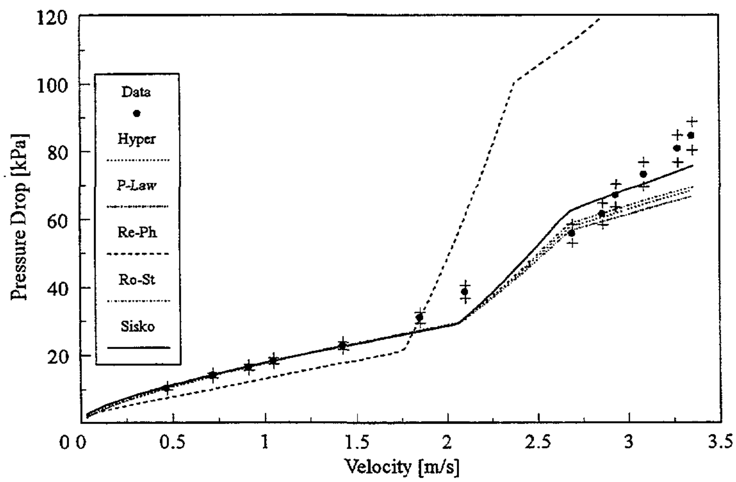

Figure G.2: Predicted and measured laminar, transitional and turbulent pressure losses for mud 'A', 1″ pipe for Hyperbolic, Power Law, Reiner-Philippoff, Robertson-Stiff and Sisko rheological models. +'s represent ±5% data measurement accuracy.

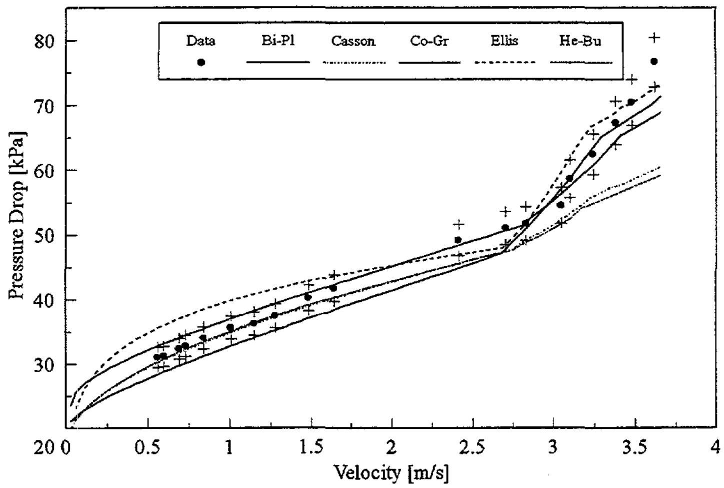

Figure G.3: Predicted and measured laminar, transitional and turbulent pressure losses for mud 'B', 1″ pipe for Bingham Plastic, Casson, Collins-Graves, Ellis *et al.* and Herschel-Bulkley rheological models. +'s represent ±5% data measurement accuracy.

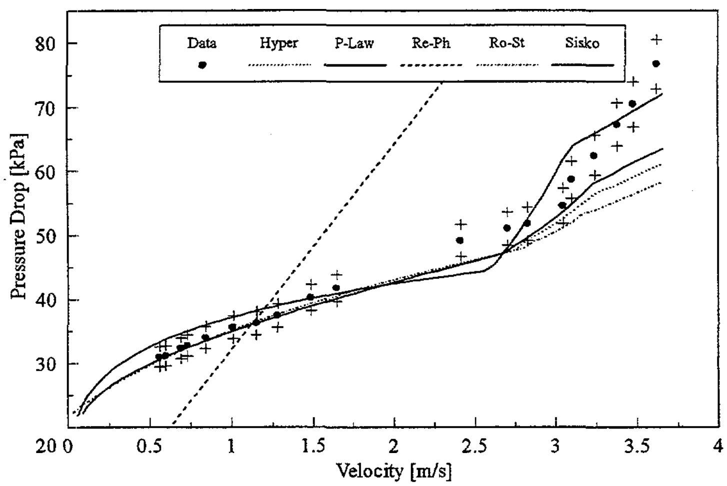

Figure G.4: Predicted and measured laminar, transitional and turbulent pressure losses for mud 'B', 1″ pipe for Hyperbolic, Power Law, Reiner-Philippoff, Robertson-Stiff and Sisko rheological models. +'s represent ±5% data measurement accuracy.

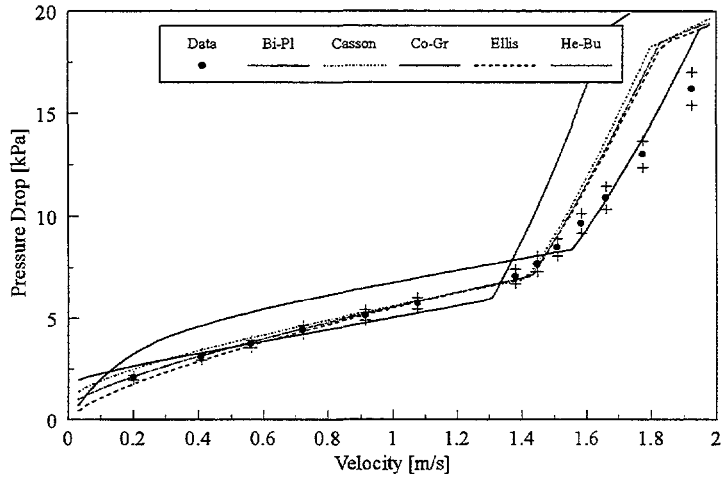

Figure G.5: Predicted and measured laminar, transitional and turbulent pressure losses for mud 'A', 2″ pipe for Bingham Plastic, Casson, Collins-Graves, Ellis *et al.* and Herschel-Bulkley rheological models. +'s represent ±5% data measurement accuracy.

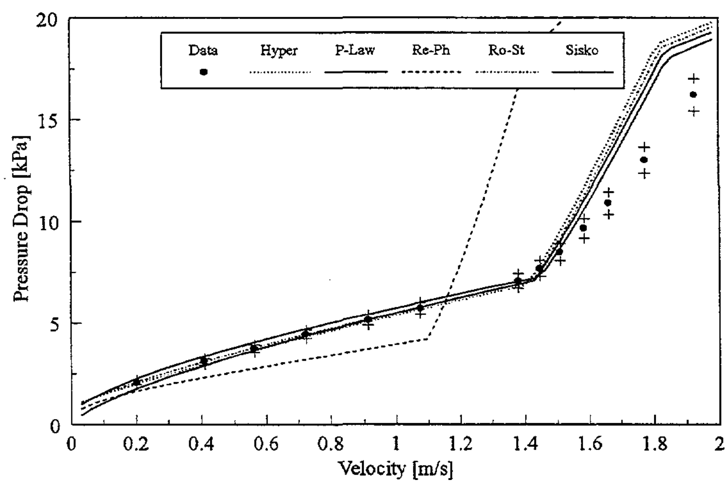

Figure G.6: Predicted and measured laminar, transitional and turbulent pressure losses for mud 'A', 2″ pipe for Hyperbolic, Power Law, Reiner-Philippoff, Robertson-Stiff and Sisko rheological models. +'s represent ±5% data measurement accuracy.

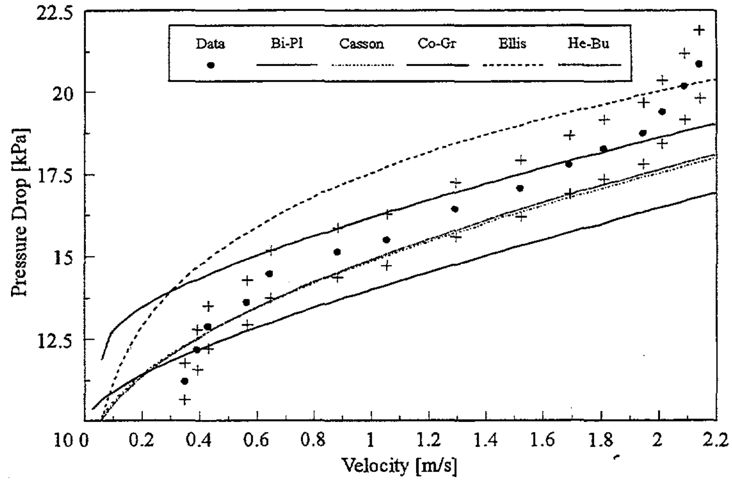

Figure G.7: Predicted and measured laminar, transitional and turbulent pressure losses for mud 'B', 2″ pipe for Bingham Plastic, Casson, Collins-Graves, Ellis *et al.* and Herschel-Bulkley rheological models. +'s represent ±5% data measurement accuracy.

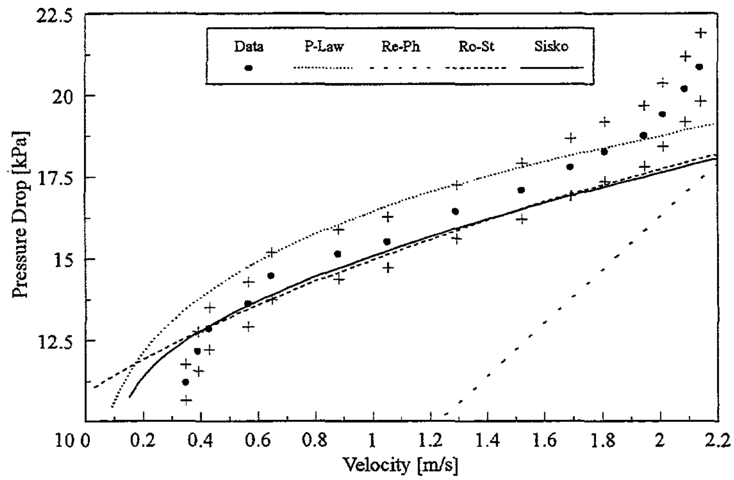

Figure G.8: Predicted and measured laminar, transitional and turbulent pressure losses for mud 'B', 2″ pipe for Power Law, Reiner-Philippoff, Robertson-Stiff and Sisko rheological models. +'s represent ±5% data measurement accuracy.

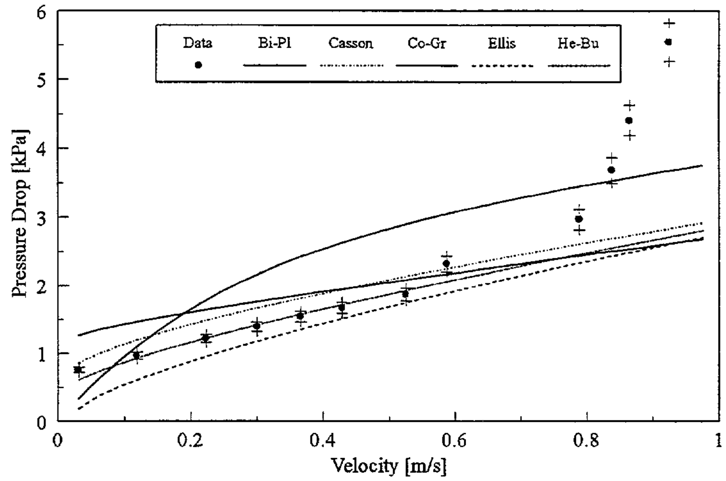

Figure G.9: Predicted and measured laminar, transitional and turbulent pressure losses for mud 'A', 3″ pipe for Bingham Plastic, Casson, Collins-Graves, Ellis *et al.* and Herschel-Bulkley rheological models. +'s represent ±5% data measurement accuracy.

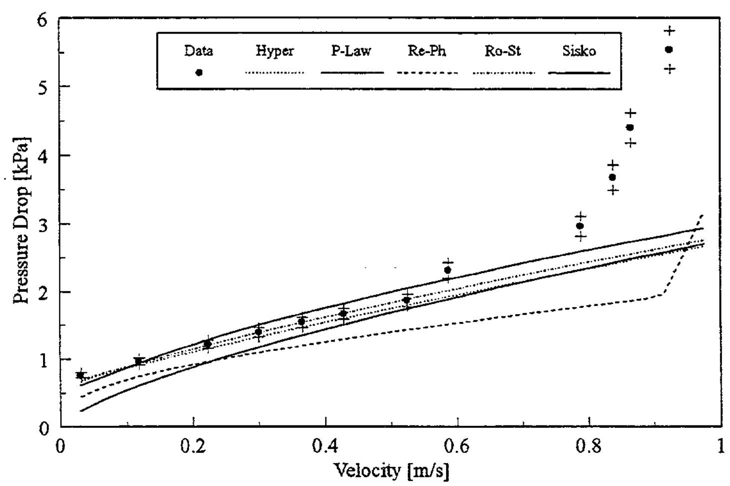

Figure G.10: Predicted and measured laminar, transitional and turbulent pressure losses for mud 'A', 3″ pipe for Hyperbolic, Power Law, Reiner-Philippoff, Robertson-Stiff and Sisko rheological models. +'s represent ±5% data measurement accuracy.

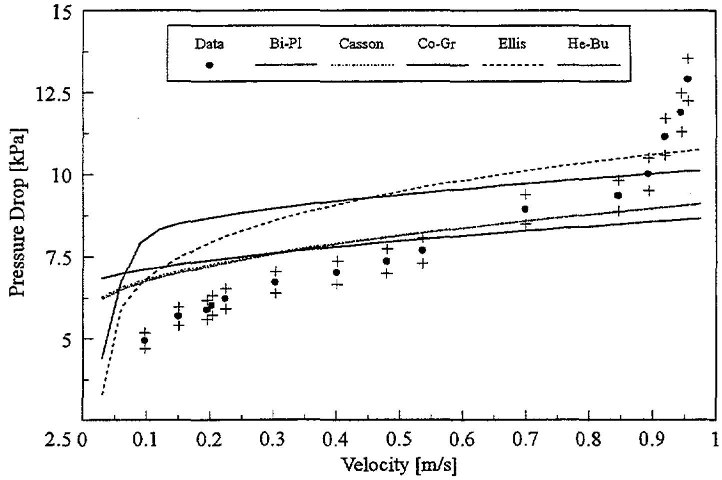

Figure G.11: Predicted and measured laminar, transitional and turbulent pressure losses for mud 'B', 3″ pipe for Bingham Plastic, Casson, Collins-Graves, Ellis *et al.* and Herschel-Bulkley rheological models. +'s represent ±5% data measurement accuracy.

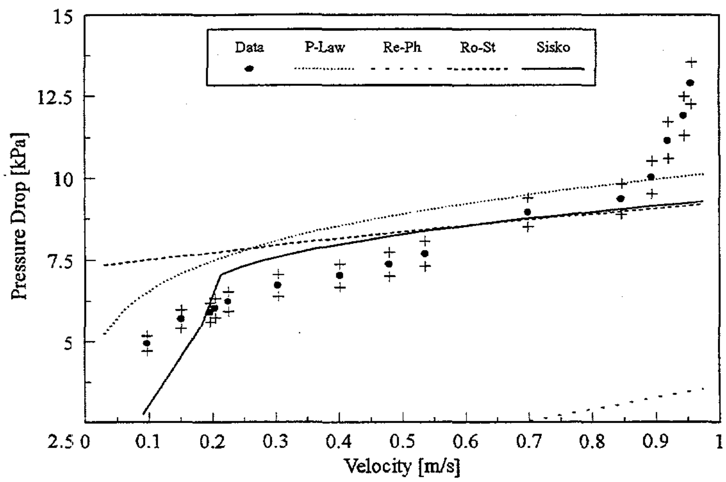

Figure G.12: Predicted and measured laminar, transitional and turbulent pressure losses for mud 'B', 3″ pipe for Power Law, Reiner-Philippoff, Robertson-Stiff and Sisko rheological models. +'s represent ±5% data measurement accuracy.

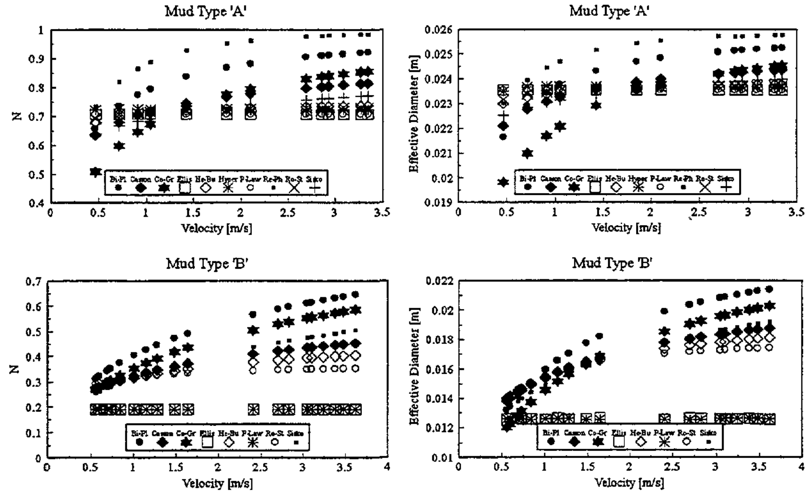

Figure G.13: Variation of N and $D_{\text{eff},G}$ against velocity for mud types 'A' and 'B'.

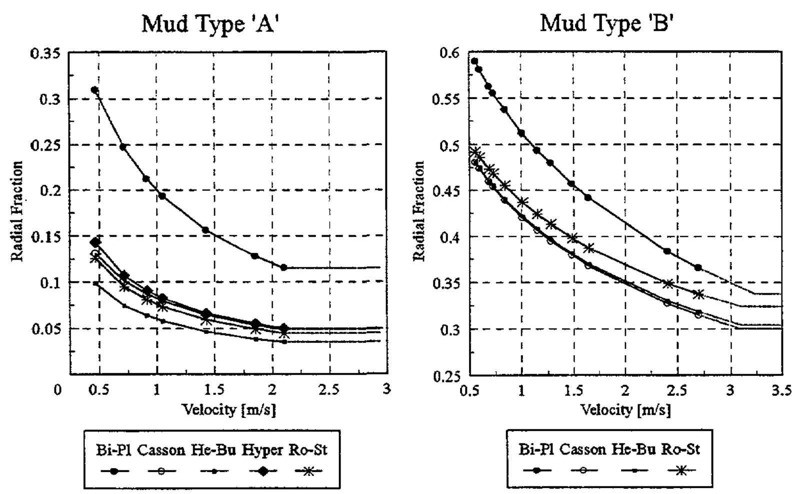

Figure G.14: Variation of plug flow boundary delimiter radial fraction (λ) with average fluid velocity for 2″ pipe. Dotted lines represent calculated, non-physical, λ values extended into transitional and turbulent flow regions.

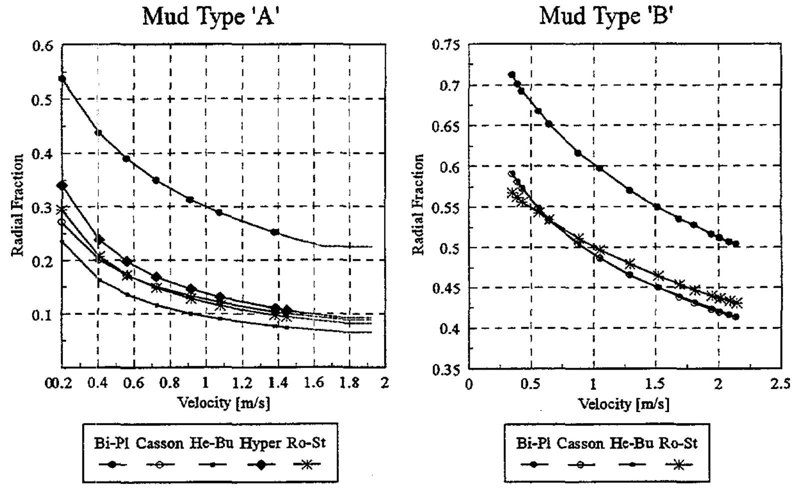

Figure G.15: Variation of plug flow boundary delimiter radial fraction (λ) with average fluid velocity for 1″ pipe. Dotted lines represent calculated, non-physical, λ values extended into transitional and turbulent flow regions.

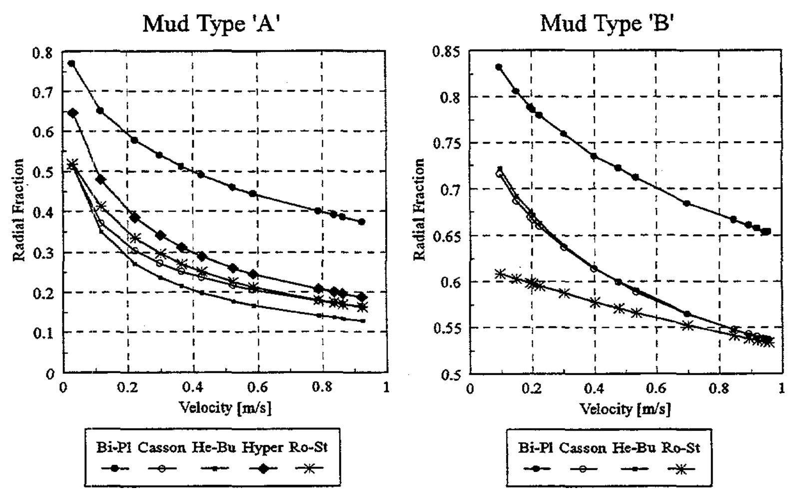

Figure G.16: Variation of plug flow boundary delimiter radial fraction (λ) with average fluid velocity for 2″ pipe. Dotted lines represent calculated, non-physical, λ values extended into transitional and turbulent flow regions.

Appendix H

Annular Flow Pressure Loss: Tables & Results

Velocity [m/s]	Pressure Drop, [kPa] Meas.	Calc.	ϵ%	N [-]	$D_{\mathrm{eff,G}}$ [m]	$\mathrm{N}_{\mathrm{Re,G}}$ [-]	τ_w [Pa]	$\dot{\gamma}_w$ [1/s]	λ [-]	$(\lambda_{[-]}, \lambda_{[+]})$ [-,-]
Mud 'A', 1″× 3″ annulus: Total RMS = 0.750, $\sigma = 17.56$, $\psi = 0.4307655$.										
0.135	2.779	4.171	50.09	0.37011	0.01571	38.9	3.088	53.053	0.6982	(0.5784, 0.8428)
0.233	3.723	4.927	32.33	0.45642	0.01754	92.4	3.578	75.817	0.7053	(0.6024, 0.8258)
0.336	4.682	5.626	20.16	0.51963	0.01868	161.5	4.049	97.677	0.7103	(0.6192, 0.8149)
0.415	5.343	6.120	14.54	0.55780	0.01930	221.3	4.399	113.905	0.7133	(0.6290, 0.8089)
0.494	6.026	6.588	9.32	0.58871	0.01977	284.7	4.730	129.251	0.7158	(0.6371, 0.8042)
0.691	7.632	7.699	0.88	0.64875	0.02062	457.5	5.538	166.785	0.7206	(0.6527, 0.7956)
0.790	8.246	8.227	-0.23	0.67237	0.02092	550.5	5.938	185.321	0.7225	(0.6587, 0.7925)
0.941	9.467	9.019	-4.73	0.70210	0.02129	696.4	6.530	212.824	0.7250	(0.6665, 0.7886)
1.008	9.735	9.366	-3.80	0.71408	0.02144	764.1	6.804	225.529	0.7259	(0.6695, 0.7871)
1.074	10.377	9.700	-6.52	0.72441	0.02156	830.5	7.059	237.368	0.7268	(0.6723, 0.7857)
Mud 'A', 1.5″× 3″ annulus: Total RMS = 5.167, $\sigma = 9.52$, $\psi = 0.6230597$.										
0.164	6.102	8.448	38.44	0.41850	0.01092	37.1	3.345	64.982	0.8128	(0.7503, 0.8806)
0.343	9.508	11.655	22.59	0.54315	0.01246	114.8	4.258	107.354	0.8178	(0.7719, 0.8665)
0.443	11.066	13.293	20.12	0.58847	0.01293	166.8	4.727	129.124	0.8196	(0.7792, 0.8620)
0.564	13.059	15.211	16.48	0.63110	0.01334	235.3	5.273	154.484	0.8212	(0.7857, 0.8583)
0.636	14.520	16.295	12.23	0.65206	0.01353	277.6	5.591	169.232	0.8220	(0.7888, 0.8565)
1.012	19.788	21.904	10.69	0.73029	0.01418	518.8	7.213	244.515	0.8247	(0.8000, 0.8502)
1.096	21.381	23.129	8.18	0.74283	0.01428	575.5	7.565	260.843	0.8252	(0.8017, 0.8493)
1.124	22.084	23.536	6.58	0.74675	0.01431	594.6	7.682	266.277	0.8253	(0.8022, 0.8490)
1.229	23.139	25.055	8.28	0.76041	0.01441	666.8	8.120	286.610	0.8258	(0.8041, 0.8480)
Mud 'B', 1″× 3″ annulus: Total RMS = 7.380, $\sigma = 1.16$, $\psi = 0.04307655$.										
0.146	14.962	16.598	10.93	0.00019	0.00002	0.0	11.347	0.000	0.6781	(0.5093, 0.9030)
0.223	15.465	17.643	14.09	0.05441	0.00392	3.2	12.188	42.850	0.6815	(0.5210, 0.8915)
0.284	15.899	18.327	15.27	0.08581	0.00572	9.3	12.607	69.871	0.6835	(0.5278, 0.8852)
0.333	16.575	18.829	13.60	0.10591	0.00675	15.9	12.890	88.138	0.6850	(0.5334, 0.8798)
0.386	17.085	19.362	13.33	0.12535	0.00769	24.9	13.177	106.636	0.6864	(0.5381, 0.8757)
0.482	17.602	20.199	14.75	0.15450	0.00897	44.7	13.631	135.952	0.6887	(0.5459, 0.8688)
0.575	18.630	20.973	12.58	0.17849	0.00994	68.2	14.030	161.648	0.6905	(0.5523, 0.8633)
0.743	19.602	22.251	13.51	0.21546	0.01130	121.1	14.691	204.344	0.6934	(0.5619, 0.8556)
0.959	20.774	23.707	14.12	0.25428	0.01259	205.3	15.455	253.650	0.6964	(0.5723, 0.8474)
1.040	21.477	24.235	12.84	0.26635	0.01296	240.1	15.710	270.109	0.6973	(0.5756, 0.8448)
Mud 'B', 1.5″× 3″ annulus: Total RMS = 57.702, $\sigma = 3.44$, $\psi = 0.6230597$.										
0.064	21.070	24.747	17.45	0.00010	0.00001	0.0	11.107	0.000	0.7979	(0.6764, 0.9411)
0.096	21.663	26.142	20.68	0.00710	0.00038	0.0	11.607	5.350	0.7992	(0.6837, 0.9342)
0.168	23.511	28.594	21.62	0.06226	0.00275	1.9	12.290	49.410	0.8013	(0.6953, 0.9235)
0.247	25.904	30.823	18.99	0.10053	0.00410	6.8	12.813	83.160	0.8031	(0.7041, 0.9161)
0.331	27.738	32.827	18.35	0.13122	0.00506	14.7	13.266	112.373	0.8045	(0.7113, 0.9100)
0.430	28.648	34.961	22.04	0.16149	0.00592	27.5	13.745	143.274	0.8059	(0.7178, 0.9048)
0.601	31.130	38.234	22.82	0.20292	0.00698	56.9	14.460	189.408	0.8077	(0.7269, 0.8975)
0.774	33.019	41.279	25.02	0.23528	0.00772	94.0	15.072	228.894	0.8093	(0.7340, 0.8923)
0.939	34.536	43.980	27.35	0.26321	0.00831	137.4	15.643	265.758	0.8106	(0.7395, 0.8884)
1.124	36.563	46.779	27.94	0.28980	0.00883	192.4	16.229	303.545	0.8116	(0.7449, 0.8843)

Table H.1: Bingham Plastic: Results for laminar flow of muds 'A' and 'B' flowing in 1″× 3″ and 1.5″× 3″ [nominal] annular conduits.

Velocity	Pressure Drop, [kPa]			N	$D_{\mathrm{eff,G}}$	$\mathrm{N_{Re,G}}$	τ_w	$\dot{\gamma}_w$	λ	$(\lambda_{[-]}, \lambda_{[+]})$
[m/s]	Meas.	Calc.	ϵ%	[-]	[m]	[-]	[Pa]	[1/s]	[-]	[-,-]
Mud 'A', 1″× 3″ annulus: Total RMS = 0.365, $\sigma = 11.32$, $\psi = 0.4307655$.										
0.135	2.779	3.565	28.28	0.42672	0.01695	29.7	2.557	31.109	0.7093	(0.6456, 0.7792)
0.233	3.723	4.434	19.11	0.48820	0.01813	71.8	3.208	51.087	0.7148	(0.6631, 0.7705)
0.336	4.682	5.215	11.38	0.52997	0.01885	126.9	3.803	71.377	0.7185	(0.6743, 0.7657)
0.415	5.343	5.762	7.85	0.55367	0.01924	174.4	4.218	86.397	0.7206	(0.6805, 0.7632)
0.494	6.026	6.284	4.28	0.57332	0.01954	226.1	4.615	101.370	0.7223	(0.6854, 0.7612)
0.691	7.632	7.472	-2.09	0.61055	0.02009	368.8	5.540	137.995	0.7256	(0.6944, 0.7581)
0.790	8.246	8.045	-2.44	0.62523	0.02030	446.8	5.983	156.271	0.7268	(0.6978, 0.7569)
0.941	9.467	8.877	-6.24	0.64416	0.02056	571.9	6.636	183.997	0.7285	(0.7022, 0.7558)
1.008	9.735	9.239	-5.09	0.65121	0.02065	629.1	6.907	195.717	0.7291	(0.7038, 0.7554)
1.074	10.377	9.595	-7.54	0.65791	0.02074	687.0	7.180	207.663	0.7294	(0.7050, 0.7547)
Mud 'A', 1.5″× 3″ annulus: Total RMS = 4.524, $\sigma = 6.89$, $\psi = 0.6230597$.										
0.164	6.102	7.866	28.91	0.45178	0.01137	27.1	2.796	38.129	0.8171	(0.7875, 0.8479)
0.343	9.508	11.402	19.92	0.53591	0.01238	86.8	3.901	74.868	0.8205	(0.7999, 0.8416)
0.443	11.066	13.166	18.97	0.56522	0.01269	128.0	4.445	94.888	0.8217	(0.8038, 0.8400)
0.564	13.059	15.168	16.15	0.59253	0.01297	183.2	5.061	118.726	0.8227	(0.8071, 0.8386)
0.636	14.520	16.299	12.25	0.60577	0.01310	217.7	5.407	132.566	0.8232	(0.8087, 0.8379)
1.012	19.788	21.906	10.70	0.65611	0.01357	421.1	7.106	204.381	0.8250	(0.8142, 0.8359)
1.096	21.381	23.116	8.11	0.66453	0.01364	470.4	7.467	220.308	0.8251	(0.8149, 0.8355)
1.124	22.084	23.512	6.47	0.66717	0.01366	487.1	7.586	225.600	0.8252	(0.8152, 0.8354)
1.229	23.139	24.985	7.98	0.67643	0.01374	550.8	8.026	245.382	0.8256	(0.8161, 0.8351)
Mud 'B', 1″× 3″ annulus: Total RMS = 6.675, $\sigma = 1.41$, $\psi = 0.4307655$.										
0.146	14.962	16.396	9.58	0.09757	0.00633	2.2	11.512	26.250	0.6796	(0.5363, 0.8612)
0.223	15.465	17.508	13.21	0.12610	0.00772	6.8	12.276	46.751	0.6823	(0.5469, 0.8511)
0.284	15.899	18.258	14.84	0.14279	0.00847	12.2	12.759	62.305	0.6838	(0.5533, 0.8451)
0.333	16.575	18.782	13.31	0.15454	0.00897	17.7	13.116	75.020	0.6849	(0.5577, 0.8413)
0.386	17.085	19.319	13.08	0.16531	0.00942	24.7	13.456	88.070	0.6860	(0.5620, 0.8372)
0.482	17.602	20.160	14.53	0.18194	0.01008	39.9	14.009	111.052	0.6876	(0.5685, 0.8316)
0.575	18.630	20.928	12.34	0.19589	0.01060	58.0	14.499	133.233	0.6889	(0.5735, 0.8276)
0.743	19.602	22.127	12.88	0.21650	0.01134	98.0	15.272	171.431	0.6910	(0.5812, 0.8215)
0.959	20.774	23.493	13.09	0.23779	0.01206	162.3	16.138	218.515	0.6931	(0.5893, 0.8152)
1.040	21.477	23.957	11.55	0.24432	0.01227	189.1	16.418	234.679	0.6937	(0.5917, 0.8132)
Mud 'B', 1.5″× 3″ annulus: Total RMS = 46.859, $\sigma = 2.28$, $\psi = 0.6230597$.										
0.064	21.070	24.386	15.74	0.07686	0.00328	0.3	11.001	15.564	0.7988	(0.6972, 0.9152)
0.096	21.663	25.954	19.81	0.09712	0.00399	0.9	11.500	25.982	0.8000	(0.7041, 0.9089)
0.168	23.511	28.554	21.45	0.12745	0.00495	3.3	12.313	47.897	0.8017	(0.7138, 0.9004)
0.247	25.904	30.769	18.78	0.15079	0.00563	7.9	13.000	70.784	0.8029	(0.7213, 0.8937)
0.331	27.738	32.746	18.05	0.16967	0.00614	14.5	13.598	93.750	0.8039	(0.7270, 0.8890)
0.430	28.648	34.755	21.32	0.18678	0.00658	24.5	14.176	118.427	0.8049	(0.7321, 0.8850)
0.601	31.130	37.745	21.25	0.21065	0.00716	47.4	15.047	159.880	0.8062	(0.7390, 0.8796)
0.774	33.019	40.370	22.26	0.22988	0.00760	77.1	15.807	200.022	0.8073	(0.7442, 0.8756)
0.939	34.536	42.627	23.43	0.24517	0.00793	111.2	16.455	236.840	0.8081	(0.7482, 0.8727)
1.124	36.563	44.973	23.00	0.25979	0.00824	155.1	17.111	276.516	0.8088	(0.7520, 0.8700)

Table H.2: Casson: Results for laminar flow of muds 'A' and 'B' flowing in 1″× 3″ and 1.5″× 3″ [nominal] annular conduits.

Velocity [m/s]	Pressure Drop, [kPa] Meas.	Calc.	ϵ%	N [-]	$D_{\text{eff},G}$ [m]	$N_{\text{Re},G}$ [-]	τ_w [Pa]	$\dot{\gamma}_w$ [1/s]	λ [-]	$(\lambda_{[-]}, \lambda_{[+]})$ [-,-]
Mud 'A', 1″× 3″ annulus: Total RMS = 1.174, $\sigma = 11.60$, $\psi = 0.4307655$.										
0.135	2.779	3.596	29.40	0.59508	0.01987	23.9	3.253	27.210	0.7326	(n/a , n/a)
0.233	3.723	4.972	33.54	0.42031	0.01682	48.9	4.572	53.504	0.7214	(n/a , n/a)
0.336	4.682	5.995	28.04	0.37503	0.01582	88.3	5.480	85.306	0.7178	(n/a , n/a)
0.415	5.343	6.623	23.96	0.39351	0.01624	130.0	6.012	108.719	0.7179	(n/a , n/a)
0.494	6.026	7.176	19.08	0.42370	0.01689	179.4	6.481	130.711	0.7185	(n/a , n/a)
0.691	7.632	8.393	9.97	0.49341	0.01822	321.2	7.483	178.972	0.7214	(n/a , n/a)
0.790	8.246	8.951	8.55	0.52184	0.01872	399.6	7.940	201.119	0.7227	(n/a , n/a)
0.941	9.467	9.758	3.07	0.56171	0.01936	527.1	8.614	233.710	0.7247	(n/a , n/a)
1.008	9.735	10.112	3.87	0.57569	0.01958	585.7	8.906	247.799	0.7255	(n/a , n/a)
1.074	10.377	10.449	0.70	0.58832	0.01977	645.5	9.186	261.848	0.7264	(n/a , n/a)
Mud 'A', 1.5″× 3″ annulus: Total RMS = 14.867, $\sigma = 11.98$, $\psi = 0.6230597$.										
0.164	6.102	9.159	50.10	0.51022	0.01209	20.6	3.907	38.014	0.8173	(n/a , n/a)
0.343	9.508	12.823	34.86	0.38149	0.01038	64.1	5.757	97.196	0.8187	(n/a , n/a)
0.443	11.066	14.553	31.51	0.42088	0.01096	103.5	6.441	128.788	0.8200	(n/a , n/a)
0.564	13.059	16.474	26.15	0.47063	0.01161	159.1	7.145	162.583	0.8214	(n/a , n/a)
0.636	14.520	17.592	21.15	0.49630	0.01193	194.5	7.528	181.135	0.8220	(n/a , n/a)
1.012	19.788	23.104	16.76	0.59568	0.01300	405.1	9.357	270.121	0.8245	(n/a , n/a)
1.096	21.381	24.301	13.66	0.61127	0.01315	455.7	9.739	288.661	0.8249	(n/a , n/a)
1.124	22.084	24.699	11.84	0.61630	0.01320	473.0	9.869	294.947	0.8251	(n/a , n/a)
1.229	23.139	26.180	13.14	0.63300	0.01336	537.7	10.325	317.058	0.8255	(n/a , n/a)
Mud 'B', 1″× 3″ annulus: Total RMS = 2.928, $\sigma = 2.52$, $\psi = 0.4307655$.										
0.146	14.962	16.416	9.72	0.32165	0.01451	1.6	12.355	8.821	0.6764	(n/a , n/a)
0.223	15.465	17.232	11.43	0.18986	0.01038	2.2	13.469	12.382	0.6795	(n/a , n/a)
0.284	15.899	17.763	11.72	0.08247	0.00554	2.1	14.194	18.428	0.6816	(n/a , n/a)
0.333	16.575	18.142	9.46	0.03690	0.00281	2.5	14.687	38.158	0.6831	(n/a , n/a)
0.386	17.085	18.536	8.49	0.06129	0.00433	7.6	15.080	66.142	0.6846	(n/a , n/a)
0.482	17.602	19.213	9.16	0.09676	0.00629	21.8	15.672	108.723	0.6872	(n/a , n/a)
0.575	18.630	19.781	6.18	0.12318	0.00758	39.9	16.145	142.616	0.6892	(n/a , n/a)
0.743	19.602	20.754	5.87	0.16147	0.00926	82.6	16.883	195.479	0.6924	(n/a , n/a)
0.959	20.774	21.906	5.45	0.19926	0.01073	152.4	17.680	252.666	0.6958	(n/a , n/a)
1.040	21.477	22.309	3.87	0.21171	0.01117	182.9	17.960	272.700	0.6969	(n/a , n/a)
Mud 'B', 1.5″× 3″ annulus: Total RMS = 23.979, $\sigma = 2.15$, $\psi = 0.6230597$.										
0.064	21.070	24.522	16.38	0.35769	0.01001	0.4	11.987	8.069	0.7980	(n/a , n/a)
0.096	21.663	25.630	18.31	0.27715	0.00859	0.7	12.785	9.890	0.7992	(n/a , n/a)
0.168	23.511	27.510	17.01	0.13251	0.00510	1.0	13.884	14.953	0.8015	(n/a , n/a)
0.247	25.904	29.192	12.69	0.04040	0.00188	1.4	14.742	42.066	0.8032	(n/a , n/a)
0.331	27.738	30.772	10.94	0.07081	0.00306	5.8	15.338	84.602	0.8048	(n/a , n/a)
0.430	28.648	32.465	13.32	0.10989	0.00440	15.5	15.904	125.306	0.8064	(n/a , n/a)
0.601	31.130	35.055	12.61	0.15231	0.00567	38.6	16.700	182.399	0.8085	(n/a , n/a)
0.774	33.019	37.474	13.49	0.18554	0.00655	69.9	17.382	231.279	0.8103	(n/a , n/a)
0.939	34.536	39.609	14.69	0.21270	0.00721	107.1	17.982	274.303	0.8116	(n/a , n/a)
1.124	36.563	41.914	14.63	0.23804	0.00778	154.8	18.581	317.203	0.8129	(n/a , n/a)

Table H.3: Collins-Graves: Results for laminar flow of muds 'A' and 'B' flowing in 1″× 3″ and 1.5″× 3″ [nominal] annular conduits.

Velocity	Pressure Drop, [kPa]			N	$D_{\text{eff,G}}$	$N_{\text{Re,G}}$	τ_w	$\dot{\gamma}_w$	λ	$(\lambda_{[-]}, \lambda_{[+]})$
[m/s]	Meas.	Calc.	ϵ%	[-]	[m]	[-]	[Pa]	[1/s]	[-]	[-,-]
Mud 'A', 1″× 3″ annulus: Total RMS = 1.974, $\sigma = 3.87$, $\psi = 0.4307655$.										
0.135	2.779	1.994	-28.24	0.70793	0.02137	47.5	1.746	26.967	0.7391	(n/a , n/a)
0.233	3.723	2.949	-20.80	0.70793	0.02137	96.4	2.581	46.821	0.7388	(n/a , n/a)
0.336	4.682	3.828	-18.24	0.70793	0.02137	154.6	3.344	67.516	0.7386	(n/a , n/a)
0.415	5.343	4.446	-16.78	0.70793	0.02137	203.1	3.884	83.393	0.7386	(n/a , n/a)
0.494	6.026	5.030	-16.53	0.70793	0.02137	254.3	4.394	99.274	0.7386	(n/a , n/a)
0.691	7.632	6.381	-16.39	0.70793	0.02137	392.3	5.573	138.874	0.7386	(n/a , n/a)
0.790	8.246	7.019	-14.88	0.70793	0.02137	466.7	6.129	158.855	0.7385	(n/a , n/a)
0.941	9.467	7.942	-16.10	0.70793	0.02137	584.7	6.935	189.130	0.7385	(n/a , n/a)
1.008	9.735	8.341	-14.32	0.70793	0.02137	639.3	7.283	202.673	0.7385	(n/a , n/a)
1.074	10.377	8.723	-15.94	0.70793	0.02137	693.8	7.616	215.909	0.7385	(n/a , n/a)
Mud 'A', 1.5″× 3″ annulus: Total RMS = 1.381, $\sigma = 3.34$, $\psi = 0.6230597$.										
0.164	6.102	5.863	-3.91	0.70793	0.01400	41.0	2.128	35.642	0.8267	(n/a , n/a)
0.343	9.508	9.890	4.02	0.70793	0.01400	106.4	3.594	74.730	0.8266	(n/a , n/a)
0.443	11.066	11.854	7.12	0.70793	0.01400	148.3	4.311	96.651	0.8266	(n/a , n/a)
0.564	13.059	14.078	7.80	0.70793	0.01400	202.9	5.121	123.228	0.8266	(n/a , n/a)
0.636	14.520	15.310	5.44	0.70793	0.01400	236.5	5.569	138.745	0.8266	(n/a , n/a)
1.012	19.788	21.268	7.48	0.70793	0.01400	431.3	7.742	220.974	0.8266	(n/a , n/a)
1.096	21.381	22.511	5.28	0.70793	0.01400	478.2	8.193	239.349	0.8266	(n/a , n/a)
1.124	22.084	22.918	3.78	0.70793	0.01400	494.1	8.341	245.473	0.8266	(n/a , n/a)
1.229	23.139	24.418	5.53	0.70793	0.01400	554.6	8.886	268.440	0.8265	(n/a , n/a)
Mud 'B', 1″× 3″ annulus: Total RMS = 6.731, $\sigma = 2.40$, $\psi = 0.4307655$.										
0.146	14.962	15.935	6.50	0.19017	0.01039	2.8	12.406	22.121	0.6904	(n/a , n/a)
0.223	15.465	17.366	12.29	0.19017	0.01039	6.3	13.567	35.412	0.6897	(n/a , n/a)
0.284	15.899	18.225	14.63	0.19017	0.01039	9.9	14.263	46.059	0.6893	(n/a , n/a)
0.333	16.575	18.806	13.46	0.19017	0.01039	13.3	14.740	54.761	0.6893	(n/a , n/a)
0.386	17.085	19.353	13.28	0.19017	0.01039	17.4	15.163	63.536	0.6891	(n/a , n/a)
0.482	17.602	20.206	14.79	0.19017	0.01039	26.2	15.839	79.916	0.6890	(n/a , n/a)
0.575	18.630	20.903	12.20	0.19017	0.01039	36.2	16.404	96.087	0.6890	(n/a , n/a)
0.743	19.602	22.004	12.26	0.19017	0.01039	58.0	17.246	125.034	0.6889	(n/a , n/a)
0.959	20.774	23.097	11.18	0.19017	0.01039	92.9	18.143	163.226	0.6891	(n/a , n/a)
1.040	21.477	23.454	9.21	0.19017	0.01039	107.5	18.421	176.852	0.6889	(n/a , n/a)
Mud 'B', 1.5″× 3″ annulus: Total RMS = 36.974, $\sigma = 2.88$, $\psi = 0.6230597$.										
0.064	21.070	23.709	12.53	0.19017	0.00667	0.4	10.500	9.199	0.8052	(n/a , n/a)
0.096	21.663	25.759	18.91	0.19017	0.00667	1.0	11.797	16.976	0.8048	(n/a , n/a)
0.168	23.511	28.773	22.38	0.19017	0.00667	2.9	13.445	33.758	0.8046	(n/a , n/a)
0.247	25.904	31.029	19.78	0.19017	0.00667	6.1	14.594	51.960	0.8044	(n/a , n/a)
0.331	27.738	32.857	18.45	0.19017	0.00667	10.5	15.500	71.320	0.8044	(n/a , n/a)
0.430	28.648	34.515	20.48	0.19017	0.00667	17.0	16.311	93.256	0.8045	(n/a , n/a)
0.601	31.130	36.868	18.43	0.19017	0.00667	31.4	17.420	131.822	0.8043	(n/a , n/a)
0.774	33.019	38.661	17.09	0.19017	0.00667	50.0	18.308	171.178	0.8043	(n/a , n/a)
0.939	34.536	40.120	16.17	0.19017	0.00667	71.3	19.013	208.847	0.8043	(n/a , n/a)
1.124	36.563	41.519	13.55	0.19017	0.00667	99.2	19.698	251.523	0.8043	(n/a , n/a)

Table H.4: Ellis *et al.*: Results for laminar flow of muds 'A' and 'B' flowing in 1″× 3″ and 1.5″× 3″ [nominal] annular conduits.

Velocity	Pressure Drop, [kPa]			N	$D_{\text{eff},G}$	$N_{\text{Re},G}$	τ_w	$\dot{\gamma}_w$	λ	$(\lambda_{[-]}, \lambda_{[+]})$
[m/s]	Meas.	Calc.	ϵ%	[-]	[m]	[-]	[Pa]	[1/s]	[-]	[-,-]
Mud 'A', 1″× 3″ annulus: Total RMS = 0.396, $\sigma = 5.80$, $\psi = 0.4307655$.										
0.135	2.779	3.015	8.51	0.42459	0.01690	21.2	1.421	12.387	0.7170	(0.6609, 0.7778)
0.233	3.723	3.917	5.20	0.51514	0.01860	57.8	1.957	24.435	0.7221	(0.6784, 0.7685)
0.336	4.682	4.735	1.13	0.56458	0.01941	105.7	2.464	37.429	0.7251	(0.6889, 0.7633)
0.415	5.343	5.316	-0.51	0.58898	0.01978	147.1	2.825	47.448	0.7268	(0.6944, 0.7606)
0.494	6.026	5.870	-2.59	0.60712	0.02004	191.7	3.171	57.547	0.7280	(0.6986, 0.7586)
0.691	7.632	7.147	-6.35	0.63734	0.02046	314.2	3.983	82.999	0.7303	(0.7061, 0.7553)
0.790	8.246	7.755	-5.96	0.64789	0.02060	381.2	4.374	96.019	0.7312	(0.7088, 0.7543)
0.941	9.467	8.629	-8.86	0.66005	0.02077	487.4	4.933	115.379	0.7323	(0.7121, 0.7530)
1.008	9.735	9.026	-7.28	0.66460	0.02082	537.0	5.180	124.222	0.7326	(0.7133, 0.7525)
1.074	10.377	9.392	-9.50	0.66857	0.02088	586.4	5.416	132.827	0.7330	(0.7144, 0.7521)
Mud 'A', 1.5″× 3″ annulus: Total RMS = 4.466, $\sigma = 3.52$, $\psi = 0.6230597$.										
0.164	6.102	7.162	17.37	0.52988	0.01231	28.5	2.084	27.580	0.8203	(0.7961, 0.8453)
0.343	9.508	10.944	15.10	0.59893	0.01303	83.4	3.005	52.632	0.8228	(0.8069, 0.8390)
0.443	11.066	12.822	15.87	0.61943	0.01323	119.8	3.458	66.284	0.8235	(0.8099, 0.8373)
0.564	13.059	14.953	14.51	0.63723	0.01340	168.0	3.979	82.872	0.8241	(0.8124, 0.8360)
0.636	14.520	16.145	11.19	0.64508	0.01347	197.5	4.262	92.254	0.8244	(0.8136, 0.8354)
1.012	19.788	21.982	11.09	0.67256	0.01371	371.3	5.677	142.483	0.8253	(0.8173, 0.8333)
1.096	21.381	23.206	8.53	0.67653	0.01374	412.9	5.964	153.273	0.8254	(0.8179, 0.8330)
1.124	22.084	23.608	6.90	0.67780	0.01375	427.0	6.061	156.993	0.8255	(0.8180, 0.8329)
1.229	23.139	25.096	8.46	0.68215	0.01379	481.1	6.421	170.894	0.8256	(0.8186, 0.8326)
Mud 'B', 1″× 3″ annulus: Total RMS = 8.098, $\sigma = 1.45$, $\psi = 0.4307655$.										
0.146	14.962	16.419	9.74	0.10335	0.00662	2.4	11.469	27.490	0.6801	(0.5364, 0.8622)
0.223	15.465	17.557	13.53	0.13368	0.00807	7.3	12.245	47.876	0.6826	(0.5473, 0.8514)
0.284	15.899	18.295	15.07	0.15180	0.00886	13.1	12.761	63.945	0.6840	(0.5535, 0.8453)
0.333	16.575	18.828	13.59	0.16317	0.00933	18.6	13.108	75.816	0.6851	(0.5579, 0.8414)
0.386	17.085	19.394	13.52	0.17390	0.00976	25.7	13.453	88.438	0.6861	(0.5619, 0.8377)
0.482	17.602	20.252	15.06	0.19024	0.01039	41.0	14.015	110.716	0.6876	(0.5682, 0.8322)
0.575	18.630	21.015	12.80	0.20336	0.01088	58.8	14.501	131.655	0.6889	(0.5731, 0.8281)
0.743	19.602	22.209	13.30	0.22244	0.01155	97.7	15.271	167.896	0.6906	(0.5808, 0.8212)
0.959	20.774	23.589	13.55	0.24224	0.01220	160.8	16.161	214.268	0.6926	(0.5882, 0.8154)
1.040	21.477	24.048	11.97	0.24854	0.01240	188.4	16.483	232.192	0.6931	(0.5906, 0.8134)
Mud 'B', 1.5″× 3″ annulus: Total RMS = 54.629, $\sigma = 2.19$, $\psi = 0.6230597$.										
0.064	21.070	24.421	15.90	0.07978	0.00339	0.3	10.930	16.219	0.7991	(0.6970, 0.9160)
0.096	21.663	26.032	20.17	0.10177	0.00414	1.0	11.431	26.619	0.8000	(0.7039, 0.9093)
0.168	23.511	28.643	21.83	0.13421	0.00515	3.5	12.260	48.299	0.8017	(0.7140, 0.9003)
0.247	25.904	30.930	19.40	0.15828	0.00584	8.1	12.957	70.517	0.8030	(0.7211, 0.8941)
0.331	27.738	32.883	18.55	0.17718	0.00634	14.9	13.562	92.595	0.8038	(0.7268, 0.8891)
0.430	28.648	34.897	21.81	0.19418	0.00677	24.8	14.157	116.697	0.8048	(0.7318, 0.8851)
0.601	31.130	37.854	21.60	0.21751	0.00732	47.8	15.064	157.799	0.8059	(0.7384, 0.8794)
0.774	33.019	40.454	22.52	0.23525	0.00772	76.9	15.835	196.741	0.8068	(0.7433, 0.8758)
0.939	34.536	42.652	23.50	0.24896	0.00801	110.0	16.488	232.443	0.8075	(0.7471, 0.8728)
1.124	36.563	44.846	22.65	0.26207	0.00829	153.0	17.164	272.028	0.8081	(0.7508, 0.8698)

Table H.5: Herschel-Bulkley: Results for laminar flow of muds 'A' and 'B' flowing in 1″× 3″ and 1.5″× 3″ [nominal] annular conduits.

Velocity [m/s]	Pressure Drop, [kPa] Meas.	Calc.	$\epsilon\%$	N [-]	$D_{eff,G}$ [m]	$N_{Re,G}$ [-]	τ_w [Pa]	$\dot{\gamma}_w$ [1/s]	λ [-]	$(\lambda_{[-]}, \lambda_{[+]})$ [-,-]
Mud 'A', 1″× 3″ annulus: Total RMS = 0.426, $\sigma = 5.84$, $\psi = 0.4307655$.										
0.135	2.779	3.046	9.61	0.49802	0.01831	36.1	1.850	25.329	0.7143	(0.6365, 0.8018)
0.233	3.723	3.913	5.11	0.58374	0.01970	82.0	2.347	39.272	0.7208	(0.6594, 0.7878)
0.336	4.682	4.725	0.91	0.63275	0.02040	137.8	2.824	53.218	0.7246	(0.6734, 0.7798)
0.415	5.343	5.305	-0.72	0.65676	0.02072	184.3	3.171	63.696	0.7266	(0.6808, 0.7755)
0.494	6.026	5.858	-2.79	0.67411	0.02095	233.3	3.511	74.216	0.7281	(0.6865, 0.7723)
0.691	7.632	7.152	-6.29	0.69998	0.02127	363.7	4.312	100.081	0.7306	(0.6964, 0.7666)
0.790	8.246	7.772	-5.75	0.70768	0.02136	433.4	4.702	113.180	0.7316	(0.6999, 0.7647)
0.941	9.467	8.672	-8.39	0.71542	0.02145	542.8	5.274	132.979	0.7325	(0.7041, 0.7620)
1.008	9.735	9.064	-6.90	0.71784	0.02148	593.3	5.525	141.897	0.7328	(0.7056, 0.7611)
1.074	10.377	9.439	-9.04	0.71974	0.02151	643.4	5.769	150.663	0.7331	(0.7070, 0.7602)
Mud 'A', 1.5″× 3″ annulus: Total RMS = 6.277, $\sigma = 2.98$, $\psi = 0.6230597$.										
0.164	6.102	7.120	16.68	0.53036	0.01232	31.8	2.006	29.641	0.8199	(0.7854, 0.8559)
0.343	9.508	10.932	14.98	0.63363	0.01336	92.2	2.835	53.542	0.8229	(0.8002, 0.8462)
0.443	11.066	12.849	16.11	0.66191	0.01362	131.1	3.262	66.480	0.8237	(0.8043, 0.8435)
0.564	13.059	15.043	15.19	0.68407	0.01381	181.5	3.761	82.138	0.8243	(0.8077, 0.8412)
0.636	14.520	16.239	11.84	0.69306	0.01388	212.3	4.042	91.199	0.8245	(0.8092, 0.8401)
1.012	19.788	22.208	12.23	0.71713	0.01408	388.0	5.447	139.096	0.8252	(0.8139, 0.8366)
1.096	21.381	23.451	9.68	0.71959	0.01410	429.7	5.747	149.878	0.8253	(0.8146, 0.8360)
1.124	22.084	23.859	8.04	0.72027	0.01410	443.9	5.847	153.500	0.8253	(0.8148, 0.8359)
1.229	23.139	25.366	9.62	0.72228	0.01412	497.1	6.202	166.592	0.8254	(0.8155, 0.8353)

Table H.6: Hyperbolic: Results for laminar flow for mud 'A' flowing in 1″× 3″ and 1.5″× 3″ [nominal] annular conduits.

Velocity	Pressure Drop, [kPa]			N	$D_{\text{eff},G}$	$N_{\text{Re},G}$	τ_w	$\dot{\gamma}_w$	λ	$(\lambda_{[-]}, \lambda_{[+]})$
[m/s]	Meas.	Calc.	ϵ%	[-]	[m]	[-]	[Pa]	[1/s]	[-]	[-,-]
Mud 'A', 1″× 3″ annulus: Total RMS = 1.739, $\sigma = 3.68$, $\psi = 0.4307655$.										
0.135	2.779	2.008	-27.76	0.70793	0.02137	57.5	2.780	52.001	0.7385	(n/a , n/a)
0.233	3.723	2.956	-20.61	0.70793	0.02137	116.6	4.093	89.814	0.7385	(n/a , n/a)
0.336	4.682	3.830	-18.21	0.70793	0.02137	187.0	5.304	129.510	0.7385	(n/a , n/a)
0.415	5.343	4.446	-16.79	0.70793	0.02137	245.6	6.158	159.929	0.7385	(n/a , n/a)
0.494	6.026	5.028	-16.56	0.70793	0.02137	307.6	6.966	190.349	0.7385	(n/a , n/a)
0.691	7.632	6.373	-16.49	0.70793	0.02137	474.5	8.834	266.225	0.7385	(n/a , n/a)
0.790	8.246	7.008	-15.01	0.70793	0.02137	564.4	9.715	304.516	0.7385	(n/a , n/a)
0.941	9.467	7.928	-16.25	0.70793	0.02137	707.1	10.992	362.541	0.7385	(n/a , n/a)
1.008	9.735	8.326	-14.48	0.70793	0.02137	773.2	11.544	388.500	0.7385	(n/a , n/a)
1.074	10.377	8.724	-15.93	0.70793	0.02137	839.0	12.072	413.872	0.7385	(n/a , n/a)
Mud 'A', 1.5″× 3″ annulus: Total RMS = 1.183, $\sigma = 3.30$, $\psi = 0.6230597$.										
0.164	6.102	5.871	-3.78	0.70793	0.01400	55.9	4.512	103.070	0.8266	(n/a , n/a)
0.343	9.508	9.885	3.97	0.70793	0.01400	144.9	7.603	215.375	0.8266	(n/a , n/a)
0.443	11.066	11.855	7.13	0.70793	0.01400	202.0	9.118	278.430	0.8266	(n/a , n/a)
0.564	13.059	14.078	7.80	0.70793	0.01400	276.3	10.828	354.903	0.8266	(n/a , n/a)
0.636	14.520	15.310	5.44	0.70793	0.01400	322.0	11.775	399.562	0.8266	(n/a , n/a)
1.012	19.788	21.268	7.48	0.70793	0.01400	587.4	16.369	636.274	0.8266	(n/a , n/a)
1.096	21.381	22.511	5.28	0.70793	0.01400	651.3	17.321	689.176	0.8266	(n/a , n/a)
1.124	22.084	22.918	3.78	0.70793	0.01400	672.9	17.634	706.810	0.8265	(n/a , n/a)
1.229	23.139	24.418	5.53	0.70793	0.01400	755.3	18.786	772.938	0.8265	(n/a , n/a)
Mud 'B', 1″× 3″ annulus: Total RMS = 1.281, $\sigma = 2.13$, $\psi = 0.4307655$.										
0.146	14.962	15.150	1.25	0.19017	0.01039	3.3	11.908	25.181	0.6888	(n/a , n/a)
0.223	15.465	16.400	6.04	0.19017	0.01039	7.1	12.901	38.358	0.6887	(n/a , n/a)
0.284	15.899	17.198	8.17	0.19017	0.01039	11.0	13.484	48.406	0.6889	(n/a , n/a)
0.333	16.575	17.709	6.84	0.19017	0.01039	14.6	13.901	56.799	0.6888	(n/a , n/a)
0.386	17.085	18.203	6.55	0.19017	0.01039	19.2	14.310	66.158	0.6887	(n/a , n/a)
0.482	17.602	19.003	7.96	0.19017	0.01039	28.7	14.925	82.565	0.6886	(n/a , n/a)
0.575	18.630	19.648	5.46	0.19017	0.01039	39.5	15.432	98.421	0.6886	(n/a , n/a)
0.743	19.602	20.631	5.25	0.19017	0.01039	62.7	16.196	126.862	0.6886	(n/a , n/a)
0.959	20.774	21.660	4.26	0.19017	0.01039	99.7	17.011	164.258	0.6886	(n/a , n/a)
1.040	21.477	21.995	2.41	0.19017	0.01039	115.8	17.287	178.754	0.6886	(n/a , n/a)
Mud 'B', 1.5″× 3″ annulus: Total RMS = 11.691, $\sigma = 2.63$, $\psi = 0.6230597$.										
0.064	21.070	22.575	7.14	0.19017	0.00667	0.6	10.719	14.479	0.8043	(n/a , n/a)
0.096	21.663	24.380	12.54	0.19017	0.00667	1.2	11.559	21.535	0.8044	(n/a , n/a)
0.168	23.511	27.088	15.21	0.19017	0.00667	3.4	12.871	37.900	0.8043	(n/a , n/a)
0.247	25.904	29.147	12.52	0.19017	0.00667	6.8	13.838	55.461	0.8044	(n/a , n/a)
0.331	27.738	30.859	11.25	0.19017	0.00667	11.7	14.643	74.668	0.8043	(n/a , n/a)
0.430	28.648	32.426	13.19	0.19017	0.00667	18.7	15.384	96.816	0.8043	(n/a , n/a)
0.601	31.130	34.505	10.84	0.19017	0.00667	34.2	16.390	135.069	0.8044	(n/a , n/a)
0.774	33.019	36.212	9.67	0.19017	0.00667	54.2	17.208	174.496	0.8043	(n/a , n/a)
0.939	34.536	37.617	8.92	0.19017	0.00667	76.9	17.847	211.356	0.8043	(n/a , n/a)
1.124	36.563	38.903	6.40	0.19017	0.00667	106.6	18.475	253.517	0.8042	(n/a , n/a)

Table H.7: Power Law: Results for laminar flow of muds 'A' and 'B' flowing in 1″× 3″ and 1.5″× 3″ [nominal] annular conduits.

Velocity [m/s]	Pressure Drop, [kPa] Meas.	Calc.	ϵ%	N [-]	$D_{\mathrm{eff},G}$ [m]	$N_{\mathrm{Re},G}$ [-]	τ_w [Pa]	$\dot{\gamma}_w$ [1/s]	λ [-]	$(\lambda_{[-]}, \lambda_{[+]})$ [-,-]
Mud 'A', 1″× 3″ annulus: Total RMS = 10.007, $\sigma = 3.42$, $\psi = 0.4307655$.										
0.135	2.779	2.020	-27.30	0.43543	0.01713	38.2	1.487	23.012	0.7190	(n/a , n/a)
0.233	3.723	2.613	-29.81	0.48080	0.01800	92.2	1.891	38.953	0.7234	(n/a , n/a)
0.336	4.682	3.153	-32.65	0.52259	0.01873	164.3	2.246	54.937	0.7270	(n/a , n/a)
0.415	5.343	3.536	-33.82	0.55165	0.01920	227.7	2.495	66.814	0.7293	(n/a , n/a)
0.494	6.026	3.908	-35.15	0.57820	0.01962	296.6	2.728	78.267	0.7312	(n/a , n/a)
0.691	7.632	4.794	-37.19	0.63690	0.02046	487.4	3.280	106.072	0.7352	(n/a , n/a)
0.790	8.246	5.229	-36.59	0.66247	0.02080	591.0	3.545	119.528	0.7368	(n/a , n/a)
0.941	9.467	5.879	-37.90	0.69749	0.02124	755.3	3.941	139.695	0.7388	(n/a , n/a)
1.008	9.735	6.168	-36.64	0.71151	0.02141	830.7	4.114	148.454	0.7396	(n/a , n/a)
1.074	10.377	6.453	-37.82	0.72445	0.02156	905.3	4.282	156.950	0.7404	(n/a , n/a)
Mud 'A', 1.5″× 3″ annulus: Total RMS = 14.968, $\sigma = 1.98$, $\psi = 0.6230597$.										
0.164	6.102	4.790	-21.50	0.45014	0.01135	34.3	1.622	28.013	0.8212	(n/a , n/a)
0.343	9.508	7.362	-22.57	0.52434	0.01225	110.2	2.261	55.634	0.8249	(n/a , n/a)
0.443	11.066	8.728	-21.13	0.55989	0.01264	163.5	2.566	70.302	0.8263	(n/a , n/a)
0.564	13.059	10.370	-20.59	0.59816	0.01303	235.4	2.909	87.304	0.8276	(n/a , n/a)
0.636	14.520	11.301	-22.17	0.61870	0.01322	280.4	3.102	97.034	0.8282	(n/a , n/a)
1.012	19.788	16.334	-17.46	0.70771	0.01400	542.7	4.066	146.032	0.8302	(n/a , n/a)
1.096	21.381	17.463	-18.33	0.72376	0.01413	604.9	4.273	156.480	0.8306	(n/a , n/a)
1.124	22.084	17.840	-19.22	0.72886	0.01417	625.9	4.341	159.942	0.8307	(n/a , n/a)
1.229	23.139	19.249	-16.81	0.74690	0.01431	705.3	4.595	172.781	0.8310	(n/a , n/a)
Mud 'B', 1″× 3″ annulus: Total RMS = 187.876, $\sigma = 15.58$, $\psi = 0.4307655$.										
0.146	14.962	1.823	-87.82	1.00000	0.02419	59.5	1.076	17.442	0.7549	(n/a , n/a)
0.223	15.465	2.780	-82.03	1.00000	0.02419	90.7	1.641	26.598	0.7549	(n/a , n/a)
0.284	15.899	3.539	-77.74	1.00000	0.02419	115.5	2.089	33.865	0.7549	(n/a , n/a)
0.333	16.575	4.147	-74.98	1.00000	0.02419	135.3	2.447	39.679	0.7549	(n/a , n/a)
0.386	17.085	4.808	-71.86	1.00000	0.02419	156.9	2.837	46.001	0.7549	(n/a , n/a)
0.482	17.602	6.004	-65.89	1.00000	0.02419	195.9	3.543	57.446	0.7549	(n/a , n/a)
0.575	18.630	7.158	-61.58	1.00000	0.02419	233.6	4.225	68.491	0.7549	(n/a , n/a)
0.743	19.602	9.254	-52.79	1.00000	0.02419	302.0	5.462	88.547	0.7549	(n/a , n/a)
0.959	20.774	11.951	-42.47	1.00000	0.02419	390.0	7.053	114.341	0.7549	(n/a , n/a)
1.040	21.477	12.957	-39.67	1.00000	0.02419	422.8	7.647	123.969	0.7549	(n/a , n/a)
Mud 'B', 1.5″× 3″ annulus: Total RMS = 241.952, $\sigma = 36.09$, $\psi = 0.6230597$.										
0.064	21.070	2.518	-88.05	1.00000	0.01591	17.1	0.449	7.287	0.8338	(n/a , n/a)
0.096	21.663	3.776	-82.57	1.00000	0.01591	25.7	0.674	10.930	0.8338	(n/a , n/a)
0.168	23.511	6.594	-71.96	1.00000	0.01591	44.8	1.177	19.084	0.8338	(n/a , n/a)
0.247	25.904	9.723	-62.47	1.00000	0.01591	66.1	1.736	28.140	0.8338	(n/a , n/a)
0.331	27.738	13.031	-53.02	1.00000	0.01591	88.6	2.326	37.716	0.8338	(n/a , n/a)
0.430	28.648	16.904	-41.00	1.00000	0.01591	114.9	3.018	48.922	0.8338	(n/a , n/a)
0.601	31.130	23.629	-24.10	1.00000	0.01591	160.6	4.218	68.386	0.8338	(n/a , n/a)
0.774	33.019	30.426	-7.85	1.00000	0.01591	206.8	5.432	88.057	0.8338	(n/a , n/a)
0.939	34.536	36.948	6.98	1.00000	0.01591	251.1	6.596	106.930	0.8338	(n/a , n/a)
1.124	36.563	44.212	20.92	1.00000	0.01591	300.5	7.892	127.953	0.8338	(n/a , n/a)

Table H.8: Reiner-Philippoff: Results for laminar flow of muds 'A' and 'B' flowing in 1″× 3″ and 1.5″× 3″ [nominal] annular conduits.

Velocity [m/s]	Pressure Drop, [kPa] Meas.	Calc.	ϵ%	N [-]	$D_{\text{eff},G}$ [m]	$N_{\text{Re},G}$ [-]	τ_w [Pa]	$\dot{\gamma}_w$ [1/s]	λ [-]	$(\lambda_{[-]}, \lambda_{[+]})$ [-,-]
Mud 'A', 1″× 3″ annulus: Total RMS = 0.331, σ = 5.58, ψ = 0.4307655.										
0.135	2.779	3.010	8.32	0.53457	0.01893	37.5	2.054	28.233	0.7237	(0.6529, 0.8022)
0.233	3.723	3.932	5.62	0.58561	0.01973	79.7	2.546	41.374	0.7252	(0.6703, 0.7846)
0.336	4.682	4.765	1.78	0.61728	0.02019	131.9	3.027	55.169	0.7270	(0.6814, 0.7757)
0.415	5.343	5.353	0.18	0.63381	0.02041	175.9	3.378	65.740	0.7281	(0.6874, 0.7712)
0.494	6.026	5.909	-1.93	0.64632	0.02058	222.7	3.716	76.310	0.7291	(0.6921, 0.7681)
0.691	7.632	7.202	-5.63	0.66736	0.02086	349.4	4.517	102.675	0.7308	(0.7003, 0.7626)
0.790	8.246	7.820	-5.17	0.67465	0.02095	417.9	4.902	115.980	0.7316	(0.7034, 0.7609)
0.941	9.467	8.704	-8.06	0.68319	0.02106	526.4	5.465	136.142	0.7324	(0.7070, 0.7586)
1.008	9.735	9.091	-6.61	0.68629	0.02110	576.7	5.711	145.162	0.7327	(0.7084, 0.7577)
1.074	10.377	9.463	-8.81	0.68899	0.02113	626.8	5.947	153.978	0.7330	(0.7096, 0.7570)
Mud 'A', 1.5″× 3″ annulus: Total RMS = 5.245, σ = 3.63, ψ = 0.6230597.										
0.164	6.102	7.238	18.62	0.53525	0.01237	29.8	2.060	28.367	0.8198	(0.7895, 0.8514)
0.343	9.508	11.040	16.11	0.61300	0.01317	86.3	2.950	52.892	0.8226	(0.8025, 0.8431)
0.443	11.066	12.933	16.87	0.63447	0.01337	123.2	3.394	66.235	0.8233	(0.8062, 0.8408)
0.564	13.059	15.073	15.43	0.65226	0.01353	171.8	3.907	82.421	0.8239	(0.8092, 0.8390)
0.636	14.520	16.281	12.13	0.66001	0.01360	201.8	4.194	91.827	0.8242	(0.8105, 0.8381)
1.012	19.788	22.158	11.98	0.68497	0.01381	375.7	5.604	141.207	0.8251	(0.8150, 0.8353)
1.096	21.381	23.389	9.39	0.68848	0.01384	417.5	5.901	152.236	0.8252	(0.8157, 0.8349)
1.124	22.084	23.793	7.74	0.68954	0.01385	431.6	5.998	155.900	0.8253	(0.8159, 0.8347)
1.229	23.139	25.288	9.29	0.69318	0.01388	485.7	6.363	169.809	0.8254	(0.8166, 0.8343)
Mud 'B', 1″× 3″ annulus: Total RMS = 9.224, σ = 1.60, ψ = 0.4307655.										
0.146	14.962	16.455	9.98	0.10042	0.00648	2.8	11.348	31.998	0.6809	(0.5291, 0.8763)
0.223	15.465	17.624	13.96	0.14258	0.00846	8.7	12.083	53.764	0.6835	(0.5404, 0.8646)
0.284	15.899	18.413	15.81	0.16536	0.00942	15.3	12.563	69.215	0.6850	(0.5470, 0.8579)
0.333	16.575	18.967	14.43	0.17961	0.00999	21.6	12.901	80.743	0.6860	(0.5515, 0.8533)
0.386	17.085	19.514	14.22	0.19252	0.01048	29.4	13.238	92.766	0.6869	(0.5559, 0.8487)
0.482	17.602	20.429	16.06	0.21207	0.01119	46.4	13.818	114.651	0.6881	(0.5621, 0.8423)
0.575	18.630	21.187	13.73	0.22623	0.01167	65.2	14.303	134.177	0.6891	(0.5674, 0.8370)
0.743	19.602	22.435	14.45	0.24588	0.01232	105.9	15.094	168.515	0.6908	(0.5746, 0.8303)
0.959	20.774	23.827	14.70	0.26410	0.01289	169.4	15.995	211.502	0.6922	(0.5822, 0.8230)
1.040	21.477	24.280	13.05	0.26964	0.01306	196.4	16.311	227.606	0.6926	(0.5847, 0.8205)
Mud 'B', 1.5″× 3″ annulus: Total RMS = 59.857, σ = 2.32, ψ = 0.6230597.										
0.064	21.070	24.508	16.32	0.06068	0.00268	0.3	10.786	16.869	0.7994	(0.6908, 0.9249)
0.096	21.663	26.127	20.60	0.09431	0.00389	1.0	11.255	29.386	0.8004	(0.6983, 0.9174)
0.168	23.511	28.853	22.72	0.14030	0.00533	4.0	12.039	52.383	0.8019	(0.7090, 0.9070)
0.247	25.904	31.204	20.46	0.17192	0.00620	9.3	12.714	74.313	0.8032	(0.7166, 0.9004)
0.331	27.738	33.256	19.89	0.19520	0.00679	16.7	13.313	95.476	0.8040	(0.7226, 0.8947)
0.430	28.648	35.287	23.17	0.21493	0.00726	27.5	13.911	118.304	0.8048	(0.7276, 0.8902)
0.601	31.130	38.290	23.00	0.23994	0.00782	51.6	14.838	157.056	0.8057	(0.7343, 0.8841)
0.774	33.019	40.806	23.58	0.25717	0.00818	81.3	15.629	193.539	0.8063	(0.7393, 0.8793)
0.939	34.536	42.985	24.46	0.26963	0.00844	114.6	16.311	227.574	0.8069	(0.7429, 0.8763)
1.124	36.563	45.096	23.34	0.28031	0.00865	156.6	16.992	264.086	0.8072	(0.7464, 0.8731)

Table H.9: Robertson-Stiff: Results for laminar flow of muds 'A' and 'B' flowing in 1″× 3″ and 1.5″× 3″ [nominal] annular conduits.

Velocity	**Pressure Drop, [kPa]**			N	$D_{\mathrm{eff,G}}$	$\mathrm{N_{Re,G}}$	τ_w	$\dot{\gamma}_w$	λ	$(\lambda_{[-]}, \lambda_{[+]})$
[m/s]	Meas.	Calc.	ϵ%	[-]	[m]	[-]	[Pa]	[1/s]	[-]	[-,-]
Mud 'A', 1″× 3″ annulus: Total RMS = 0.766, $\sigma = 4.19$, $\psi = 0.4307655$.										
0.135	2.779	2.762	-0.62	0.55465	0.01925	36.8	2.428	32.193	0.7248	(n/a , n/a)
0.233	3.723	3.687	-0.97	0.57699	0.01960	80.6	3.237	53.543	0.7274	(n/a , n/a)
0.336	4.682	4.518	-3.49	0.59434	0.01986	135.9	3.964	75.667	0.7293	(n/a , n/a)
0.415	5.343	5.103	-4.48	0.60521	0.02001	183.3	4.471	92.495	0.7300	(n/a , n/a)
0.494	6.026	5.643	-6.36	0.61555	0.02016	234.4	4.951	109.229	0.7307	(n/a , n/a)
0.691	7.632	6.894	-9.67	0.63448	0.02042	374.8	6.038	150.367	0.7322	(n/a , n/a)
0.790	8.246	7.492	-9.14	0.64244	0.02053	451.3	6.551	170.846	0.7328	(n/a , n/a)
0.941	9.467	8.339	-11.91	0.65305	0.02067	573.6	7.293	201.647	0.7336	(n/a , n/a)
1.008	9.735	8.714	-10.49	0.65735	0.02073	630.5	7.615	215.388	0.7338	(n/a , n/a)
1.074	10.377	9.072	-12.57	0.66136	0.02078	687.4	7.926	228.877	0.7341	(n/a , n/a)
Mud 'A', 1.5″× 3″ annulus: Total RMS = 2.263, $\sigma = 3.22$, $\psi = 0.6230597$.										
0.164	6.102	6.890	12.91	0.56596	0.01270	33.1	2.822	42.097	0.8224	(n/a , n/a)
0.343	9.508	10.631	11.82	0.59989	0.01304	94.9	4.218	83.953	0.8237	(n/a , n/a)
0.443	11.066	12.448	12.49	0.61354	0.01318	136.3	4.891	107.163	0.8243	(n/a , n/a)
0.564	13.059	14.538	11.32	0.62788	0.01331	191.3	5.639	134.658	0.8247	(n/a , n/a)
0.636	14.520	15.693	8.08	0.63475	0.01337	226.1	6.055	151.030	0.8249	(n/a , n/a)
1.012	19.788	21.362	7.96	0.66308	0.01363	428.4	8.064	234.901	0.8258	(n/a , n/a)
1.096	21.381	22.570	5.56	0.66818	0.01367	477.5	8.484	253.531	0.8260	(n/a , n/a)
1.124	22.084	22.939	3.87	0.66980	0.01369	494.2	8.622	259.718	0.8261	(n/a , n/a)
1.229	23.139	24.405	5.47	0.67537	0.01373	557.1	9.113	281.996	0.8262	(n/a , n/a)
Mud 'B', 1″× 3″ annulus: Total RMS = 0.870, $\sigma = 3.15$, $\psi = 0.4307655$.										
0.146	14.962	13.043	-12.83	1.00000	0.02419	7.2	8.762	17.140	0.6960	(n/a , n/a)
0.223	15.465	14.760	-4.56	0.11008	0.00696	1.9	11.048	13.373	0.6898	(n/a , n/a)
0.284	15.899	15.585	-1.98	0.11707	0.00730	5.0	11.998	28.045	0.6896	(n/a , n/a)
0.333	16.575	16.083	-2.97	0.12400	0.00762	8.5	12.553	40.805	0.6900	(n/a , n/a)
0.386	17.085	16.593	-2.88	0.13323	0.00805	13.6	13.042	54.934	0.6906	(n/a , n/a)
0.482	17.602	17.410	-1.09	0.14809	0.00870	25.5	13.757	80.631	0.6918	(n/a , n/a)
0.575	18.630	18.066	-3.03	0.15924	0.00917	40.0	14.320	104.782	0.6929	(n/a , n/a)
0.743	19.602	19.136	-2.38	0.17991	0.01000	75.4	15.200	148.939	0.6950	(n/a , n/a)
0.959	20.774	20.309	-2.24	0.20310	0.01087	135.6	16.117	202.367	0.6974	(n/a , n/a)
1.040	21.477	20.743	-3.42	0.21127	0.01116	162.6	16.431	222.079	0.6982	(n/a , n/a)
Mud 'B', 1.5″× 3″ annulus: Total RMS = 3.934, $\sigma = 4.31$, $\psi = 0.6230597$.										
0.064	21.070	19.371	-8.06	1.00000	0.01591	2.1	3.725	7.287	0.8100	(n/a , n/a)
0.096	21.663	21.839	0.81	1.00000	0.01591	3.1	5.587	10.930	0.8049	(n/a , n/a)
0.168	23.511	24.548	4.41	1.00000	0.01591	5.4	9.945	19.455	0.8048	(n/a , n/a)
0.247	25.904	26.623	2.77	0.12199	0.00478	3.2	12.186	31.965	0.8056	(n/a , n/a)
0.331	27.738	28.390	2.35	0.13480	0.00517	7.8	13.138	58.045	0.8064	(n/a , n/a)
0.430	28.648	30.127	5.16	0.15013	0.00561	15.6	13.917	87.136	0.8074	(n/a , n/a)
0.601	31.130	32.736	5.16	0.17400	0.00626	35.4	14.952	135.681	0.8089	(n/a , n/a)
0.774	33.019	35.062	6.19	0.19390	0.00676	62.2	15.760	180.779	0.8101	(n/a , n/a)
0.939	34.536	37.111	7.46	0.21175	0.00719	95.0	16.449	223.224	0.8111	(n/a , n/a)
1.124	36.563	39.215	7.25	0.22893	0.00758	137.6	17.103	266.516	0.8120	(n/a , n/a)

Table H.10: Sisko: Results for laminar flow of muds 'A' and 'B' flowing in 1″× 3″ and 1.5″× 3″ [nominal] annular conduits.

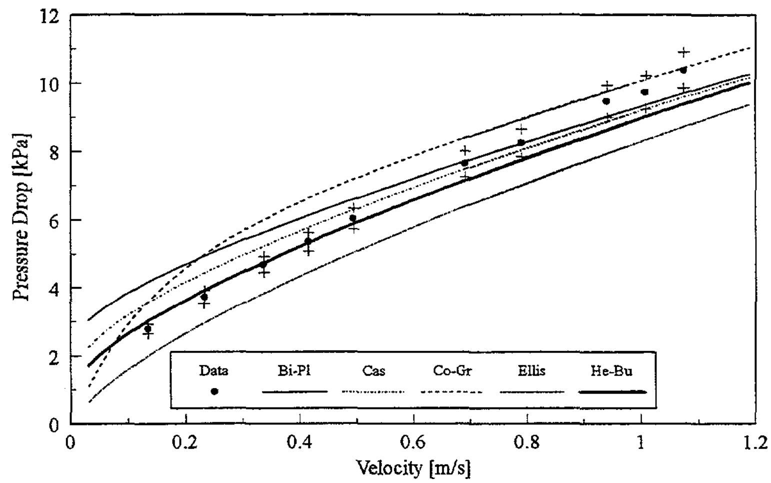

Figure H.1: Predicted and measured laminar pressure losses for mud 'A', 1″× 3″ concentric annulus for Bingham Plastic, Casson, Collins-Graves, Ellis *et al.* and Herschel-Bulkley rheological models. +'s represent ±5% measurement accuracy.

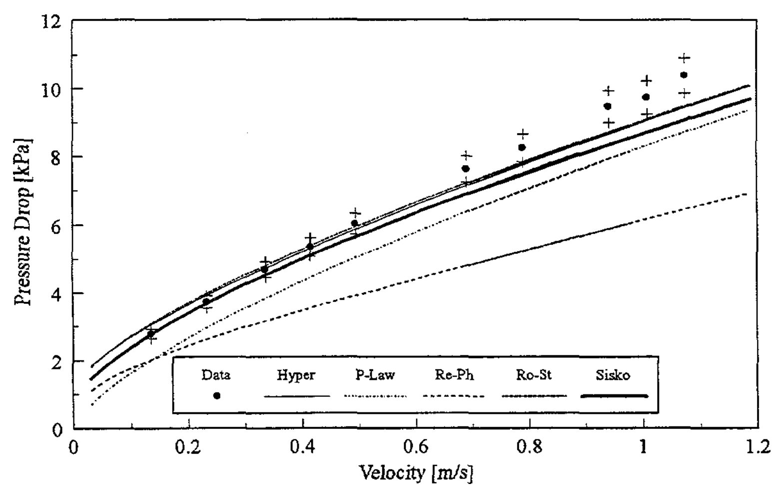

Figure H.2: Predicted and measured laminar pressure losses for mud 'A', 1″× 3″ concentric annulus for Hyperbolic, Power Law, Reiner-Philippoff, Robertson-Stiff and Sisko rheological models. +'s represent ±5% measurement accuracy.

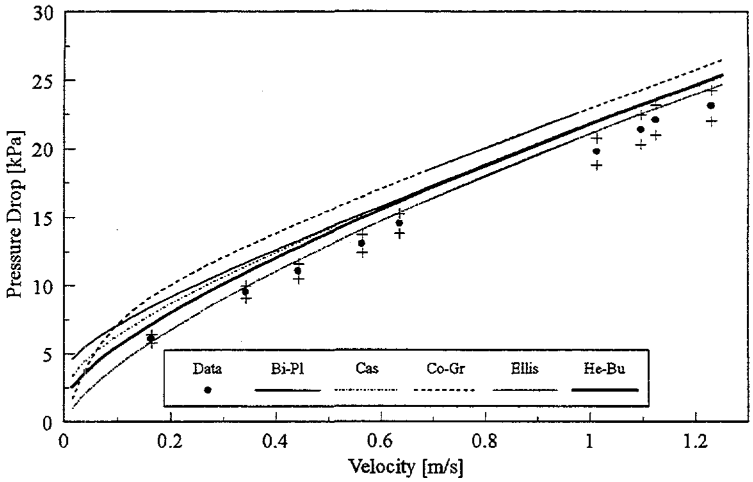

Figure H.3: Predicted and measured laminar pressure losses for mud 'A', 1.5″× 3″ concentric annulus for Bingham Plastic, Casson, Collins-Graves, Ellis *et al.* and Herschel-Bulkley rheological models. +'s represent ±5% measurement accuracy.

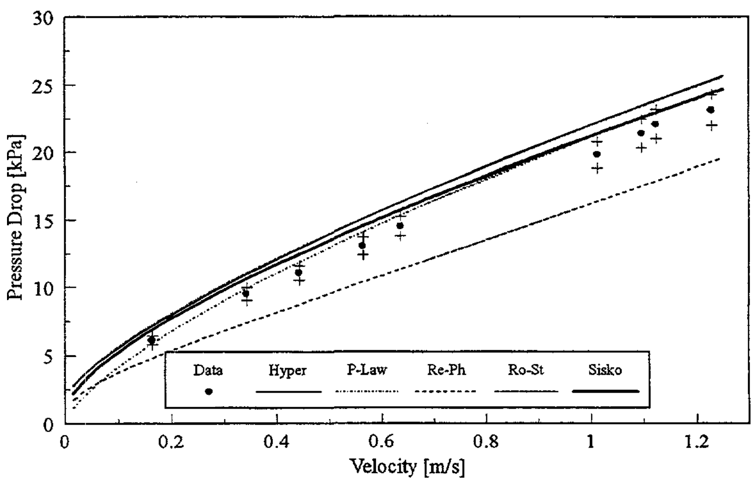

Figure H.4: Predicted and measured laminar pressure losses for mud 'A', 1.5″× 3″ concentric annulus for Hyperbolic, Power Law, Reiner-Philippoff, Robertson-Stiff and Sisko rheological models. +'s represent ±5% measurement accuracy.

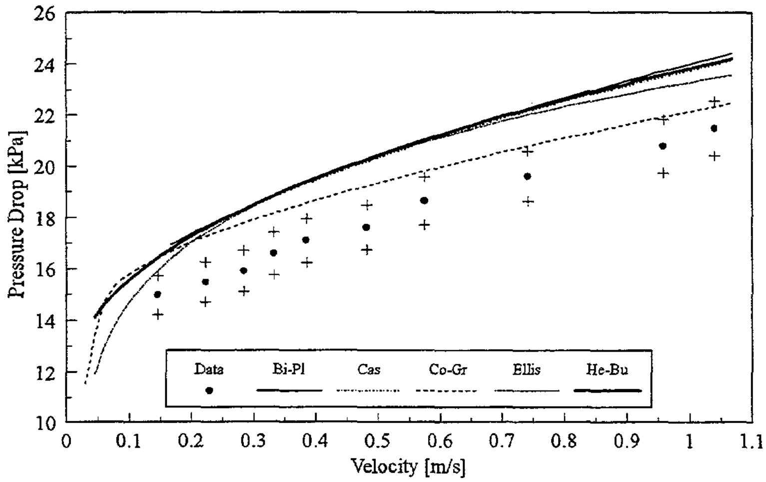

Figure H.5: Predicted and measured laminar pressure losses for mud 'B', 1″× 3″ concentric annulus for Bingham Plastic, Casson, Collins-Graves, Ellis *et al.* and Herschel-Bulkley rheological models. +'s represent ±5% measurement accuracy.

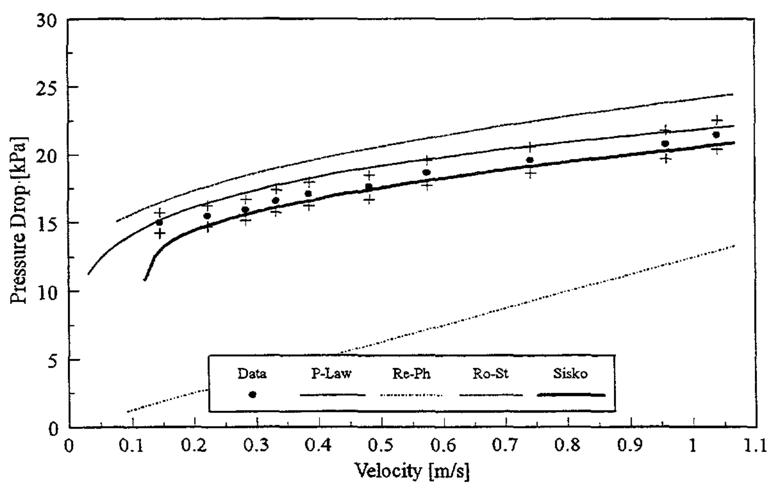

Figure H.6: Predicted and measured laminar pressure losses for mud 'B', 1″× 3″ concentric annulus for Power Law, Reiner-Philippoff, Robertson-Stiff and Sisko rheological models. +'s represent ±5% measurement accuracy.

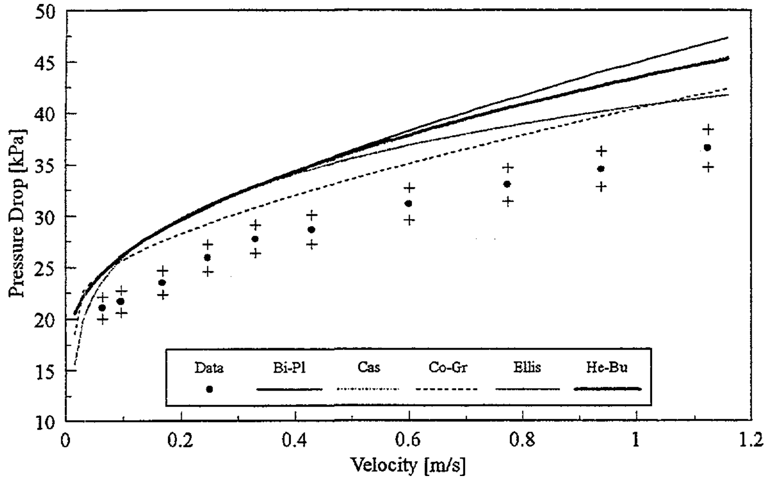

Figure H.7: Predicted and measured laminar pressure losses for mud 'B', 1.5″× 3″ concentric annulus for Bingham Plastic, Casson, Collins-Graves, Ellis *et al.* and Herschel-Bulkley rheological models. +'s represent ±5% measurement accuracy.

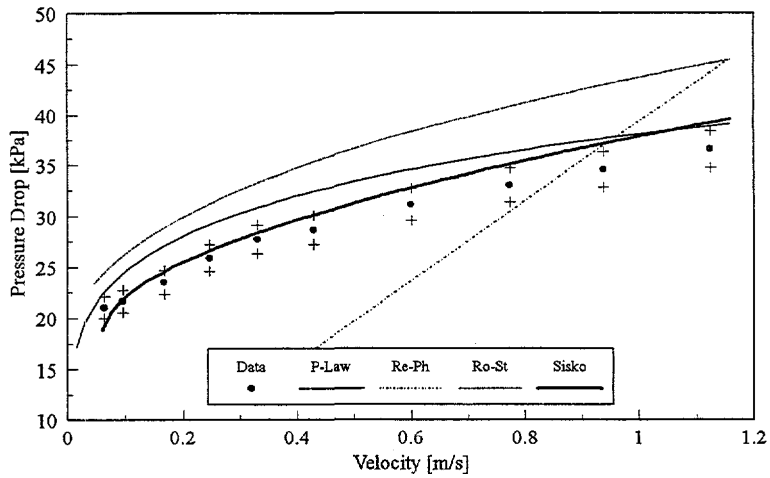

Figure H.8: Predicted and measured laminar pressure losses for mud 'B', 1.5″× 3″ concentric annulus for Power Law, Reiner-Philippoff, Robertson-Stiff and Sisko rheological models. +'s represent ±5% measurement accuracy.

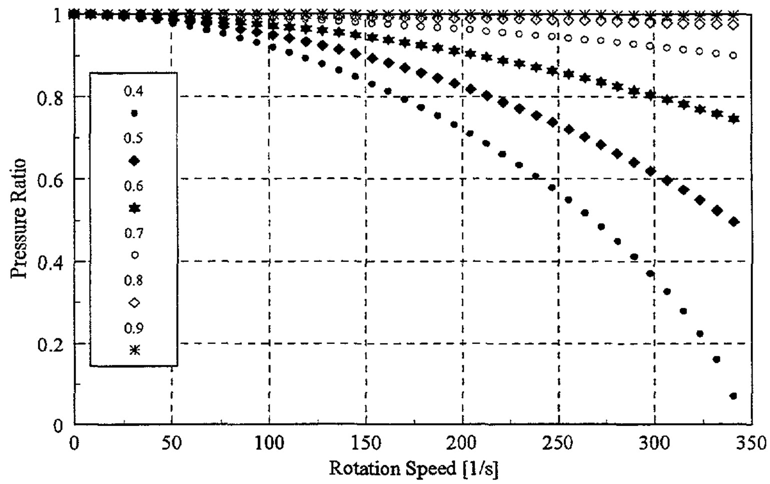

Figure H.9: Effect of pipe rotation on laminar annluar pressure losses for mud 'A' for six different aspect ratios. Pressure ratio represent $(\Delta p)_\omega \,/\, (\Delta p)_{\omega=0}$. Decay exponent: $m = 3$. Average velocity: $\bar{v} = 0.636$ m/s.

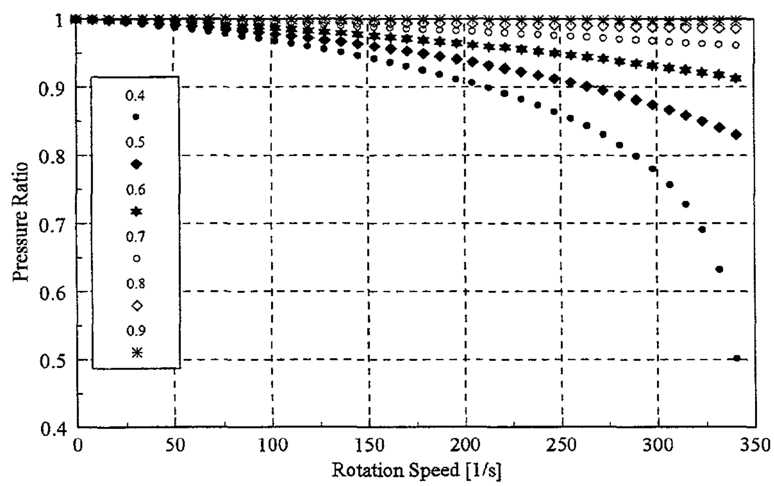

Figure H.10: Effect of pipe rotation on laminar annluar pressure losses for mud 'B' for six different aspect ratios. Pressure ratio represent $(\Delta p)_\omega \,/\, (\Delta p)_{\omega=0}$. Decay exponent: $m = 3$. Average velocity: $\bar{v} = 0.636$ m/s.

Appendix I

Simulation Data

DRILLING HYDRAULICS PROGRAM INPUT FILE

```
####################################################################################
# Part 1:  Administrative Information
####################################################################################
BIT_RUN                 25      $Bit run number$
BIT_NAME                        $Lyng LA250BX M646$
BHA_NUMBER              30      $Bottom hole assembly record number$
WELL_NAME                       $North Sea Well 'A'$
DATE                    $01/01/96$    $Date of simulation (UK format)$
####################################################################################
# Part 2:  General Hydraulics Input Data
####################################################################################
BIT_DEPTH               4874.0  $meters MD$
BIT_DISCOEFF            0.95    $Bit discharge coefficient$
BOTTOM_DEPTH            6119.9  $meters MD$
FANN                    127 75 56 36 28 21 12 11 $Eight Fann readings from 600 to 3$
FLOWRATE                2100    $litres per minute$
FV_SOLIDS               26.5    $Volume fraction of fluid weighting agent$
MEASURED_SPP            290     $measured pressure (bars)$
NOZZLES                 26 26 26 26 $Nozzle sizes in 1/32nd of an inch$
OUTLET_PRESSURE         0       $0:  atmospheric; else value in bars$
OWR                     80.0 20.0 $Oil/Water Ratio [% of oil & water]$
POLYMER_PPM             1000    $Drag reducing polymer content (ppm)$
POV_RATING              330     $Pop-Off Valve rating (bars)$
ROP                     12.8    $ROP in meters per hour$
ROTATION                200     $Drillstring rotation in rpm$
RPM                     200     $Drillstring rotation [in rpm]$
RTF                     1.0     $Reactive Torque Factor$
SALINITY                10.0    $Salinity, wt.  salt/wt.  pure water$
SPHERICITY              0.95    $Sphericity of cuttings$
SG                      1.65    $Specific Gravity of Drilling Fluid$
TEMP_TOP                20      $Flowline Temperature (degrees Celcius)$
TEMP_BOTTOM             75      $Bottom hole temperature (degrees Celcius)$
WOB                     12      $Weight on bit (metric tonnes)$
YP                      11.5    $Yield Point (milli-Pa)$
####################################################################################
# Part 3:  Program Control Switches
#
# Key for rheological model switch:
# 1:  Power Law; 2:  Bingham Plastic; 3:  Herschel-Bulkley; 4:  Robertson-Stiff
# 5:  Casson; 6:  Modified (API) Power Law; 7:  Sisko; 8:  Collins-Graves
# 9:  Hyperbolic; 10:  Ellis et al; 11:  Reiner-Philippoff; 12:  Inverse ln-cosh
####################################################################################
BIT_TYPE                2       $1:  Roller Cone; 2:  PDC; 3:  Diamond; 4:  Core Barrel$
COMPRESSIBILITY         0       $Fluid compressibility 0:  Off, 1:  On$
ECCENTRICITY            0       $Annular eccentricity 0:  Off, 1:  On$
NODE_LENGTH             100.0   $Node length (meters).  0.0 sets automatic$
OIL_TYPE                1       $1:  Diesel, 2:  A, 3:  B, 4:  C, 5:  D$
PLUG_FLOW               1       $0:  Off; 1:  On [calculate]; 2:  On [Newtonian]$
RHEOLOGICAL_MODEL       9       $See key$
WATER_TYPE              1       $1:  Kutasov; 2:  Melbouci$
####################################################################################
```

```
###########################################################################################
# Part 4:  Tally-Book Description (Drillstring description table)
#
# arg1:  String section number (excl.  bit); arg2:  ID of main Drill Pipe section (inches)
# arg3:  OD of main Drrill Pipe section (inches); arg4:  Total length (meters)
# NOTE: For MWD & PDM input formatting requirements see key
###########################################################################################
SECTIONS
1        PDM      1        7.53
2        2.937    6.625       1.15  $Float Sub$
3        2.750    6.650       1.81  $Stabilizer Straight IB$
4        2.900    6.500       6.54  $CDR$
5        2.900    6.650       1.51  $Stabilizer Sleeve NM$
6        MWD      2        8.34
7        3.000    7.000       0.50  $XO Sub$
8        3.000    5.000      18.20  5     $HWNM Drill Pipe$
9        2.750    6.500       9.39  $Jar$
10       3.500    5.000      27.02  13    $Drill Pipe$
11       2.750    6.375       9.72  $Accelerator$
12       3.500    5.000    2981.40  13    $Drill Pipe$
13       3.063    7.500       0.89  $XO Sub$
14       4.734    5.500    9999.99  8     $Drill Pipe$
END_SECTIONS
###########################################################################################
# Part 5:  Welly-Book Description
#
# arg1:  Start Depth (meters); arg2:  End Depth (meters)
# arg3:  ID (inches); arg4:  '$' delimetered descriptive text string
###########################################################################################
CASING
   0.0     29.0    21.250   $LP Riser$
  29.0     39.1    20.750   $HP Riser$
  39.1   3499.9    12.415   $13 3/8" Casing P-110 68 (lbs/ft)$
3433.0   4865.5     8.535   $9 5/8" Liner L-80 53.5 (lbs/ft)$
END_CASING
###########################################################################################
# Part 6:  Deviation Survey
#
# arg1:  Measured Depth (m MD); arg2:  Total Vertical Depth (m TVD)
# arg3:  Inclination (degrees from vertical)
###########################################################################################
DEVIATION_SURVEY
   0.0       0.00   0.00
 300.0     300.00   0.00
 416.0     415.53   5.29
 552.0     550.14  10.78
 617.0     613.75  13.50
 665.0     660.06  17.00
 750.0     740.50  19.60
 804.0     790.91  22.60
 857.0     839.08  26.60
 909.0     885.03  29.40
 964.0     932.07  33.10
 991.0     954.34  35.70
1042.0     995.02  36.50
1097.0    1038.32  38.30
1151.0    1079.50  42.70
1178.0    1098.90  45.40
1288.0    1169.69  52.60
```

```
1329.0    1194.02   54.90
1384.0    1224.76   57.30
1465.0    1266.24   61.90
1492.0    1278.41   64.50
1519.0    1289.59   66.60
1573.0    1309.27   70.70
1627.0    1325.13   75.10
1681.0    1338.01   77.10
1946.0    1394.72   78.40
2331.0    1474.47   77.60
2665.0    1551.96   75.50
3077.0    1632.41   78.80
3296.0    1672.00   80.80
4086.0    1798.80   79.50
4737.0    1910.44   80.40
4998.0    2031.52   88.20
5623.0    2029.10   90.90
5808.0    2052.87   86.90
6235.0    2031.14   88.80
6372.0    2029.03   91.70
END_SURVEY
END_OF_FILE
###########################################################################################
```

Table I.1: Sample drilling hydraulics program input file (spread over 3 pages).

	Data for Hole Sections			
	24″	17 1/2″	8 1/2″	8 1/2″
Nominal Casing Size	32″	20″	13 3/8″	9 5/8″
Casing Depth [mMD]	365	1269	3499	4865
Casing Depth [mTVD]	365	1159	1700	2017
Measured SPP [bars]	145	275	253	260
Flowrate [lpm]	4100	4260	1900	1850
Bit Depth [mMD]	1021.0	3151.0	5580.0	6437.0
ROP [m/hr]	21.8	21.9	50.9	22.5
Min. WOB [ton]	4.0	2.0	1.0	1.0
Max. WOB [ton]	12.0	5.0	8.0	9.0
RPM (min/max)	106/182	120/270	210/338	215/345
LOT/FIT [g/cm^3]	1.57	1.63	1.83	1.90
Pore Pressure [g/cm^3]	0.93	1.19	1.59	1.60
BHA Number	2	6	9	20
BIT Nozzles [1/32″]	2x24;18;16	3x15;4x16	4x20	4x26
Bit TFA [in^2]	1.328	1.303	1.227	2.074
Bit Type (catalogue ID)	SS33SGJ4	PDQ19L	DS56H	LA250BX
Bit Munufacturer	Security	Diamant	Hycalog	Lyng
Bit Type (IADC Code)	115G	S611	PDC	M646
Mud Type	Seawater/Pac	KCl/Pac	OBM	OBM
Mud Weight [g/cm^3]	1.19	1.53	1.65	1.65
Solids [vol.%]	11.7	22.5	26.5	26.5
Gel @ 10s [Pa]	2.0	4.0	5.5	7.5
Gel @ 10m [Pa]	10.0	5.5	9.5	16.5
pH	8.0	7.9	-	-
PV [mPa·s]	20.0	37.0	42.0	44.0
YP [Pa[	10.0	21.5	7.0	8.5
Chlorides [1000 mg/l]	22	79	100	110
Calcium [mg/l]	600	580	-	-
Magnesium [mg/l]	1094	680	-	-
Oil/Water Ratio [%/%]	n/a	n/a	82/18	80/20
Flowline Temp. [°C]	34	60	41	46
$\theta_{600}/\theta_{300}$	60/40	117/80	98/56	105/61
$\theta_{200}/\theta_{100}$	32/21	65/45	41/26	44/28
θ_{60}/θ_{30}	16/11	35/24	20/15	22/16
θ_{6}/θ_{3}	4/3	11/7	8/7	10/9
Sisko Rheological Model Parameters				
$a \times 10^{-2}$	0.12551	0.53848	3.97930	4.35205
b	0.58818	1.68758	2.48728	3.35762
c	0.56437	0.50076	0.19161	0.14737

Table I.2: Relevent data required for drilling hydraulics calculation for the well-sections analysed.

	Component Description	O.D. [in]	I.D. [in]	Length [m]	Component Description	O.D. [in]	I.D. [in]	Length [m]
	BHA #2 Description				**BHA #6 Description**			
1	Tri Cone Bit	24.000	-	0.56	PDC/Diamond Bit	17.500	-	0.60
2	Dyna-Drill PDM	9.626	-	8.14	Dyna-Drill PDM	9.625	-	8.14
3	Float Sub	9.438	2.438	0.91	Float Sub	9.438	2.438	0.91
4	Pony Collar (NM)	9.500	3.000	2.76	Pony Collar (NM)	9.500	3.063	2.77
5	Stab. Sleeve	21.750	3.000	2.05	Stabilizer (NM)	16.000	3.000	2.00
6	Sub Pin X Pin	9.438	3.344	0.45	Sub Pin X Pin	9.438	3.000	0.45
7	Anadrill MWD	9.500	-	8.98	Anadrill MWD	9.500	-	12.18
8	Filter Sub	9.500	3.000	0.41	Filter Sub	9.500	3.500	0.42
9	Sub	9.500	3.000	0.78	Stabilizer (NM)	17.000	3.000	2.23
10	Stab. Sleeve	22.750	3.000	2.06	XO Sub	9.500	3.688	1.21
11	Drill Collar (NM)	9.500	3.000	18.63	Drill Collar (NM)	8.000	2.875	16.98
12	Stabilizer	17.500	3.000	2.38	Jar	8.000	3.000	9.78
13	Drill Collar	9.500	3.000	9.39	XO Sub	7.500	3.500	0.88
14	XO Sub	9.500	3.500	1.21	HW Drill Pipe	6.625	4.734	27.85
15	Drill Collar	8.000	3.000	54.85	Drill Pipe	5.500	4.734	2246.67
16	Jar	8.000	3.000	9.78	HW Drill Pipe	6.625	4.734	305.30
17	Drill Collar	8.000	3.000	18.45	Drill Pipe	5.500	4.734	522.63
18	XO Sub	7.500	3.500	0.88				
19	HW Drill Pipe	6.625	3.000	138.73				
20	Drill Pipe	5.500	4.730	739.60				

Table I.3: Description table for BHA #2 (24″ hole) and BHA #6 (17 1/2″ hole).

	Component Description	O.D. [in]	I.D. [in]	Length [m]	Component Description	O.D. [in]	I.D. [in]	Length [m]
	BHA #9 Description				**BHA #20 Description**			
1	PDC/Diamond	8.500	-	0.34	PDC/Diamond Bit	8.500	-	0.28
2	Stabilizer Rotary	8.375	2.250	0.28	Dyna-Drill PDM	6.750	-	9.25
3	Dyna-Drill PDM	6.750	-	7.55	Stab. Float Sub	7.000	2.875	2.92
4	Float Sub	6.375	2.750	0.93	Geosteering Sub.	6.750	2.875	6.51
5	Stabilizer	8.250	2.250	1.80	Stabilizer	7.000	2.875	1.51
6	Pony Collar (NM)	6.750	2.875	3.06	Anadrill MWD	6.750	-	10.43
7	Sub Pin X Pin	6.750	2.750	0.34	LWD Tool CDN	6.750	-	8.74
8	Anadrill MWD	6.750	-	19.44	Stabilizer	7.000	2.875	1.42
9	NMHW Drill Pipe	5.000	3.000	22.81	HW NM Drill Pipe	5.000	3.125	18.21
10	Jar	6.313	3.000	9.46	Jar	6.375	2.750	9.24
11	HW Drill Pipe	5.000	3.000	27.05	HW Drill Pipe	5.000	3.125	28.05
12	Accelerator	6.500	3.000	9.79	Accelerator	6.375	2.750	9.72
13	HW Drill Pipe	5.000	3.000	27.41	HW Drill Pipe	5.000	3.125	27.96
14	Drill Pipe	5.000	3.250	2078.66	Drill Pipe	5.000	4.276	1544.19
15	HW Drill Pipe	5.000	3.000	27.36	HW Drill Pipe	5.000	3.125	27.41
16	Jar	6.313	3.000	9.46	Jar	6.375	2.750	9.32
17	HW Drill Pipe	5.000	3.000	28.06	HW Drill Pipe	5.000	3.125	28.08
18	XO Sub	5.000	3.500	0.90	Drill Pipe	5.000	4.276	1521.90
19	Drill Pipe	5.500	3.250	3305.30	XO Sub	7.500	3.063	0.89
20					Drill Pipe	5.500	4.778	3172.36

Table I.4: Description table for BHA #9 (8 1/2″ hole) and BHA #20 (8 1/2″ hole).

ID	Description	Diameters [m],[m]	Depths [m MD] Top	Bottom	Depths [m TVD] Top	Bottom	Av. Vel. [m/s]
Drillstring Assemblage and Geometry							
2.1	Drill Pipe	0.12014	0.00	740.16	0.00	731.19	6.02765
2.2	HW Drill Pipe	0.07620	740.16	878.89	731.19	858.42	14.9842
2.3	XO Sub	0.08890	878.89	879.77	858.42	859.20	11.0088
2.4	Drill Collar	0.07620	879.77	898.22	859.20	875.50	14.9842
2.5	Jar	0.07620	898.22	908.00	875.50	884.15	14.9842
2.6	Drill Collar	0.07620	908.00	962.85	884.15	931.09	14.9842
2.7	XO Sub	0.08890	962.85	964.06	931.09	932.12	11.0088
2.8	Drill Collar	0.07620	964.06	973.45	932.12	939.86	14.9842
2.9	Stabilizer	0.07620	973.45	975.83	939.86	941.83	14.9842
2.10	NM Drill Collar	0.07620	975.83	994.46	941.83	957.10	14.9842
2.11	Stab. Sleeve	0.07620	994.46	996.52	957.10	958.74	14.9842
2.12	Sub	0.07620	996.52	997.30	958.74	959.37	14.9842
2.13	Filter Sub	0.07620	997.30	997.71	959.37	959.69	14.9842
2.14	MWD Tool	n/a	997.71	1006.69	959.69	966.86	n/a
2.15	Sub Pin X Pin	0.08494	1006.69	1007.14	966.86	967.21	12.0599
2.16	Stab. Sleeve	0.07620	1007.14	1009.19	967.21	968.85	14.9842
2.17	NM Pony Collar	0.07620	1009.19	1011.95	968.85	971.05	14.9842
2.18	Float Sub	0.06193	1011.95	1012.86	971.05	971.78	22.6886
2.19	PDM Tool	n/a	1012.86	1021.00	971.78	978.27	n/a
2.20	Bit TFA ($\times 10^{-4}m^2$)	8.570482	1021.00	1021.56	978.27	978.46	n/a
Annulus Configuration and Geometry							
2.21	PDM in 24″ OH	0.24448 , 0.60960	1012.86	1021.00	971.78	978.27	0.27900
2.22	Float Sub in 24″ OH	0.23973 , 0.60960	1011.95	1012.86	971.05	971.78	0.27696
2.23	PC (NM) in 24″ OH	0.24130 , 0.60960	1009.19	1011.95	968.85	971.05	0.27763
2.24	Stab. Slv. in 24″ OH	0.55245 , 0.60960	1007.14	1009.19	967.21	968.85	1.31009
2.25	Sub Pin in 24″ OH	0.23973 , 0.60960	1006.69	1007.14	966.86	967.21	0.27696
2.26	MWD in 24″ OH	0.24130 , 0.60960	997.71	1006.69	959.69	966.86	0.27763
2.27	Filter Sub in 24″ OH	0.24130 , 0.60960	997.30	997.71	959.37	959.69	0.27763
2.28	Sub in 24″ OH	0.24130 , 0.60960	996.52	997.30	958.74	959.37	0.27763
2.29	Stab. Slv. in 24″ OH	0.57785 , 0.60960	994.46	996.52	957.10	958.74	2.30772
2.30	DC (NM) in 24″ OH	0.24130 , 0.60960	975.83	994.46	941.83	957.10	0.27763
2.31	Stab. in 24″ OH	0.44450 , 0.60960	973.45	975.83	939.86	941.83	0.49994
2.32	DC in 24″ OH	0.24130 , 0.60960	964.06	973.45	932.12	939.86	0.27763
2.33	XO Sub in 24″ OH	0.24130 , 0.60960	962.85	964.06	931.09	932.12	0.27763
2.34	DC in 24″ OH	0.20320 , 0.60960	908.00	962.85	884.15	931.09	0.26339
2.35	Jar in 24″ OH	0.20320 , 0.60960	898.22	908.00	875.50	884.15	0.26339
2.36	DC in 24″ OH	0.20320 , 0.60960	879.77	898.22	859.20	875.50	0.26339
2.37	XO Sub in 24″ OH	0.19050 , 0.60960	878.89	879.77	858.42	859.20	0.25947
2.38	HWDP in 24″ OH	0.16828 , 0.60960	740.16	878.89	731.19	858.42	0.25344
2.39	DP in 24″ OH	0.13970 , 0.60960	365.00	740.16	364.74	731.19	0.24711
2.40	DP in 32″ Casing	0.13970 , 0.76200	0.00	365.00	0.00	364.74	0.15505

Table I.5: Geometry of drillstring assemblage and annulus configurations for BHA# 2. MWD: Anadrill 9.5″ CDR; PDM: Halliburton/Dyna-Drill 9-5/8″ Medium Speed F2000S; DP: Drill Pipe; DC: Drill Collar; HP: High Pressure; HWDP: Heavy Weight Drill Pipe; LP: Low Pressure; NM: Non-Magnetic; OH: Open Hole; PC: Pony Collar; Stab.: Stabilizer; Slv.: Sleeve.

ID	Description	Diameters [m],[m]	Depths [m MD] Top	Bottom	Depths [m TVD] Top	Bottom	Av. Vel. [m/s]
Drillstring Assemblage and Geometry							
6.1	Drill Pipe	0.12024	0.00	513.23	0.00	511.77	6.25237
6.2	HW Drill Pipe	0.12024	513.23	818.53	511.77	804.12	6.25237
6.3	Drill Pipe	0.12024	818.53	1818.53	804.12	1367.44	6.25237
6.4	Drill Pipe	0.12024	1818.53	2818.53	1367.44	1581.94	6.25237
6.5	Drill Pipe	0.12024	2818.53	3065.20	1581.94	1630.11	6.25237
6.6	HW Drill Pipe	0.12024	3065.20	3093.05	1630.11	1635.50	6.25237
6.7	XO Sub	0.08890	3093.05	3093.93	1635.50	1635.67	11.4384
6.8	Jar	0.07620	3093.93	3103.71	1635.67	1637.55	15.5689
6.9	DC (NM)	0.07303	3103.71	3120.69	1637.55	1640.78	16.9522
6.10	XO Sub	0.09368	3120.69	3121.90	1640.78	1641.01	10.3019
6.11	Stab. (NM)	0.07620	3121.90	3124.13	1641.01	1641.43	15.5689
6.12	Filter Sub	0.08890	3124.13	3124.55	1641.43	1641.51	11.4384
6.13	MWD Tool	n/a	3124.55	3136.73	1641.51	1643.76	n/a
6.14	Sub Pin X Pin	0.07620	3136.73	3137.18	1643.76	1643.84	15.5689
6.15	Stab. (NM)	0.07620	3137.18	3139.18	1643.84	1644.19	15.5689
6.16	Pony Collar (NM)	0.07780	3139.18	3141.95	1644.19	1644.68	14.9351
6.17	Float Sub	0.06193	3141.95	3142.86	1644.68	1644.84	23.5740
6.18	PDM Tool	n/a	3142.86	3151.00	1644.84	1646.29	n/a
6.19	Bit TFA ($\times 10^{-4}m^2$)	8.407188	3151.00	3151.60	1646.29	1646.32	n/a
Annulus Configuration and Geometry							
6.20	PDM in 17.5″ OH	0.24448 , 0.44450	3142.86	3151.00	1644.84	1646.29	0.65597
6.21	Float Sub in 17.5″ OH	0.23973 , 0.44450	3141.95	3142.86	1644.68	1644.84	0.64520
6.22	PC (NM) in 17.5″ OH	0.24130 , 0.44450	3139.18	3141.95	1644.19	1644.68	0.64871
6.23	Stab. (NM) in 17.5″ OH	0.24448 , 0.44450	3137.18	3139.18	1643.84	1644.19	0.65597
6.24	Sub Pin in 17.5″ OH	0.23973 , 0.44450	3136.73	3137.18	1643.76	1643.84	0.64520
6.25	MWD in 17.5″ OH	0.24130 , 0.44450	3124.55	3136.73	1641.51	1643.76	0.64871
6.26	Filter Sub in 17.5″ OH	0.24130 , 0.44450	3124.13	3124.55	1641.43	1641.51	0.64871
6.27	Stab. (NM) in 17.5″ OH	0.25400 , 0.44450	3121.90	3124.13	1641.01	1641.43	0.67937
6.28	XO Sub in 17.5″ OH	0.24130 , 0.44450	3120.69	3121.90	1640.78	1641.01	0.64871
6.29	DC (NM) in 17.5″ OH	0.20320 , 0.44450	3103.71	3120.69	1637.55	1640.78	0.57841
6.30	Jar in 17.5″ OH	0.20320 , 0.44450	3093.93	3103.71	1635.67	1637.55	0.57841
6.31	XO Sub in 17.5″ OH	0.19050 , 0.44450	3093.05	3093.93	1635.50	1635.67	0.56048
6.32	HWDP in 17.5″ OH	0.16828 , 0.44450	3065.20	3093.05	1630.11	1635.50	0.53408
6.33	DP in 17.5″ OH	0.13970 , 0.44450	2065.20	3065.20	1419.41	1630.11	0.50768
6.34	DP in 17.5″ OH	0.13970 , 0.44450	1269.00	2065.20	1157.46	1419.41	0.50768
6.35	DP in 20″ Casing	0.13970 , 0.46833	818.53	1269.00	804.12	1157.46	0.45242
6.36	HWDP in 20″ Casing	0.16828 , 0.46833	513.23	818.53	511.77	804.12	0.47327
6.37	DP in 20″ Casing	0.13970 , 0.46833	142.50	513.23	142.50	511.77	0.45242
6.38	DP in HP Riser	0.13970 , 0.52705	59.00	142.50	59.00	142.50	0.35003
6.39	DP in LP Riser	0.13970 , 0.53975	0.00	59.00	0.00	59.00	0.33258

Table I.6: Geometry of drillstring assemblage and annulus configurations for BHA# 6. MWD: Anadrill 9.5″ CDR; PDM: Halliburton Dyna-Drill 9-5/8″ Medium Speed F2000S; Casing: L-80 Casing. See Table I.5, page 223, for acronyms descriptions.

ID	Description	Diameters [m],[m]	Depths [m MD] Top	Depths [m MD] Bottom	Depths [m TVD] Top	Depths [m TVD] Bottom	Av. Vel. [m/s]
Drillstring Assemblage and Geometry							
9.1	Drill Pipe	0.08255	0.00	1000.00	0.00	961.52	5.91668
9.2	Drill Pipe	0.08255	1000.00	2000.00	961.52	1405.91	5.91668
9.3	Drill Pipe	0.08255	2000.00	3000.00	1405.91	1617.37	5.91668
9.4	Drill Pipe	0.08255	3000.00	3305.60	1617.37	1673.54	5.91668
9.5	XO Sub	0.08890	3305.60	3306.50	1673.54	1673.69	5.10163
9.6	HW Drill Pipe	0.07620	3306.50	3334.56	1673.69	1678.19	6.94389
9.7	Jar	0.07620	3334.56	3344.02	1678.19	1679.71	6.94389
9.8	HW Drill Pipe	0.07620	3344.02	3371.38	1679.71	1684.10	6.94389
9.9	Drill Pipe	0.08255	3371.38	4371.38	1684.10	1847.74	5.91668
9.10	Drill Pipe	0.08255	4371.38	5371.38	1847.74	2030.07	5.91668
9.11	Drill Pipe	0.08255	5371.38	5450.08	2030.07	2029.77	5.91668
9.12	HW Drill Pipe	0.07620	5450.08	5477.49	2029.77	2029.66	6.94389
9.13	Accelerator	0.07620	5477.49	5487.28	2029.66	2029.63	6.94389
9.14	HW Drill Pipe	0.07620	5487.28	5514.33	2029.63	2029.52	6.94389
9.15	Jar	0.07620	5514.33	5523.79	2029.52	2029.48	6.94389
9.16	HWDP (NM)	0.07620	5523.79	5546.60	2029.48	2029.40	6.94389
9.17	MWD Tool	n/a	5546.60	5566.04	2029.40	2029.32	n/a
9.18	Sub Pin X Pin	0.06985	5566.04	5566.38	2029.32	2029.32	8.26380
9.19	Pony Collar (NM)	0.07303	5566.38	5569.44	2029.32	2029.31	7.56083
9.20	Stabilizer	0.05715	5569.44	5571.24	2029.31	2029.30	12.3447
9.21	Float Sub	0.06985	5571.24	5572.17	2029.30	2029.30	8.26380
9.22	PDM Tool	n/a	5572.17	5579.72	2029.30	2029.27	n/a
9.23	Stabilizer Rotary	0.05715	5579.72	5580.00	2029.27	2029.27	12.3447
9.24	Bit TFA ($\times 10^{-4}$m^2)	7.917304	5580.00	5580.34	2029.27	2029.27	n/a
Annulus Configuration and Geometry							
9.25	Stab. Rot. in 8.5″ OH	0.21273 , 0.21590	5579.72	5580.00	2029.27	2029.27	29.6272
9.26	PDM in 8.5″ OH	0.17145 , 0.21590	5572.17	5579.72	2029.30	2029.27	2.34173
9.27	Float Sub in 8.5″ OH	0.16193 , 0.21590	5571.24	5572.17	2029.30	2029.30	1.97710
9.28	Stab. in 8.5″ OH	0.16510 , 0.21590	5569.44	5571.24	2029.31	2029.30	2.08317
9.29	PC (NM) in 8.5″ OH	0.17145 , 0.21590	5566.38	5569.44	2029.32	2029.31	2.34173
9.30	Sub Pin in 8.5″ OH	0.17145 , 0.21590	5566.04	5566.38	2029.32	2029.32	2.34173
9.31	MWD in 8.5″ OH	0.16510 , 0.21590	5546.60	5566.04	2029.40	2029.32	2.08317
9.32	HWDP (NM) in 8.5″ OH	0.12700 , 0.21590	5523.79	5546.60	2029.48	2029.40	1.32264
9.33	Jar in 8.5″ OH	0.16035 , 0.21590	5514.33	5523.79	2029.52	2029.48	1.92909
9.34	HWDP in 8.5″ OH	0.12700 , 0.21590	5487.28	5514.33	2029.63	2029.52	1.32264
9.35	Accelerator in 8.5″ OH	0.16510 , 0.21590	5477.49	5487.28	2029.66	2029.63	2.08317
9.36	HWDP in 8.5″ OH	0.12700 , 0.21590	5450.08	5477.49	2029.77	2029.66	1.32264
9.37	DP in 8.5″ OH	0.12700 , 0.21590	4450.08	5450.08	1861.24	2029.77	1.32264
9.38	DP in 8.5″ OH	0.12700 , 0.21590	3499.00	4450.08	1704.58	1861.24	1.32264
9.39	DP in 13 3/8″ Casing	0.12700 , 0.31178	3371.38	3499.00	1684.10	1704.58	0.49727
9.40	HWDP in 13 3/8″ Casing	0.12700 , 0.31178	3344.02	3371.38	1679.71	1684.10	0.49727
9.41	Jar in 13 3/8″ Casing	0.16035 , 0.31178	3334.56	3344.02	1678.19	1679.71	0.56392
9.42	HWDP in 13 3/8″ Casing	0.12700 , 0.31178	3306.50	3334.56	1673.69	1678.19	0.49727
9.43	XO Sub in 13 3/8″ Casing	0.12700 , 0.31178	3305.60	3306.50	1673.54	1673.69	0.49727
9.44	DP in 13 3/8″ Casing	0.13970 , 0.31178	2305.60	3305.60	1469.21	1673.54	0.51895
9.45	DP in 13 3/8″ Casing	0.13970 , 0.31178	1305.60	2305.60	1180.13	1469.21	0.51895
9.46	DP in 13 3/8″ Casing	0.13970 , 0.31178	305.60	1305.60	305.58	1180.13	0.51895
9.47	DP in 13 3/8″ Casing	0.13970 , 0.31178	142.50	305.60	142.50	305.58	0.51895
9.48	DP in HP Riser	0.13970 , 0.52705	59.00	142.50	59.00	142.50	0.15612
9.49	DP in LP Riser	0.13970 , 0.53975	0.00	59.00	0.00	59.00	0.14833

Table I.7: Geometry of drillstring assemblage and annulus configurations for BHA# 9. Long uniform sections are described in 1000 m [MD] lengths. MWD: Anadrill 6-1/2″ CDN; PDM: Halliburton Dyna-Drill 6-3/4″ Medium Speed F2000M; Casing: N-80 Casing. See Table I.5, page 223, for acronym descriptions.

ID	Description	Diameters [m],[m]	Depths [m MD] Top	Depths [m MD] Bottom	Depths [m TVD] Top	Depths [m TVD] Bottom	Av. Vel. [m/s]
Drillstring Assemblage and Geometry							
20.1	Drill Pipe	0.12136	0.00	1000.00	0.00	961.52	2.66545
20.2	Drill Pipe	0.12136	1000.00	2000.00	961.52	1405.91	2.66545
20.3	Drill Pipe	0.12136	2000.00	3000.00	1405.91	1617.37	2.66545
20.4	Drill Pipe	0.12136	3000.00	3171.24	1617.37	1649.88	2.66545
20.5	XO Sub	0.07780	3171.24	3172.13	1649.88	1650.03	6.48588
20.6	Drill Pipe	0.10861	3172.13	4172.13	1650.03	1813.57	3.32803
20.7	Drill Pipe	0.10861	4172.13	4694.03	1813.57	1903.07	3.32803
20.8	HW Drill Pipe	0.07938	4694.03	4722.11	1903.07	1907.89	6.23108
20.9	Jar	0.06985	4722.11	4731.43	1907.89	1909.48	8.04633
20.10	HW Drill Pipe	0.07938	4731.43	4758.84	1909.48	1920.32	6.23108
20.11	Drill Pipe	0.10861	4758.84	5758.84	1920.32	2028.86	3.32803
20.12	Drill Pipe	0.10861	5758.84	6303.04	2028.86	2029.10	3.32803
20.13	HW Drill Pipe	0.07938	6303.04	6331.00	2029.10	2029.11	6.23108
20.14	Accelerator	0.06985	6331.00	6340.72	2029.11	2029.12	8.04633
20.15	HW Drill Pipe	0.07938	6340.72	6368.77	2029.12	2029.13	6.23108
20.16	Jar	0.06985	6368.77	6378.01	2029.13	2029.13	8.04633
20.17	HWDP (NM)	0.07938	6378.01	6396.22	2029.13	2029.13	6.23108
20.18	Stab.	0.07303	6396.22	6397.64	2029.13	2029.13	7.36186
20.19	MWD Tool	n/a	6397.64	6416.81	2029.13	2029.13	n/a
20.20	Stab.	0.07303	6416.81	6418.32	2029.13	2029.13	7.36186
20.21	Geosteering	0.05347	6418.32	6424.83	2029.13	2029.13	13.7328
20.22	Stab. Float Sub	0.07303	6424.83	6427.75	2029.13	2029.13	7.36186
20.23	PDM Tool	n/a	6427.75	6437.00	2029.13	2029.13	n/a
20.24	Bit TFA ($\times 10^{-3}$m^2)	1.388024	6437.00	6437.28	2029.13	2029.13	n/a
Annulus Configuration and Geometry							
20.25	PDM in 8.5″ OH	0.17145 , 0.21590	6427.75	6437.00	2029.13	2029.13	2.28011
20.26	Stab. Float Sub in 8.5″ OH	0.17780 , 0.21590	6424.83	6427.75	2029.13	2029.13	2.61722
20.27	Geosteering in 8.5″ OH	0.17145 , 0.21590	6418.32	6424.83	2029.13	2029.13	2.28011
20.28	Stab. in 8.5″ OH	0.17780 , 0.21590	6416.81	6418.32	2029.13	2029.13	2.61722
20.29	MWD in 8.5″ OH	0.16510 , 0.21590	6397.64	6416.81	2029.13	2029.13	2.02835
20.30	Stab. in 8.5″ OH	0.17780 , 0.21590	6396.22	6397.64	2029.13	2029.13	2.61722
20.31	HWDP (NM) in 8.5″ OH	0.12700 , 0.21590	6378.01	6396.22	2029.13	2029.13	1.28784
20.32	Jar in 8.5″ OH	0.16193 , 0.21590	6368.77	6378.01	2029.13	2029.13	1.92507
20.33	HWDP in 8.5″ OH	0.12700 , 0.21590	6340.72	6368.77	2029.12	2029.13	1.28784
20.34	Accelerator in 8.5″ OH	0.16193 , 0.21590	6331.00	6340.72	2029.11	2029.12	1.92507
20.35	HWDP in 8.5″ OH	0.12700 , 0.21590	6303.04	6331.00	2029.10	2029.11	1.28784
20.36	DP in 8.5″ OH	0.12700 , 0.21590	5303.04	6303.04	2028.66	2029.10	1.28784
20.37	DP in 8.5″ OH	0.12700 , 0.21590	4865.00	5303.04	1968.35	2028.66	1.28784
20.38	DP in 9 5/8″ Casing	0.12700 , 0.22050	4758.84	4865.00	1920.32	1968.35	1.20831
20.39	HWDP in 9 5/8″ Casing	0.12700 , 0.22050	4731.43	4758.84	1909.48	1920.32	1.20831
20.40	Jar in 9 5/8″ Casing	0.16193 , 0.22050	4722.11	4731.43	1907.89	1909.48	1.75265
20.41	HWDP in 9 5/8″ Casing	0.12700 , 0.22050	4694.03	4722.11	1903.07	1907.89	1.20831
20.42	DP in 9 5/8″ Casing	0.12700 , 0.22050	3694.03	4694.03	1735.89	1903.07	1.20831
20.43	DP in 9 5/8″ Casing	0.12700 , 0.22050	3172.13	3694.03	1650.03	1735.89	1.20831
20.44	XO Sub in 9 5/8″ Casing	0.19050 , 0.22050	3171.24	3172.13	1649.88	1650.03	3.18426
20.45	DP in 9 5/8″ Casing	0.13970 , 0.22050	2171.24	3171.24	1441.38	1649.88	1.34894
20.46	DP in 9 5/8″ Casing	0.13970 , 0.22050	1171.24	2171.24	1094.04	1441.38	1.34894
20.47	DP in 9 5/8″ Casing	0.13970 , 0.22050	171.24	1171.24	171.24	1094.04	1.34894
20.48	DP in 9 5/8″ Casing	0.13970 , 0.22050	142.50	171.24	142.50	171.24	1.34894
20.49	DP in HP Riser	0.13970 , 0.52705	59.00	142.50	59.00	142.50	0.15201
20.50	DP in LP Riser	0.13970 , 0.53975	0.00	59.00	0.00	59.00	0.14443

Table I.8: Geometry of drillstring assemblage and annulus configurations for BHA# 20. Long uniform sections are described in 1000 m [MD] lengths. MWD: Anadrill composite 6-3/4″ LWD/MWD; PDM: Halliburton Dyna-Drill 6-3/4″ Slow Speed F2000S; Casing: P-110 Casing. See Table I.5, page 223, for acronym descriptions.

Vita

A British national, William John Bailey was awarded a Master of Engineering (M.Eng) degree (with honours) in Petroleum Engineering from Imperial College of Science, Technology and Medicine, University of London in 1989. He also holds a Masters in Business Administration (MBA) from Warwick Business School, University of Warwick, UK, is an Associate of the Royal School of Mines (ARSM) and a Member of the Society of Petroleum Engineers. He was a prize winner in the 1991 SPE student paper contest.

Before entering university William Bailey worked in The City of London as an insurance broker and as a unit trust dealer. After graduation from Imperial College he worked for an internationally renowned American strategic management consultancy firm and was involved in investment, technical and strategic analysis for a number of clients in the UK, Italy, United Arab Emirates and Bahrain. He later worked in Norway for an oil service company and headed the development of the HYCAT drilling hydraulics simulation package. As well as working experience he managed all drilling hydraulic simulations for a major North Sea operator and a number of service companies. He has also acted as a consultant for an oil service company in the USA.

William Bailey ran, on a part-time basis, a dance-orientated record label (with a couple of club 'hits') and has played in several musical groups. He enjoys cricket, cats, football, motor bikes, music (all sorts) and weight training.